1988

Effects of reactor configuration on the performance of static-bed submerged media anaerobic reactors

Chow-Feng Chiang
Iowa State University

Order Number 8825378

Effects of reactor configuration on the performance of static-bed submerged media anaerobic reactors

Chiang, Chow-Feng, Ph.D.

Iowa State University, 1988

U·M·I
300 N. Zeeb Rd.
Ann Arbor, MI 48106

PLEASE NOTE:

In all cases this material has been filmed in the best possible way from the available copy. Problems encountered with this document have been identified here with a check mark ✓.

1. Glossy photographs or pages _____
2. Colored illustrations, paper or print _____
3. Photographs with dark background _____
4. Illustrations are poor copy _____
5. Pages with black marks, not original copy _____
6. Print shows through as there is text on both sides of page _____
7. Indistinct, broken or small print on several pages ✓
8. Print exceeds margin requirements _____
9. Tightly bound copy with print lost in spine _____
10. Computer printout pages with indistinct print _____
11. Page(s) _____ lacking when material received, and not available from school or author.
12. Page(s) _____ seem to be missing in numbering only as text follows.
13. Two pages numbered _____. Text follows.
14. Curling and wrinkled pages ✓
15. Dissertation contains pages with print at a slant, filmed as received _____
16. Other _____

_____

_____

Effects of reactor configuration on the performance of static-bed submerged media anaerobic reactors

by

Chow-Feng Chiang

A Dissertation Submitted to the
Graduate Faculty in Partial Fulfillment of the
Requirements for the Degree of
DOCTOR OF PHILOSOPHY

Department: Civil and Construction Engineering
Major: Sanitary Engineering

Approved:

Signature was redacted for privacy.

In Charge of Major Work

Signature was redacted for privacy.

For the Major Department

Signature was redacted for privacy.

For the Graduate College

Iowa State University
Ames, Iowa

1988

TABLE OF CONTENTS

LIST OF FIGURES

LIST OF TABLES

DEDICATION

Dedicated to my parents and Mao-Mao

who love me

LIST OF ABBREVIATIONS

AA	Atomic absorption
AE	Atomic emission
AMA	Acetoclastic methanogenic activity
CoA	Coenzyme A
CoM	Coenzyme M
COD	Chemical oxygen demand
CSTR	Continuously stirred tank reactor
EPS	Extracellular polymetric substance
F/M	Food vs. microorganisms ratio
FAS	Ferrous ammonium sulfate
F_{420}	Factor 420
G+C	Guanine + Cytosine
IA	Intermediate alkalinity
KHP	Potassium hydrogen phthalate
MCRT	Mean cell residence time
NAD	Nicotinamide adenine dinucleotide
NFDM	Non-fat dry milk
PA	Partial alkalinity
SCOD	Soluble COD
SF	Substrate gradient factor
SMAR	Submerged media anaerobic reactor
SRT	Solid retention time
STP	standard temperature and pressure

TAlk	Total alkalinity
TC	Titration-calibration COD method
TCA	Tricarboxylic acid cycle
TCOD	Total COD
TOA	Total organic acids (Chromatography)
TS	Total solids
TVA	Total volatile acids (Steam distillation)
UASB	Upflow anaerobic sludge reactor
USEPA	United State Environmental Protection Agency
VS	Volatile solids
VSS	Volatile suspended solids

INTRODUCTION

In recent years, concerns over treatment of organic industrial wastes have resulted in the development of several high-rate anaerobic processes (Speece, 1983). These processes can be classified into upflow or downflow, packed bed or unpacked bed. Depending on the type of packing used and the hydraulic regime operated, the upflow packed-bed process can be further classified into static bed, expanded bed, or fluidized bed. Figure 1 shows schematics of these processes. The term "submerged media anaerobic reactor" (SMAR) was coined for the upflow packed-bed processes by an ad hoc committee to alleviate confusion in nomenclature (Argonne National Laboratory, 1980).

Characteristics of Static-Bed SMAR

The static-bed SMAR is basically a column packed with some type of media. The influent enters a bottom distribution panel and flows upward through the packing where biomass develops. The biomass occurs either in the voids (biofloc) or on the surface (biofilm) of the packing. Biogas is produced as the end product of anaerobic digestion. Biogas consists mainly of methane and carbon dioxide with small quantities of nitrogen, hydrogen sulfide, and hydrogen. This characterizes the SMAR system as a complex, three-phase (liquid, biomass, and biogas) anaerobic system (Figure 2).

The SMAR process has been of special interest because of its better biomass retention capability over the unpacked process (Frostell, 1981).

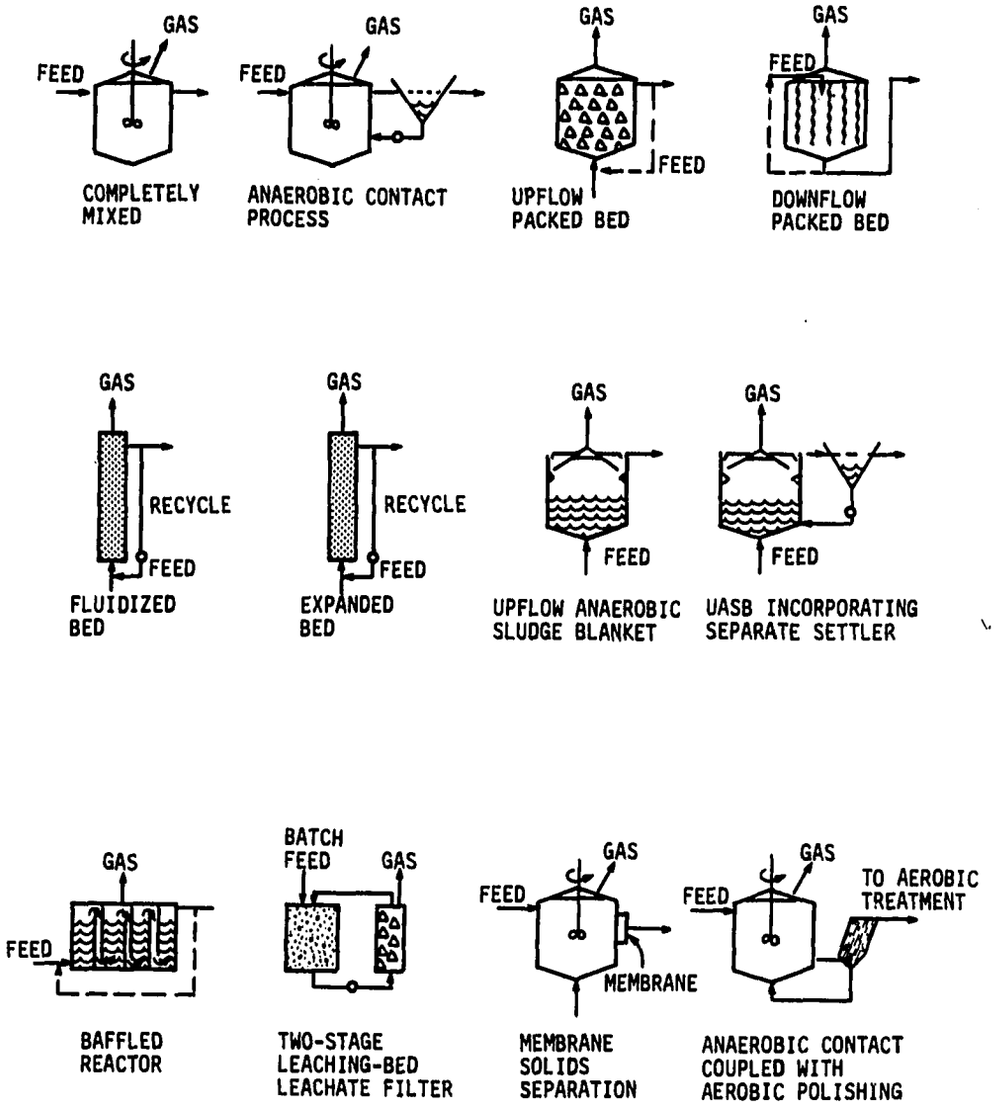

FIGURE 1. Schematics of modern high-rate anaerobic processes (Speece, 1983)

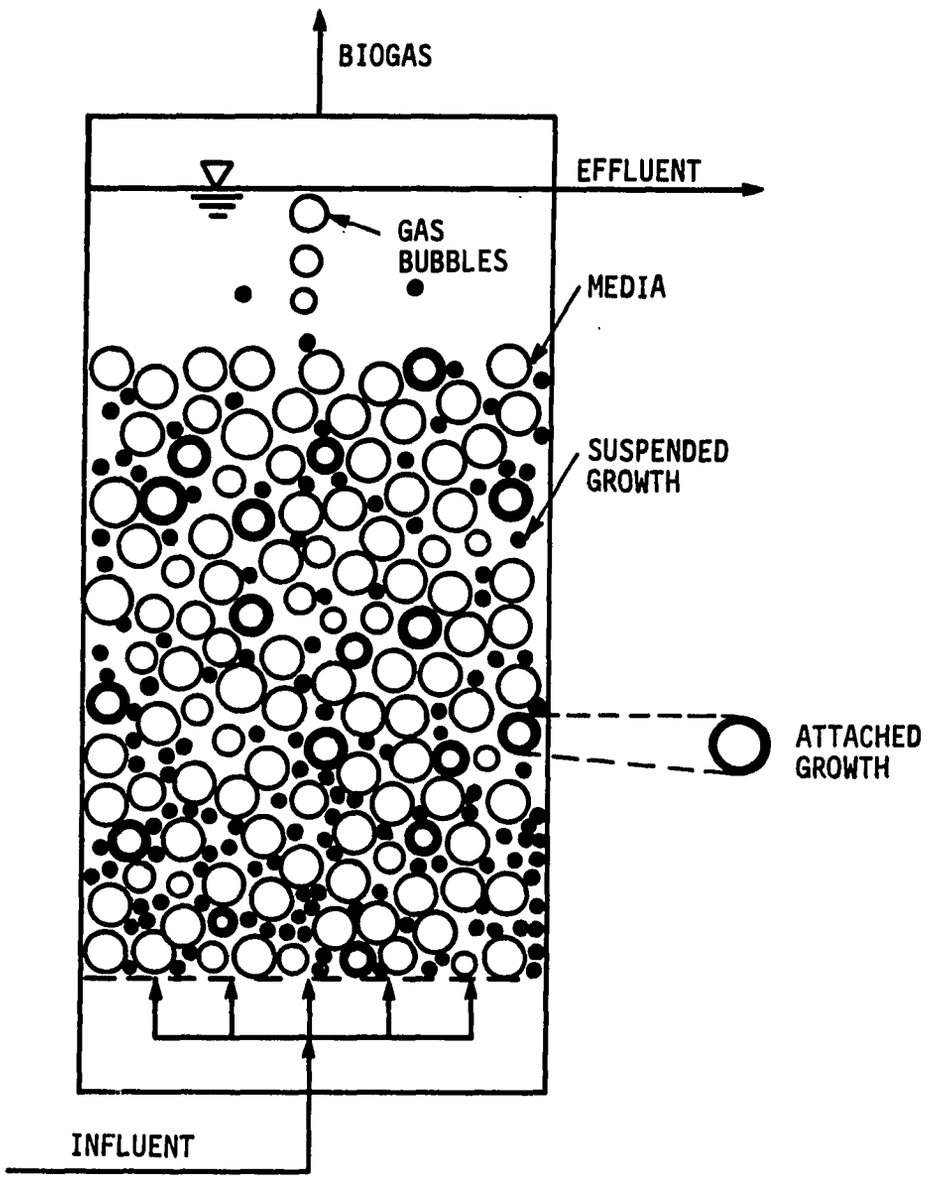

FIGURE 2. Schematics of a static-bed submerged media anaerobic reactor, showing a three-phase anaerobic system

Consequently, a longer solids retention time (SRT) can be achieved. An SRT of over 500 days has been reported (Young and McCarty, 1969; Jennett and Dennis, 1975). A long SRT is essential for successful treatment (Dague *et al.*, 1970). Pilot studies over the past 20 years indicate that a long SRT is also important in successful operation under non-optimal conditions, such as ambient temperature operation (Young and McCarty, 1969; Rittmann *et al.*, 1982; Oleszkiewicz and Koziarski, 1982; Kelly and Switzenbaum, 1984), pH between 6 to 8 (Clark and Speece, 1970; Dague and Porter, 1982), and high toxicants levels (Parkin *et al.*, 1983; Blum *et al.*, 1986).

The SMAR process is characterized by a highly heterogeneous distribution of biomass mainly resulting from the upflow operation. The lower part of the SMAR, which is often responsible for a major portion of substrate removal, often contains a high concentration of biomass (10-15 g TSS/L) with self-induced mixing due mainly to internally produced biogas. The substrate utilization behavior of the biomass under this environment has not yet been well studied.

The biogas mixing intensity has been estimated using the isothermal energy dissipation theory (USEPA, 1979). Assuming a single point biogas production at pressure p_2 and allowing for an isothermal expansion to pressure p_1, the energy dissipation rate (E) and the mean velocity gradient (G) resulting from the expansion are:

$$E = p_1 Q_g \ln(p_1/p_2) \quad (1)$$

$$G = \left(\frac{E}{V\mu}\right)^{1/2} \quad (2)$$

where, "E" is the energy dissipation rate (power) in kW; "G" is the mean velocity gradient in 1/sec; "p_1" and "p_2" are the biogas pressure at the production point and at the expansion point, respectively, in kN/m^2; "Q_g" is the biogas flowrate at p1 in m^3/s; "V" is the liquid volume of the reactor in m^3; and "μ" is the Newton's viscosity of the liquid in kN-sec/m^2.

As a result of biogas mixing, the growth is often developed into granular aggregates with excellent settling properties (Dague *et al.*, 1970). The granules have typical diameters of 1-5 mm (Lettinga *et al.*, 1980) and settling velocities of approximately 1.2 cm/s (Sahm, 1984). The granules are negatively charged with extracellular polymeric substances, which are important to the aggregation (Mahoney *et al.*, 1984). It has also been found that the granules are capable of significant absorption of many organic compounds (Johnson and Young, 1983).

The ultrastructure morphology of anaerobic biofilm (from down-flow stationary reactors) was recently studied using the scanning electron microscopy (SEM). The biofilm consists of two distinct layers of methanogens with *Methanothrix* interweaving at the surface and *Methanosarcina* embedded in deeper layers. The biofilm structure is

characterized with an extensive network of channels that may facilitate biogas and nutrient exchanges into the deeper regions of growth (Robinson *et al.*, 1984). As the biofilm grows, electron-dense mineral deposition, enriched with calcium and phosphorus, may occur and eventually block the transport sites and retard methanogenic activity (Harvey *et al.*, 1984).

With recent advances in anaerobic microbiology, the advantage of highly concentrated biomass over dispersed biomass in hydrogen interspecies transfer becomes better understood. Process designs that encourage hydrogen producers (H_2-producing acetogens) and hydrogen utilizers (methanogens) to live in close proximity, such as in the SMAR process, are more favorable to high rates of H_2 conversion in the system. Without the transfer, H_2 may quickly build up and inhibit the system (Bryant, 1979). The H_2 partial pressure normally ranges from 0.1 to 2.0 $\times 10^{-4}$ atm, depending on loading rates. At a COD loading rate of 10 g/L/d, it is estimated that the H_2 1st-order rate constant can reach as high as about 80 1/s with the two H_2-transfer species living within a distance of about 10 μm. At a higher COD removal rate of 40 g/L/d, the distance has to be about 5 μm (McCarty and Smith, 1986).

Another feature of the SMAR process is related to the limited self-induced biogas mixing intensity. The substrate gradient across the liquid film is greater for the SMAR system than for systems with higher mixing intensity. Consequently, when the SMAR is exposed to toxicants (as the secondary substrate), the actual toxicant levels reaching the biomass are reduced as the toxicants diffusion through the liquid film.

This might explain why the SMAR system is more tolerant to higher toxicant levels than the CSTR system (Parkin *et al.*, 1983).

Packing media are another important feature in the SMAR process. The role of the packing media and their design criteria are now better understood with the efforts of Young and his associates (Young and Dahab, 1982; Young, 1985; Song and Young, 1986). The media should be designed to provide a better biomass retention capability and to increase the intermixing and contact efficiency between substrate and organisms.

Need for Research

Scale-up and SMAR height. In sizing a SMAR, the volume and height are of concern (Dague, 1982). This brings up two questions. First, can the removal rate (g COD/L/d) obtained from pilot studies be directly used for scale-up in the determination of the full-scale SMAR volume? Second, what should be the depth for a given volume? Considering the effect of different biogas mixing intensity resulting from different reactor heights, these two questions are actually interrelated, since, in many cases, pilot SMARs are much shallower than the full-scale SMARs to be designed. The question is whether or not there is an optimal height for a given volume.

Theoretically, higher hydrostatic pressures resulting from higher SMAR heights have both positive and negative effects on treatment performance. As shown in Equations (1) and (2), higher hydrostatic pressures increase mixing intensity and improve the contact efficiency

between substrate and organisms. Figure 3 shows the relationship between G and SMAR height at various TCOD removal rates. Figure 3 is plotted assuming: (1) a single biogassing point at the bottom of the SMAR, (2) clean water density (not considering the sludge) for calculating P_2, (3) a methane content of 70%, (4) p_1 of 1 atm, (5) at a temperature of 35° C, and (6) TCOD removal rates of 2, 6 and 12 g/L/d.

On the other hand, higher SMAR heights tend to result in higher hydrogen partial pressures, which may inhibit methanogenesis, especially under heavy loading conditions. This can be calculated using the Lewis equation:

$$\Delta G = \Delta G^{o} - RT \ln Q \qquad (3)$$

where, "ΔG^{o}" is the standard Gibbs free energy change in J; "R" is the universal gas constant of 8.314 J/deg/mole; "T" is the absolute temperature in degree Kelvin; and "Q" is the reaction molar quotient. Figure 4 illustrates the Gibbs free energy change (ΔG^{o}) as a function of SMAR height at a range of hydrogen partial pressures of interest, using propionate acetogenesis as an example:

$$Propionate^{-} + 3H_2O \leftrightarrow Acetate^{-} + HCO_3^{-} + 3H_2 + H^{+} \qquad (4)$$

$$\Delta G^{o} = +76.1 \text{ kJ/rxn}$$

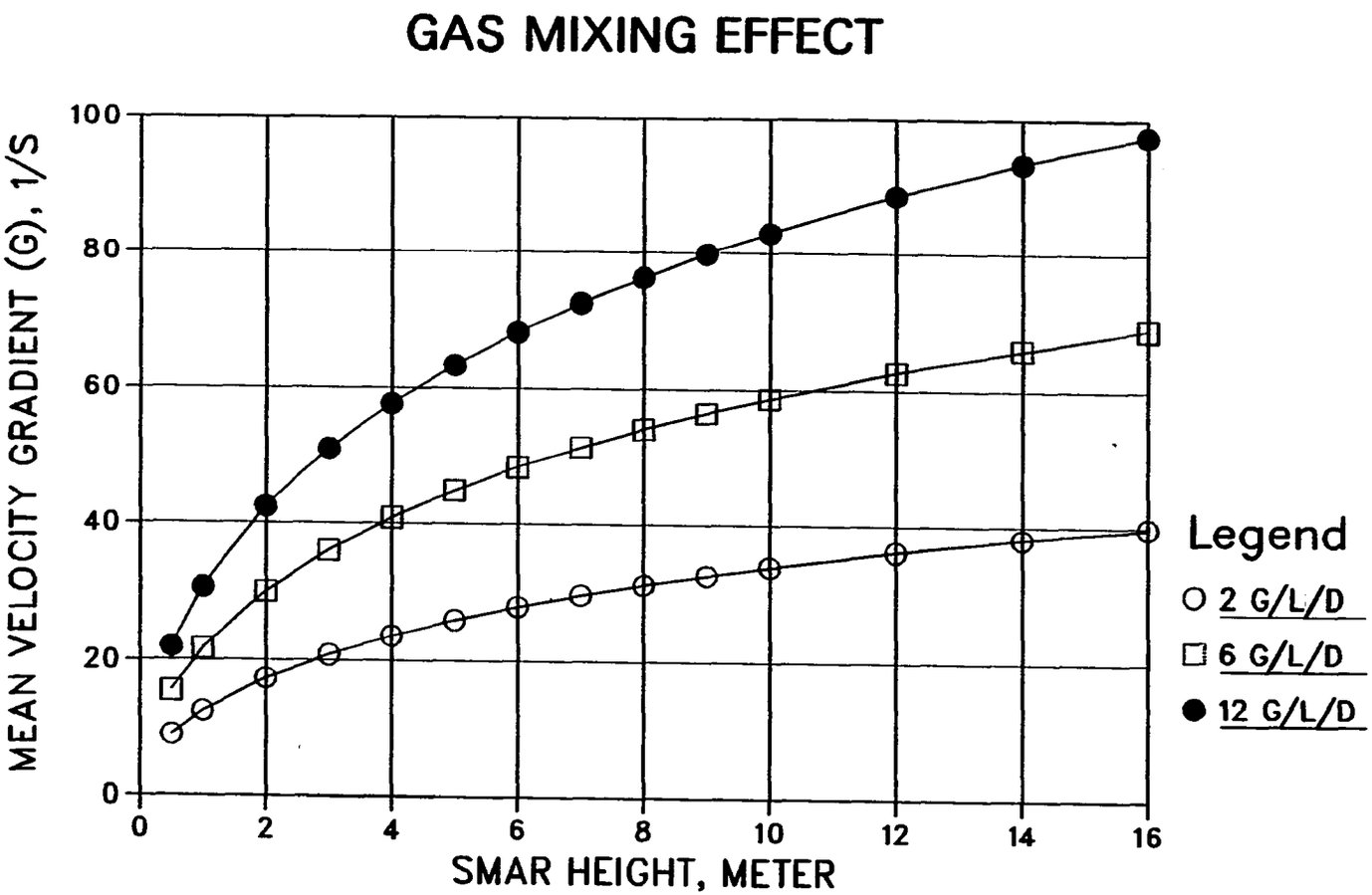

FIGURE 3. Biogas mixing mean velocity gradient as a function of SMAR depth at various TCOD removal rates, assuming (1) a single gassing point at the bottom of SMARs, (2) clean water density, (3) methane content of 70%, (4) p_1= 1 atm, and (5) 35° C

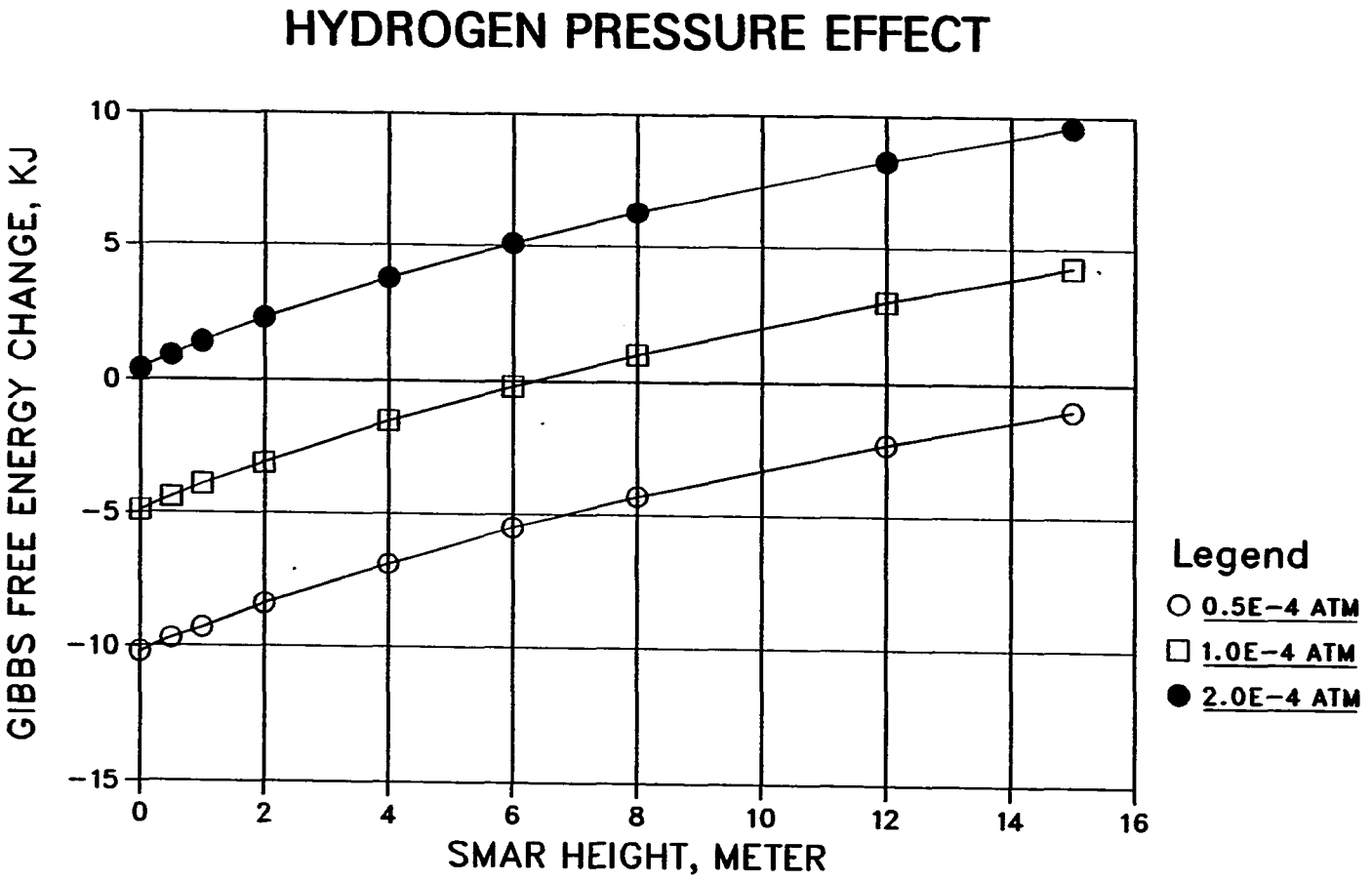

FIGURE 4. Gibbs free energy change as a function of SMAR height for propionate acetogenesis at various exit H_2 partial pressures, assuming (1) [acetate]/[propionate]=0.5, (2) exit CO_2 partial pressure= 0.3 atm, (3) pH=7, and (4) 35° C

Figure 4 is plotted using: exit pCO_2 = 0.3 atm, CO_2 Henry's constant = 2230 atm (at 35° C), pK_{a1} = 6.31 for H_2CO_3 (at 35° C), pH = 7.0, and [Acetate$^-$]/[Propionate$^-$] = 0.5, for a range of pH_2 = 0.5-2.0 × 10^{-4} atm. Both Figures 3 and 4 suggest that SMAR height may be an important factor affecting treatment performance. However, this had not been experimentally studied.

Dirty-bed tracer study. Biogas mixing can also affect SMAR hydraulic patterns. Young (1968) assumed an ideal plug flow in simulating the SMAR process according to clean-bed tracer studies. It is not well understood that, under operating conditions, how much dispersion and short circuiting could result from biogas mixing and biomass accumulation in the system.

Methanogenic activity. Another question arises in applying the SRT concept to the SMAR process. Unlike the CSTR system, biomass distribution in a SMAR is highly heterogeneous. Consequently, biomass activity may also vary at different depths (Bull *et al.*, 1984). Although it is well known that the SMAR can achieve a very long SRT with a great amount of biomass accumulation in the system, there is a lack of information on the distribution of the biomass activity that actually occurs in *situ*. Also, methods and procedures involving the determination of the activity are not presently available for practical use.

Rate-limiting step. The question concerning what is the overall rate-limiting step in anaerobic digestion has frequently been asked and debated. It is generally accepted that acetate methanogenesis is the

overall rate-limiting step under normal digestion conditions treating non-polymer wastes (Zeikus, 1985). However, when digestion is upset and H_2 partial pressure builds up, acetogenesis, especially of the low-carbon organic acids such as propionate and butyrate, may become the rate-limiting step (Kaspar and Wuhrmann, 1978; Bryant, 1979). Finney and Evans (1975), however, claim that the detachment rate of the minute gas bubbles from the cell surface, which tends to block substrate transfer sites, is the limiting step. This was evidenced by a great increase in substrate removal rate under vacuum operations.

Harper and Pohland (1987) studied the effect of biogas removal on treatment performance for the SMAR process. The biogas was removed at several intermediate points along the SMAR height. Their data clearly show that gas removal improves TOC removal even up to 10%. Their H_2 data further suggest that the better performance was associated with the lower pH_2 in the system. Podolak *et al.* (1984) also found that vacuum operation of an anaerobic rotating biological contactor (AnRBC) can significantly improve the treatment efficiency, especially at high loading rates.

It is questioned, however, why the fast growing H_2-utilizing methanogens cannot rapidly remove the hydrogen while it is built up. It is hypothesized, in this study, that the H_2 dissolution (from the gas phase into liquid phase) is the rate-limiting step and only the dissolved H_2 can be directly used. The hypothesis is supported by the fact that H_2 gas is very insoluble (1.6 g/L at 25 ^{o} C) and strong mixing can greatly increase the H_2 utilization rate by methanogens (Daniels *et al.*, 1984a).

Half-velocity constant. Another question which has not brought attention is the wide variation of K_s reported in literature for acetate methanogenesis. Lawrence and McCarty (1969) reported a K_s of 154 mg/L as acetic acid (HAc) for chemostat cultures on acetate, while Wang *et al.* (1986) found that the Ks has to be 8.4 mg/L as HAc to accurately simulate their fluidized-bed (completely mixed) SMAR treating acetate. This might be due to difference in mixing intensity used in these two studies. The contact efficiency factor (η) can be estimated of about 0.05 (8.4/154) as a result of inadequate mixing for the anaerobic system used by Lawrence and McCarty, assuming 8.4 is the true K_s.

Interestingly, McCarty (1985), in a recent paper, has also addressed the problem of this high K_s value. In estimating the minimum concentration of substrate that can be achieved in a system at steady state, the following equation is used:

$$S_{min} = k_d K_s/(Yk_m - k_d) \qquad (5)$$

where, "Y" is the growth yield in gm substrate utilized/gm biomass produced and "k_d" is the decay constant in 1/d. It was found that the calculated S_{min} for anaerobic treatment of domestic sewage, based on the data reported by Lawrence and McCarty (1969), was much higher than that achieved in pilot studies. This again indicates the inadequacy of the Monod model to account for differences in mixing intensity used in different studies.

Another reason that may further result in the high K_S value is the improper use of mathematical techniques in obtaining the value by linearizing the Monod equation and applying a linear least squares method. Kouadio (1984) has addressed this problem. When compared with the K_S obtained with a non-linear maximum likelihood optimization model, the K_S obtained with the linear models tend to be overestimated, even up to 60%.

Purposes and Objectives

Three pilot-scale SMARs were designed and operated using an enriched synthetic waste of powdered milk solution. The three SMARs have the same operating volume but different heights and diameters. Biogas production rate, methane content, COD, individual volatile acids, biomass concentrations, and acetoclastic methanogenic activity were determined under steady-state conditions at various organic loading rates. The major purpose of the study was to see whether difference in SMAR configuration could result in different treatment performance, due mainly to different biogas mixing patterns as a result of different hydrostatic pressures. This is thought to be an important factor in process design and operation, especially at heavy loading conditions.

The specific objectives of this study were:

(1) To compare the steady-state treatment performance and biomass retention capability among the three different shapes of SMARs, in considering, specifically, the biogas mixing effects.

(2) To compare the hydraulic patterns among the three SMARs and to determine the effect of biogas mixing and biomass accumulation on short circuiting by conducting tracer studies under clean and dirty-bed conditions.

(3) To develop an activity test and use the test to determine the activity profiles for biomass obtained from various heights in the three SMARs.

(4) To understand the relative importance of acetogenic pathways, as proposed in Wood scheme (9161), especially under heavy loading conditions, by determining the individual volatile acids at different heights in the three SMARs.

(5) To substantiate the hypothesis that hydrogen dissolution is the rate-limiting step, as proposed in this study, by recycling the biogas under heavy loading conditions.

(6) To propose a rational design procedure for the SMAR process based on the results of this study.

LITERATURE REVIEW

Fundamentals of Anaerobic Digestion

An anaerobic process is a series of biochemical reactions in which free molecular oxygen plays no part as an electron acceptor. Fermentation refers to any process in which only substrate level phosphorylation (SLP) is used by bacteria to obtain energy. Respiration, however, involves the use of electron transport phosphorylation (ETP) to obtain energy. Anaerobic digestion is a process of fermentation with the last step being respiration to methane.

The methanogenic anaerobic system is an extremely complex system in which many trophically diverse groups of bacteria are involved. Zeikus (1985) has classified these bacteria into four distinctive groups based on their trophic levels: Group I hydrolytic/fermentative bacteria, Group II H_2-producing acetogens, Group III homoacetogens, and Group IV methanogens. This is shown in Figure 5. Group II and III are usually referred to as the "syntrophic bacteria" to characterize their symbiotic relationship with the methanogens.

The Zeikus scheme presents the current understanding of the anaerobic systems and is important in several aspects. First, it corrects the misconception that propionate can be directly used by methanogens, as previously believed (Barker, 1956; McCarty, 1964a; Andrews and Pearson, 1965; Lawrence and McCarty, 1969). Second, it details an over-simplified, two-stage (acid and methane formation) scheme

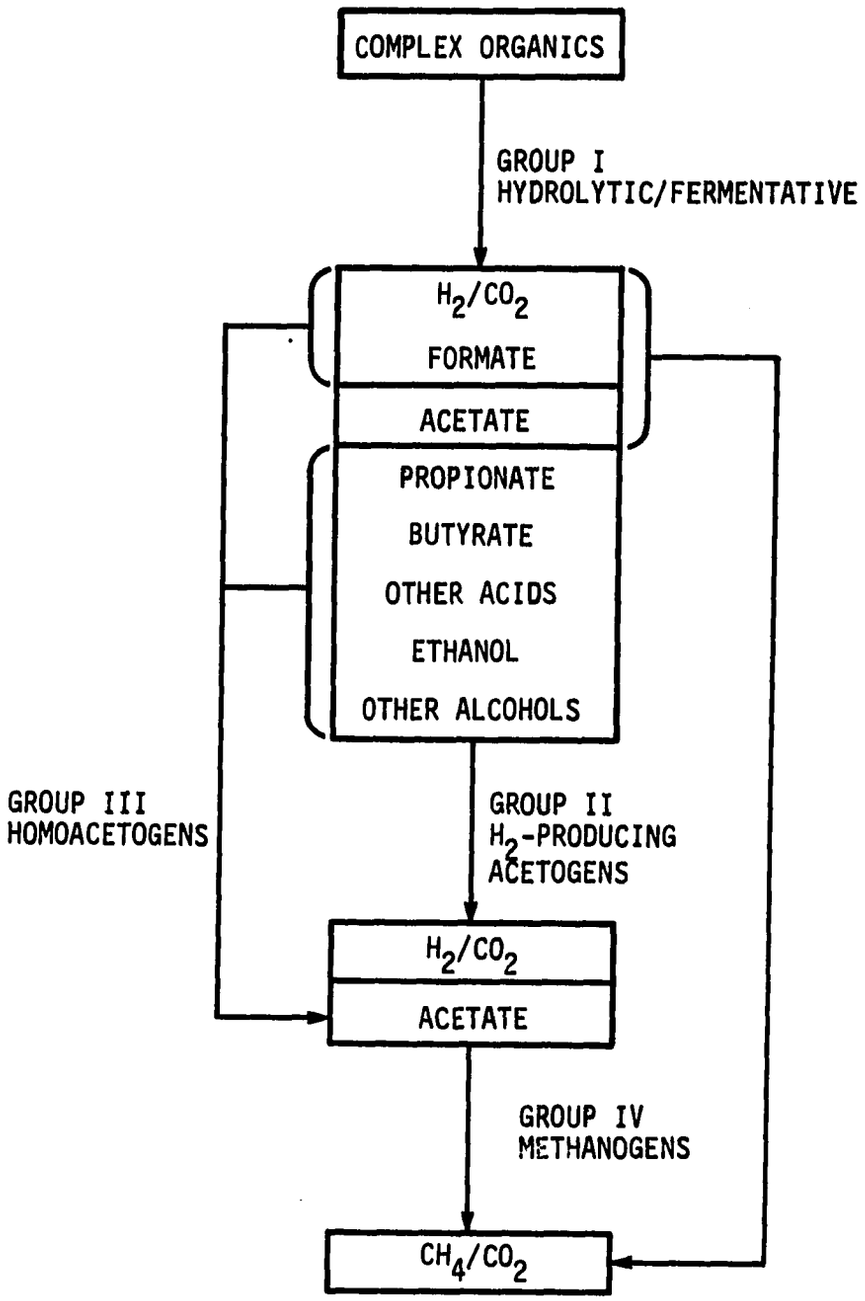

FIGURE 5. Schematics of anaerobic degradation, showing four levels of syntrophic groups, adapted and modified from Zeikus (1985) and Daniels (1984)

that was previously accepted (McCarty, 1964a). And third, it shows the syntrophic relationship between the acetogens and methanogens and the importance of hydrogen interspecies transfer in process control.

The importance of species diversity in providing system stability in anaerobic digestion has been discussed by Zeikus (1985). The species diversity, as reflected in different physiological requirements for optimal growth, accounts for the process stability. However, the need for species diversity leads to difficulty in process control in maintaining balanced growth rates and species populations for different groups of bacteria in anaerobic digestion. Table 1 shows the estimated maximum specific growth rate (μ_m, 1/day) and population density (in MPN, #/mL) for the five groups of bacteria most commonly found in successfully operated anaerobic sludge digesters.

Fermentative Hydrolysis

Organic compounds found in wastes are usually insoluble, high-molecular weight polymers, such as polysaccharides, lipids, and proteins. For instance, the sludge produced from primary settling of sewage contains 8-15% cellulose, 6-30% lipids, and 20-30% proteins (USEPA, 1979). In this case, hydrolysis has to be carried out to depolymerize these compounds into soluble, smaller molecules to allow for substrate diffusion into bacterial cells in which most of the reactions take place. Hydrolysis is carried out by a group of anaerobic or facultative bacteria using extracellular enzymes (exoenzymes). Energetically, hydrolysis is an irreversible reaction with a small decrease in free energy.

TABLE 1. Typical growth rates and population density for five groups of bacteria most commonly found in anaerobic sludge digesters

Group	μ_m[a] (1/day)	MPN[b] (#/mL)	Reference
Hydrolytic bacteria			Zeikus (1985)
Total	2.4	10^8-10^9	
Proteolytic	-	10^7	
Cellulolytic	-	10^5	
H_2-producing acetogenic bacteria	0.1-0.2	10^6	Boone and Bryant (1980)
Cocultures	0.1-1.2		Heyes and Hall (1983)
Homoacetogenic bacteria	0.7-2.8	10^5-10^6	Zeikus (1985)
Methanogens		10^6-10^8	Zeikus (1985)
H_2/CO_2	1.4-8.3		
Acetate	0.7		
Sulfate reducers	0.3-0.7	10^4	Sorensen *et al.* (1981)

[a]Maximum specific growth rate = 0.693/regeneration time.

[b]Most probable number, from Zeikus (1985).

Polysaccharides are hydrolyzed to monosaccharides and then degraded to pyruvate via the Embden-Meyerhof-Parnas (glycolysis) scheme. Lipids are hydrolyzed to glycerols and fatty acids which are further fermented to pyruvate via β-oxidation with 2-C reduction. Unsaturated fatty acids are saturated by hydrogenation. Long chain fatty acids such as stearate (18-C) and palmitate (16-C) may be important products for some fermentative bacteria (Chynoweth and Mah, 1971). Proteinaceous materials are fermentated to various α-amino acids which, in turn, are deaminated (with the production of NH_3) to various fatty acids including isobutyrate, isovalerate, 2-methyl-butyrate, n-valerate, and various aromatic acids such as phenylacetate and indoleacetate (Barker, 1961).

The rate of hydrolysis is highly dependent on the availability of exoenzymes that can be adaptive to a specific substrate. In their study of anaerobic digestion of urban organic refuse, Pfeffer and Liebman (1976) indicate that the hydrolysis of cellulose (β-linked hexose) is the overall rate-limiting step. Lignin found in pulping wastes is also recognized as having a very low hydrolysis rate, probably due to a low solubility. Novak and Carlson (1970) found that the degradation of long-chain fatty acids is limited by β-oxidation, not by dissolution. However, hydrolysis of compounds other than cellulose, lignin, or lipids is considered much faster and not to be the rate-limiting step in anaerobic digestion.

The size of particles also plays an important role in determining the hydrolysis rate. Studies in anaerobic sludge digestion indicate that

materials larger than supracolloidal size (100μm) are essentially not degraded while the materials smaller than the supracolloidal size are effectively degraded (Levine *et al.*, 1985). It is explained that the greater surface resulting from a smaller particle size is essential in accelerating the exoenzymatic hydrolysis. Assuming that the majority of materials in sewage sludge is larger than supracolloidal size, hydrolysis can become the limiting step.

Wood Scheme of Pyruvate Fermentation

Pyruvate is the key intermediate product of the three primary polymers discussed above. Under aerobic conditions, pyruvate enters the TCA cycle and ends at H_2O and CO_2. Under anaerobic conditions, pyruvate may undergo conversion via other metabolic pathways to various volatile acids. The general pattern of pyruvate fermentation have been presented by Wood (1961). Figure 6 shows Wood scheme for pyruvate fermentation, which was modified by Bryant (1979). Under Wood scheme, pyruvate can undergo three pathways via: (1) acetyl-CoA, (2) lactate and oxaloacetate, and (3) acetaldehyde and acetolactate. The last pathway (alcohol fermentation), which is more important in the wine industry, will not be further discussed in this review. The first two pathways are important to this study and are detailed below.

In the acetyl-CoA pathway, along with acetate, formate and H_2/CO_2 are also produced, and can be readily used by methanogens. The acetyl-CoA then ends as acetate, ethanol, and butyrate via acetoacetate. The

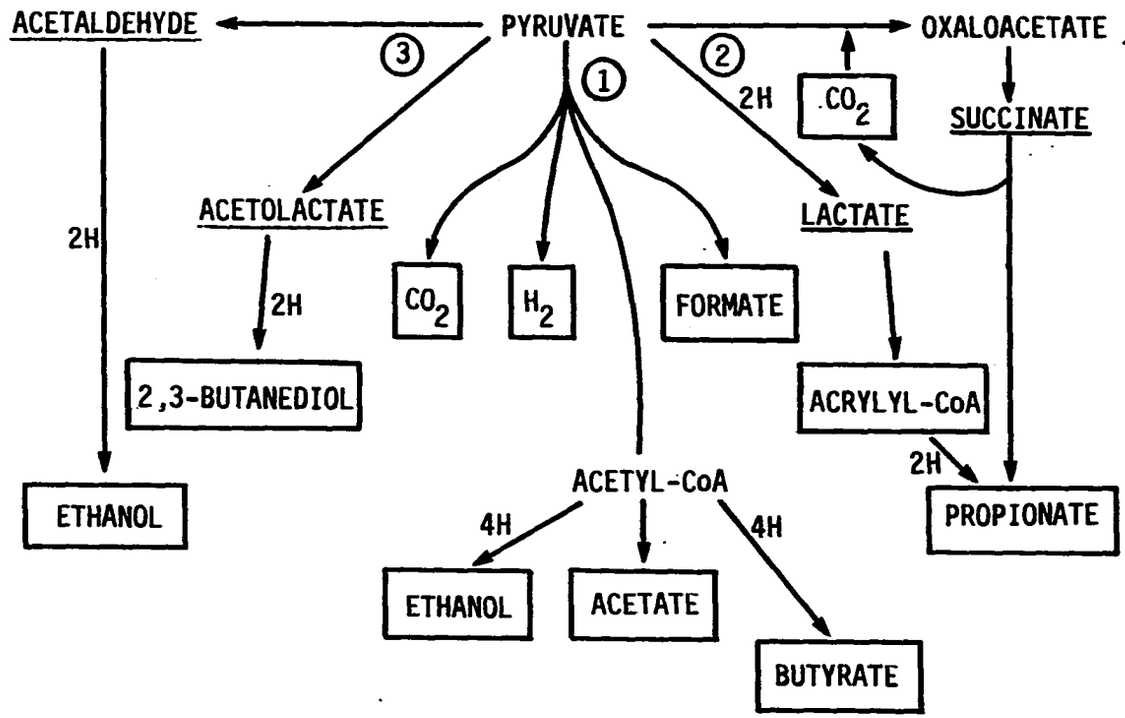

FIGURE 6. Wood scheme of pyruvate fermentation (Wood, 1961)

acetyl-CoA pathway, which generates formate, H_2/CO_2, and acetate for methanogenesis is of most importance in the anaerobic treatment of wastes.

On the other hand, the pathway of lactate and oxaloacetate ends at propionate via either acrylyl-CoA or succinate. It has been found that cattle wastes contain a relatively high amount of lactate (6-7 % of the dry matter); thus it may be an important substrate as well as an intermediate (Bryant, 1979). Succinate is also an important extracellular intermediate for some fermentative bacteria and is subsequently decarboxylated to propionate by syntrophic bacteria (Scheifinger and Wolin, 1973).

Probably the most important implication of the Wood scheme is that it suggests a central role of H_2 in controlling the proportions of the various products produced by fermentative bacteria. Bryant (1979) is probably one of the pioneering researchers who recognized this fact. Under normal operating conditions, nicotinamide adenine dinucleotide (NAD^+) is generated with the production of H_2 as follows:

$$NADH + H^+ \leftrightarrow H_2 + NAD^+ \qquad (6)$$

NAD^+ serves as the electron carrier and is essential for the entire process to proceed. The H_2 produced is directly used by methanogens and/or sulfate reducers.

Under overloaded conditions or conditions that do not favor H_2 utilizers, H_2 builds up and retards the NAD^+ regeneration via the H_2 production, as shown above. Instead, the regeneration of NAD^+ tends to shift to reactions which do not produce H_2, such as:

$$4NADH + Acetyl\text{-}CoA \leftrightarrow Butyrate^- + NAD^+ \quad (7)$$

$$2NADH + Acrylyl\text{-}CoA \leftrightarrow Propionate^- + NAD^+ \quad (8)$$

The result of this shifting is to increase the catabolism of pyruvate to other products, especially propionate, rather than acetate, CO_2, or H_2, as shown in Figure 6. Butyrate, valerate, and caproate may also increase and, in more extreme cases, ethanol and lactate may increase significantly.

Characteristics of Syntrophic Bacteria

Degradation of volatile acids is performed by a group of syntrophic bacteria, especially the acetogenic bacteria. This group of bacteria have very recently been studied (McInerney *et al.*, 1979; McInerney and Bryant, 1981). Depending on whether or not H_2 is produced, acetogenic bacteria can be grouped into two categories: homoacetogens and H_2-producing acetogens. H_2-producing acetogens that utilize low-carbon fatty acids such as propionate and butyrate are most important in this study. All of the H_2-producing acetogens studied so far can not grow alone and require an obligate coculture with H_2 utilizers such as

methanogens and/or sulfate reducers. The obligate association is unique and is explained in the following:

$$\text{Propionate}^- + 3H_2O \leftrightarrow \text{Acetate}^- + HCO_3^- + H^+ + 3H_2 \qquad (9)$$

$$\Delta G^o = +76.1 \text{ kJ/rxn}$$

$$\text{Butyrate}^- + 2H_2O \leftrightarrow 2\text{Acetate}^- + H^+ + 2H_2 \qquad (10)$$

$$\Delta G^o = +48.1 \text{ kJ/rxn}$$

$$4H_2 + HCO_3^- + H^+ \leftrightarrow CH_4 + 3H_2O \qquad (11)$$

$$\Delta G^o = -135.6 \text{ kJ/rxn}$$

Propionate and butyrate acetogenesis are not thermodynamically possible unless they are coupled with H_2/CO_2 methanogenesis as follows:

$$4\text{Propionate}^- + 3H_2O \leftrightarrow 4\text{Acetate}^- + HCO_3^- + H^+ + 3CH_4 \qquad (12)$$

$$\Delta G^o = -102.1 \text{ kJ/rxn}$$

$$2\text{Butyrate}^- + HCO_3^- + H_2O \leftrightarrow 4\text{Acetate}^- + H^+ + CH_4 \qquad (13)$$

$$\Delta G^o = -39.3 \text{ kJ/rxn}$$

Brand and Markovetz (1984) have estimated that the maximum H_2 partial pressures (pH_2) for the reactions to proceed are 1.25×10^{-4} atm for propionate acetogenesis and 1.9×10^{-3} atm for butyrate acetogenesis, assuming pH = 7, 40 °C, 1 atm, and [Acetate$^-$] = [Propionate$^-$] = [Butyrate$^-$]. This indicates that propionate acetogenesis is more sensitive to H_2 buildup than butyrate acetogenesis. Under normal

operating conditions, pH_2 is about 1-20 x 10^{-5} atm, depending on the loading conditions (McCarty and Smith, 1986). This is below the level that would result in the inhibition of propionate acetogenesis. Barnes *et al.* (1983), studying the anaerobic fluidized-bed process, reported that H_2 partial pressure could reach up to 10^{-3} atm under shock loading conditions. Under these conditions, volatile acids can build up to a very significant amount. The consequence of the increased volatile acids, as occurs in digester failure, is to drop the pH, which can further stress the methanogens.

Another group of syntrophic bacteria do not produce H_2. The group of bacteria found so far can use a wide variety of substrates including single-carbon compounds such as methanol, formate, carbon monoxide (Kerby *et al.*, 1983); and methoxylated aromatic acids (Bache and Pfennig, 1981). Homoacetogens can use H_2 and CO_2 to form acetate. The importance of the reaction is not well understood, but likely playing the role of regulating H_2 partial pressure in the system (Zeikus, 1985). In general, this group of bacteria require different conditions for optimal growth than do the methanogens.

Kerby *et al.* (1983) have proposed a single-carbon catabolism model for acetogenic bacteria that synthesize acetate or butyrate (Figure 7). The model suggests that acetyl-CoA is the direct precursor of acetate and butyrate. This scheme also predicts that two distinct formyl-level intermediates ([HCOOH] and [CO]) are linked by formate, CO_2, and a carboxyl intermediate of [CO_2].

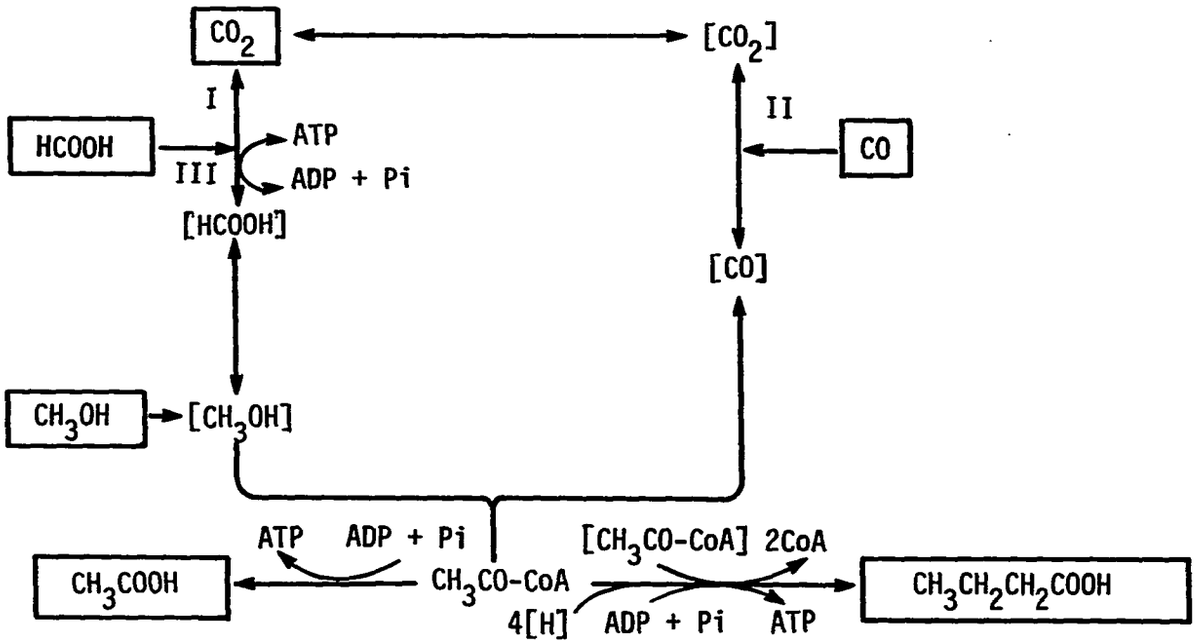

FIGURE 7. Single-carbon catabolism model for acetogenic bacteria that synthesize acetate or butyrate, showing acetyl-CoA is the direct precursor; I:formate dehydrogenase, II:CO dehydrogenase and III:formyl-THF synthetase (Kerby *et al.*, 1983)

Nutrition of Methanogens

The role of methanogens in the biosphere nutritional cycle was not clear until the pioneering works of Sohngen (1906) and Barker (1936). Today, we know that methanogens obtain their energy and carbon from only a few simple molecules, therefore primarily playing the role of degraders at the very bottom of the biosphere nutritional cycle.

Energy and Carbon Sources Methanogens found so far can only use two types of substrates for their energy source. These substrates are either proton-bearing or methyl-bearing. The proton-bearing substrates include H_2/CO_2 and formate (HCOOH), and the methyl-bearing substrates include acetate (CH_3COOH), methanol (CH_3OH), and methylamines (CH_3NH_2, $(CH_3)_2NH$, and $(CH_3)_3N$). Methanogens, which use the same type of substrates, are proven to be more phylogeny-related (Balch *et al.*, 1979). Growth on CO is possible but slight, despite the high free energy of CO (Daniels *et al.*, 1977). Table 2 shows these methanogenic reactions and their free energy.

Virtually, all the methanogens studied so far can use H_2/CO_2 as the single energy and carbon source, except for six species. These species are *Methanosarcina* strain TM-1 (Zinder and Mah, 1979), *Methanothrix soehngenii* (Huser *et al.*, 1982), *Methanolobus tindarius* (Konig and Stetter, 1982), a coccus from human feces (Miller and Wolin, 1983a), *Methanococcoides methylutens* strain TMA-10 (Sowers and Ferry, 1983), and *Mc.*[1] *acetivorans* (Sowers *et al.*, 1984). It is interesting to note that

---

[1]To avoid confusion, the abbreviation scheme for genus names

TABLE 2. Reactions[a] used by methanogenic bacteria (Daniels et al., 1984b)

Reaction	ΔG^o (kJ/rxn)	ΔG^o (kJ/CH_4)
$4H_2 + CO_2 \rightarrow CH_4 + 2H_2O$	-138.8	-138.8
$4HCOOH \rightarrow 3CO_2 + CH_4 + 2H_2O$	-119.5	-119.5
$4CH_3OH \rightarrow 3CH_4 + CO_2 + 2H_2O$	-310.5	-103.5
$4CH_3NH_3^+ + 2H_2O \rightarrow 3CH_4 + CO_2 + 4NH_4^+$	-225.7	- 75.2
$4CO + 2H_2O \rightarrow CH_4 + 3CO_2$	-185.6	-185.6
$CH_3COOH \rightarrow CH_4 + CO_2$	- 27.6	- 27.6

[a] ΔG^o at 25 °C, 1 atm, and pH 7 in water.

some of them do use H_2 as their energy source but require a carbon source other than CO_2 such as methanol (Appendix A).

Formate can also serve as the energy source for most methanogens capable of using H_2/CO_2. However, formate is not used by methyl-bearing substrate utilizers. A study has shown that formate, as a carbon source, requires an obligatory splitting to H_2/CO_2 for methanogenesis (Hungate *et al.*, 1970). This may explain the phylogenic similarity between these two groups of methanogens.

Besides H_2/CO_2 and formate, methyl-bearing substrates can also serve as the energy and carbon source for some methanogens, particularly the isolates from anaerobic digesters. *Methanosarcina* and *Methanothrix* species are the two groups of methanogens best known as methyl-bearing substrate utilizers.

Some methanogens, especially the *Ms.* species, have been characterized as mixotrophic--being capable of obtaining energy from both proton-bearing substrates (autotrophic) and methyl-bearing substrates (heterotrophic). The best example is *Ms. barkeri*. When grown on acetate alone, the *Ms.* species generates 80 % of the methane produced from acetate. However, when grown on acetate in conjunction with H_2/CO_2 and methanol, the methane percentage from acetate is inhibited to 42 % and 5 %, respectively (Weimer and Zeikus, 1977).

---

proposed by Daniels *et al.* (1984b) are adopted in this paper as follows: *Methanobacterium (Mb.), Methanobrevibacterium (Mbr.), Methanogenium (Mg.), Methanospirillum (Msp.), Methanosarcina (Ms.), Methanococcus (Mc.), Methanothrix (Mtx.), Methanoplanus (Mpl.), Methanothermus (Mt.), Methanolobus (Ml.), Methanoccoides (Mcc.), Methanomicrobium (Mm.).*

Baresi *et al.* (1978) further pointed out that the inhibition depends on the culture age grown on acetate. Their data show that 9-day cultures are inhibited 100% after a 168-hour exposure, while 1-day cultures can recover from 100% inhibition after a 24-hour exposure to only 37% inhibition when the exposure time is prolonged to 168 hours. More interestingly, their data also showed that the inhibition can be reduced by diluting the cultures. This might suggest that the SMAR system, which has a very long sludge age and highly concentrated biomass in the system, is more likely to be upset by an increase in hydrogen partial pressure.

Methanogens which use methyl-bearing substrates are considered to be much slower growing than the proton-bearing substrate utilizers, probably due to a thermodynamic preference (Table 2). However, preference over a specific energy source may not only relate to its thermodynamic preference but also relates to enzyme specificity and the activated enzyme levels existing (Zeikus, 1985; Daniels *et al.* 1984b).

Nitrogen and Sulfur Sources Methanogens, like other bacteria, require nitrogen for biosynthesis. Speece and McCarty (1962) suggested a chemical formula, $C_5H_9NO_3$, for anaerobic growth on sewage sludge. This formula show a lower nitrogen percentage than $C_5H_7NO_2$ for activated sludge suggested by Hoover and Porges (1952).

It is well known that all methanogens can obtain their nitrogen source from NH_4^+. Recent studies demonstrate that *Methanosarcina barkeri* strain 227 and *Methanococcus thermolithotrophicus*, in addition, can fix N_2 as the sole nitrogen source (Belay *et al.*, 1985). However,

experimental data show that methanogens grown on $H_2/CO_2/N_2$ yield fewer cells than those grown on $H_2/CO_2/NH^{+4}$ by about 2/3. This suggests an energy demand for using the N_2 fixation pathway. *Methanococcus thermolithotrophicus* can also grow well on NO_3^- as the sole nitrogen source.

Sulfur-containing compounds, such as Na_2S and cysteine, have been used as sulfur sources and oxygen reductants in media preparation for anaerobic growth. Stetter and Gaag (1983) have shown that a variety of methanogens from volcanic sources have the ability to use molecular sulfur as the electron acceptor (with the H_2 as the electron donor) to form H_2S in the dissimilatory sulfur reduction, especially for the thermophile *Methanococcus thermolithotrophicus*. They also found that competition between sulfur reduction and methanogenesis exists as a composite result of energy preference and H_2S toxicity.

Daniels *et al.* (1986) demonstrated that, in the preparation of culturing media, sulfide leads to full reduction; thiosulfate, elemental sulfur, and sulfite result in partial reduction; and sulfate does not reduce the medium at all. Traditionally, sulfide in the form of Na_2S is used as the sulfur source in methanogenic studies. Viewing the problems associated with $S^=$ depletion and H_2S odor, they suggested a substitution of elemental sulfur, sulfate, sulfite, or thiosulfate as the sulfur source. It was also pointed out that preference and concentration requirements vary for different species of methanogens.

Taxonomy of Methanogens

Barker (1956) proposed the first classification of methanogens and suggested that they be placed in one family, the *Methanobacteriacea*. His suggestion was reflected in the 1974's edition of Bergey's Manual of Determinative Bacteriology (1974). The classification is based on the physiological and morphological characteristics of methanogens.

Fox *et al.* (1977) found that the 16S rRNA[2] of methanogens is distinct from microbes in Eubacteria (Prokaryotes) and Eukaryotes, and proposed a new kingdom of "Archaebacteria". The name reflects an untested conjecture about their revolutionary status. Archaebacteria, in many aspects, are very different from the other two kingdoms. Among the most prominent features, the Archaebacteria lack muramic acid in their cell walls and contain ether-linked branched isoprenoid chains in membrane lipids.

Based on the 16S rRNA sequence homologies, Balch *et al.* (1979) proposed a now widely accepted taxonomic scheme for methanogens. The scheme consists of three orders: *Methanobacteriales*, *Methanococcales*, and *Methanomicrobiales*. The new taxonomy reflects the consistency of the hierarchy with other classical characteristics including morphology, Gram stain, DNA base composition (mole % of guanine and cytosine), cell wall structure, cell membrane, and nutritional features for the methanogens considered at that time.

---

[2]S Stands for the Svedberg unit, a measurement of the rate of sedimentation in an ultracentrifuge and hence an indirect measure of molecular size; 16S is about 1500 nucleotide long.

Based on Balch's taxonomy, Chiang (1985) has additionally tabulated some recent isolates of methanogens with 3 order, 6 families, 12 genera, 31 species, and 45 strains. This is shown in Appendix A. The history of the species, DNA base composition, energy source, maximum specific growth rate, and optimal growth conditions (pH, temperature, and NaCl) are also tabulated. Several important features can be observed in the Table as discussed below.

The DNA base composition (G+C %) has been used to characterize many bacterial species. If two organisms have very different base ratios, they are obviously not closely related. As shown in Appendix A, base composition within genera shows a relatively narrow range for the three Orders. Order III on average has the highest percentage of G+C among the three Orders. *Methanobacterium* species show the largest variation in G+C percentage. *Mb. wolfei*, a tungsten-requiring thermophile isolated from sewage digesters, shows an exceptionally high G+C%. A survey to find if methanogens from the same type of habitats have closer G+C values does not suggest any correlation. Chemical structure, rather than the G+C composition of DNA, is a more important factor in determining proper enzyme functions in a specific habitat.

As to optimal growth conditions, most methanogens can best grow at neutral pH, 30-40^{o} C, and 1-2% NaCl. Exceptions are often habitat-related. For example, the two unnamed *Mb.* species (strain Kuznetsov and strain Omeliansky), isolates from deep oil fields, require more than 14% NaCl for optimal growth. Seven species are labeled as thermophiles which

grow best at temperatures higher than 55° C. They are *Mb. thermoautotrophicum* strain ΔH, *Mb. wolfei* strain W, *Mt. fervidus* strain V24S, *Mc. thermolithotrophicus* strain SN1, *Mc. jannaschii* strain JAL-1, *Mg. thermophilicum*, and *Mg. frittony* strain FR4. It is interesting to note that none of the above thermophiles uses acetate as the major energy source. This might suggest that the faster digestibility in thermophilic digesters is due to enhancement of these faster growing H_2/CO_2 methanogens.

Methanococcoides, *Methanosarcina*, *Methanothrix*, and *Methanolobus* of Order III represent the only groups found so far capable of using methyl-bearing substrates as the major energy source. However, *Methanococcoides*, an isolate from deep sea, and *Methanolobus*, an isolate from marsh ponds, do not use acetate as the energy source. *Methanothrix*, an isolate from sewage digesters, uses only acetate as the energy source. *Methanosarcina* represents the highest mixotrophic nature, capable of using both proton- and methyl-bearing substrates as the energy sources. For this reason, the optimum growth conditions for *Methanosarcina* are difficult to define.

As shown in Appendix A, all the groups capable of using methyl-bearing substrates have slower maximum growth rates than do the proton utilizers. This might be ascribed to lower free energy in methyl-bearing substrates. However, this does not imply that the methyl utilizers have less efficient growth. This will be discussed in more detail below.

Continuous Culture Theory

Continuous culture theory relates to the continuity of energy flow occurring in a metabolic process. It is a theory of energy conservation in biological systems, i.e., bacterial cells in this study. The major questions in continuous culture theory are three:

(1) What are the mechanisms involved in the energy conservation process, such as ATP formation, electron transport system?

(2) What is the energy capture efficiency of bacteria cells, such as the cell growth yield? and

(3) What is the electron (energy) transport rate, such as the kinetics of cell growth rates.

Classical thermodynamics has been used for years to study the energetics of anaerobic systems (McCarty, 1969; Thauer *et al.*, 1977). However, there are several limitations in applying thermodynamics to bacterial systems. First, bacterial cells are open systems while classical thermodynamics deals with closed systems. Therefore, a more defined cell boundary is necessary. Second, the energy flow in a cell is highly dependent on a specific pathway that is regulated by enzymes, while classical thermodynamics deals with only the energy flow disregarding the pathway. And third, classical thermodynamics deals with only steady-state conditions disregarding kinetics.

Electron and Carbon Transport in Methanogens In the following, major electron and carbon transfer reactions for methanogens are discussed. For a more detailed discussion, the paper by Daniels *et al.*

(1984b) is suggested. How the methanogens obtain their energy for cell synthesis and methanogenesis has been of great interest. More knowledge in this area remains to be documented.

Figure 8 shows a now widely accepted electron transport model for methanogens. The model proposes a central electron pool of F_{420}, a 8-hydroxy 5-deazaflavin cofactor, accepting electrons from energy sources. F_{420} has been found in all methanogens isolated so far with a level of approximately 1.1-4.7 nmol/mg protein. One group of non-methanogenic bacteria, *Streptomyces* species, also contains F_{420} but at a much lower level. Like other deazaflavins, F_{420} is chemically restricted to 2-electron transfers. It is not clear if F_{420} is bound to proteins in cells or freely diffuses.

As shown in Figure 8, various electron-transfer enzymes are required to liberate electrons from energy sources. These include hydrogenase, formate dehydrogenase, and CO dehydrogenase. These enzymes can reduce F_{420} to provide reducing power for cell synthesis and methanogenesis.

NADP, rather than NAD, is specifically reduced by F_{420} to form NADPH using the NADP-F_{420} oxidoreductase. The enzyme catalyzes the reduction of NADP optimally at a pH of about 8, and in the opposite direction at a pH of about 5. The enzyme is estimated to be about 0.09% of the protein in the cell. Zinc is associated with the enzyme.

As to methanogenesis, CoM serves as a carbon transfer cofactor in the last step of methanogenesis. The methyl CoM reductase is used to catalyze the reaction. The reductase is the most abundant enzyme found

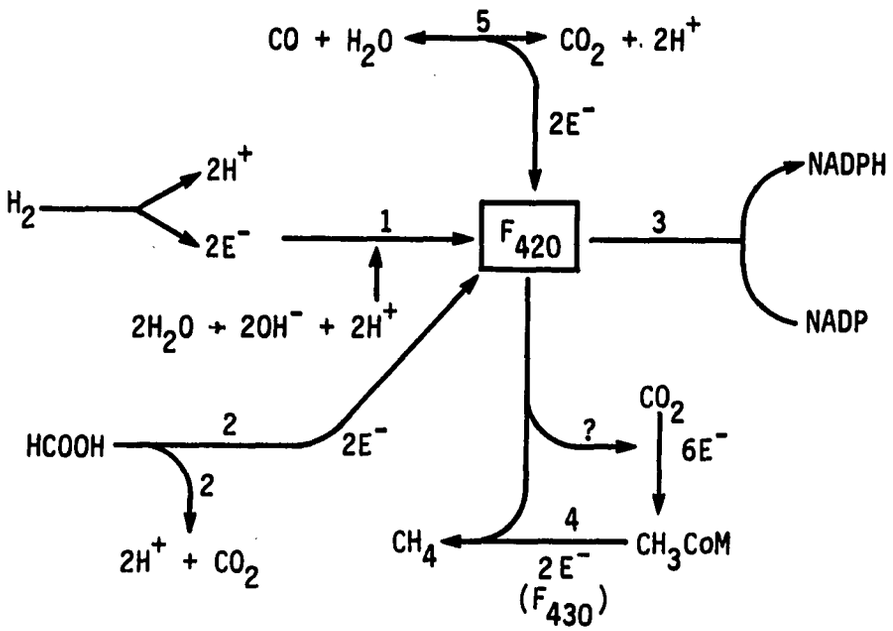

FIGURE 8. Major electron transfer reactions for methanogens (1) Hydrogenase (2) Formate dehydrogenase (3) NADP-F_{420} oxidoreductase (4) Methyl CoM reductase (5) CO dehydrogenase (Daniels et al., 1984b)

so far in methanogens, at a level of 3-12% of the cell protein. The catalysis requires Mg:ATP for activity. The activity is fully inhibited by several compounds including chloroform, azide, and nitromethane, but not by CO, cyanide, nitroxide, or dithionite. CO_2 can act as a positive effector. However, Hansson and Molin (1981) has reported that CO_2 partial pressure can strongly retard propionate acetogenesis. The retardation can be up to 70% at a pCO_2 of 1 bar (0.99 atm).

In the methanogenesis from methyl-bearing substrates (methanol, acetate, and methylamines), splitting of CH_3^- requires an intermediate complex of B_{12} corrinoids. The assimilation of cell carbon in methanogens is virtually through a reverse TCA cycle.

Figure 9 shows a now widely accepted ATP generation model for methanogens. According to the chemiosmotic theory, ATP is generated by a protonmotive force (E_p) across the cell membrane as follows:

$$E_p = E_p^o - 2.3(RT/F)(\Delta pH) \qquad (14)$$

$$E_p = E_p^o - 61(\Delta pH) \quad \text{at } T = 35\ ^oC \qquad (15)$$

where, "F" is the Faraday constant, or 96.493 J/mv; "R" is the universal gas constant, or 8.314 J/degree/mole; "T" is the temperature in Kelvin; ΔpH is the pH difference between inside and outside of the cell; and "E_p^o" is the potential inside the membrane at standard conditions in mv.

Currently, there are three different perceptions concerning the extrusion that protons in methanogens carry out electron transport

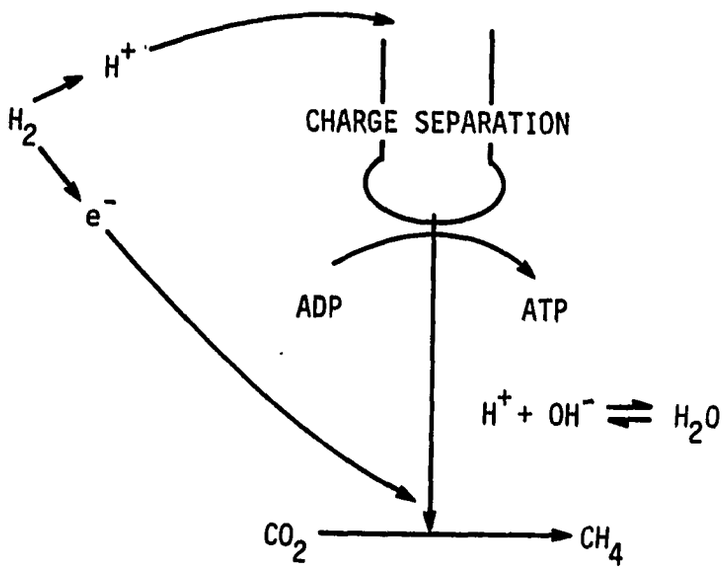

FIGURE 9. Chemiosmotic generation of ATP for methanogens (Daniels et al., 1984b)

according to the Mitchell hypothesis. The traditional view suggests a clearcut separation of protons outside the membrane so that all the protons are readily exchangeable with bulk water. The more recent views are that the protons are either associated on or in the membrane, and are not readily exchangeable to the bulk water.

It was not possible to prove the chemiosmotic theory until E_p^o can be experimentally determined. The E_p^o was determined to be 120-140 mv in *Mb. thermoautotrophicum* (inside alkaline and negative). The theory is also supported by a recent finding that, in H_2/CO_2 methanogenesis, the 'H' on the produced methane arises from the protons in water, not from the H_2 substrate as previously thought.

Energetics and Bacterial Growth In a well defined system, the relationship of bacterial growth (dX/Xdt) and substrate utilization (dS/Xdt) can be described as follows:

$$\frac{dX}{Xdt} = Y_m \frac{dS}{Xdt} - k_d \qquad (16)$$

where, "S" and "X" are the concentrations of substrate and biomass, respectively, in mg/L; "Y_m" is the true yield coefficient in mg biomass produced per mg substrate utilized; and "k_d" is the first order decay rate constant in 1/day. The decay may occur through death, lysis, endogenous metabolism, predation, as well as energy utilization for maintenance (such as respiration). The k_d typically ranges from 0.01-0.05 1/day in mixed culture. The true yield (Y_m) is different from the net yield (Y) as follows:

$$Y = Y_m/(1+k_d\theta_c) \quad (17)$$

Equation (16) states the law of continuity in the bacterial system and can be expressed in a more general form as follows:

$$\mu = Y_m k - k_d \quad (18)$$

where, "μ" is the specific growth rate in mg biomass produced/mg biomass in the system/day, and "k" is the specific substrate utilization rate, in mg substrate utilized/mg biomass in the system/day. For a completely mixed system, the above equation can be related to solids retention time (SRT, θ_c) or mean cell residence time (MCRT) as follows:

$$1/\theta_c = Y_m k - k_d \quad (19)$$

The above equation can be used for a system with or without biomass recycling.

In anaerobic systems, volatile solids (VS) or volatile suspended solids (VSS) are often used as measures of biomass, and chemical oxygen demand (COD) as the measure of substrate. This should be cautiously interepreted, since not all the VS or VSS are viable and not all the COD is biodegradable. Biomass can also be estimated by turbidity with a spectrophotometer at a wavelength that gives a maximum reading, as often used by microbiologists in pure culture studies. A correlation between biomass concentration and turbidity reading can then be used.

Lawrence and McCarty (1969) estimate biomass by measuring the nitrogen content (mg) of VSS and multiplying the nitrogen content with a conversion factor of 11.4 mg VSS/mg cell nitrogen obtained by Speece and McCarty (1962). This may greatly increase the accuracy of biomass estimation since the nitrogen content can be determined with better precision. However, none of the methods discussed above can differentiate between viable biomass and dead biomass.

Equation (18) has been modified to include biomass activity as follows:

Young (1968)

$$\mu = eY_m k - k_d \qquad (20)$$

Grady and Lim (1980)

$$\mu = Y_m k - \gamma - b \qquad (21)$$

In Young's expression, "e" is the active fraction (about 0.8) of biomass. In Grady and Lim's model, biomass is separated into viable and dead cells. The purpose of the separation is that viable cells may undergo death (γ) and decay (b) while the dead cells only undergo decay. The separation is desired when a precise analysis is needed. However, this may complicate data analysis.

To obtain Y_m and k_d, Equation (19) is often directly used by plotting "$1/\theta_c$" against "k". In a completely mixed system at steady state without biomass recycling, $1/\theta_c$ and k can be determined as follows:

$$1/\theta_c = 1/\tau \tag{22}$$

$$k = (S - S_o)/(X\tau) \tag{23}$$

where, "S" and "S_o" are the substrate concentration in the reactor and influent concentration, in mg/L respectively; and "τ" is the hydraulic detention time in day. The direct plot of using Equation (19) has been criticized as being insensitive to system parameters (Y_m and K_d) due to the reciprocal of τ. Instead, the Jordon plot (Grady and Lim, 1980) is preferred:

Jordon plot

$$(S_o-S)/X = (k_d/Y_m)\tau + 1/Y_m \tag{24}$$

The above equation can be derived by substituting Equations (22) and (23) into Equation (19). By plotting $(S_o-S)/X$ against τ, Equation (24) gives a slope of k_d/Y_m and y intercept of $1/Y_m$.

Growth yield coefficients (Y_m or Y) of some selected fermentative and methanogenic reactions for both pure and mixed cultures are listed in Appendix B. In most pure culture studies, the optical (turbidity) method is used as a direct measure of biomass. This would give the Y (net yield) measurement with no k_d determination. For those listed with k_d, the yield is the Y_m (total yield) and either Equation (19) or (24) was used.

The yield is expressed as gram biomass produced/electron equivalent of substrate utilized. The use of electron equivalent for energy substrates provides a wider basis than does COD of substrate (McCarty, 1969). Substrate expressed in electron equivalents can be converted to COD using an equivalent of 1/8 g COD per electron equivalent (e). In order to justify the energy capture efficiency by bacteria, the ratio of $Y_m/\Delta G^o$ is calculated. The ratio estimates the gram of biomass produced per kcal of free energy of substrate utilized. A higher $Y_m/\Delta G^o$ ratio indicates a better energy capture efficiency by the cell.

As shown in Appendix B, growth yield varies over a wide range from 3.68 to 0.14 g/e, depending upon the type of reactions and the type of bacteria. In general, the yield and $Y_m/\Delta G^o$ for pure cultures are in close agreement with those for mixed cultures as shown for H_2/CO_2 and acetate methanogenesis.

In the group III reaction of homoacetogenesis, homopropionogenesis, and homobutyrogenesis, insufficient data were available to make a general conclusion. This group of bacteria do not produce H_2 and can be cultured without a syntrophic association with the H_2 utilizers. Mixed culture studies of this group might not be feasible unless their biomass can be differentiated from the total biomass. Comparisons between *A. woodii* and *P. modestum* suggest that energy capture efficiency is greater for reactions with less free energy. The two listed values of $Y_m/\Delta G^o$ are among the higher values in Appendix A, suggesting that this group of bacteria can grow well and are not likely to be the limiting species in anaerobic digestion.

In the group of methanogens, reactions with greater ΔG^o, in general, give greater yield but less energy capture efficiency. Organic supplements can greatly increase the yield as shown in acetate methanogenesis by *Ms. barkeri*. It is noted that *Ms. barkeri*, which is the predominant species in anaerobic digestion of organic wastes, yields twice more on H_2/CO_2 than on acetate. Also, the yield differs remarkably for different species that use the same reaction. It appears that *Mtx. soehngenii*, which uses only acetate, has a less efficient growth. On the average, acetate utilizers yield about 0.2-0.4 g/e with a capture efficiency of 0.2-0.4 g/kcal.

Kinetics and Growth Rate The Monod (1949) equation is often used to describe bacterial growth kinetics as follows:

$$\mu = \mu_m \, S/(K_s+S) \qquad (25)$$

where, "μ_m" is the maximum specific growth rate in mg biomass produced/mg biomass/d; and "K_s" is the half-saturation constant, in mg substrate/L.

Another expression often used to describe bacterial kinetics is the Michaelis-Menten equation:

$$k = k_m \, S/(K_s+S) \qquad (26)$$

The Michaelis-Menten equation is similar to the Monod equation, but expresses the bacterial kinetics in terms of substrate utilization. The

"K_s" has been characterized as the "required driving force" to achieve 1/2 of the maximum specific growth rate (μ_m) or specific utilization rate (k_m). Factors such as the nature of cell membranes, biomass concentration, and mixing intensity all can greatly affect K_s.

Contois (1959) noticed that, in addition to substrate concentration (S), the biomass concentration (X) is also a function of the specific growth rate (μ). He further proposed a kinetic model as follows:

$$\mu = \mu_m S/(BX+S) \qquad (27)$$

where, "B" presents a growth parameter that is constant under defined conditions. The Contois equation has the same mathematical form as the Monod equation with a hyperbolic function with respect to "S". The Contois model has been intensively evaluated experimentally using *Aerobactor aerogenes* and proven to have general applicability. However, unlike Monod kinetics, which can be derived from fundamentals of enzymatic reactions, Contois kinetics lacks a theoretical background.

On the other hand, Contois kinetics suggests an important fact that "BX", which is equivalent to "K_s" in Monod kinetics, increases as biomass concentration (X) increases. This agrees with the modified Monod kinetics by Dague and Chiang (1984), which states that "operating K_s (K_s/η)" increases as contact efficiency factor (η) decreases due to a decrease in mixing intensity by an increase in biomass concentration:

$$k = k_m S_b/(K_s/\eta+S_b) \qquad (28)$$

where, S_b refers to the substrate concentration in bulk solution. Equation (28) can be obtained by substituting $S = \eta S_b$ into Equation (26).

To obtain the Monod constants (μ_m and K_s), Equation (25) is often linearized so that linear least-squares optimization can be used. Three forms of linearization are often used (Grady and Lim; 1980):

Lineweaver-Burk Plot

$$\frac{1}{k} = \frac{Y_m K_s}{\mu_m}\left(\frac{1}{S}\right) + \frac{Y_m}{\mu_m} \qquad (29)$$

Hanes plot

$$\frac{S}{1/\tau + k_d} = \frac{S}{\mu_m} + \frac{K_s}{\mu_m} \qquad (30)$$

Hofstee plot

$$\frac{1/\tau + k_d}{S} = \frac{\mu_m}{K_s} - (1/\tau + k_d) \qquad (31)$$

The proper use of the above linearization models is important in obtaining accurate Monod constants. The double reciprocal Lineweaver-Burk plot gives a deceptively good fit, even with unreliable data. This should be avoided in any event. If the line is to be drawn by eye, the Hanes plot is preferred. However, the least-squares technique cannot be used to find the line of best fit because both axes contains a term (i.e., S) which is subject to error. If the least-squares technique is to be used, the Hofstee plot should be used. The use of the reciprocal

of "S" may amplify the error in "S" and make it difficult to get a line by eye (Grady and Lim, 1980).

It should be known that any form of linearization will inevitably cause error in the estimation of Monod constants (Cornish-Bowden and Eisenthal, 1974). Kouadio (1984) has developed a very rigorous mathematical model to estimate the two Monod constants (μ_m, K_s), yield (Y_m), and decay (k_d) coefficients, using a maximum likelihood optimization technique. The results of his study indicate that any linear least-squares methods tend to overestimate μ_m and K_s, sometimes even up to 60%, and slightly underestimate k_d and Y_m. Kouadio also suggested that if the linear least-squares method has to be used, the Jorden (Equation 24) and Hanes (Equation 30) plots should be used.

Appendix B also shows K_s and μ_m data for some selected fermentative and methanogenic reactions. For those studies with no K_s listed, μ_m is calculated either from the slope of the exponential growth phase or from the regeneration time (t_r) as follows:

$$\mu_m = \ln 2/t_r \qquad (32)$$

The above equation can be derived with a zero-order growth assumption. Also, as listed in Appendix B, the ratio of μ_m/Y_m gives the electron transport rate (e/g biomass/d). This is equivalent to the expression for the maximum specific utilization rate (k_m).

In general, μ_m ranges from 0.2 to 1.2 1/d and electron transport rates from 0.2 to 3.0 e/g/d. As expected, methanogens that use H_2/CO_2 transport electrons at a rate about five times faster than those using acetate. Data from Finney and Evans (1975) show a exceptionally high transport rate among acetate utilizers. The data were obtained under vacuum conditions (13.2% atm). Based on this, they suggested that the CO_2 detachment rate from the biomass is the overall limiting step, which can be accelerated under vacuum conditions.

The K_s shown in Appendix B is in least agreement among all studies. This is probably due to the difference in mixing intensity, operating biomass concentrations, and mathematical handling techniques among different studies. The K_s varies remarkably with different substrates and temperatures used. For example, simple compounds such as acetate give lower values than do complex compounds such as lipids. Lower temperatures tend to give higher K_s values, indicating a higher required driving force at lower temperatures.

System Controls and Monitoring

Solids Retention Time The concept of solids retention time (SRT) has been used as an unified control parameter in design and operation of biological processes for years. Under steady-state conditions, the SRT of a system can be defined as follows:

$$\text{SRT (day)} = \frac{\text{Total biomass in the system}}{\text{Biomass daily wasting rate}} \qquad (33)$$

The above definition is virtually based on hydraulic considerations. However, under steady-state conditions, biomass regeneration rate equals biomass wasting rate; thus SRT can be related to the mean cell residence time (MCRT), which is a biological index, as shown in Equation (19).

An adequate SRT is essential for successful treatment. For anaerobic systems treating sewage sludge at 35° C, Dague *et al.* (1970) observed a minimum SRT of 10 days for efficient treatment and no waste stabilization at 3 days. Parkin *et al.* (1983) studied the effect of four toxicants (nickel, ammonium, sulfide, and formaldehyde) on anaerobic systems. They concluded that the toxicity effect can be greatly reduced by using a sufficiently long SRT. Studies on the dewaterability of digested sludge by Lawler *et al.* (1986) also show that, in addition to solids stabilization, digesters should be designed to obtain a good dewaterability of digested sludge with an adequate SRT.

An adequate SRT can be achieved in several ways. For a completely mixed system without biomass recycling, SRT equals hydraulic retention time (HRT). SRT can be increased to greater than the HRT by recycling biomass after separation to increase the total biomass in the system. The concept brought up the development of "anaerobic activated sludge" (Dague *et al.*, 1966).

With the development of many modern high-rate anaerobic processes, a very long SRT can be achieved within a relatively short HRT. Young and McCarty (1969) reported an SRT of over 500 days for an anaerobic filter treating dilute organic wastes at 25° C. The use of the extremely long

SRT makes possible the treatment of the dilute waste at low temperatures. Also, with the extremely long SRT, the system can be operating in the endogenous phase with low net solids production, as shown in Equation (17).

However, there are several limitations to applying the SRT concept to modern high-rate anaerobic processes. Such processes are characterized by a highly non-uniform distribution of biomass activity in the system. As a result, SRT based on biomass alone can not fully estimate the treatment capability of a system. More importantly, the use of an extremely long SRT in the modern high-rate processes makes the parameter insensitive as a control index as in the conventional and contact anaerobic processes.

Another aspect of using SRT as a design parameter is the scale-up problem. By directly applying the the lab-scale SRT to full-scale systems, it is assumed that the biological similarity is the same as the hydraulic similarity between the lab-scale and full-scale system. Unfortunately, this may not be the case. Many full-scale anaerobic systems are operated under much higher hydrostatic pressures than are the lab-scale systems, such as 40 ft (12 m) vs. 0.5 ft (0.15 m). Morgan (1954) and Torpey (1955), in studying the anaerobic treatment of sewage sludge, noticed that lab-scale digesters can successfully operate at loading rates at least three times those commonly accepted for design of full-scale digesters. The scale-up problem has not been well understood.

pH, Alkalinity, and Volatile Acids One of the most important environmental requirements for anaerobic digestion is a proper pH. Previous studies concluded that anaerobic digestion proceeds well at pH 6.6-7.6 with an optimum range of 6.8-7.2 (McCarty, 1964b). Since most acetogens can grow well under more acidic conditions, the primary consideration of pH is for optimum growth of methanogens (Appendix A). Also, in many cases, the pH consideration is associated with the toxicity of NH_3 and H_2S. The pH effect on the production of these two toxic forms are opposite. High pH is associated with high NH_3 while low pH is associated with high H_2S.

Despite its importance, pH appears to be an insensitive control index and cannot be used for early detection of digester failure (USEPA, 1976). As a digester fails, with a gradual increase in volatile acids, pH might remain relatively constant for a period with the consumption of bicarbonate alkalinity.

The maintenance of an adequate alkalinity in anaerobic systems is important for process control. However, the choice of a suitable titration endpoint for alkalinity determination has been a constant debate. For routine monitoring, Standard Methods (1985) suggests a pH of 4.3 as the titration endpoint while the USEPA Anaerobic Sludge Digestion Manual (1976) uses 4.5. In the method of dual titration (DiLallo and Albertson, 1961), a pH of 4.0 was chosen.

Nevertheless, the importance of a meaningful alkalinity measurement is to provide insight into how much buffering capacity a digestion system

can provide at a desired operating pH. Many volatile acids have pk_A values above 4.5 (for example acetic acid 4.76 and propionic acid 4.85). Consequently, these volatiles, which are not normally considered as buffers in digester operation, will also be included in the alkalinity measurement when endpoints are below 4.5. For this reason, it is necessary to differentiate the useful bicarbonate alkalinity (BAlk) from the the less useful total volatile acids (TVA) alkalinity (McCarty, 1964b):

$$BAlk = TAlk - (0.85)(0.83)(TVA) \qquad (34)$$

where, "BAlk" and "TAlk" are the bicarbonate alkalinity and total alkalinity, respectively, in mg/L as $CaCO_3$; and "TVA" is the total volatile acid determined by the steam-distillation method (Standard Methods, 1985) in mg/L as acetic acid; and "0.83" (50/60) is a factor to convert the acetic acid equivalent of "TVA" to the $CaCO_3$ equivalent of alkalinity. Use of the above equation assumes that only 85% of the TVA (determined by the steam distillation method) is measured in TAlk titration to pH 4.0 (McCarty, 1964b).

Due to the tedious procedure involving the determination of the volatile acids, Jenkins *et al.* (1983) have suggested a "alkalimetric titration method" for estimating BAlk. The method uses a titration endpoint of pH 5.75 as a direct measurement of BAlk. The method assumes that, for normal sewage sludge digesters, 80% of bicarbonate and less than 20% of volatile acids are titrated at pH 5.75.

In considering a sensitive index for digestion process control, USEPA (1976) proposed the use of TVA/TAlk ratio. When digestion starts to fail, the TVA will build up with a possible decrease in TAlk. This will tend to exagerate theT VA/TAlk ratio even in the early stages of process failure. The TVA/Talk ratio between 0.1 to 0.25 (in mg/L as acetic acid per mg/L as calcium carbonate) has been considered to be necessary for successful digester operation. This ratio simply suggests that, in order to neutralize 1 equivalent of volatile acids, 5 to 12 equivalents of alkalinity should be maintained in the system for successful digester operation.

DiLallo and Albertson (1961) have developed a now widely used volatile acids method by direct titration. The sample is first titrated with H_2SO_4 solution to pH 4 for TAlk measurement. The sample is further acidified to a pH of 3.3-3.5 and gently boiled for 3 minutes to remove the CO_2 resulting from the acidification of bicarbonate. After cooling to room temperature, the sample is then back-titrated to pH 7.0 with NaOH solution to determine the TVA. With the dual titration method, the TVA/TAlk ratio can be obtained in 30 minutes. However, this method has been criticized because inconsistent boiling leads to the method lack of reproducibility.

Ripley *et al.* (1986), recognizing the importance of alkalinity between pH 4.3 and 5.75, suggest the use of a "IA/PA" ratio. The IA stands for the intermediate alkalinity which is equivalent to the TVA alkalinity determined between pH 4.3 to 5.75. The PA stands for the

partial alkalinity which is equivalent to the bicarbonate alkalinity with the titration endpoint of pH 5.75, as suggested by Jenkins *et al.* (1983). The IA/PA ratio is considered more sensitive than the TVA/TAlk ratio suggested by USEPA because the buildup of TVA may result in a TAlk increase too. The IA/PA ratio can be obtained with only one titration in a few minutes. In addition, there is no need to boil the sample and standardize the titrant, as required in the dual titration method.

Static-Bed SMAR Process

Applications

Applications of the static-bed SMAR process are primarily for pretreatment of high-strength organic wastes. Pilot-scale studies over the past 20 years have shown that the SMAR process is capable of efficient pretreatment of a wide variety of wastes at high loading rates and at short retention times. The system is also capable of intermittent operation and shock loadings. The net growth yield (Y) is generally very low, i.e., 0.015 g VSS/g COD removed for treating volatile acids and 0.12 for treating protein-carbohydrate wastes (Young and McCarty, 1969), as compared to the conventional and contact processes, i.e., 0.05 for treating volatile acids and 0.24 for treating carbohydrate wastes (McCarty, 1964a). The SMAR process has also proven to be capable of treating wastes containing organic priority pollutants, such as hydroxyl and methoxyl benzenes. In many aspects, the SMAR is an "ideal" process for the pretreatment of organic wastes.

Table 3 lists five categories of complex organic wastes that have been studied using the static-bed SMAR process. This includes food-processing carbohydrate wastes, pharmaceutical wastes, thermal sludge conditioning wastes, dairy wastes, and landfill leachates. Two studies on simple synthetic wastes are also listed for comparison. Total COD (TCOD) removal rate (g/L/d) and theoretical retention time (hours) are based on clean-bed liquid volume. TCOD, instead of soluble COD, is used to include the consideration of solids retention ability of the SMAR process. Clean-bed liquid volume is used so that comparison in TCOD removal rate and hydraulic retention time with different media porosity in different studies can be more meaningful. Unless specified, TCOD removal rates are calculated only for those runs achieving 80% or better TCOD removal efficiencies.

In the category of carbohydrate waste (Table 3), a food-processing waste was treated by Plummer *et al.* (1969). The waste was characterized with a COD of about 8.5 g/L and low solids, an ideal waste for the SMAR process. The SMAR used was packed with a mixture of Raschig rings and berl saddles which resulted in a porosity of about 0.7. The TCOD removal rate was 2.2 g/L/d at a retention time of 83 hrs and temperature of 35° C. The TCOD removal rate is similar to the rate for the more complex flour-processing starch waste treated by Mosey (1978) and the simpler synthetic protein-carbohydrate (nutrient broth and glucose) waste of Young and McCarty (1969). It can be generally concluded that carbohydrate food-processing wastes can be efficiently treated at a TCOD removal rate of 2-3 g/L/d within a retention time of 80-90 hrs.

One vegetable tanning waste, containing high lime solids (20 g TS/L) and COD (16 g/L), was treated at a high COD loading rate of 16.0 g/L/d with a COD removal rate of 13.8 g/L/d (Arora and Chattopadhya, 1980). Doubling the loading rate resulted in almost a doubling of the removal rate, indicating the system was not overloaded. Solids were "captured" in the system at a rate as high as 30 g TS/L/d with a retention time of 12 hours. In spite of the low-porosity media used, no clogging problem was reported. This seems to extend the SMAR application to wastes containing high solids, which were not previously thought treatable with the SMAR process (Young and McCarty, 1969).

For the treatment of pharmaceutical wastes with the SMAR process, two studies are tabulated in Table 3. Both wastes are rich in methanol (95% of total COD) which can be readily used by methanogens. However, they were very different in pH. The waste treated by Jennett and Dennis (1975) was slightly basic and the other was extremely acidic (pH 1.5). Both wastes are short of nitrogen and phosphorus nutrients. Consequently, pH adjustment and nutrient supplements were required for successful treatment. Surprisingly, the reported TCOD removal rates for these two pharmaceutical wastes differed remarkably.

The waste treated by Jennett and Dennis (1975) had a TCOD removal rate of 5-8 g/L/d which is 3-6 times the removal rate for the waste by Sachs *et al.* (1982). The difference is partly due to the different influent COD concentrations, as shown in Table 3. Closer examination reveals that the waste of Sachs *et al.* is high in sulfate (1.4-3.5 g/L).

TABLE 3. Treatability[a] of some selected organic wastes by static-bed SMARs

Wastes	COD_{in} (mg/L)	T_d[b] (hours)	$TCOD_r$[b] (g/L/d)	Temp (°C)	porosity (-)	References
Simple synthetic wastes						
Methanol	2.1	12	3.8	25	0.40	McCarty (1966)
Methanol+Acetate	2.4	12	4.0	25	0.40	
Meth.+Acet.+propionate	2.7	12	4.5	25	0.40	
Meth.+Acet.+Propionate	2.2	6	8.5	25	0.40	
Acet.+propionate	2.2	6	7.4	25	0.40	
Acetate+propionate	6.0	18	7.0	25	0.42	Young & McCarty (1969)
	6.0	36	4.0	25	0.42	
Acetate+Propionate	3.0	36	1.9	25	0.42	
Complex wastes						
Food processing	8.5	83	2.2	35	0.68	Plummer *et al.* (1969)
Flour processing	10.0	96	2.3	35	0.90	Mosey (1978)
	18.0	96	3.7	35	0.90	Mosey (1978)
Nutrient broth+ Glucose	1.5	18	1.9	25	0.42	Young & McCarty (1969)
	3.0	36	1.8	25	0.42	
Vegetable tanning	16.0	144	2.4	22-33	0.42	Arora & Chattopadhya (1980)
	16.0	96	3.6	22-33	0.42	
	16.0	72	4.4	22-33	0.42	
	16.0	48	6.5	22-33	0.42	
	16.0	24	13.8	22-33	0.42	
	16.0	12	28.8	22-33	0.42	

[a]TCOD removal equal to or greater than 80% (unless specified).

[b]Based on clean-bed liquid volume.

[c]TCOD removal less than 80%.

Table 3. (continued)

Wastes	COD_{in} (mg/L)	T_d[b] (hours)	$TCOD_r$[b] (g/L/d)	Temp (°C)	porosity (-)	References
Pharmaceutical	4.0	18	5.1	35	0.44	Jennett & Dennis (1975)
	4.0	12	7.5	35	0.44	
	8.0	24	7.6	35	0.44	
	16.0	48	7.8	35	0.44	
Pharmaceutical	2.0	36	1.3	35	0.43	Sachs *et al.* (1982)
Thermal sludge conditioning	20.1	32	6.9[c]	35	0.90	Dague *et al.* (1980)
	20.1	64	3.8[c]	35	0.90	
Thermal sludge conditioning	6.0	6	16.0[c]	35	0.90	Crawford *et al.* (1980)
	6.0	12	8.9[c]	35	0.90	
Thermal sludge conditioning	9.5	32	3.6[c]	32	0.43	Haug *et al.* (1977)
Dairy	1.0	7	2.3	35	0.96	Backman *et al.* (1986)
	1.0	12	1.5	35	0.96	
	1.0	22	0.9	35	0.96	
	2.7	22	2.1	35	0.96	
	2.7	34	1.5	35	0.96	
	3.2	44	1.4	35	0.96	
	3.2	87	0.8	35	0.96	
Dairy	3.8	24	1.1[c]	23	0.91	Rittmann *et al.* (1982)
	3.8	72	1.2	23	0.91	
Landfill leachate	27.0	8	3.3	25	0.94	DeWalle & Chian (1976)

Although sulfate reduction with H_2 is thermodynamically more favorable than H_2 methanogenesis, a sulfur balance indicates that most of sulfate was reduced to sulfide and precipitated with metals originally existed in the waste. The sulfide precipitates in the biomass, which can greatly reduce biomass activity, may account for the lower treatment performance of the sulfate-rich waste. It is suggested that, with the type of waste, sulfide-metal precipitates be removed first before the SMAR treatment. Also, effluent recycling is used to neutralize the influent pH and dilute any potential toxicants such as sulfate.

In the SMAR treatment of thermal sludge conditioning wastes, three pilot studies are listed in Table 3. The type of waste was characterized as having a high temperature, high COD (6-20 g/L), and low non-volatile solids, an ideal waste for SMAR treatment. TCOD removal rates in these studies vary with the strength of the wastes. It appears that the waste treated by Crawford *et al.* (1980) is more treatable. Dague *et al.* (1980) reported that TCOD removal efficiency increases only 13% by doubling the SMAR volume in series. All the data listed in this category show a TCOD removal of less than 80%, indicating the refractory and complex nature of the wastes.

Dairy wastes are also good candidates for SMAR treatment. This type of waste is rich in lactose and protein and has a well-balanced nutrition for anaerobic treatment. Unlike thermal sludge conditioning wastes, which are highly dissolved, dairy wastes contain colloidal particles. As shown in Table 3, the TCOD removal rate is in the range of about 1.0-2.0

g/L/d, which is similar to the synthetic protein-carbohydrate waste treated by Young and McCarty (1969). It is noted that TCOD removal rate for the dairy wastes is the lowest among the five groups of wastes listed. Operation at low temperatures does not lower the removal rate, suggesting it is probably diffusion-limited. It is interesting to note that Kelly and Switzenbaum (1984) also reported a weak temperature dependence of their fluidized-bed SMAR treating synthetic whey wastes, even with higher mixing intensity than the static-bed SMAR.

DeWalle and Chian (1976) also reported successful treatment of a landfill leachate rich in fatty acids and heavy metals. The SMAR was operated in a completely mixed mode with an effluent recycle ratio of 25:1. The TCOD removal rate was about 3.3 g/L/d at 25° C. In another report, Fe (430 mg/L) and Zn (16 mg/L) in the leachate were removed to above 94% (Chian and Dewalle, 1977). It is estimated that if all the sulfate in the influent were reduced to sulfide, only 30% of the metals in the influent would be removed as sulfides. Precipitation of the metals as carbonates was the major removal mechanism.

In addition to organics and heavy metals, the SMAR process has been studied for the destruction of coliforms and bacteriophages in raw sewage (Polprasert and Hoang, 1983). It was found that the coliform MPN could be reduced by about 75% at a hydraulic retention time of 2 days.

Recently, applications of the SMAR process have been extended to the treatment of coal gasification wastes (Blum *et al.*, 1986). This waste contains a large amount of hydroxyl and methoxyl benzenes which, in

general, are toxic to anaerobic bacteria. Comparison studies between SMARs and serum bottle cultures reveal that SMARs are superior in their ability to rapidly acclimate to high concentrations of benzenes. Phenol concentrations as high as 1885 mg/L could also be reduced to less than 1 mg/L with a hydraulic retention time of 18 hours.

Johnson and Young (1983) studied inhibition of anaerobic digestion with some organic priority pollutants. Their data suggested that adsorption plays an important role in removing soluble organics. For instance, up to 99% of the hexachloroethane can be adsorbed after 48-hour contact with sterilized cultures. The importance of adsorption in regulating substrate utilization behavior under the SMAR environment is not well understood.

Parkin *et al.* (1983) studied the toxicity of cyanide, chloroform, formaldehyde, ammonium, nickel, and sulfide to anaerobic growth, using serum bottles and SMARs. It was shown that methanogens are capable of acclimating to relatively high concentrations of these toxicants. They explained that the provision of a long SRT is the key to preventing the process from deteriorating due to toxicant exposure and to allowing acclimation to occur.

Packing media

The importance of the packing media in the SMAR process can be understood by comparing the SMAR with the upflow anaerobic sludge blanket (UASB) reactor. In UASB, no packing media are used. Therefore,

successful operation has to rely entirely on the development of highly settleable granules (Lettinga *et al.*, 1980). Frostell (1981) has demonstrated that the SMAR is more capable of handling hydraulic shock loadings and has lower effluent solids than the UASB. However, the use of packing media in SMAR may increase initial costs and create plugging problems, if not properly designed and operated.

In any event, optimum media design attempts to maximize active biomass in the system and avoid plugging problems during operation. Both attached and suspended biomass can be present in a SMAR. Van Den Berg and Lentz (1979) have shown that the relative importance of attached and suspended biomass by comparing upflow to downflow reactors with different area/volume ratios. Their experimental data show that there is a fundamental difference in operation between downflow and upflow reactors. Downflow reactors operate exclusively as fixed film reactors, while upflow reactors depend on the surface area/volume ratio. Activity of the fixed film (in L CH_4 STP/cm^2/d) decreases from 62% of the total activity (including suspended growth activity) for the downflow reactor with the area/volume ratio of 105 m^2/m^2 to 25% with the ratio of 53 m^2/m^2.

If this is the case for the static-bed SMAR, one can speculate that the relative importance of attached and suspended growth might actually vary with the type of media being used. Dague *et al.* (1980) used 16 mm Raschig rings to treat a thermal sludge conditioning waste. The Raschig rings had a porosity of 0.9 and a specific surface of area of 344 m^2/m^3, resulting an area/liquid volume ratio of about 380 (344/0.9) m^2/m^3. The

ratio is about three times the ratio for the cross-flow media used by Young and Dahab (1982), which had a porosity of 0.95 and specific surface area of 98 m^2/m^3. It is not well understood if such a large difference in the area/liquid volume ratio can actually affect SMAR treatment performance.

Song and Young (1986) studied the effects of specific surface area using 60-degree cross-flow media. Three media were compared. The media each had a porosity of 0.93 and specific surface areas of 98, 138, and 223 m^2/m^3. Their results showed that the differences in SCOD removal between media with specific surface areas of 138 and 223 m^2/m^3 were very small, compared to the differences in specific surface area. An increase of over 60% in specific surface area produced less than a 2% increase in SCOD removal for all the loadings tested. It was explained that most of the COD removal was associated with the biomass held loosely in the interstitial void spaces in the media. However, the difference in SCOD removal between media with specific surface areas of 98 and 138 m^2/m^3 was greater. A 40% increase in specific surface area produced approximately a 7% increase in SCOD removal. If the major SCOD removal was attributed to suspended growth, this difference in SCOD removal cannot be explained, unless some other factors were involved.

Song and Young further explained that one factor that needs to be considered is the media opening size. Media with small openings may hinder solids transport and eventually cause plugging. Also, very small openings may lead to severe short-circuiting through the small void

spaces, thus lowering treatment efficiency. The media with the smallest specific surface area had the largest media pore size (79 mm by 54 mm compared with 48 mm by 38 mm and 28 mm by 23 mm for the other two). It was explained that the larger media pore size was beneficial and compensated for the smaller surface area in SCOD removal.

The importance of media pore size was also demonstrated in an earlier study by Young and Dahab (1982). Two of 60-degree cross-flow media (with equivalent pore sizes of 46 mm and 32 mm, respectively), and one of 90-mm Pall rings (20 mm), and the other of 90-mm perforated spheres (15 mm) were compared. It was found that the SCOD removal efficiencies were strongly correlated with the media type, size, and shape. Media which had the largest pore size performed best in SCOD removal for all the loadings tested. Media with the greater pore sizes were less likely to have channeling at lower pore velocities of liquids and biogas. Also, lower pore velocities allowed solids to settle and not to be lifted easily by the upflowing gas stream. It was also found that channeling was more likely to occur in randomly packed media such as the Pall rings and the perforated spheres, since the openings in these media have more chance to be vertically oriented.

The effects of orientation of media were also studied by Song and Young (1986) using cross-flow (22.5^{o}, 45^{o}, 67.5^{o}) and tubular media (90^{o}). It is concluded that better SCOD removal is associated with the flatter orientation for all the loadings tested. The differences in COD removal between media with 22.5^{o} and 45^{o} were small while differences

between these two media and the media with 67.5° orientation were relatively significant. The tubular media performed significantly worse than did the cross-flow media with the same specific surface area. It was explained that media with the flatter slopes have a greater ability to redistribute the flow within the media matrix, therefore increasing the intermixing and contact efficiency between substrates and organisms. Also, the media with flatter slopes were more effective in holding the solids in the reactors. In any event, an increase in mixing and solids in the system can result in better treatment performance. However, the media with the 60° orientation was suggested for practical use to avoid clogging problems.

For all the reasons discussed above, when conducting pilot studies, media with the exact type, size, and shape as for the full-scale reactors to be designed should be used. It is also suggested that, in full-scale design, the bottom portion of SMARs should not be packed to avoid clogging problems (Young, 1985; Roe and Love, 1984).

SMAR Mathematical Simulation

Simulation of the SMAR system requires knowledge of at least two aspects: (1) substrate transfer and utilization, and (2) solids (biomass) transport.

Substrate Transfer And Utilization The SMAR process has been described as a complex phase-heterogeneous (liquid, biomass, and biogas) system with a highly concentrated growth and limited mixing intensity

(Chiang, 1983). Consequently, the concept of biofilm and biofloc is used to describe the substrate transfer and utilization in the SMAR system. The concept of biofilm arose in the early 1960s and was based on the classical mass transfer theory (Gulevich *et al.*, 1968). The biofilm concept states that (Figure 10):

(1) The substrate has to diffuse through a liquid film adhered to the biofilm surface before it can be utilized. This step is often termed "external diffusion."

(2) The diffusion of substrate into the cell matrix needs to be considered and occurs simultaneously with the utilization by the biofilm. The second step of diffusion is termed "internal diffusion."

Williamson and McCarty (1976a) have used the concept to develop a now widely accepted biofilm model, using Monod kinetics and Fick's 1st Law under steady-state conditions:

$$\frac{d^2S_f}{dz^2} = \frac{k_m}{D_f} \frac{S_f X_f}{(K_s+S_f)} \qquad (35)$$

Using the same approach, the above relationship can also be developed for biofloc model (Figure 11):

$$\frac{d^2S_f}{dr^2} + \frac{2}{r} \frac{dS_f}{dr} = \frac{k_m S_f X_f}{D_f(K_s+S_f)} \qquad (36)$$

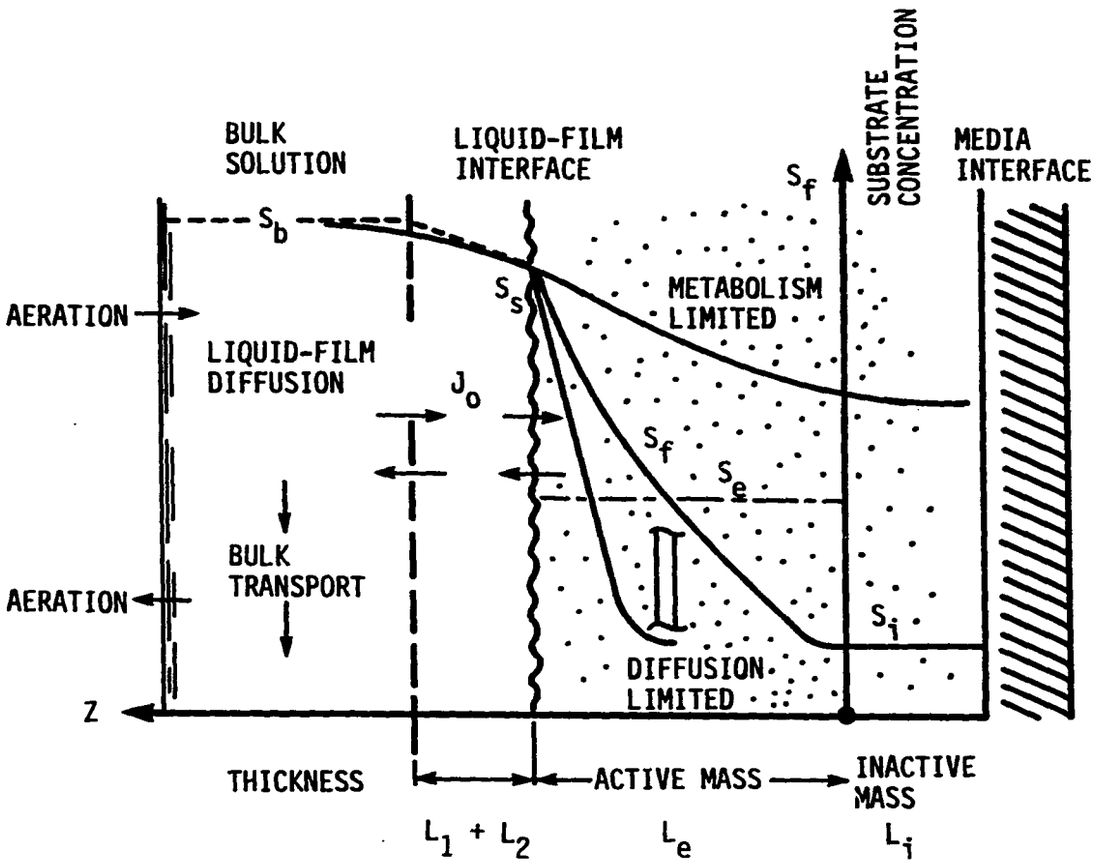

FIGURE 10. Conceptual illustration of biofilm model

In Equations 35 and 36, "S_f" is the limiting substrate concentration in the biofilm/biofloc in g/cm^3; "X_f" is the biofilm/biofloc density in g/cm^3; "k_m" is the maximum substrate specific utilization rate in g/d/g biomass; "K_s" is the half-saturation constant of Monod kinetics in g/cm^3; "D_f" is the substrate diffusion coefficient within the biofilm/biofloc in cm^2/d; and "z" and "r" are the biofilm and biofloc depth, in cm, perpendicular to the direction of the substrate flux. The D_f is often determined as a fractional portion of the substrate diffusion coefficient in water (D_W). Williamson and McCarty (1976b) have reported a value of D_f as 0.8 of D_W for nitrifier biofilm.

Equations (35) and (36) describe substrate utilization within the biofilm and biofloc under steady-state conditions. The biofloc equation has also been used to describe oxygen utilization kinetics for aerated packed-bed reactors (Lee and Stensel, 1986) and filamentous bacterial growth kinetics for activated sludge bulking (Lau *et al.*, 1984).

As to internal and external substrate diffusion, Fick's first Law may be used as follows (Figures 10 and 11):

$$J_f = D_f \frac{dS_f}{dz} \tag{37}$$

$$J_W = D_W \frac{S_b - S_s}{L_W} \tag{38}$$

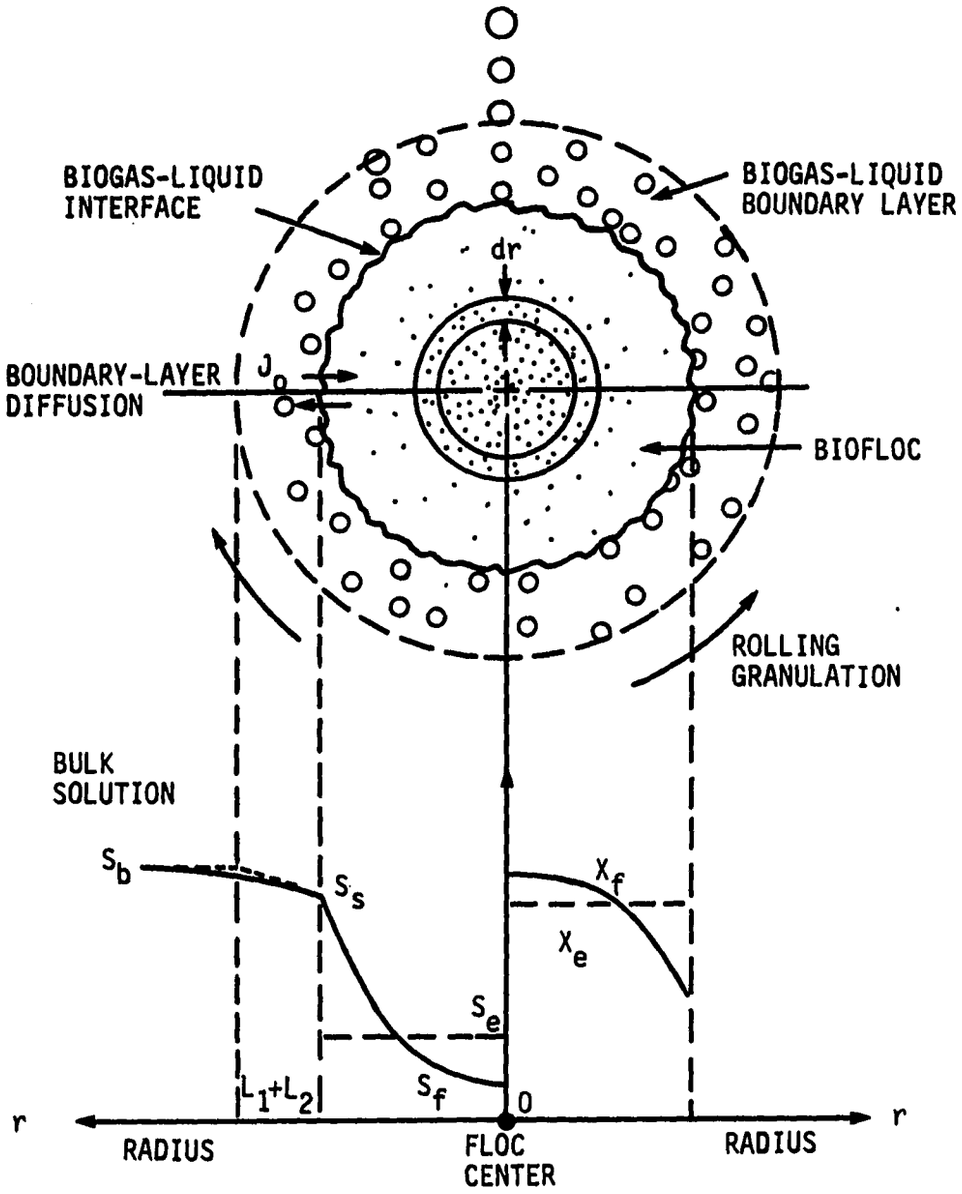

FIGURE 11. Conceptual illustration of biofloc model

where, "J_f" and "J_w' are the internal and external diffusion fluxes of the limiting substrate, respectively, in g/s/cm^2; "D_f" and "D_w" are the diffusion coefficients of the limiting substrate in the biofilm and liquid film, respectively, in cm^2/s; "S_b" and "S_s" are the substrate concentrations in the bulk solution, and on the interface, respectively, in g/cm^3; "L_w" is the liquid film thickness in cm; and "dz" is the differential biofilm thickness in cm. Fick's law simply states that the diffusion flux is directly proportional to the substrate gradient across the diffusion depth of concern.

From the viewpoint of boundary layer theory, L_w is considered the distance from the biofilm surface out to where the fluid velocity is 99% of the superficial velocity (Shames, 1982). In their model verification study using rotating cylinders, Williamson and McCarty (1976b) further found that the liquid film consisted of two layers. The outer layer, L_1, may be reduced to zero by mixing. The layer next to L_1, which is L_2, cannot be removed by mixing and is believed to result from the uneven nature of the liquid-biofilm interface. The thickness of L_2 was determined as 56 μm for the nitrifier biofilm in their study. It was stated that whether such a layer exists in the biofilm is currently unknown. Interestingly, in studying fluidized-bed acetoclastic methanogenesis, Wang *et al.* (1986) have determined L_w as 22 μm which is smaller that the L_2 of 56 μm determined by Williamson and McCarty (1976b) for nitrifier biofilm.

The two second-order differential equations, which describe the substrate profile within biofilm and biofloc, do not have an analytical solution. A numerical method, such as a Runge-Kutta finite difference method, must be used. The calculation normally starts from the biofilm depth where the slope of the substrate profile is zero and the substrate concentration is very small. This is normally referred to as the effective depth (L_e). For deep film growth, the effective depth is located at the interface between the biofilm and supporting media.

The calculation proceeds with an incremental biofilm depth. By incrementally increasing the biofilm depth, a tentative surface substrate concentration (S_s) is determined with each iteration. The S_s is then used to calculate the internal flux (J_f) at the biofilm depth currently simulated and the external flux at (J_w) at the liquid-biofilm interface, using Equations 37 and 38. The calculation continues until J_f equals J_w. This determines the surface flux (J_o), surface substrate concentration (S_s), and the effective biofilm thickness (L_e).

Despite the sound theoretical basis, there are several difficulties in applying the biofilm/biofloc model to the SMAR system. First, the model requires an assumption that the biofilm is a relatively thin plate and the biofloc is relatively small so that the substrate is only diffusing into the cell in a direction perpendicular to the cell surface. This is unlikely to be true for the SMAR system treating high strength wastes. Also, the model does not consider the effects of bacteria decay and shear loss, which may be important to the SMAR system (Rittmann, 1982).

Second, the use of the model requires accurate inputs of all the four system parameters (k_m, K_S, D_f, and D_W) and the biofilm density (X_f). This often complicates the calibration procedure if experimental determination of these parameters are not performed. Wang *et al.* (1986) have developed a calibration procedure by minimizing the sum of the squares of the deviations between the experimentally determined amount of biomass and the model-predicted biomass. The method has been successfully used in their studies of the fluidized-bed SMAR.

Finally, and most importantly, the model requires the use of some empirical equations to estimate liquid film thickness (L_W), which may not be applicable to a SMAR system in which biogas mixing predominates. Currently, three expressions have been used to estimate L_W for upflow packed-bed reactors in waste treatment:

Snowdon and Turner model (Meunier and Williamson, 1981)

$$L_W = 1.23(\mu/\rho)^{1/6}(d_p/v_O)^{1/2}(\varepsilon)^{3/2}(D_W)^{1/3} \qquad (39)$$

Gupta and Thodos (Wang et al., 1986; Suidan, 1986)

$$L_W = \frac{D_p}{(J_D)(Re)(Sc)^{1/3}} \qquad (40)$$

in which,

$$J_D = (0.010 + \frac{0.863}{Re^{0.58} - 0.483})(\frac{1}{\varepsilon}) \qquad Re=1-2140$$

$$Re = (\rho d_p v_O)/\mu m$$

$$Sc = \mu/(\rho D_W)$$

In Equations 39 and 40, "μ" and "ρ" are the absolute viscosity and density of liquid, in g/cm/s (poise) and g/cm^3, respectively; "d_p" is the diameter of the packing media in cm; "ϵ" is the specific porosity of packing media under operation in cm^3/cm^3; and "v_o" is the superficial velocity in cm/s. Also "J_D" is the Colburn J factor for mass and momentum transfer; "Re" is the packing Reynolds number; and "Sc" is the Schmidt number. The equation is valid only within a packing Re (not reactor Re) of 1 to 2140, which covers laminar and turbulent flow in packed-bed reactors.

The third expression for estimating liquid film thickness is similar to Equation 40 and requires the use of a plot (Williamson and McCarty, 1976a):

$$L_l = \frac{D_w^{1/3}}{v_o Y} (\mu/\rho)^{2/3} \qquad (41)$$

in which, "Y" is a function of Reynolds number and can be obtained from a plot with Y vs. Reynolds number (R_e), shown in Williamson and McCarty's paper (1976a).

Gulevich *et al.* (1968) also developed a direct expression for calculating J_W as follows:

$$J_W = \frac{D_W}{1.61} \left(\frac{\rho D_W}{\mu}\right)^{1/3} \left(\frac{\mu}{\omega}\right)^{1/2} S_b \qquad (42)$$

where, "ω" is the rotational speed of the cylinders on which biofilm grows, in 1/s. The above equation is based on the universal Navier-Stokes mass transfer equation (Equation 42 shown in the original paper of Gulvich *et al.* (1968) uses an incorrect power of -1/3 on the D_W term and -1/2 on the ω term).

All the above expressions of liquid film thickness (L_W or L_1) show a relationship of a power of 1/3 to D_W, 1/6 to μ, and a stronger power of 1/2 to d_p. Interestingly, the Snowdon and Turner expression shows a power of 3/2 to expansion bed porosity (ϵ), suggesting the liquid film thickness is a strong function of bed porosity. According to this, media with a greater porosity might result in a thicker liquid film, thus a poorer contact efficiency and lower treatment performance.

All of the above expressions for L_W are derived for the expanded-bed reactors mixed by flowing liquids and may not be directly applied to static-bed SMAR reactors in which mixing results primarily from biogas produced in the system. It is this property of the liquid-biogas interface encountered in the SMAR system that makes it difficult to apply the above expressions for L_W in the SMAR system.

Young (1968), in developing an anaerobic filter model, also considered a substrate gradient associated with the biofilm/biofloc concept. Instead of using the complicated biofilm/biofloc approach (as described above), Young took a much simpler approach of using a "substrate gradient factor" to describe the substrate gradient developed in the liquid film and cell matrix. The substrate gradient factor (SF), as defined by Young, is:

$$SF = S_b/S_e \tag{43}$$

where, "S_b" is the substrate concentration in the bulk solution (where no substrate gradient occurs) and "S_e" is the equivalent substrate concentration that will result in the same rate of utilization as if the biofilm/biofloc were completely dispersed and mixed with the substrate in a controlled finite element ($A\Delta h$). Although not mentioned by Young (1968), the equivalent concentration can be elucidated by using the following relationship:

$$\frac{k_m S_e X_e}{K_s+S_e} \Delta h = \int \frac{k_m S_f X_f}{K_s+S_f} dz \tag{44}$$

where, the integration runs across the entire effective cell depth (from 0 to L_e). X_e is the equivalent biomass concentration as if the biofilm were completely dispersed in the control element of $A\Delta h$. In Young's anaerobic filter model, "SF" is taken as an exponential function of bulk substrate concentration (S_b) as follows:

$$SF = 1 + (SF_o-1)e^{-k_g S_b} \tag{45}$$

where, "SF_o" is a maximum value for the substrate gradient factor (Figure 12) and "k_g" is a coefficient that must be obtained experimentally. By definition, "SF" approaches 1.0 for a completely mixed system.

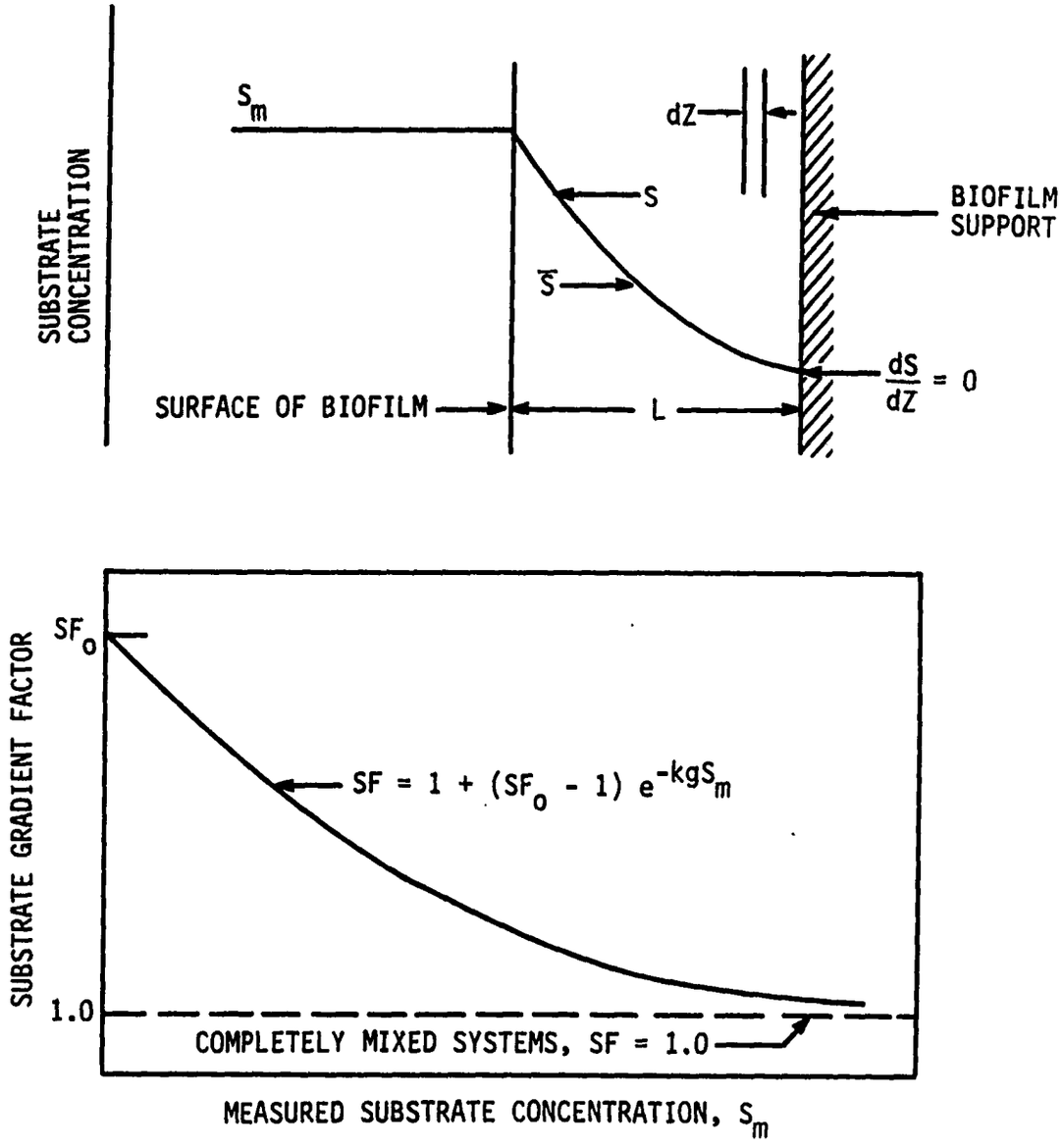

FIGURE 12. Conceptual illustration of Young's substrate gradient factor (Young, 1968)

From the viewpoint of the biofilm concept used today, the expression lacks the consideration of the biogas mixing effect which tends to reduce liquid film resistance. Dague and Chiang (1984), in developing a theoretical SMAR model, modified the "SF" expression to include the biogas mixing effect as follows:

$$SF = 1 + (SF_o - 1)e^{-k_g Q_o S_b} \qquad (46)$$

where, "Q_o" is the superficial biogas flow rate in $L/d/cm^2$, which changes along the height of SMAR. The expression assumes that the mixing effect on the substrate gradient is an exponential function of the superficial biogas flowrate. This might not be appropriate since, based on the power dissipation theory as discussed in the previous chapter, the biogas pore velocity and biogas pressure should be considered.

In many aspects, the use of "SF" greatly simplifies the mathematical procedure. The difficulties that occur in using the biofilm/biofloc model disappear. The use of equivalent biomass concentration (X_e) in the bulk solution is more experimentally measurable than is biofilm/biofloc density (X_f), especially for the static-bed SMAR system. However, a big drawback is that the validity of the expressions for estimating SF has not been proven either theoretically or experimentally.

Solids Transport and Granulation Solids (biomass) transport in the static-bed SMAR system may result from shearing and uplifting of biogas produced in the system. The shearing loss of attached growth

occurs when it grows sufficiently thick or the biogas mixing is sufficiently high. As a result, attached growth is sheared into the bulk solution. It is not well understood how much of this can actually occur in a normally operating SMAR. However, one would speculate that this could be important in the upper portion of SMARs, where biogas produced in the lower portions has a greater effect. This may be especially true in over-loaded SMARs if the rising biogas is not properly managed. The direct effect of biomass shearing in the upper portion of SMARs is to deteriorate the effluent quality due to suspended solids loss.

Van Der Meer and De Vletter (1982) have shown that the use of an internal gas-liquid separator in the top of a UASB can greatly enhance solids settling efficiency. Roe and Love (1984), however, have proposed a method of recycling liquids from the bottom active zone through a vacuum gas separator to reduce the uplifting effects of the biogas stream in the upper zones of SMARs.

Rittmann (1982) has shown how the shear loss can be incorporated into his steady-state biofilm model by relating the loss to shear stress ($dyne/cm^2$). His equation shows that the loss rate ($mg/cm^2/d$) is proportional to shear stress by a fractional order of 0.58, using data from Trulear and Characklis (1982). It should be noted that their data were derived under aerobic conditions using rotating cylinders. Therefore, the shear-loss relationship, derived by Rittmann, would only account for the liquid mixing and not for the biogas mixing effect.

Young (1968) stated that scouring and mixing of biogas flowing through the porous bed of a SMAR was the most important factor in solids transport. He assumed that the fraction of biomass transported upwards is directly proportional to the superficial biogas flowrate.

As biogas moves upwards, a rolling action occurs and causes the biomass particles to take on a granular shape. It is believed that this granulation plays an important role in the successful operation of the SMAR process in producing highly settleable granules (Lettinga *et al.*, 1980).

In a anaerobic bioflocculation study, Dague *et al.* (1970) also observed a low value of sludge volume index (SVI) of 13.6, giving a sludge concentration of 7.3 g/L. The anaerobic sludge was described as flocculating in a manner similar to activated sludge.

Mahoney *et al.* (1984) studied chemical aggregation of granules obtained from a UASB reactor, and found that the existence of negatively charged extracellular polymeric substance (EPS) is important for divalent bridging.

The mechanism of granulation may also affect biomass activity in a SMAR. Previous studies (Young, 1968; Hydroscience, Inc., 1981) indicated that a higher activity, in terms of g COD removed/g VSS/day, for the suspended biomass in the lower parts of a SMAR than in the upper parts. For example, Young (1968) reported an activity of 1.75 vs. 0.1 for growth treating volatile acids and 0.65 vs. 0.15 for growth treating protein/carbohydrates. They explained that the variation in the biomass

activity was due to "granulation decay" as a result of a decrease in the substrate level surrounding the biomass when the biomass transports upwards. Without the decay, a plugging problem might occur at a faster rate in the lower parts of a SMAR in which highly concentrated biomass accumulates.

Static-Bed SMAR Models Young (1968) developed the first SMAR model using the concept of substrate gradient factor (SF), as described previously. The model also considers biomass transport resulting from biogas lifting effects. The model assumes an ideal plug-flow which may not be applicable to the SMAR system, especially under heavy loading conditions.

Young's model corrects for short-circuiting due to biogas lifting and biomass accumulation by reducing the effective reactor volume (V_e) as follows:

$$V_e = \epsilon\ V\ (1-k_V X)(1-r_S Q_O) \qquad (47)$$

where, "ϵ" is the porosity of packing media and "k_V" and "r_S" are the first-order correction coefficients for biomass accumulation (X, in g VSS/L) and biogas flow rate (Q_O in L/d/ft^2), respectively. K_V and r_S were estimated to be about 0.01-0.02 L/g VSS/L liquid volume and 0.0025 (L biogas/d/ft^2)$^{-1}$. The model over-predicted effluent substrate and biomass concentrations for treating complex protein-carbohydrate wastes. As was pointed out, this might be due to inadequate descriptions of the substrate utilization and biomass transport in the system.

Mueller and Mancini (1976) modeled the SMAR as a series of completely mixed reactors for both the liquid and biogas phases. No biofilm growth and substrate gradient were assumed. The major advantage of the model was to indicate the chemical equilibria among nitrogen, volatile acids, alkalinity, carbon dioxide, and pH. In addition, the non-ideal plug flow, resulting from the longitudinal dispersion, could be simulated with mathematical techniques. They suggested that the non-ideality of their SMAR was on the order of three to four reactors in series. Unfortunately, the model neither extends an explicit perception of the SMAR process nor provides an approach to practical design.

Meunier and Williamson (1981) proposed a "simplified model" for packed-bed biofilm reactors. The model is based on Williamson and McCarty's biofilm model (1976a) as previously described. The "simplified model" first set a criterion to determine if the electron donor or electron acceptor is the limiting species. Instead of calculating the substrate profile within the biofilm, an iterative equation was developed to directly calculate the surface substrate concentration (S_s). The iteration is computed by a method of subsequent substitution until a desired accuracy between two consecutive computations in S_f is met, for example within 0.01 mg/L. The substrate flux (J_o) is then calculated using Fick's 1st Law and substrate is again checked for limiting species using the same criterion. If there is no change in the limiting species, the required incremental volume (V_i) for the ith segment is then calculated as:

$$V_i = \frac{(\Delta S_i)Q}{(J_{o,i})a} \qquad (48)$$

where, "ΔS_i" is the incremental decrease of the limiting substrate concentration (g/cm^3) in segment i, which can be calculated as (S_{in}-S_{eff})/N; "N" is the number of segments chosen for use; "Q" is the substrate flow rate in cm^3/d; "a" is the biofilm surface area per unit reactor volume (or the specific surface area of packing media) in cm^2/cm^3; and "$J_{o,i}$" is the surface flux in segment "i" in $g/d/cm^2$.

When applied to the SMAR system, the model inherits the same difficulties as for the biofilm/biofloc model described previously. More importantly, the model provides no insight into the solids transport actually occurring in the SMAR system. It is noted that the "simplified model" is more suitable for fluidized-bed systems.

Dague and Chiang (1984) also proposed a theoretical mathematical model for static-bed SMARs. The model is termed a "two-culture" model to differentiate the attached growth (biofilm) and the suspended growth (biofloc). As stated, such a differentiation is necessary to account for differences in substrate utilization and biomass transport. The model uses a "contact efficiency factor" (η), which is defined as the inverse of the "substrate gradient factor" of Young (1968), to elucidate the effects of biogas mixing on reducing liquid film resistance and therefore increasing contact efficiency between growth and substrates. In addition to the uplift solids transport, as considered in Young's model, the model also considers shear loss of attached growth. The model assumes an ideal plug-flow, which may not be appropriate.

The advantage of the two-culture model is that important design parameters, such as the surface area and porosity of packing can be directly related. The relative importance of porosity and surface area can be evaluated, if the model parameters are properly determined. However, as with Young's model, the "two-culture" model requires the determination of "contact efficiency factors", which are difficult to determine. It is the writer's opinion that none of the models discussed above are applicable because of the complex nature of the SMAR system.

As indicated in many pilot-scale studies (Young, 1985), it becomes clear that, in the SMAR system, the major growth responsible for utilization is biofloc rather than biofilm. In other words, the porosity is a more important factor than the surface area of packing for the upflow static-bed system. Therefore if the "two-culture" model can be simplified into a "one-culture" model for biofloc alone, it might become more feasible to determine the "contact efficiency factor" for biofloc.

Evaluation of Full-Scale SMARs

Two full-scale static-bed SMARs are evaluated and compared below (Table 4). The Centennial Mills plant (Taylor, 1972) is located in Spokane, Washington, and the Celanese plant in Vernon, Taxas (Witt *et al.* 1979). Both plants treat carbohydrate wastes. However, the sugar-refining wastes treated by the Vernon plant contains some polymers of guar gum which are considered less susceptible to hydrolysis. The Vernon plant received a flowrate of 0.22 mgd (832.7 m^3/d), which is about twice

that of the Spokane plant. The Vernon plant has one SMAR unit, 40 ft in diameter and 30 ft high (12.2 m by 9.1 m) and is packed with plastic packing with a porosity of about 0.95. The Spokane plant has three SMAR units, each is 30 ft in diameter and 20 ft high (9.1 m by 6.1 m), operating in parallel with rock packing and a porosity of about 0.40.

The Vernon plant was operating at a COD loading rate of 7.9 g/L liquid volume/d with a theoretical retention time of 28.6 hrs and a temperature of 37° C, while the Spokane plant at 9.5 g/L liquid volume/d, 22.2 hrs, and 32° C.

Several conclusions regarding the operation and performance of the Vernon and Spokane plants can be made:

(1) The loading rates used by these two plants are close to the loading rates obtained in many pilot studies in treating food-processing wastes at a COD loading rate of 8-10 g/L/d and a retention time of about 1 day.

(2) The total COD (TCOD) removal rate is higher for the Spokane plant (6.1 g COD/L/d) than for the Vernon plant (4.7 g TCOD/L/d). The higher TCOD removal rate for the Spokane plant was likely due to the starch waste, which was believed to be easier to treat than the sugar gum polymer wastes for the Vernon plant. The higher loading rate at the Spokane plant might not be the reason for its higher removal rate, since both plants were believed to be operating at their saturated loading rates.

TABLE 4. Comparisons between two full-scale SMARs

Parameter	Unit	Centennial Mills Spokane plant	Celanese Chemical Vernon plant
Waste		Wheat starch	Guar gum
Flowrate	m^3/d	515	833
TCOD	mg/L	8800	9140
BOD_5	mg/L	6500	
TSS	mg/L	2650	
SMAR			
Dimensions	m	9.1 dia. by 6.1 ht.	12.2 dia. by 9.1 ht.
Units	no.	3	1
Total volume	m^3	1190	1046
Packing			
Media		Rock	Plastic
Porosity	(-)	0.40	0.95
Operation			
Temp	^oC	32	37
TCOD load	$g/L/d^a$	9.5	7.7
Detent. time	$hour^a$	22.2	28.6
Recycling		No	Yes
Performance			
$TCOD_r$	(%)	64	61
$TCOD_r$	$g/L/d^a$	6.1	4.7
$TCOD_{eff}$	mg/L	3170	3590
TSS_{eff}	mg/L	1460	210
Methane	(%)	-	73
Reference		Taylor (1972)	Witt *et al.* (1979)

[a]Based on the clean-bed liquid volume.

(3) The Spokane plant effluent solids was as high as 1460 mg TSS/L, which accounts for 53% of the effluent TCOD of 3170 mg/L. The Vernon plant discharged only 210 mg TSS/L. This gives a daily solids discharge of 752 and 175 kg TSS for the Spokane and Vernon plants, respectively. Further analysis indicates that the effluent suspended solids at the Spokane plant can be reduced to 370 mg TSS/L within a 30-minute lab-sedimentation period. It is clear that the Spokane SMAR system was poorer in retaining solids in spite of the fact that the Spokane SMAR had a much lower liquid superficial velocity (2.5 m/d) than does the Vernon SMAR (7.1 m/d). This suggests that the packing used at the Vernon plant (with a porosity of 0.95) was superior to the rock packing used at the Spokane plant (with a porosity of 0.40) in retaining biomass in the system. This comparison confirms Young and Dahab's finding in their pilot-scale studies (1982) that higher pore velocities resulting from the packing media with random-packed smaller openings is more likely to hinder settling of well-flocculated solids and discharge more solids in the effluent.

(4) The Vernon plant reported that effluent recycling resulted in extremely smooth operation, excellent COD removal and operation with un-neutralized or partially neutralized feed. However, the Spokane plant did not recycle effluent during normal operations but recycled 100% when the plant received no feed. It is not clear if the recycling practice used in the Vernon plant can be used in the

Spokane plant to give any benefit, such as a better mixing intensity, as suggested by DeWalle and Chian (1976).

(5) It was reported that the Spokane plant could fully recover within 3 hours at the full loading rate after one month recession. This confirms many previous pilot-scale studies. This also suggests that the slow decaying anaerobic system is highly suited to industries that have seasonally varying waste streams.

EXPERIMENTAL STUDY

The experimental study was conducted in the Environmental Engineering Laboratory located in the Town Engineering Building, Iowa State University, Ames, Iowa. The study included the operation of three 85-L, static-bed, submerged-media, anaerobic reactors (SMARs) with continuous feeding of a synthetic waste of animal-grade low-heat non-fat dry milk (NFDM) solution. The entire setup was operated in a 35° C constant temperature room.

Equipment and Substrate

Pilot-Scale SMARs

As shown in Figure 13, three cylindrical columns[3] were used as the pilot-scale SMARs with approximately the same operating volume of 85 liters but different heights and diameters. The shortest column (SMAR A) was constructed of 0.48-cm PVC, with dimensions of 44.8 cm I.D. by 59.7 cm height. The other two columns (SMARs B and C) were constructed of 0.32-cm Plexiglas, with dimensions of 29.8 cm I.D. by 128.3 cm height and 19.7 cm I.D. by 288.1 cm height, respectively. A photograph of the SMAR set-up is shown in Figure 14.

Each column was equipped with a bottom inlet distribution panel to provide a uniform influent feed (Figures 15 through 17). The height/diameter ratios, which characterize the slenderness of the SMARs,

---

[3]Manufactured by the ERI Machine Shop, Iowa State University, Ames, Iowa 50010.

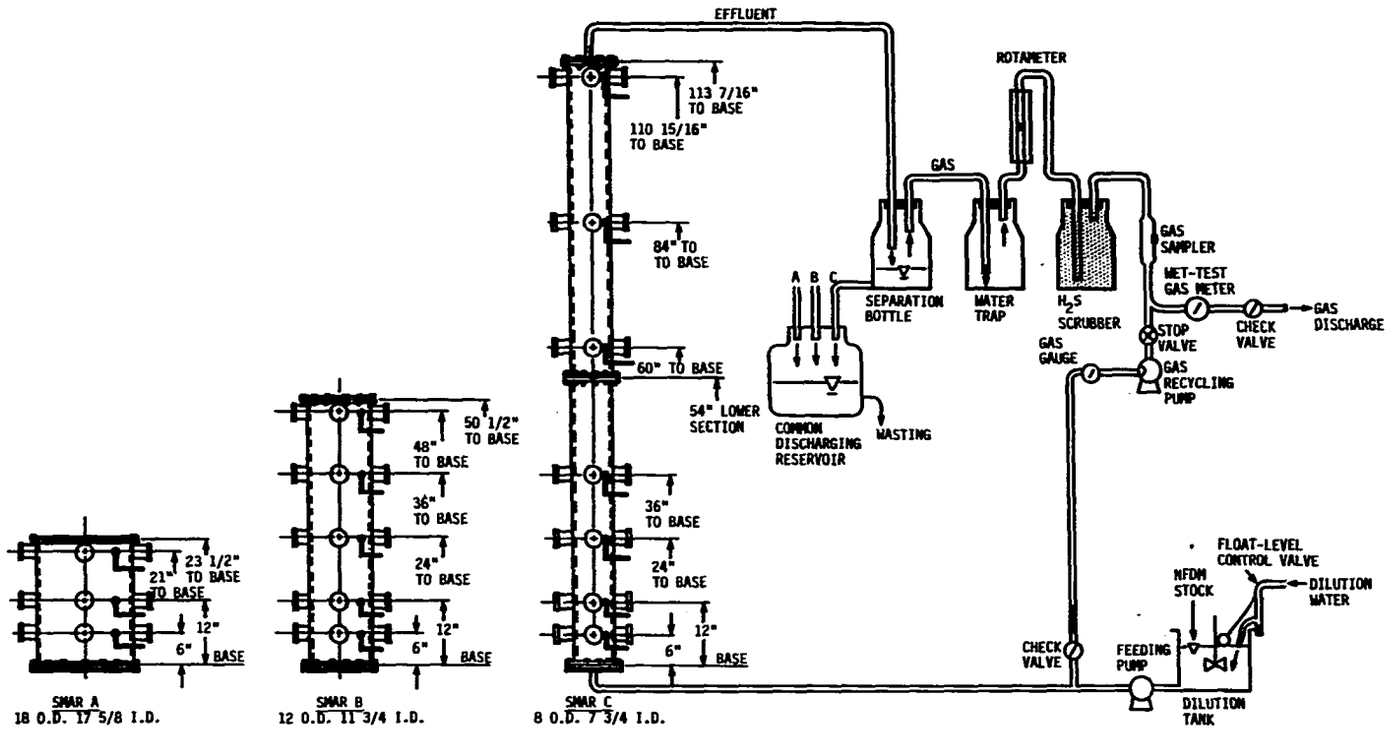

FIGURE 13. Schematics of SMAR line-up and sampling heights

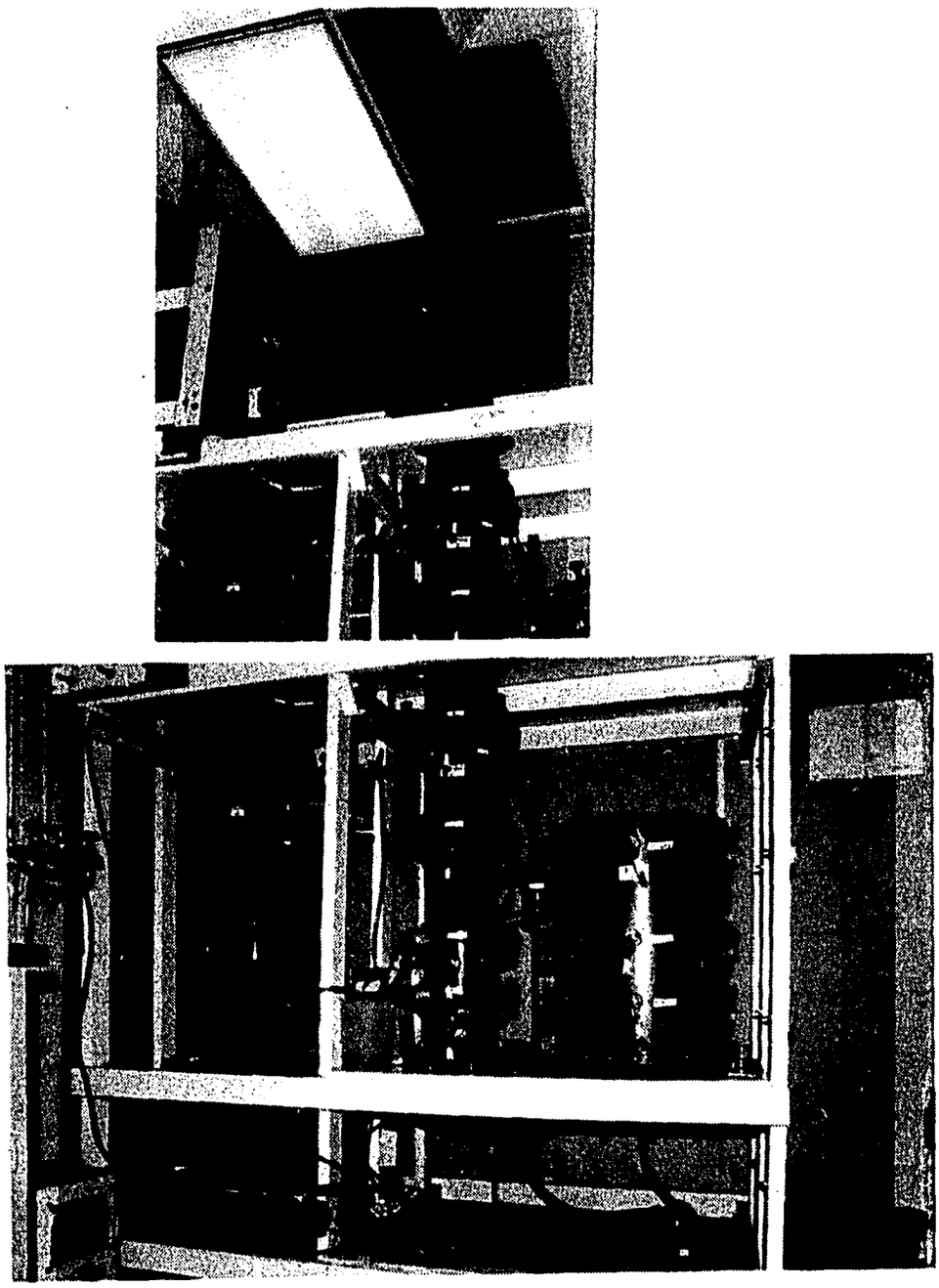

FIGURE 14. Photograph of the SMAR setup used in this study

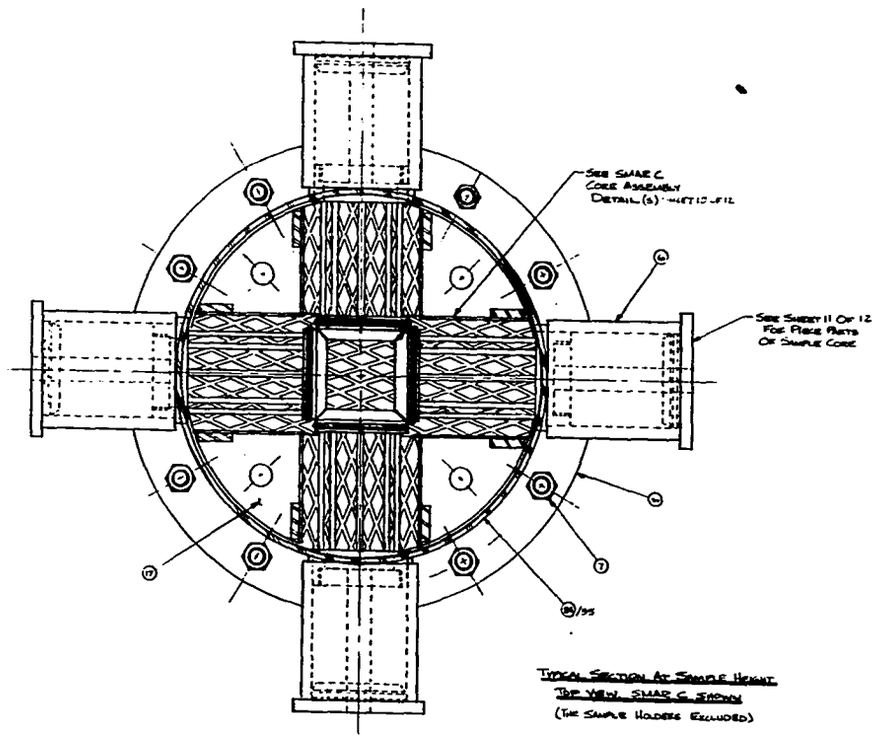

FIGURE 15. Schematics of bottom distribution plate for SMAR A

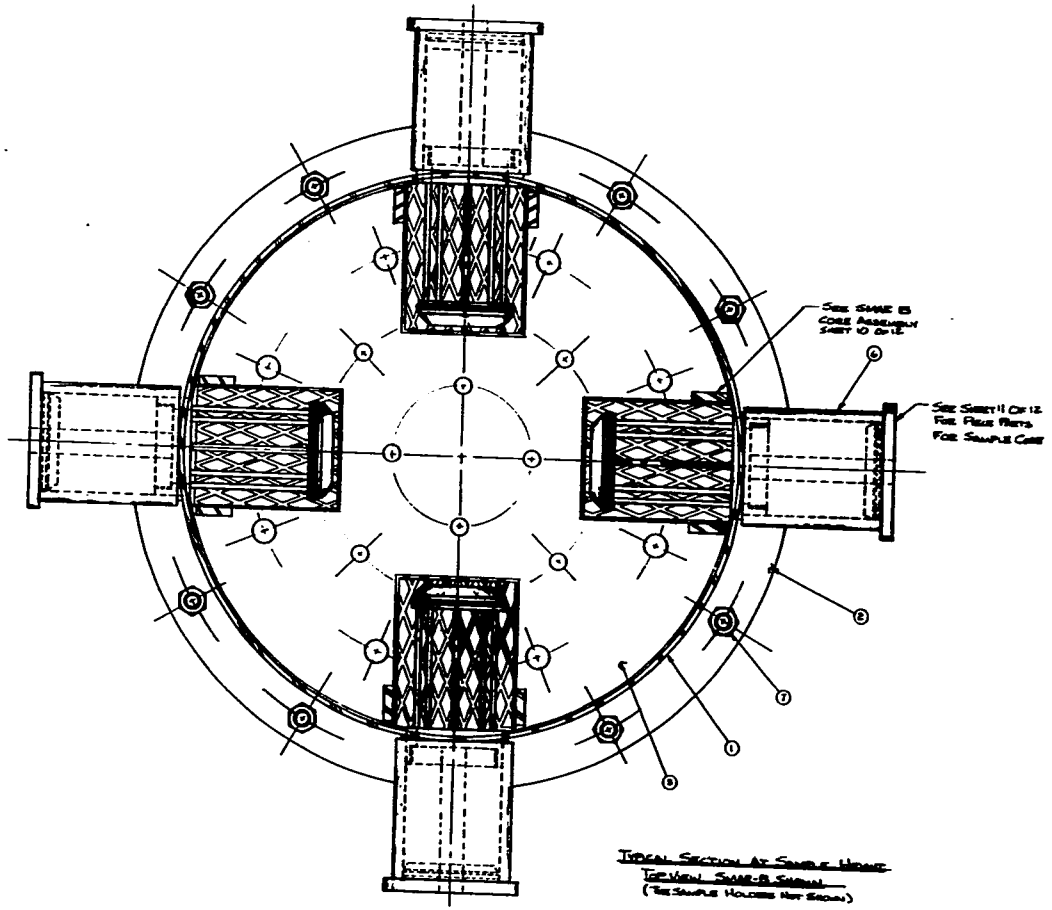

FIGURE 16. Schematics of bottom distribution plate for SMAR B

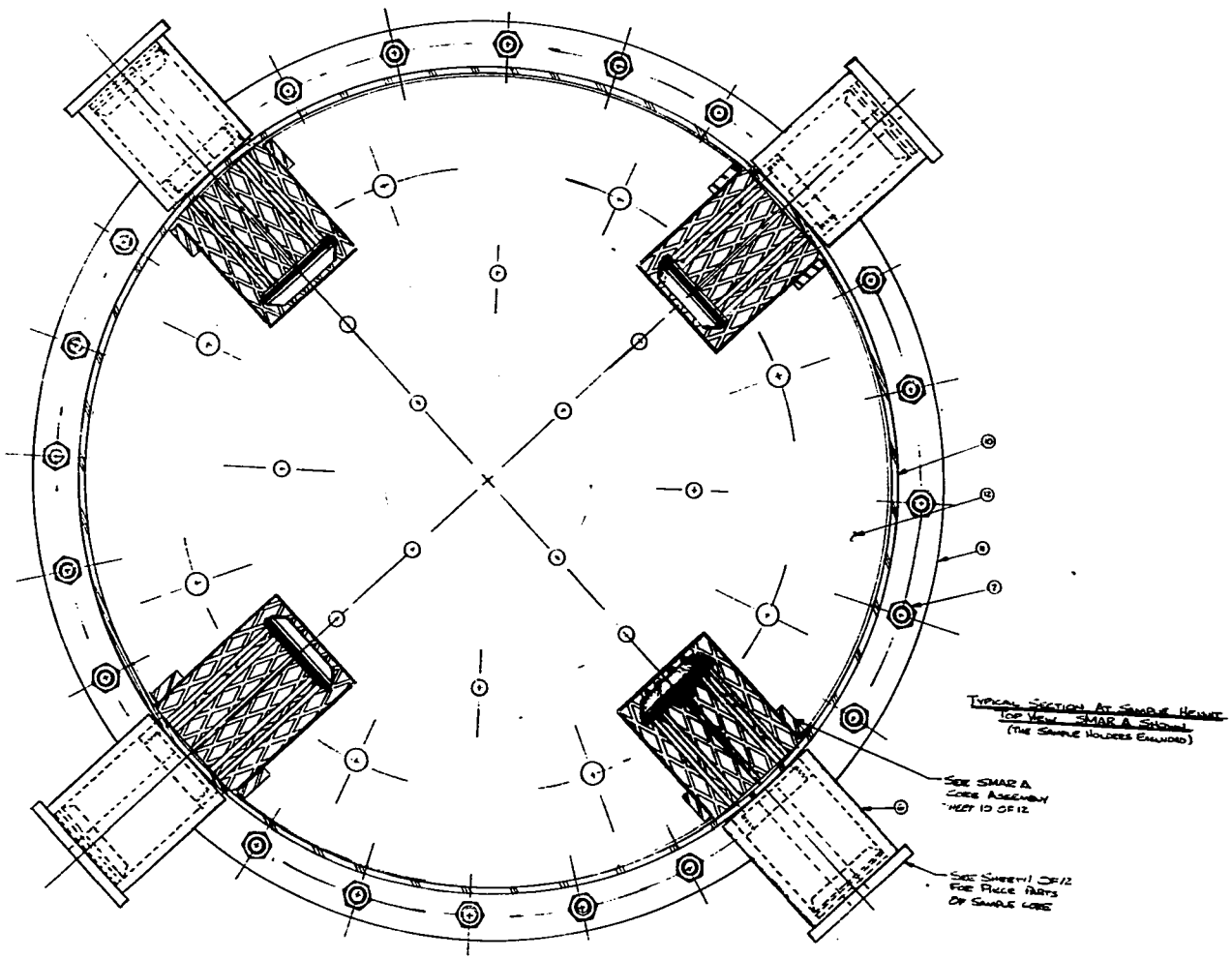

FIGURE 17. Schematics of bottom distribution plate for SMAR C

are 1.2, 4.1, and 14.3 for SMARs A, B, and C, respectively.

Each SMAR was packed with 16-mm (nominal size) plastic Flexiring[4] up to the height of the highest sampling ports, i.e., 53.3 cm, 121.9 cm, and 281.8 cm for SMARs A, B, and C, respectively. The bed porosity was determined to be 0.9. A media-specific surface area of 344 m^2/m^3 is reported by the manufactures. Table 5 shows the dimensions of the three SMAR units.

TABLE 5. Dimensions of SMAR units used in this study

SMAR	I.D. (cm)	Reactor height (cm)	Packing height (cm)	Reactor volume (L)	Packing volume (L)	Reactor liquid volume (L)	Packing liquid volume (L)
A	44.8	59.7	53.3	94.1	84.0	84.7	75.6
B	29.8	128.3	121.9	89.5	85.1	80.6	76.6
C	19.7	288.1	281.8	87.8	85.9	79.0	77.3

Each SMAR was equipped with two types of sampling devices, i.e., suspended growth sampling ports and attached growth sampling cages at several different heights. There are three sampling heights for SMAR A, five for SMAR B, and seven for SMAR C. The sampling ports were constructed of 5.6-mm stainless steel tubes and extended to the center of the reactor. Four sampling cages, separated by 90 degrees, were

[4]Koch Engineering Company Inc., Wichita, Kansas 67208.

fabricated at each height of the sampling port. The sampling cages were constructed of 1-mm stainless steel wire with dimensions of 3.5 cm diameter by 8.0 cm length and can hold 10-12 units of 16-mm plastic Flexiring.

The sampling cage was held in a Plexiglas core which could be slid out of the reactor along an outer Plexiglas sleeve to fetch the attached growth. The sleeves (Figure 18) were extended out of the reactor wall and could also serve as a dispersion ring to reduce wall effects. The sampling cage holder was fabricated with 3 o-rings at both ends and center. The outside and central o-rings seal the reactor when the holder is in the reactor under normal operating conditions. However, when the sampling holder is slid out for sampling, the inside and the central o-rings are used to seal the reactor. Unfortunately, because of the long-term exposure of these inside o-rings to the digestion environments, they became worn out and failed to function properly.

The feed stock solution was stored in a refrigerator (10^{o} C) and pumped by a #14 Masterflex pump into a small agitated Plexiglas tank where the stock solution was diluted with warm tap water to produce the desired concentration of feed. The dilution tank has inside dimensions of 30.5 cm by 25.4 cm by 10 cm water depth (7.7 liters). In order to obtain a stable tap water flowrate, the dilution tank was equipped with a tap water pressure reducer (reduced to about 5 psig) and a float control valve. The reduced pressure was necessary to increase the sensitivity of the float control valve. The diluted feed was then pumped by a #15,

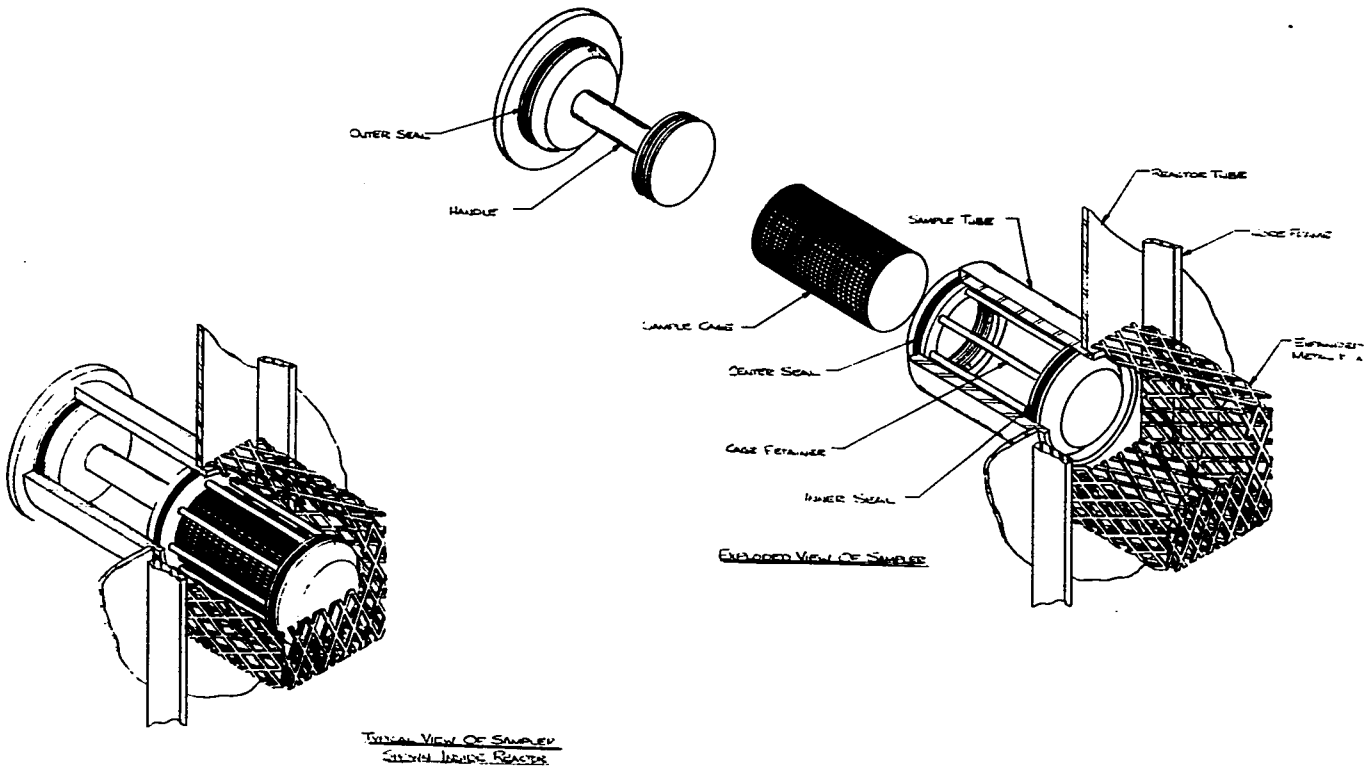

FIGURE 18. Schematics of SMAR attached growth sampling cage

3-headed Masterflex pump into the bottom inlet distribution plate of each SMAR. By adjusting the speed of the stock and feeding pumps, any combination of organic and hydraulic loading rates could be obtained.

The liquid effluent and produced biogas passes through a #18 Tygon tubing (8.0 mm I.D.) and discharges into a 250-mL respiratory bottle where the biogas is separated from the effluent. The effluent line is adapted to the bottom side arm of the separation bottle and bent into the shape of an inverted siphon with a siphon break on the downstream side. By controlling the level of the siphon break, the liquid level in the separation bottle can be adjusted. A liquid level in the separation bottles of approximately 8 cm was maintained to ensure a proper seal on the SMAR system. The effluent then passed into a common reservoir for wasting.

The biogas, after separation, passes into a 1000-mL glass bottle to remove some carry-over water vapor before running into an H_2S scrubber. This is important to prevent the scrubber from flooding. The H_2S scrubber was made by filling Fe_2O_3-coated wooden chips into a 1000-mL wide-mouth glass bottle. After H_2S is removed, the biogas volume is then measured with a Wet Test gas meter.[5] A glass gas sampler, equipped with a septum,[6] was installed in the line between the scrubber and the gas meter to allow for gas sampling by using a syringe. Figure 13 shows the sampling heights and the entire lineup of the SMAR system.

---

[5]Precision Scientific Co., Cat. no. 63110, Chicago, Illinois.

[6]Thermogreen™ LB-1 cylindrical, 6.0 mm diameter, cat. no. 20668, Supelco Inc., Bellefonte, PA 16823-0048.

Substrate

The substrate used in this study was a synthetic waste of animal-grade, low-heat, non-fat, dry milk[7] (NFDM) solution supplemented with minerals important to anaerobic microorganisms. The NFDM was relatively cheap and had a well balanced nutrition and could be stored for a long period through the entire study. The low-heat milk was chosen because it contains a higher nitrogen content than the high-heat milk. The NFDM has a COD equivalent of 1.13 g/g NFDM. Table 6 shows the ingredients of the NFDM.

For SMAR feeding, the NFDM stock solution was made up each time in 30-L volume with a concentration varying from 50 to 300 g COD/L, depending upon loading requirement. In order to obtain suitable buffering, bicarbonate ($NaHCO_3$) alkalinity (as $CaCO_3$) was added at a alkalinity/COD ratio of 1/40 to 1/4. During the acclimation period, a higher alkalinity/COD ratio was used. Once the system was acclimated, a ratio of 1/10 to 1/40 was used during normal operating periods.

Five trace metals (Fe, Zn, Ni, Co, and Mn) were added in the stock solution at a concentration of 200 ppm (of the NFDM) for Fe and 20 ppm for the other four metals. Table 7 gives the recipe for preparing 30-L of 150 g COD/L NFDM stock solution.

To obtain a well dissolved homogenous stock solution, a milk paste was first prepared by hand and then churned by a homogenizer[8] at a low

---

[7]Swiss Valley Farms Co., Davenport, IA 52808.

[8]TR-5 Homogenizer, Tekmar Company, Cincinnati, Ohio 45222.

TABLE 6. Ingredients of NFDM substrate

Parameter	Values	Units	Reference
COD	1.13	g/g NFDM	This study
TOC	0.21	g/g NFDM	This study
TKN	5.4	g/100 g NFDM	This study
T-PO_4	2.2	g/100 g NFDM	This study
Fat	≤1.0	g/100 g NFDM	Swiss Valley
Lactose	51.0	g/100 g NFDM	Swiss Valley
Particle size	98% thru #40 sieve		Swiss Valley
Ash	8.2	%	Swiss Valley
Solub. index	≤1.25	%	Swiss Valley
Standard Plate Bacterial count	50,000	counts/g NFDM	Swiss valley
Trace metals			
Fe	4.6	ppm of NFDM	This study
Ni	1.0	ppm of NFDM	This study
Co	0.8	ppm of NFDM	This study
Mo	3.0	ppm of NFDM	This study
Zn	15.0	ppm of NFDM	This study

TABLE 7. Recipe of NFDM stock solution (30 L-150 g COD/L)

Ingredients	Quantity	Criteria
NFDM	3982 g	COD/NFDM = 1.13
$NaHCO_3$	756 g	Alk/COD = 1/10
Mineral stock	80 mL	
$FeCl_2.4H_2O$ (10 g/L)	35.60 g/L	Fe/NFDM = 200 ppm
$ZnCl_2$ (1 g/L)	2.08 g/L	Zn/NFDM = 20 ppm
$NiCl_2.6H_2O$ (1 g/L)	4.05 g/L	Ni/NFDM = 20 ppm
$CoCl_2.6H_2O$ (1 g/L)	4.04 g/L	Co/NFDM = 20 ppm
$MnCl_2.4H_2O$ (1 g/L)	3.61 g/L	Mn/NFDM = 20 ppm

speed for about 5 minutes. This is important to avoid any floating chunks, which are difficult to dissolve when more water is added later to get the total volume. After a homogenous milk paste was prepared, bicarbonate and mineral solution and tap water were added to bring the total volume to 30 L and then rapidly mixed by the homogenizer at a higher speed for about 30 minutes. To ensure a well dissolved solution, the homogenized stock was then screened through a #100 sieve before use. When well homogenized, the stock solution could easily pass the sieve.

SMAR Operating Procedures

Tracer Study

The purpose of the tracer study was to investigate the hydraulic characteristics of the three SMARs both before seeding with and without

external air gassing (clean bed) and after seeding at some selected loading rates (dirty bed). The tracer study was done by injecting a slug of 50 mL of 2000 mg Li^+/L into the influent line of each SMAR. Lithium nitrate was used before seeding. However, lithium chloride was used after seeding as nitrate could inhibit methanogenic bacteria. Four runs were done during different phases of the study, as shown in Table 8.

TABLE 8. Operating conditions for SMAR tracer studies

Run	Bed Conditions	Flowrate (mL/min)	COD_{in} (g COD/L)	Type of gassing
1.	Clean	146	0.0	No gassing
2.	Clean	167	0.0	External air gassing
3.	Dirty	109	2.1	Internal biogassing
4.	Dirty	110	4.0	Internal biogassing

Air gassing was done by running a #18 Masterflex pump into the bottom influent line with a single point application. Although this can not exactly simulate SMAR gassing patterns at normal operating conditions, it is considered proper since most of biogas occurs in the lower parts of the SMAR. Runs 3 and 4 represent a middle and the highest organic loading conditions, respectively, with the highest nominal hydraulic loading rate (or 0.5 day detention time) used in the study. Comparisons between the clean-bed with gassing (Run 2) and dirty-bed

studies (Runs 3 and 4) help to understand the effect of biomass accumulation on the hydraulics of the SMAR system.

Upon injection of the lithium tracer, approximately 25 mL of effluent samples were collected over a period of about twice the detention time (about 24 hours). The sampling frequency was every thirty minutes within the period of the theoretical detention time and every one hour thereafter. For the dirty-bed studies, samples were filtered with a fiber glass filter[9] right after collection. The filtration was necessary to use atomic emission for Li^+ analysis (see the following section on Analytical Methods). The SMAR influent flowrate was also measured every hour during the study. The average flowrate was used to calculate the theoretical detention time.

Start-up and Acclimation

Before the three SMARs were seeded, the reactors were emptied from the previous tracer studies to determine the porosity of the packing media. All the influent, effluent, and gas lines were connected. Gas-liquid separation bottles, vapor traps, H_2S gas scrubbers, and Wet Test gas meters were on line and tested for leaks.

Seed was obtained from the primary anaerobic digester at the City of Ames Wastewater Treatment plant on August 4, 1986. The digester was in a healthy condition and operating at an SRT of about 15 days and mixed by intermittent biogas recycling. The sludge obtained from the digester was

[9]Whatman GF/C glass microfiber filter, 4.25 cm.

immediately screened with a #10 sieve to remove large chunks and pumped into each SMAR with a #18 Masterflex pump right after the screening.

Routine Maintenance and Daily Monitoring

Successful operation of the SMARs relied on consistent, careful, and thorough routine maintenance. A single outbreak might disturb the entire system and require additional time for a steady-state test. In some cases, it even caused failures of operating devices. A daily inspection checklist was therefore established as shown in Table 9. The checklist kept expanding to include the problems not in the current list throughout the entire study.

SMAR daily monitoring included flowrate measurement and gas meter readings. Influent flowrate was measured by volume of the combined flow of stock solution and dilution tapwater into the dilution tank. Gas meter readings, gas temperature, and barometric pressure were recorded daily and used to calculate daily average gas production at standard conditions (0^{o} C and 1 atm). The influent was also sampled from the dilution tank daily for COD analysis during steady-state operation.

Loading Schedule

The loading schedule for the three SMARs was performed on the basis of volumetric COD loading rate and theoretical detention time (Table 10). The loading rate and detention time were based on clean-bed liquid volume. The COD load was gradually increased after each steady-state study with a testing range from 1 to 12 g/L/d and three detention times

TABLE 9. SMAR daily inspection list

A. Stock solution
1. Is the stock solution enough for the next 24 hours?
2. Is the stock line getting clogged?
3. Are the connecting joints around the stock pump getting loose?
4. Is the Masterflex pump tubing getting broken?
B. Influent and effluent
1. Is the tapwater pressure reducer getting clogged (indicated by a low reading in pressure gauge)?
2. Is the float control valve of the dilution tank too insensitive due to high operating pressure in the pressure reducer (adjust to about 5 psig)?
3. Is the dilution tank mixer operating at a suitable speed (too high rpm causes unstable regulation in the float control valve; too low rpm causes inadequate mixing)?
4. Is the feeding Masterflex tubing getting broken?
5. Are the common effluent reservoir and effluent line getting clogged?
C. Liquid-gas separation
1. Are liquid levels in separation bottles suitable (low level causes inadequate sealing and indicates a unusual back pressure from a flooding or tight-packing scrubber if the siphon break is high enough; and higher levels might flood the gas line)?
2. Are H_2S gas scrubbers getting flooded?
3. Are H_2S gas scrubbers getting black as a result of too much iron sulfide precipitation?
4. Are the liquid levels in Wet Test gas meters appropriate?

of 0.5, 1.0, and 2.0 days. Exit gas recycle was studied at high loading conditions with a COD loading rate of about 10 g/L/d and a retention time of about 2 days. A total of sixteen steady-state runs were conducted.

TABLE 10. SMAR scheduled loading rates

Run No	COD load (g/L/d)	Deten. time (hour)	COD_{in} (g/L)
1a	1.0	48	2.0
2a	2.0	48	4.0
2b	2.0	24	2.0
2c	2.0	12	1.0
4a	4.0	48	8.0
4b	4.0	24	4.0
4c	4.0	12	2.0
6b	6.0	24	6.0
8a	8.0	48	16.0
8b	8.0	24	8.0
8c	8.0	12	4.0
10a	10.0	48	20.0
10b	10.0	24	10.0
10c	10.0	12	5.0

Steady-State Sampling

Steady-state conditions at a specific loading are assumed to exist if daily average gas production rate is relatively constant for at least three detention times. This is termed "pseudo steady-state" conditions. Samples are taken at various depths in each SMAR using the following procedures:

(1) Gas meters are first read and gas is sampled for immediate methane analysis using a GC.

(2) Influent flowrate is measured and influent is sampled, acidified, and refrigerated for later COD analysis.

(3) Gas line is disconnected at location between vapor traps and separation bottles.

(4) With the influent running, liquid samples and/or attached samples are taken from various heights of each SMAR from top to bottom.

In the runs when samples are analyzed for activity, additional care is taken to avoid oxygen exposure. This is done by purging sampling bottles (1 L, plastic) with N_2 gas right before sampling. Also, when taking samples from the SMARs, a tube is used to discharge samples below the liquid levels in the sampling bottles.

Analytical Methods

Operation of the SMAR system involves very intensive analytical work on a routine basis. Table 11 summarizes the analyzed items and the methods used in this study. These methods were constantly checked for reliability and efficiency as the study progressed, using the quality control program suggested by USEPA (1979). The TC method of COD analysis developed in this study is the outcome of application of the quality control program.

TABLE 11. Summary of analytical methods used in this study

parameter	Method	Samples	Frequency
Biogas			
Gas production	Wet Test meter	Biogas	Daily
Methane content	GC	Biogas	Weekly and S.S.[a]
Biomass			
Solids	Standard Methods	Effluent	Weekly and S.S.
		Ports	S.S. only
Activity	AMA[b]	Ports	S.S. only
Liquids			
pH	pH meter	Effluent and ports	Daily and S.S.
Alkalinity & Total V.A.	Titration	Effluent	Initially only
SCOD & TCOD	TC method[c]	Inf & Eff	Weekly and S.S.
SCOD		Ports	S.S. only
C2-C5 acids	GC	Ports	S.S. only
Nitrogen	Standard Methods	Feed	Initially only
Phosphate	Standard Methods	Feed	Initially only
Li	AE[d]	Effluent	Tracer study
Co,Ni,Ca,Mn,Zn	AE	Feed	Initially only

[a]Steady state.
[b]Acetoclastic methanogenic activity test (this study).
[c]Titration-calibration curve method (this study).
[d]Atomic emission.

Gas Production and Analysis

Gas production of each SMAR is measured using a Wet Test gas meter.[10] These meters are of the liquid-sealed, rotating-drum type and have been calibrated in the factory with an accuracy within 0.5% and a smallest division of 0.001 ft^3. Daily average gas production rate (L at STP/day) is calculated as follows:

$$GSTP = 28.3 \left(\frac{r2-r1}{t2-t1}\right)\left[\frac{(P1+P2)/2}{760}\right]\left[\frac{273}{273+(T1+T2)/2}\right] \qquad (49)$$

where, subscripts "1" and "2" refer to readings at Day 1 and Day 2 respectively; "r" is the gas meter reading in ft^3; "t" is the time of reading in day; "P" is the barometric pressure in mm Hg; and "T" is the gas temperature in ^oC. The above equation uses an average measurement of Day 1 and Day 2 for temperature and pressure corrections to STP conditions, i.e., 0^o C and 1 atm. Vapor pressure was not corrected for since it is considered to be minor for this study.

Gas is analyzed for methane content using a gas chromatograph with a thermal conductivity detector. Gas samples are taken in the line between H_2S scrubbers and gas meters using a syringe[11] and are analyzed immediately. Table 12 shows the operating conditions of the gas chromatograph for gas analysis. Two standards used for calibration

---

[10]Precision Scientific Co., Cat. No 63110, Chicago, Illinois.

[11]Gastight series 1000, Model #1001-TTL, Stock #81320, Hamilton Company, Reno, Nevada 89520.

contain 10% methane and 10% carbon dioxide,[12] respectively, each in a 90% nitrogen bottle. The standards are accurate to within 2%. Peak area was used for calculating the response factor. Peak identification and integration were done with a Sigma Console[13] data station.

TABLE 12. GC operating conditions for biogas analysis

Gas chromatograph	Packard Model 7411S
Column	10 ft by 4 mm glass
Packing	Porapak Q, 80/100 mesh
Temperature	60° C
Carrier gas	Helium
Flowrate	25 mL/min
Column pressure	60 psig
Detector	Thermal conductivity
Temperature	80° C
Bridge current	225 mA
Sensitivity	10 mA
Injector block temperature	80° C
Sample size	600 μL

[12] CO_2 standard--Stock # 61224, CH_4 standard--Stock #60124, Hamilton Company, Reno, Nevada 89520.

[13] Perkin-Elmer Corporation, Norwalk, Connecticut.

Solids and Activity

Suspended solids concentrations were determined for both total and volatile fractions. The Standard Methods (1985) 209D (103-105° C for TS) and 209E (550° C for VSS) were followed. A sample size of 10 to 100 mL was used, depending on the solids contents. The fiber glass filters used were of 4.25 cm Whatman GF/C.[14] An aluminum planchet was used to hold the filter. The planchet and filter were weighed together because the filter often got stuck with the planchet after filtration. Analyses were run in duplicate. When an activity test was performed, suspended solids were analyzed after the activity test using samples from the incubation flasks.

In order to determine the activity of biomass taken from various depths of each SMAR, an activity test was developed as a part of this study. Appendix C outlines the experimental procedure. The theory of the activity test is only briefly discussed here. A more detailed discussion is in the chapter on Results and Discussion.

The activity test used in this study measures the biomass specific methane production rate in terms of L CH_4 (STP) produced/gm VSS/day. A suitable volume (300-400 mL) of biomass is first obtained from each SMAR and directly transferred into a 500-mL incubation flask previously purged with N_2 gas. The flask is immediately capped and a certain amount of Na_2S is added to reduce oxygen exposure. After stabilization for 1-2 hours in a 35° C constant temperature room, an excess amount of acetate

[14]Whatman Ltd., England.

is added into the flask using a syringe. Gas production is then measured with a manometer throughout the entire incubation period. Figure 19 shows the experimental setup for the activity test.

After incubation, the manometer is calibrated by withdrawing a certain volume (such as 2 μL) of gas from the flask and recording the corresponding changes in manometer reading. A calibration curve can then be established with several withdrawals. To convert daily gas production (v_p, 35^0 C) from operating to STP conditions (v_s at 0^o C and 1 atm), the following equation is used:

$$v_s = v_p\left(\frac{T_s}{T_p}\right)\left(\frac{P_p - e + h}{P_s}\right) \qquad (50)$$

where, the subscript "s" and "p" refer to the standard and operating conditions, respectively; "T" is the absolute temperature in Kelvin; "P" is the barometric pressure in cm of manometer liquid (P_s = 76.0 cm Hg = 349.2 cm M.L.); "e" is the water vapor pressure at the incubation temperature in cm of M.L. (e = 4.22 in Hg = 19.4 cm M.L., at 35^0 C); and "h" is the manometer reading in cm of M.L.

Methane production is taken as 50% of the gas production according to the stoichiometric relationship for acetate methanogenesis. Methane production is then converted to STP conditions (0^o C and 1 atm). Finally, total incubation volume is measured and VSS are determined. The acetoclastic methanogenic activity (AMA) can then be calculated as the initial linear slope of the methane production curve divided by the total

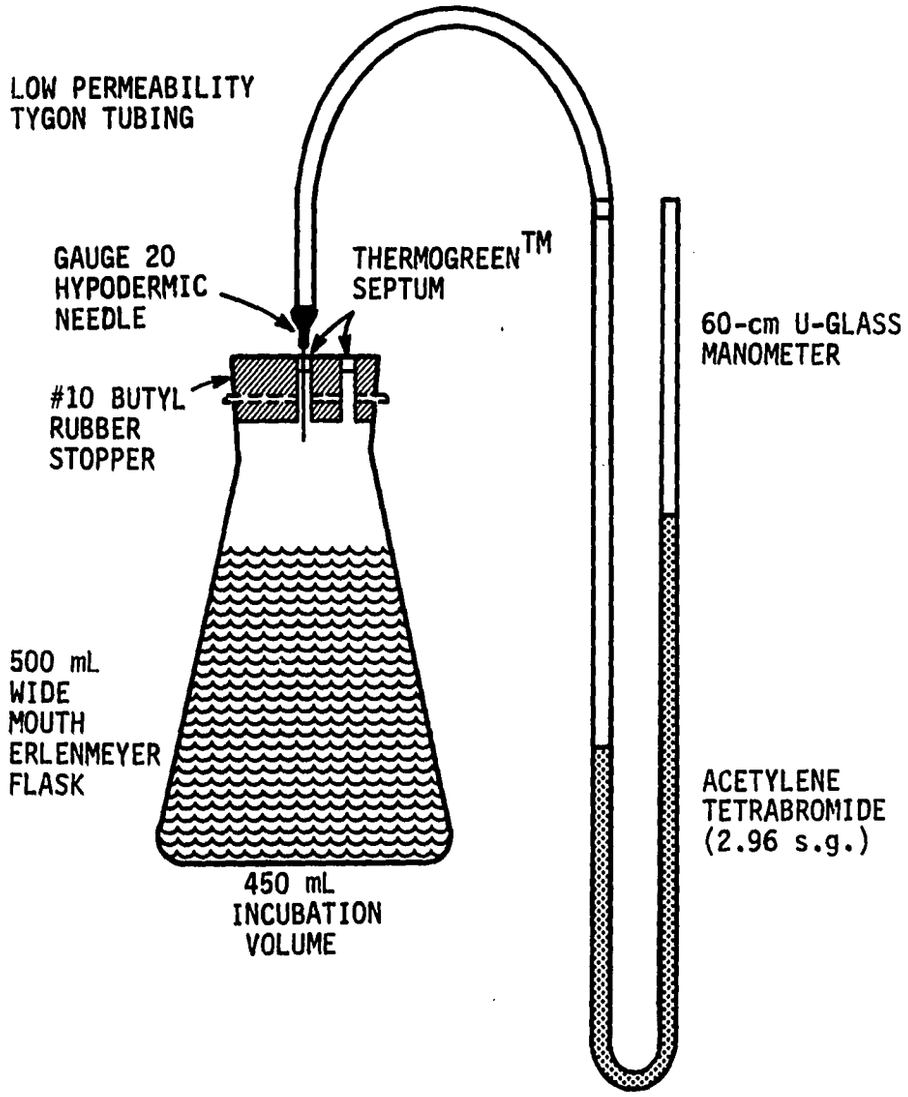

FIGURE 19. Schematic setup for AMA test

incubation biomass (as VSS), and expressed in mL CH_4 (STP) produced/d/g VSS.

The test is based on the assumption that the methanogenic biomass growth is minimal during the incubation period (usually less than 10 hours) and that a zero-order substrate utilization rate exits. It is felt proper for the test since most of the acetoclastic methanogens found so far have regeneration times of over 24 hours. Also, according to Michealis-Menten kinetics, the substrate utilization rate approaches zero order at high substrate concentrations which can be controlled by an F/M (Food/Microorganism) ratio. The minimum growth ensures a fixed amount of biomass to be tested, while the zero-order utilization rate ensures the independence of the methanogenesis rate on substrate concentration so that a constant rate can be established throughout the incubation period. Table 13 summarizes the test criteria for the AMA test.

pH, Alkalinity, and Total Volatile Acids

pH was measured using a digital pH meter.[15] The pH probe used is a glass electrode with a separate temperature-compensation probe. The accuracy of the meter is 0.01 pH unit. Two standard buffer solutions of pH 7.0 and 4.0 were used for the calibration. The same pH meter was used during alkalinity measurements to determine the titration endpoint.

[15]Hanna Instruments, HI 8417 microprocessor bench pH meter, Risorgimento, 3510 LIMENA (Padova), Italy.

TABLE 13. Summary of test criteria for AMA test

No.	Parameters	Test criteria
1.	Incubation flask	500-mL wide mouth Erlenmeyer flask
2.	Incubation volume	300-400 mL
3.	Maximum AMA assumed	1.0 L CH_4 (STP)/gm VSS/d
4.	Maximum biomass used	0.5 gm VSS
5.	Substrate added	1.67 gm HAc
6.	Minimum F/M	2.23-3.35
7.	Minimum degree of substrate saturation	94.3-96.1%
8.	Mixing	Gentle hand mixing 30 sec every 30 min.
9.	ORP control	1-2 mM sulfide

Alkalinity was determined by potentiometric titration with an endpoint pH of 4.0. The alkalinity and total volatile acids were intensively studied using the direct titration method of DiLallo and Albertson (1961) during an upset period for the SMAR process. A sample size of 50 mL was used. Both the titrants of H_2SO_4 and NaOH solutions had a normality of 0.05 N.

Chemical Oxygen Demand

COD was used as the major index to indicate treatment efficiency for the SMARs. Both total COD (TCOD) and soluble COD (SCOD) were run for SMAR effluents. SCOD refers to the COD of the sample filtrate with a glass fiber filter, which was also used for suspended solids analysis.

The micro closed-reflux method was used since this allowed many samples to be run more efficiently. The closed-reflux method generally gives a higher COD recovery ratio than the Standard Methods 50-mL open-reflux method (about 10% higher). Throughout this study, many versions of the micro method were tested. This includes the USEPA method 410.4 of 2.5 mL sample size (1978), the Zimpro method of 5.0 mL (1980), and the Standard Methods 508B of 5.0 mL (1985). Unfortunately, none of the above methods were considered suitable for this study. The USEPA method uses a sample size that is too small to be adequately reproducible and is only good for use with an Auto Analyzer. The Zimpro method is highly subject to interference by the silver-mercury precipitates in spectrophotometric reading. The Standard Method is not efficient when dealing with a large

number of samples as in this study. Consequently, a new method was developed for this study (Chiang and Seagren, 1987). Table 14 compares all these methods by sample size, dichromate normality, maximum COD measuring capacity, and sensitivity.

TABLE 14. Comparisons of several micro COD methods

	USEPA Method 410.4		Zimpro 166	Standard 508 B	TC Method
	(Auto)	(Others)			
Sample size (mL)	2.5	10.0	5.0	5.0	5.0
Dichromate (N)	0.208	0.208	0.67	0.10	0.25
(mL)	1.5	6.0	1.5	3.0	3.0
Acid (mL)	3.5	14.0	6.5	7.0	7.0
Total (mL)	7.5	30.0	13.0	15.0	15.0
Max. COD (mg/L)	1000	1000	1608	480	1200
FAS (N)	Spec.	Spec.	Spec.	3.0	5.0
Sens. (mg/L/mL)				160	240
(mg/L/Abs)	3300	-	2900		

The new method uses a titration procedure in conjunction with a calibration curve which is established using standard solutions. The method is therefore termed the titration-calibration curve (TC) method.

The method is considerably faster than the Standard Method and has an equal or better reproducibility. As with the Standard Methods, the TC method developed in this study uses a nominal volume of 5 mL for samples, 3 mL for potassium dichromate solution, and 7 mL for sulfuric acid reagent. The mercury and silver requirements are also the same as in the Standard Method. However, the dichromate normality is raised to 0.25N to give a maximum measuring capacity of 1200 mg/L COD. The normality of the ferrous ammonium sulfate (FAS) titrant is raised to 0.15 N. This gives the TC method a sensitivity of 240 mg/L COD per mL of FAS added. Five potassium hydrogen phthalate (KHP) standard solutions (50, 100, 250, 100 mg/L COD) were used to establish the calibration curve. An Autopipet[16] with a maximum volume of 5 mL and reproducibility of 0.5% was used to add the samples and all the reagents for the TC method.

The test tubes used for the TC method were 20 mm by 150 mm Pyrex with a Teflon-lid screw cap. The titrations were performed directly into the test tubes after a 2-hour digestion period at 150° C in an oven. The endpoint of the titration was considered to be the first sharp color change from blue-green to reddish brown. Mixing was done by a magnetic stirrer with a 1/2" stirrer bar. The buret used had a smallest division of 0.1 mL and a total volume of 25 mL.

---

[16]Fisher Scientific, Cat. No. 13-689-25.

Individual and Total Organic Acids

Besides the total volatile acids measured by the direct titration method, as described previously, the individual organic acids were also measured using a gas chromatograph. A Hewlett-Packard[17] chromatography system and data-processing software of Maxima[18] Chromatography Workstation (Version 2.1, 1985) were used in the study. The glass column used was 6 feet long by 2 mm in diameter and was packed with GP 60/80 Carbopack C.[19] The column was capable of separating ppm levels of 2-methyl and 3-methyl butyric acids. Table 15 lists the GC operating conditions for the organic acids analyses.

The samples for organic acids analysis were taken from the SMARs and immediately filtered with a fiber glass filter. The filtrates were acidified with concentrated phosphoric acid to pH 2-3 (sulfuric acid will destroy the column packing materials used in this study). The acidified filtrates were then preserved in 2-mL vials,[20] which were covered with Teflon-coated lids and clamped with aluminum caps. A microsyringe[21] was used to withdraw samples from vials and adjusted to 1 μL for direct injection into the column. Four standard solutions, which contained six

---

[17]Hewlett-Packard, Avondale, PA 19311.

[18]Dynamic Solution Corporation, Ventura, CA 93003.

[19]Supelco, Inc., Bellefonte, PA 16823-0048.

[20]Cat. no. 3-3121, Supelco, Inc., Bellefonte, PA 16823-0048.

[21]Microliter series 700, Model #701-L, Stock #80300, Hamilton Company, Reno, Nevada 89520.

TABLE 15. GC operating conditions for volatile acids analysis

Gas chromatograph	Hewlett-Packard 5730A
Column	4 ft by 4 mm ID glass
Packing	GP Carbopack C/0.3% Carbowax 20 M/0.1 % H_3PO_4
Detection limit	ppm level
Temperature	120° C
Carrier gas	Helium
Flowrate	50 mL/min
Detector	Flame ionization
Hydrogen/air flowrate	40/240 mL/min
Temperature	200° C
Injection port temperature	200° C
Sample size	1.0 μL
Data station	Maxima data station

volatile acids of interest (acetic, propionic, iso-butyric, n-butyric, isovaleric, and n-valeric acid), were used to establish the calibration curves. Table 16 shows their concentrations. In some cases, where the 2-methyl butyric acid was also identified, the average response factor of 3-methyl butyric (isovaleric) and the n-butyric was used for determining the 2-methyl butyric concentrations. The Maxima data station allows for automatic data acquisition during the analysis. With the data station,

output signals can be retrieved to identify all of the possible peaks. These peaks were then re-integrated for peak areas. Without the data station, meaningful analysis would be difficult.

TABLE 16. Volatile organic acids standard solutions in mg/L

Volatile Acids	Std 1	Std 2	Std 3	Std 4
Acetic	50	250	500	1000
Propionic	50	150	300	500
iso-Butyric	10	50	100	150
n-Butyric	10	50	100	100
iso-Valeric	10	50	75	100
n-Valeric	10	50	75	100

Nitrogen and Phosphate

Total Kjeldahl nitrogen and total phosphate were analyzed to determine if they were adequate in the feed milk solution for nutritional requirements. These tests were done by the Analytical Services Laboratory (ASL) at Iowa State University. The procedures of Standards Methods were followed using a Technicon Auto Analyzer.[22]

[22]Technicon Industrial Systems, Tarrytown, NY 10591.

Metals (Li, Co, Ni, Ca, Mn, Zn)

All metals were measured using a Perkin-Elmer Atomic Absorption Spectrophotometry System[23] with a flame emission (AE) method. Except Li^+, all metals were determined by the Analytical Services Laboratory at Iowa State University. Li^+ was determined for tracer studies and the other metals were for a nutritional check on the feed milk solution. Table 17 shows the AA operating conditions for Li^+ analysis.

TABLE 17. AA operating conditions for Li^+ analysis

Chopper mode	Flame emission
Burner head	2 and 3/4 inches
Burning gases	C_2H_2-N_2O
C_2H_2 pressure	8 psig
N_2O. pressure	30 psig
Flame wavelength	323.3 nm (VIS)
Flame angle	0°
Slit width	0.7 nm
Sensitivity	10.0 mg/L

[23]Model 305B, Perkin-Elmer Corporation, Norwalk, CT 06856.

Effluent samples from the clean-bed tracer studies were analyzed directly while samples from dirty-bed studies required filtration. Approximately 30-mL samples were collected at each sampling. Samples were then ionized by adding about 0.5 gm of NaCl. Five standard solutions of Li^+ (0.05, 0.1, 0.5, 1.0, 2.0 mg/L as Li^+) were used. The standards were run every 20 sample analyses and the two standard runs before and after the sample runs were averaged for calibration. A method of averaging ten consecutive determinations by GC was used for each sample to even the noise for better reproducibility.

RESULTS AND DISCUSSION

Design and Operation

Design of the SMAR System

The three SMARs used in this study were built with height to inside diameter ratios of 1.2, 4.1, and 14.3 for SMARs A, B, and C, respectively. The range of the ratios covered those used in many other pilot studies, such as 3.6 by Young and Dahab (1982), 12.2 by Song and Young (1985), and 13.1 by Young and McCarty (1969). Three full-scale SMARs, however, have very low ratios of 1.3 (Taylor, 1972), 0.7 (Witt *et al.*, 1975), and 0.6 (Roe and Love, 1984).

The height of SMAR C was 282.8 cm (9.3 ft) and might be the highest lab-scale SMAR ever studied. Most lab-scale SMARs have dimensions similar to those of Young and McCarty (1969) with a height of 180 cm (6.0 ft) and a diameter of 14 cm (5.5 in). Two full-scale SMARs packed with low-porosity stones are much deeper, with heights of about 20 ft (6.1 m) by Taylor (1972) and 30 ft (9.1 m) by Witt *et al.* (1979). One recently designed full-scale SMAR, termed the "shallow bed anaerobic reactor", has a height of 10 ft (3.3 m) and is packed with high-porosity cross-flow plastic media (Roe and Love, 1984). The packing volume of the three SMARs used in this study is about 85 L, which is 2-5 times larger than most other pilot studies but about one-third the volume used by Young and Dahab (1982).

Operation of the SMAR system

The suspended growth sampling ports appear to be properly sized for all the loadings studied, except for one run with the highest loading rate (Run 10a), in which the lowest sampling port of SMAR C was clogged. The attached growth sampling devices failed to seal properly due to degradation of the internal o-rings under long-term exposure to the anaerobic environment. This was especially serious in SMAR C at the lower sampling heights, probably due to higher hydrostatic pressures.

The use of the bottom distribution plates and the attached growth sampling devices to prevent short circuiting appears appropriate as indicated in the clean-bed tracer study with no air recycling (Run 0c). However, as also indicated in the clean-bed tracer study with air recycling (Run 0cG), it seems that the top distribution plates should have been designed to reduce short circuiting under operating conditions. The packing used in this study was plastic Flexiring with a nominal size (D_p) of 5/8 inch (16 mm). This gives I.D./D_p ratios of 28.0, 18.6, and 12.3 for SMARs A, B, and C, respectively. The I.D./D_p ratio should be greater than 8 to minimize wall effects (Young, 1985).

The entire line-up of the SMAR system appears to be appropriate after several corrections during the first few months of operation. This is discussed briefly below. A T-tube was initially used for each SMAR to serve as a gas-liquid separator at a height of about 50 cm above the common discharge reservoir. The H_2S gas scrubbers were placed about 50 cm above the T-tubes. It was found that liquid was carried over through

the gas line and flooded the H_2S gas scrubbers. Also, the siphon breaks often spilled and resulted in inconsistent gas measurement. Replacing the T-tubes with three 500-mL respiratory bottles and placing each bottle at the effluent height of each SMAR solved the problem.

The use of rotameters to measure gas recycle flowrate in the latter phases of the study created some unexpected problems. The gas produced was wet at the operating temperature of 35° C, even after passing the gas through a water trap. Measurement of the wet gas recycle flowrate had never been possible because the floats in the glass tubes of the rotameters often got stuck. Removal of the water vapor from the gas with a desiccating agent, such as $CaCl_2$, is possible but requires very frequent replacement. Also, rotameter pressure reducers cannot be used for flow adjustment since they created back pressure and caused spilling in the siphon breaks.

The positive displacement Masterflex pump was not suitable for gas recycle to provide continuously smooth flow for accurate flowrate measurements using rotameters. Two big glass bottles (10 L) were then installed before and after the rotameters to dampen the surging, but accurate flowrate measurement with the rotameters was still difficult. Consequently, gas recycle flowrate had to be estimated by counting the rpm of the pumping rate and multiplying the rpm with mL/revolution of the tubing used. This is not likely to be accurate when the tubing is out of shape after a period of operation.

H_2S gas scrubbers were prepared by filling Fe_2O_3-coated wooden chips in 1000-mL glass bottles. The bottles often turned black within a few weeks, especially during operation at high loading rates. Uncovering of the bottles revealed that the scrubbers were not efficiently used due to an uneven packing of the wooden chips. On several occasions, packing in scrubbers was found to be too tight and created back pressure to cause spilling in siphon breaks. It is felt that wooden chips are not suitable to make efficient scrubbers due to their irregular shapes. Iron sponge with a proper size opening might be a better material for more efficient scrubbers.

The use of the dilution tank was the right choice. It was initially thought that direct injection of the stock solution and dilution tap water into the influent line was better, since this could save any routine cleaning of the dilution tank, which could easily allow growth at 35^{o} C. The direct injection method was used by Young and his associates (Young and McCarty, 1969; Young and Dahab, 1982; Song and Young, 1986). However, it was found that, with the substrate milk solution, uniform stock feeding with the Masterflex pumps was not possible due to deposition of milk in the tubes. The use of the dilution tank minimized the problem.

The SMAR system was operated for 415 days from the first seeding. The most serious and frequent operating problem was the clogging in the stock line. It was estimated that the clogging occurs in at least 50 day-times and caused tremendous delays. It was then decided to screen

the stock solution after it was prepared and clean the stock tank and stock line on a more frequent and routine basis. However, this did not completely solve the problem. The problem was inherent in the precipitating nature of the milk solution, especially when the concentrations of the stock solution increased to 150 g COD/L or above, as the loading rates increased. Sometimes the clogging occurred within hours.

In the latter phases of this study, it was also found that the milk solution coagulated and deposited in the bottom zone of the SMARs, especially for the SMAR C. It is felt that, although the powdered milk has a well-balanced nutrition and is relatively cheap, it is not suitable for the study like this, which required the use of a highly concentrated stock solution. In addition, preparation of a well homogenized milk solution with the powdered milk is laborious and time-consuming without a good mixing device.

Analytical Methods

The two analytical methods developed in this study, the acetoclastic methanogenic activity (AMA) test and the closed-reflux titration-calibration curve (TC) method for COD analysis, are discussed below.

AMA Test

The proposed AMA test procedure (Appendix C) was used to analyze over a hundred samples with a fair success rate. In general, the

anaerobic procedures of N_2 gas purging and sulfide addition are adequate in providing the anaerobic requirement. Stabilization for one hour after seeding is adequate for the depletion of air contamination obtained in sample transfer. Gentle hand mixing appears to be appropriate in data reproducibility. Reagent blank controls (no seed addition) often gave a vacuum reading of 1-2 cm M.L. (manometer liquid), probably due to CO_2 adsorption by the added sulfide. The vacuum became stable after about one-hour incubation.

A study was conducted to determine the reproducibility of manometer calibration and the effect of incubated volume on manometer calibration. Acetylene tetrabromide ($C_2H_2Br_4$) with a yellow dye added was used for the manometer liquid. This gives the manometer liquid a density of about 2.96 g/cm^3. Three 450 mL, one 460 mL, and one 440 mL were used for the incubation volume. The calibration procedures listed in Appendix C were followed, except that air was injected in, instead of being drawn out.

Figure 20 shows the calibration curves for the five runs used for manometer calibration. It can be seen from the curves that a greater incubation volume causes a smaller slope ($\Delta v_s/\Delta h$), and vice versa. Table 18 gives results of the least squares linear regression of the five calibration curves in Figure 20. The slopes ($\Delta v/\Delta h$) for the three 450-mL runs are essentially the same. All the runs show an almost perfect linear correlation.

One sample, obtained from SMAR A, was analyzed by four repetitions to determine the reproducibility of the AMA test. Figure 21 shows the

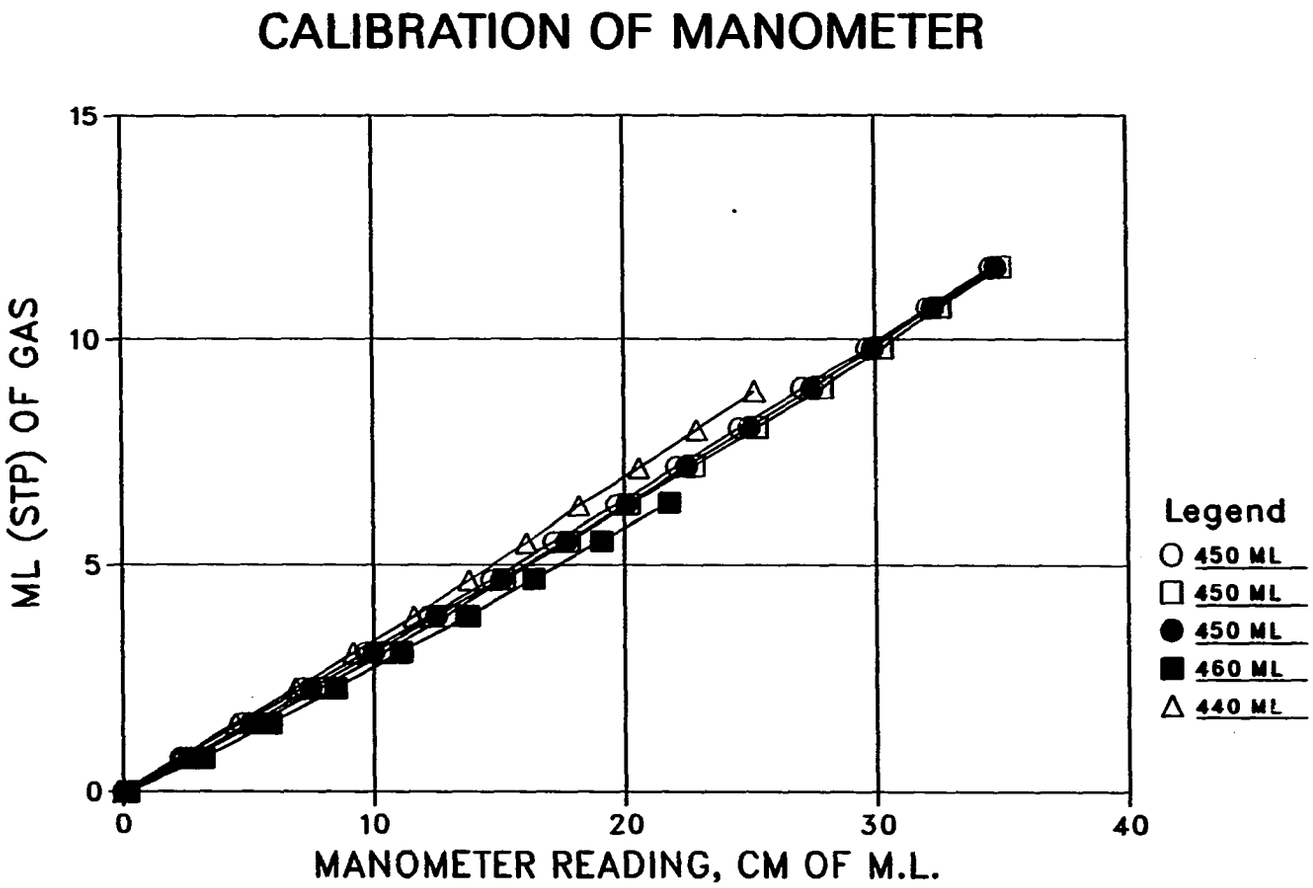

FIGURE 20. Effect of incubation volume on manometer calibration for AMA test, showing a greater slope with a smaller incubation volume, and vice versa

TABLE 18. Reproducibility study for manometer calibration

#Run	Incubation volume (mL)	Slope (mL/cm)	Intercept (mL)	Corr. coeff. (-)	Volume deviat. (%)	Slope deviat. (%)
1	450	0.334	-0.131	1.000	0.0	0.0
2	450	0.334	-0.299	0.999	0.0	0.0
3	450	0.334	-0.235	0.999	0.0	0.0
4	460	0.298	-0.186	1.000	2.2	-10.8
5	440	0.351	-0.103	1.000	-2.2	5.1

specific methane production curves. In general, the curves show a pattern of starting a short period of irregular gas production followed by a linear gas production. The linear gas production lasts for 5-6 hours and starts showing some degree of retardation if the gas was not removed from the incubation flasks. The retardation was likely resulting from the build-up of pressure (20-25 cm M.L.) in the incubation flasks.

The least squares linear regression of the linear sections of the curves indicates a correlation coefficient of over 0.99 for all four repetitions. The coefficient of sample standard deviation of AMA is 6.5% with a mean AMA of 0.39 L CH_4 (STP)/gm VSS/d.

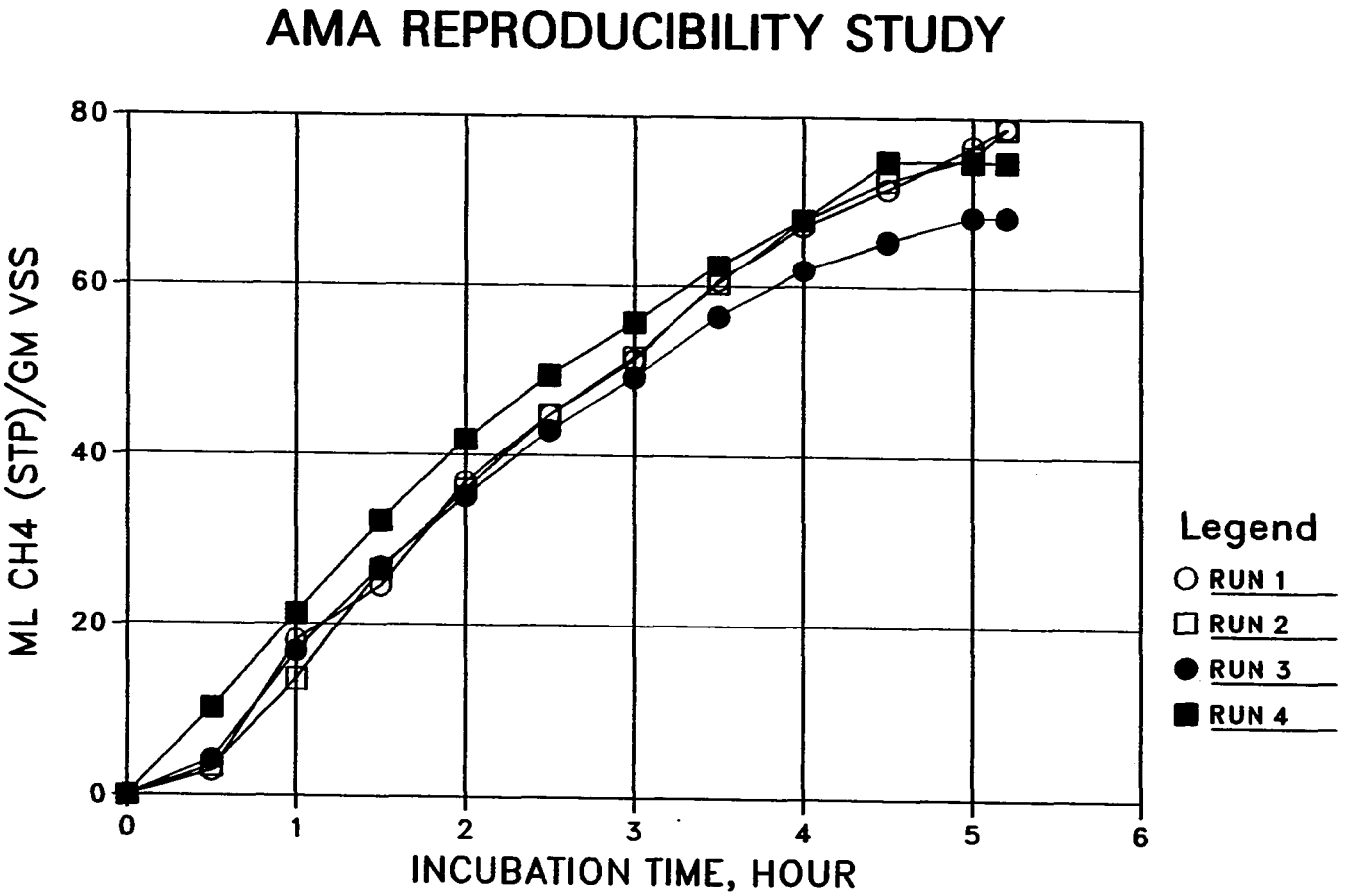

FIGURE 21. Reproducibility study for AMA test with four repetition runs, showing a good agreement in slope

TC method for COD Analysis

An experimental study was conducted to make a comparison between the TC method and the closed-reflux titrimetric method of Standard Methods with regard to reproducibility, speed, and variations in analyst for both high and low COD samples. The samples used for analysis were made using non-fat dry milk (NFDM). The low sample was estimated to have a strength of about 400 mg/L COD and the high sample a strength of about 1000 mg/L COD. The high NFDM sample required a dilution ratio of 2.5 to be within the measuring capacity of the Standard Method. Three repetitions were analyzed for both the low and high COD NFDM samples for each method. Two blanks for both the Standard and TC method and two FAS standardizations for the Standard Method were done along with the sample analyses.

Table 19 gives the COD analysis results performed by two operators. One is considered to be more skillful with the TC method. A comparison of the COD values shows that the results are close for the standards and samples between these two methods, except for the low NFDM samples done by operator A with the TC method. Even though the COD of the low NFDM sample done by operator A with the TC method gives a higher COD result, it appears to have the same degree of reproducibility as the other runs.

Figure 22 shows the two calibration curves obtained by the two operators with the TC method. Both curves show an almost perfect least squares linear regression with a correlation coefficient of 0.9998 and 0.9999 and a y intercept of 3.9 and 8.2, respectively. This suggests that the standard solutions were properly prepared and that the autopipet gave good reproducibility.

TABLE 19. Reproducibility and comparison study for TC method, COD in mg/L

Sample ID	Operator A		Operator B	
	Standard[a] Method	TC Method	Standard Method	TC Method
Std 50[b]	54	53	49	ERROR
Std 100	100	98	115	98
Std 250	255	243	254	246
Std 500	-	508	-	509
Std 1000	-	998	-	997
Low NFDM 1[c]	354	386	362	363
Low NFDM 2	355	378	369	365
Low NFDM 3	355	383	360	365
High NFDM 1	928[d]	940	930	929
High NFDM 2	940[d]	930	941	931
High NFDM 3	932[d]	943	937	926

[a]Standard Method 508B, closed-reflux, titrimetric method.

[b]Standard solutions of potassium hydrogen pthalate.

[c]Non-fat dry milk solutions, 3 repetitions.

[d]Samples were analyzed with a dilution rate of 2.5.

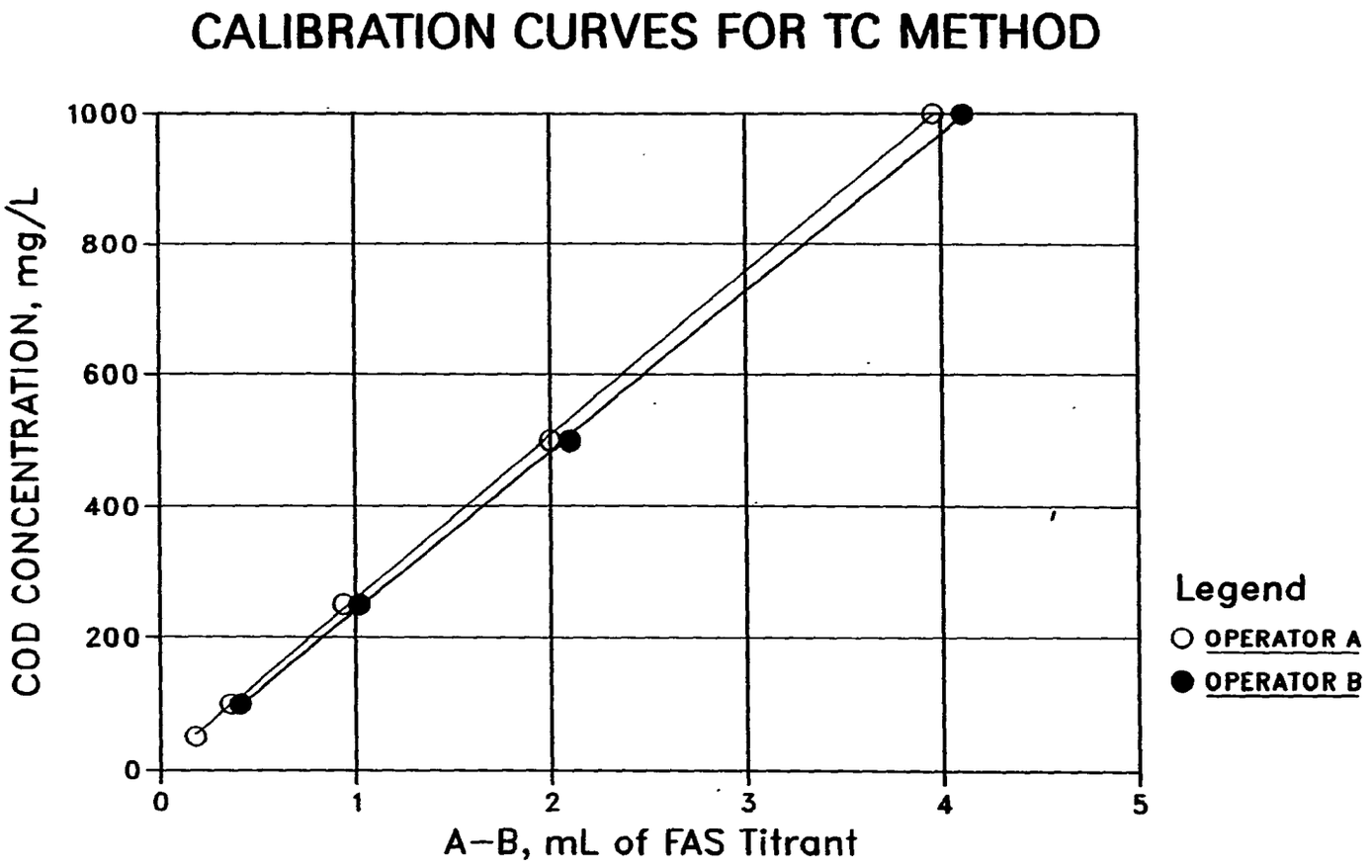

FIGURE 22. Calibration curves for TC method done by two operators

The results in Table 19 were used for a statistical analysis. As shown in the Table 20, the coefficient of variation (C_V) obtained with the TC method is higher than the coefficient of variation with the Standard method for operator A but lower for operator B. This suggests that the TC method developed in this study is at least as good as the Standard Method with regard to reproducibility. There was no significant difference in the reproducibility between the low and high NFDM samples being analyzed by both methods.

As also shown in the Table 20, the total setup time with the TC method for both operators was significantly reduced, with a time saving of 5-9 minutes out of a total run time of 20-40 minutes for analyzing 5 standards and 6 samples with 2 blanks. The setup time was defined as the time required to add the samples, dichromate solution, and sulfuric acid reagent to all of the test tubes used in each method. This suggests an advantage for the TC method when dealing with a large number of samples.

There are several other advantages to the TC method developed in this study. First, a calibration curve can always be established with a constant slope, even for a range of COD concentration not applicable to Beer's law. Second, with the establishment of the calibration curve, the system error due to that such as inadequate recovery can be minimized. And third, there is no need for standardizing the FAS titrant. However, caution should be taken to ensure that the volume used for samples, standards, blanks, and all reagents are close to the nominal volume specified in this method. This is especially important for dichromate in order that the maximum COD measuring capacity is maintained.

TABLE 20. Statistical analysis of COD data in Table 19

Sample ID	Standard Method			TC Method		
	$\bar{X}$[a] (mg/L)	s[b] (mg/L)	Cv[c] (%)	$\bar{X}$ (mg/L)	s (mg/L)	Cv (%)
			(Operator A)			
Low NFDM	355	1	0.2	383	4	1.0
High NFDM	933	6	0.6	938	7	0.7
Time[d] used	22 min. 28 sec.			17 min. 35 sec.		
			(Operator B)			
Low NFDM	364	5	1.3	365	1	0.4
High NFDM	936	6	0.6	929	3	0.3
Time[d] used	37 min. 41 sec.			28 min. 27 sec.		

[a] $\bar{X}$ = Sample average.

[b] s = square root of $[(X_i-\bar{X})^2/(n-1)]$.

[c] C_v = Variation of coefficient $=(100)(s/\bar{X})$.

[d] Time spent for samples and reagents addition only.

Tracer Studies

Two clean-bed tracer studies (before seeding) and two dirty-bed tracer studies (after seeding) were conducted during four different testing periods. All the studies were done with a retention time of about of 0.5 day, which was the shortest retention time used in this study. The responses of lithium concentrations (C_i) were normalized with the average influent lithium concentration (C_o = Total slug input/SMAR clean-bed liquid volume) and the time (T_i) with the theoretical retention time (T_d = SMAR clean-bed liquid volume/flowrate). Figures 23 through 26 compare the slug responses of the three SMARs for the four tracer studies.

All the response curves were analyzed for the mean time (T, the time length between the injection time and the centroid of the area under the curve), the standard deviation (σ), and the recovery ratio (R), using the following expressions:

$$T = \frac{\Sigma(t_{ai}C_{ai}\Delta t)}{\Sigma(C_{ai}\Delta t)} \tag{51}$$

$$\sigma^2 = \frac{\Sigma[(t_{ai}-T)^2C_{ai}\Delta t]}{\Sigma(C_{ai}\Delta t)} \tag{52}$$

$$R = \Sigma(C_{ai}\Delta t) \tag{53}$$

where,

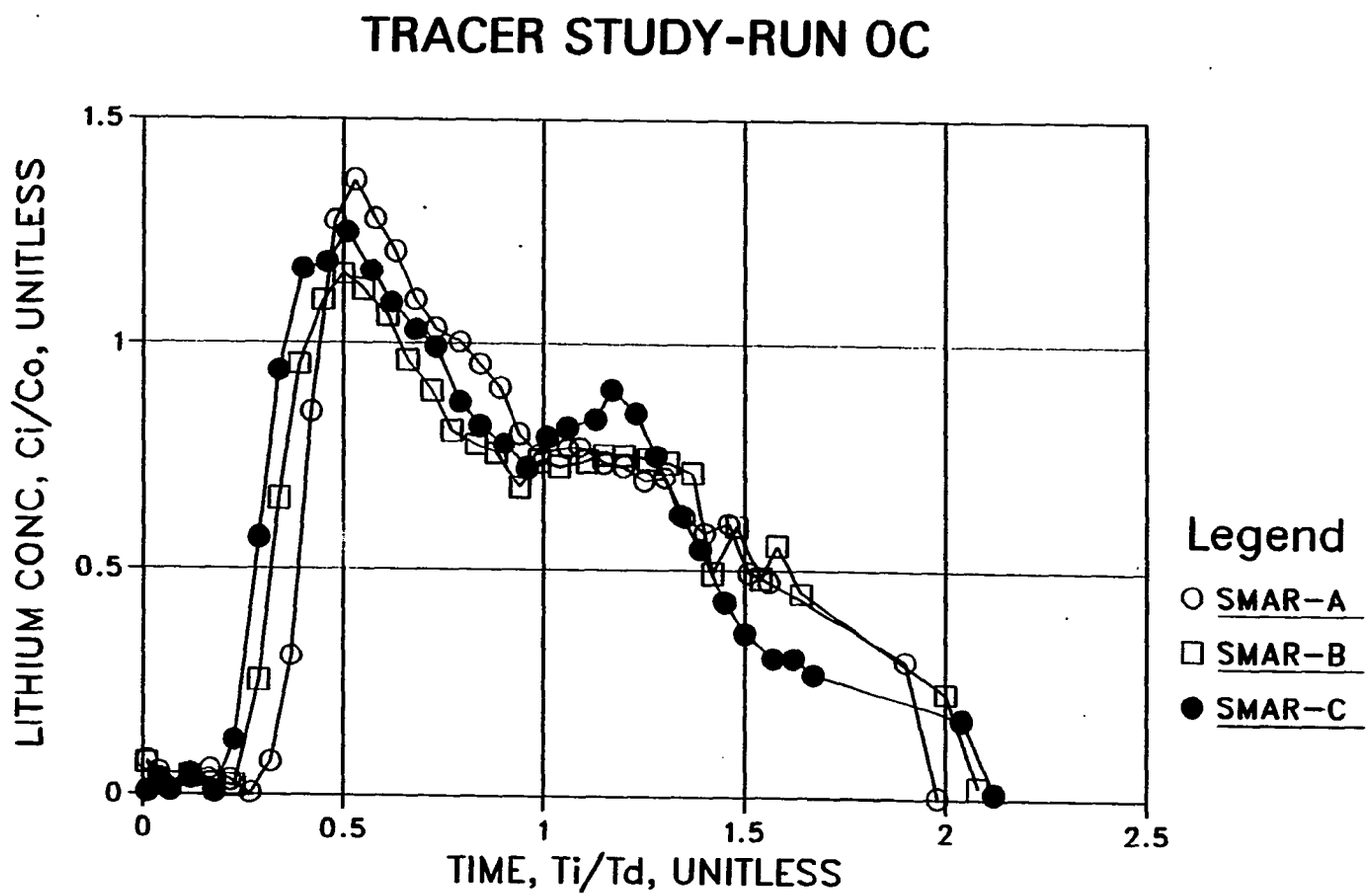

FIGURE 23. Clean-bed tracer slug responses with no gassing, Run 0c

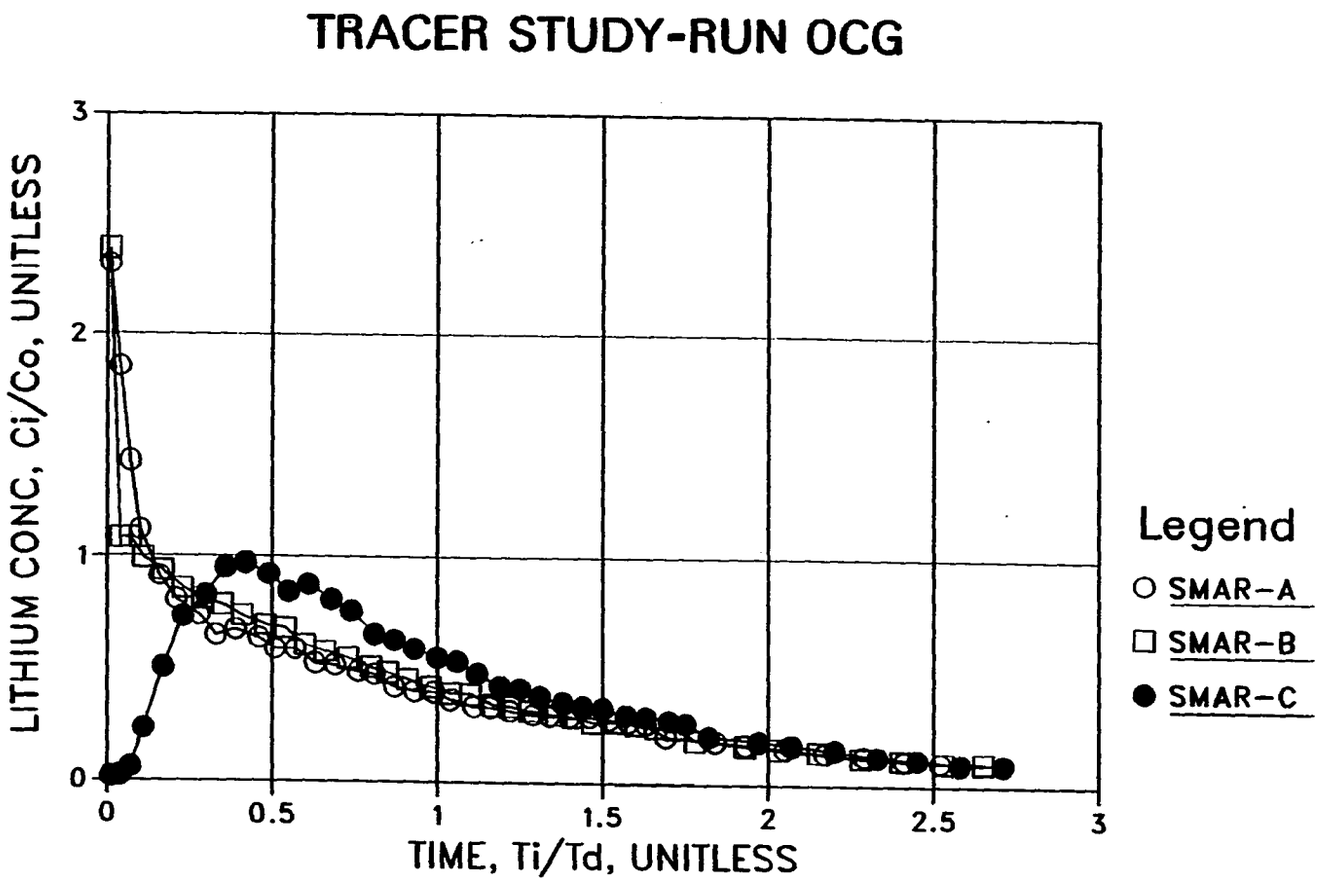

FIGURE 24. Clean-bed tracer slug responses with air gassing, Run 0cG (gassing G of about 40 1/s)

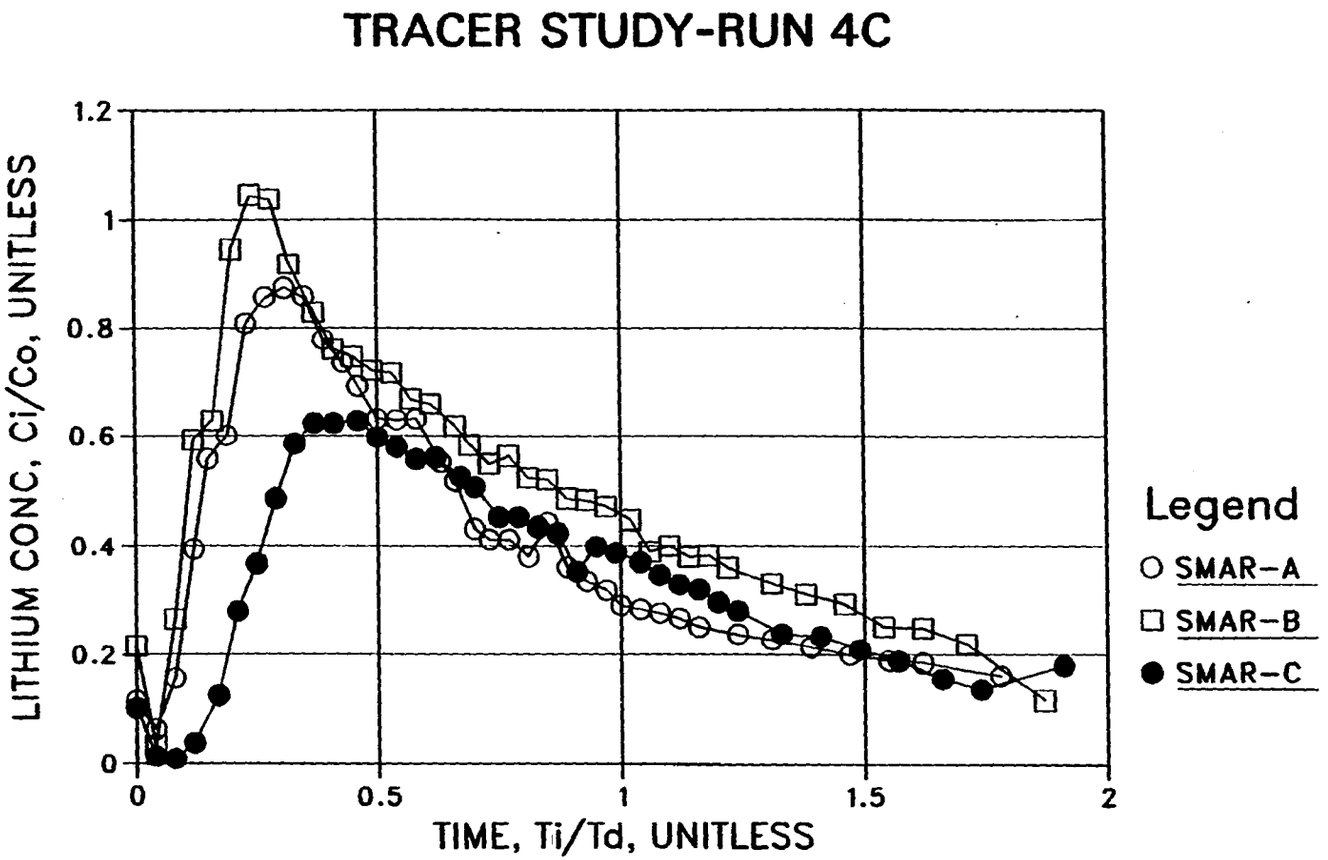

FIGURE 25. Dirty-bed tracer slug response, Run 4c (COD loading rate of about 4 g/L/d)

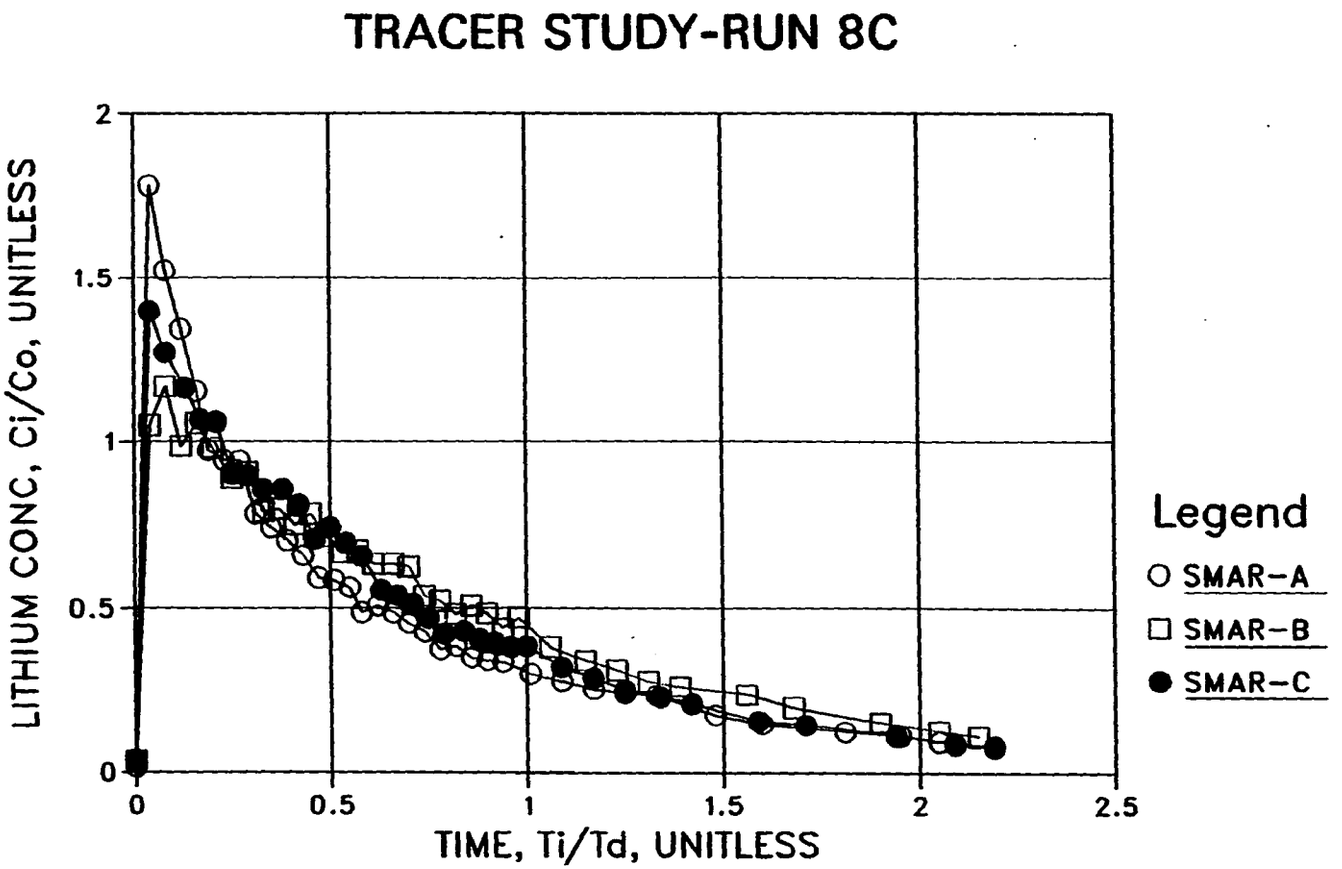

FIGURE 26. Dirty-bed tracer slug responses, Run 8c, (COD loading rate of about 8 g/L/d)

$$t_{ai} = (t_i + t_{i-1})/2$$

$$\Delta t_i = t_i - t_{i-1}$$

$$C_{ai} = (C_i + C_{i-1})/2.$$

The T and σ of each response curve were then used to calculate the dispersion number (N_d) using a longitudinal dispersion model (Levenspiel and Smith, 1957):

$$\sigma^2 = 2T^2[N_d - N_d^2(1-e^{N_d})] \qquad (54)$$

Table 21 shows the results of N_d, T, T/T_d, and the recovery rate (R) for the four tracer studies.

Clean-Bed Studies

Figures 23 and 24 were obtained under clean-bed conditions (before seeding) with and without air gassing, respectively. The following criteria for N_d are used to justify the flow patterns: 0 plug flow, between 0 and 0.002 small dispersion, between 0.002 and 0.025 intermediate dispersion, between 0.025 and 0.2 large dispersion, and ∞ completely mixed flow (Weber, 1972). With the flowrate tested under no gassing, Figure 23 shows that the three SMARs had about the same degree of dispersion with a dispersion number of 0.10-0.12. Based on the T/T_d, SMARs A and B had very little short-circuiting, while SMAR C (the tallest column) had a slight short-circuiting, probably due to a higher

TABLE 21. Results of SMAR tracer studies

Run#	SMAR	Flowrate (mL/min)	T_d[a] (hr)	Gasing (mL/L/min)	G[b] (1/s)	N_d[c] (-)	D_d[d] (cm^2/min)	T[e] (hr)	T/T_d (-)	R[f] (%)
0c	A	146	9.7	0.0	0	0.1	0.5	9.6	1.0	106
	B	146	9.2	0.0	0	0.1	2.9	9.2	1.0	107
	C	146	9.1	0.0	0	0.1	15.8	8.4	0.9	109
0cG	A	167	8.5	10.0	40[g]	0.9	5.7	6.6	0.8	93
	B	167	8.0	6.0	40[g]	0.8	22.9	6.5	0.8	96
	C	167	7.9	3.0	40[g]	0.3	48.0	7.5	1.0	99
4c	A	109	12.9	1.5	10[h]	0.3	1.2	9.0	0.7	63[i]
	B	109	12.3	1.5	20[h]	0.3	5.5	9.1	0.8	80
	C	109	12.1	1.5	30[h]	0.2	17.5	10.2	0.8	56[i]
8c	A	110	12.8	3.0	15[h]	1.0	4.3	7.6	0.6	80
	B	110	12.2	3.0	25[h]	0.5	10.4	8.7	0.7	89
	C	110	12.0	3.0	40[h]	0.9	92.1	7.2	0.6	81

[a]Retention time, based on clean-bed liquid volume.

[b]Mean velocity gradient.

[c]Dispersion number= $D_d/(v_x L)$.

[d]Eddy diffusion coefficient.

[e]Time length between injection and centroid.

[f]Lithium recovery ratio.

[g]By external air gassing.

[h]By internal biogas mixing.

[i]Due to loss in injection.

superficial velocity. The little short-circuiting for the three SMARs under clean-bed conditions indicates that the bottom distribution plates and the dispersion rings were properly designed.

Under external air gassing conditions, SMARs A and B had a very large dispersion with some degree of short-circuiting (Figure 24). Interestingly, with gassing, SMAR C became less short-circuiting, although the dispersion number (N_d) increased. Comparison between Figures 23 and 24 shows that single point air gassing at a mean velocity gradient (G) of about 40 1/s had a significant effect on the SMAR hydraulics; and the shorter the SMAR height, the greater the effect. Both clean-bed tracer studies had tracer recovery ratios of almost 100% for the three SMARs.

Dirty-Bed Studies

Figures 25 and 26 show the slug responses for the two dirty-bed studies with a COD loading rate of about 4 and 8 g COD/L/d, respectively. These two studies illustrate the SMAR hydraulic pattern under actual operating conditions, i.e., with (internal) gas mixing and biomass accumulation. In general, the hydraulic pattern was characterized by a large dispersion (N_d of 0.2-0.3) at about 4 g COD/L/d and a very large dispersion (N_d 0.5-1.0) at about 8 g COD/L/d. Compared with the clean-bed study with air gassing, both the dirty-bed studies indicate that biomass accumulation could cause significant short-circuiting with a T/T_d of 0.7-0.8 at a COD loading rate of about 4 g/L/d, and a T/T_d of 0.6-0.7

at about 8 g COD/L/d; and the greater the dispersion number, the greater the short-circuiting.

The configuration of the SMAR had significant effects on both N_d and T/T_d under dirty-bed conditions. Under operating conditions, it appears that the taller the SMAR, the less the short circuiting. However, at higher COD loadings (such as 8 g/L/d), SMARs that are too tall (such as SMAR C), might develop very serious short-circuiting due to a higher gas superficial velocity and accumulation of concentrated biomass in the lower parts of the SMAR. The slug responses of the four studies were also plotted for each SMAR in Figures 27 through 29.

The tracer recovery ratios of the two dirty-bed studies ranged from 80 to 88%, except for SMARs A and C with the 4 g/L/d run. These two exceptions were due to a loss in tracer injection and should not affect the estimation of N_d and T/T_d. However, inadequate recovery due to adsorption or absorption of the biomass could cause over-estimation of N_d and T/T_d.

Start-up and Acclimation

First Seeding

The start-up and acclimation procedures described in the previous chapter on Equipment and Substrate were followed. SMARs B and C were fully seeded. SMAR A was seeded only to about 70 L due to a shortage of seed. Warm tap water was pumped to SMAR A to make up for the full volume. It was estimated that 2.4 kg of solids were seeded to SMARs B and C and 2.1 kg to SMAR A, assuming a solids concentration of 3%.

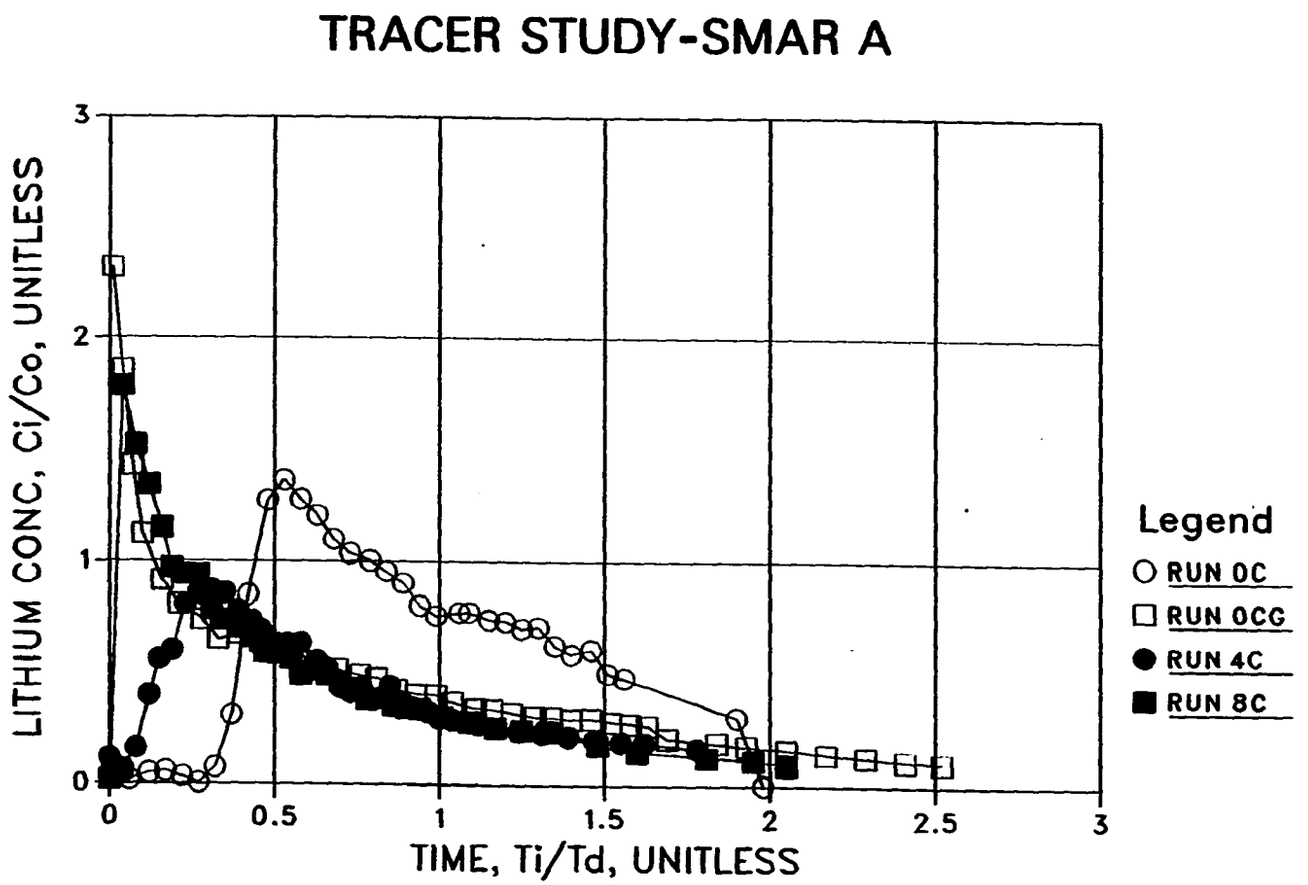

FIGURE 27. Tracer slug responses for SMAR A, Run 0c (clean bed, no gassing), Run 0cG (clean bed, gassing G of about 40 1/s) Run 4c (dirty bed, COD loading rate of about 4 g/L/d) Run 8c (dirty bed, about 8 g/L/d)

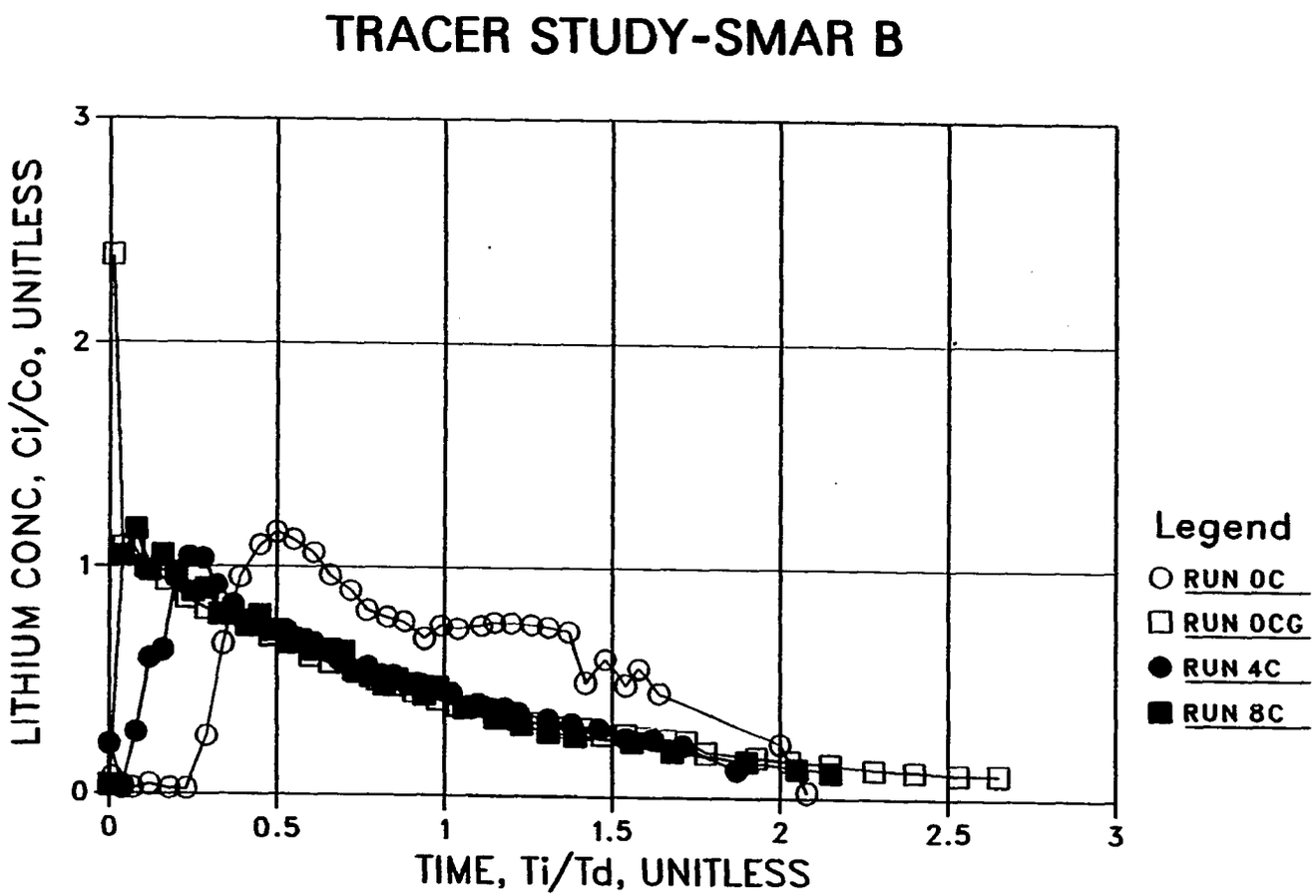

FIGURE 28. Tracer slug responses for SMAR B, Run 0c (clean bed, no gassing), Run 0cG (clean bed, gassing G of about 40 1/s) Run 4c (dirty bed, COD loading rate of about 4 g/L/d) Run 8c (dirty bed, about 8 g/L/d).

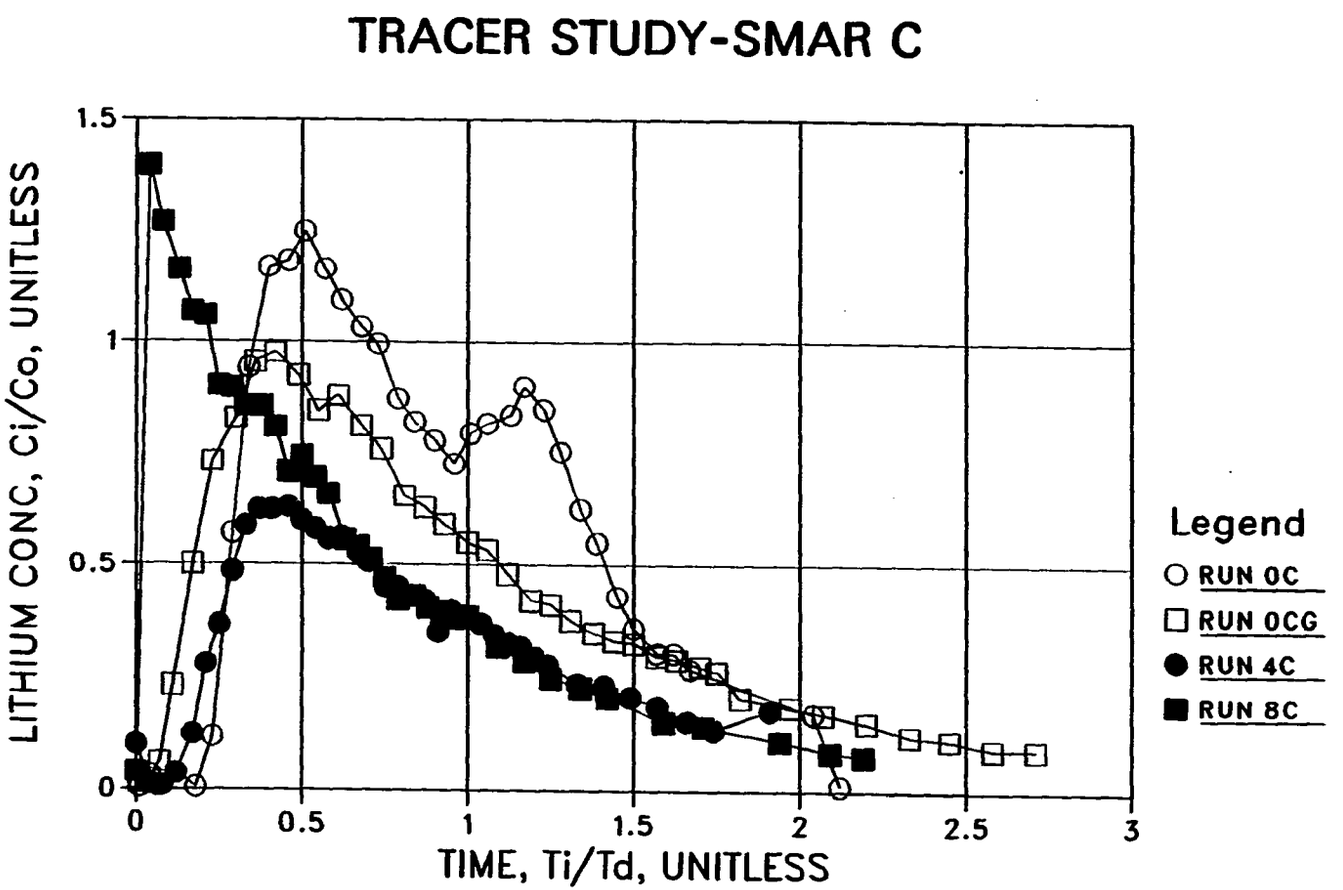

FIGURE 29. Tracer slug responses for SMAR C, Run 0c (clean bed, no gassing), Run 0cG (clean bed, gassing G of about 40 l/s) Run 4c (dirty bed, COD loading rate of about 4 g/L/d) Run 8c (dirty bed, about 8 g/L/d)

After seeding, the system was allowed to stand for 4 days to eliminate oxygen. The system was then fed with a solution of equal amounts of COD (about 60 g) of sodium acetate and NFDM in a batch mode once a day (for about 30 minutes) for 3 days before continuous feeding began. Continuous feeding started on day 8 after seeding with a COD loading rate of about 0.1 g/L/d and retention time of about 2.0 days.

Since the seeding was obtained from an anaerobic digester, acclimation in this study should have meant the requirement of (1) adapting the fermentative and acetogenic, but not the methanogenic, bacteria to the new NFDM substrate; and (2) establishing a new population balance among the three groups of bacteria at the operating conditions.

A certain amount of gas production was observed soon after seeding for all three SMARs, indicating a successful seeding. During the first few days after seeding, SMAR A had a gas production rate of about 15 L/day,[24] while SMARs B and C produced about 30 L/day. SMAR A produced less gas because it contained less seed. By the time of continuous feeding on day 8, the gas production rate was at about 10 L/day for all three SMARs. On day 14, approximately 3.0 L/day was metered for all SMARs with an initial COD loading rate of about 0.1 g COD/L/d. The COD loading was then increased to about 0.2 g/L/d on day 16 and then to about 0.4 g/L/d on day 21, with a corresponding gas production of about 3 and 6 L/d, respectively, for all SMARs.

---

[24]The standard conditions of 0° C and 1 atm are hereafter used for the daily average gas production in this study, unless specified.

During the initial acclimation period, the gas production for SMARs A and B were essentially the same at a rate of about 10 L/d (with a COD loading of about 0.4 g/L/d) until day 30, which was the 5th day after the loading was increased to about 1.5 g/L/d on day 26, with a greater gas production rate for SMAR A. After the 21st day, SMAR C, which is the tallest column, started showing a lower gas production rate than SMARs A and B, despite SMAR C being seeded heavier than SMAR A. The initial acclimation pattern is interesting and suggests that a greater hydrostatic pressure, as resulting from a deeper SMAR, might be a likely cause of inhibition in initial acclimation (Appendix D).

Unfortunately, the initial acclimation could not be further studied because gas production started dying off on day 31 due to a lack of buffering. On day 35, analyses on the effluent showed a pH of 5.5 and a COD greater than 1000 mg/L for all SMARs. Sodium bicarbonate was then added to the stock solution to give an alkalinity of 30 gm/L, as $CaCO_3$, on day 36. This unexpectedly increased the stock feeding rate to about 4.0 g/L/d (from 1.5 g/L/d), due to the addition of bicarbonate which reduced pump friction. Gas analyses on day 38 showed a methane percentage of about 30% for all the SMARs. The failure of the initial acclimation indicates that, without the addition of alkalinity, the SMAR system could not be acclimated to a COD loading rate higher than 1.5 g/L/d with the NFDM solution. The influent was shut off on day 40.

It was then decided to take the opportunity to study restarting acclimation by intensively analyzing effluent total volatile acids (TVA)

and total alkalinity (TAlk), using the dual titration method of DiLallo and Albertson (1961). The monitoring technique of TVA/TAlk, suggested by USEPA (1976) for digester operation, was also used. More bicarbonate (about 80 gm/d) was added to the dilution tank with warm tap water and pumped into the SMARs in a batch mode on days 43, 44, and 47.

The effluent TVA maintained at a level of about 1100 mg/L with a TVA/TAlk ratio of about 0.9 between days 42 and 47 for all the SMARs (Figure 30). The TVA/TAlk ratio was far beyond the range of 0.1-0.35, suggested by USEPA for successful digester operation. Despite showing a trend of decreasing TVA/TAlk ratio to about 0.7 on day 49, gas production was still extremely low at about 2.0 L/d for all the SMARs. This suggests that the restoration of the three SMARs during initial acclimation by simply adding bicarbonate was slow and not practical.

Second Seeding

It was then decided to partially reseed all the SMARs on day 50. Approximately 20 L of screened primary digester liquid (from the City of Ames Wastewater Treatment Plant) was pumped to each SMAR. In order to disperse the volatile acids accumulated in the lower parts of the SMARs, gas was recycled with a mean velocity gradient of about 20 1/s right after reseeding. The partial reseeding with gas recycle was remarkably effective. On the second day after reseeding, effluent TVA/TAlk dropped to about 0.15 (Figure 30) with an increase of TAlk to about 6000 mg/L as $CaCO_3$, and the effluent pH increased to about 8.0, for all the SMARs.

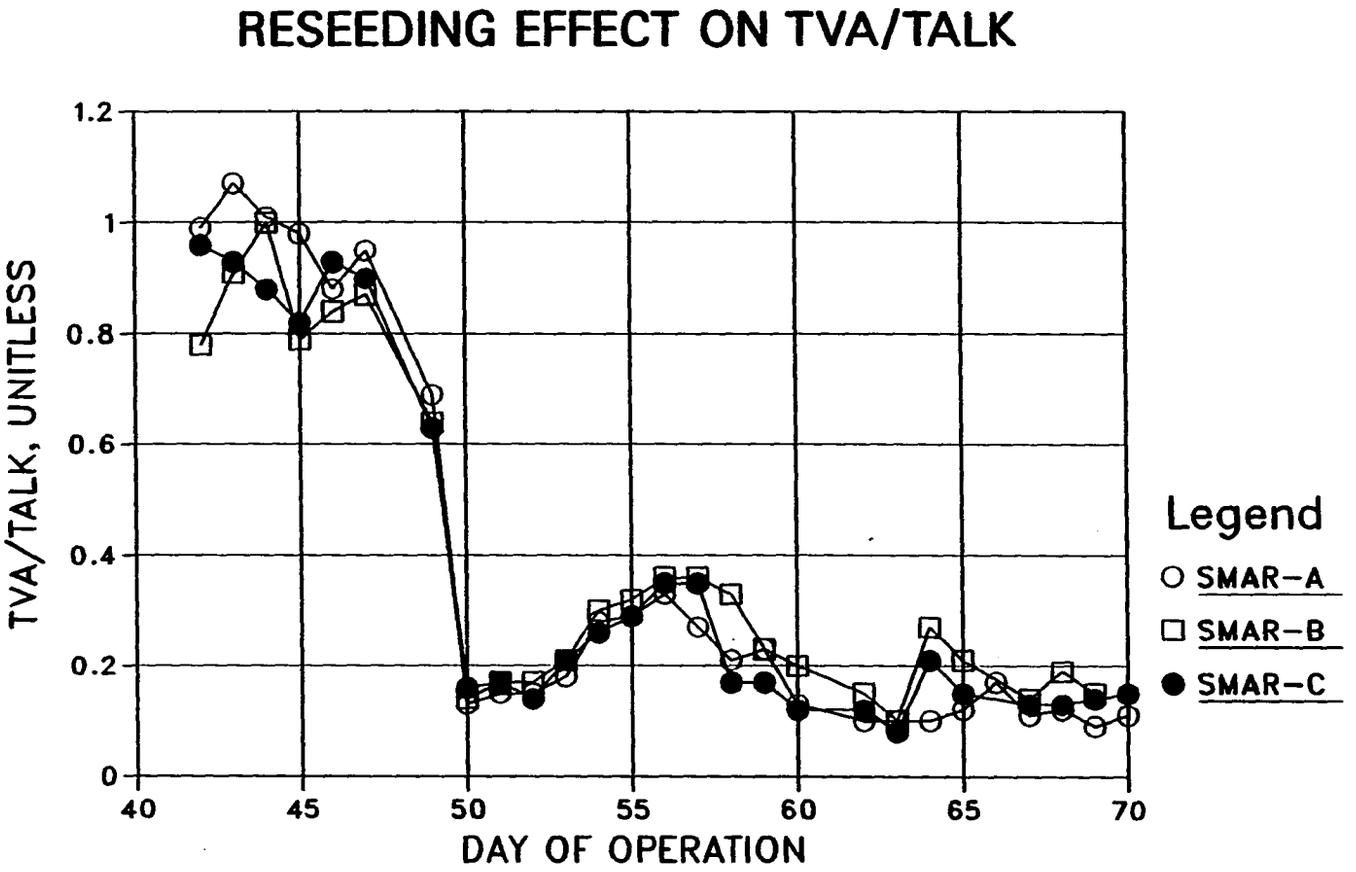

FIGURE 30. Effect of reseeding on the ratio of TVA/TAlk during initial acclimation period

Continuous feeding resumed on day 51 with a retention time of 2 days and a COD loading rate of about 0.2 g/L/d. An alkalinity addition of 1/4 of the feed COD was used. Gas recycle stopped on day 52 due to difficulties in metering the net gas production rate. Gas production started to take off and reached about 5 L/d on day 60 for all SMARs. By day 70, gas production had reached about 10 L/day at a COD loading rate of about 0.5 g/L/d. Gas analyses on day 72 showed methane content of about 88% for SMAR A and 85% for SMARs B and C. Interestingly, during the initial acclimation after the second seeding, SMAR C again produced the least gas, even under gas recycle conditions. However, there was no significant difference in gas production among the three SMARs after the initial period (Appendix D). The three SMARs were well acclimated on day 70 and ready for steady-state studies.

Pseudo Steady-State Performance

Pseudo steady state was assumed to be achieved at a specific operating condition if the gas production rate was relatively constant for a period of at least three hydraulic retention times under operation. Seventeen steady-state runs were conducted during the entire study. Table 22 lists the operating conditions of these steady-state runs.

In Table 22, the hydraulic retention times (HRT, hr) and COD loading rates (g/L/d) were calculated based on the clean-bed liquid volume at the packing height of each SMAR, i.e., the height of the highest sampling port. Alkalinity addition was based on the ratio of total

TABLE 22. SMAR pseudo steady-state operating conditions

#Run	Day	Alk[a] (g/g)	Q_{in} (mL/min)	COD_{in} (g/L)	SMAR	HRT[b] (hr)	OLR[c] (g/L/d)
					A	45.8	1.00
1a	225-228	1/4	27.5	1.91	B	46.4	0.99
					C	46.8	0.98
					A	45.2	2.19
2a1	173-177	1/4	27.9	4.13	B	45.8	2.17
					C	46.3	2.14
					A	46.3	1.95
2a2	250-257	1/4	27.2	3.76	B	46.8	1.93
					C	47.3	1.91
					A	23.2	1.82
2b	241-248	1/4	54.4	1.76	B	23.4	1.80
					C	23.7	1.78
					A	11.4	1.84
2c	258-269	1/4	110.8	0.87	B	11.5	1.81
					C	11.6	1.80
					A	43.7	4.28
4a	309-319	1/40	28.8	7.79	B	44.2	4.23
					C	44.7	4.18
					A	23.7	3.86
4b1	274-278	1/4	53.1	3.82	B	24.0	3.82
					C	24.3	3.78
					A	22.6	4.42
4b2	287-294	1/10	55.6	4.17	B	22.9	4.37
					C	23.2	4.32
					A	11.7	3.52
4c	295-300	1/20	107.5	1.72	B	11.9	3.48
					C	12.0	3.44

[a]Added alkalinity as $CaCO_3$/influent COD.
[b]Hydraulic retention time based on clean-bed liquid volume.
[c]Organic loading rate = influent COD/HRT.

TABLE 22. (continued)

#Run	Day	Alk[a] (g/g)	Qin (mL/min)	COD_{in} (g/L)	SMAR	HRT[b] (hr)	OLR[c] (g/L/d)
					A	23.4	6.47
6b1	336-345	1/40	53.9	6.31	B	23.7	6.40
					C	23.9	6.33
					A	22.8	6.55
6b2	346-361	1/40	55.3	6.22	B	23.1	6.47
					C	23.3	6.41
					A	46.0	8.90
8a.	326-335	1/40	27.4	17.07	B	46.6	8.80
					C	47.1	8.71
					A	43.9	10.20
10a	407-410	1/40	28.0	18.66	B	44.4	10.08
					C	44.9	9.98
					A	43.7	9.97
10aG1	411-412	1/40	28.8	18.18	B	44.3	9.86
					C	44.7	9.75
					A	46.2	9.22
10aG2	413-415	1/40	27.3	17.74	B	46.7	9.12
					C	47.2	9.02
					A	11.2	9.77
10c	383-391	1/40	112.7	4.55	B	11.3	9.65
					C	11.4	9.55
					A	12.0	11.87
12c	398-406	1/40	104.6	5.96	B	12.2	11.73
					C	12.3	11.61

alkalinity/influent COD (TAlk/COD). Lower alkalinity ratios were used at higher COD loading rates.

Treatment Performance

Treatment performance of the three SMARs was evaluated and compared on the basis of TCOD removal rate in g/L/d and methane production rate in L CH_4 (STP)/L/d. SCOD removal rate in g/L/d and TSS effluent rate in g/L/d were also calculated for comparison. Because of the slight volume difference among the three SMARs, TCOD removal rate, SCOD removal rate, and TSS effluent rate were normalized with the clean-bed liquid volume at the highest port of each SMAR. The methane production rate was normalized with the total clean-bed liquid volume. Table 23 shows the pseudo steady-state performance for the three SMARs.

Theoretically, TCOD removal rate and CH_4 production rate are related with a constant ratio of 0.35 L CH_4 (STP)/gm TCOD removed. However, there is some difference between these two criteria. At steady state, TCOD removal rate accounts for the total COD removal in the liquid phase, while CH_4 production rate accounts for only the part of removal recovered as methane in the gas phase. The COD removal by hydrogen-producing acetogens will be accounted for in the liquid-phase TCOD removal, but will not be accounted in the methane production if the hydrogen gas is not utilized by methanogens, or by sulfate-reducers, or simply not utilized. Normally, hydrogen in the exit gas is in the order of 10^{-4} atm (or about 0.01% in the exit gas). Therefore, the difference between

TABLE 23. SMAR pseudo steady-state performance

Run	SMAR	SCODr[a] (g/L/d)	TCODr[a] (g/L/d)	Eff.[a] TSS (g/L/d)	Methane (%)	Methane[b] (L/L/d)	Methane[c] recovery (L/g)	Out/In[d] (-)
	A	0.87	0.84	0.03	80.2	0.28	0.34	0.97
1a	B	0.92	0.91	0.01	80.0	0.31	0.34	0.96
	C	0.93	0.91	0.01	80.0	0.28	0.30	0.87
	A	2.12	2.08	0.03	84.0	0.65	0.31	0.89
2a1	B	1.98	1.93	0.05	82.9	0.56	0.29	0.84
	C	2.03	1.95	0.08	83.2	0.61	0.31	0.91
	A	1.90	1.84	0.04	68.7	0.56	0.31	0.88
2a2	B	1.83	1.78	0.06	68.4	0.60	0.34	0.97
	C	1.87	1.81	0.05	68.8	0.62	0.34	0.98
	A	1.74	1.66	0.08	70.2	0.51	0.31	0.89
2b	B	1.71	1.64	0.05	70.5	0.58	0.35	1.01
	C	1.73	1.67	0.04	70.8	0.60	0.36	1.03
	A	1.62	1.50	0.09	77.0	0.33	0.22	0.70
2c	B	1.61	1.15	0.38	77.1	0.43	0.38	1.05
	C	1.71	1.62	0.06	77.1	0.43	0.27	0.79
	A	4.20	4.03	0.13	63.3	1.27	0.32	0.91
4a	B	4.14	3.83	0.33	64.1	1.30	0.34	0.97
	C	4.10	3.99	0.11	64.7	1.38	0.35	0.99
	A	3.67	3.57	0.13	65.5	1.02	0.29	0.83
4b1	B	3.64	3.49	0.21	66.0	1.12	0.32	0.92
	C	3.67	3.58	0.12	65.4	1.15	0.32	0.92
	A	4.25	4.09	0.12	64.4	1.11	0.27	0.79
4b2	B	4.11	3.85	0.29	65.4	1.27	0.33	0.95
	C	4.13	4.03	0.10	64.0	1.24	0.31	0.89
	A	3.30	3.13	0.45	71.4	0.93	0.30	0.86
4c	B	3.37	3.08	0.69	70.5	1.03	0.33	0.96
	C	3.32	3.17	0.42	71.3	1.02	0.32	0.93

[a]Based on the clean-bed liquid volume to the highest ports.

[b]Based on the total reactor clean-bed liquid volume.

[c]Theoretical value=0.35 L CH_4 (STP)/g TCODr.

[d](Methane COD + Effluent TCOD)/(Influent COD).

TABLE 23. (continued)

Run	SMAR	SCODr[a] (g/L/d)	TCODr[a] (g/L/d)	Eff.[a] TSS (g/L/d)	Methane (%)	Methane[b] (L/L/d)	Methane[c] recovery (L/g)	Out/In[d] (-)
	A	6.16	5.21	1.25	60.9	1.83	0.35	1.00
6b1	B	6.22	5.39	1.41	60.4	1.91	0.36	1.01
	C	6.13	5.58	0.95	61.2	2.06	0.37	1.05
	A	6.29	5.54	0.88	60.3	1.88	0.34	0.97
6b2	B	6.31	5.33	0.69	60.9	1.97	0.37	1.04
	C	6.23	5.90	0.27	61.1	2.02	0.34	0.98
	A	8.69	8.01	0.66	58.5	2.30	0.29	0.84
8a	B	8.70	7.62	1.07	58.0	2.31	0.30	0.88
	C	8.53	7.63	0.88	58.9	2.57	0.34	0.97
	A	9.91	8.32	1.39	55.0	2.49	0.30	0.88
10a	B	9.86	8.28	1.52	55.6	2.68	0.32	0.94
	C	9.79	8.89	0.99	53.4	2.37	0.27	0.79
	A	9.73	8.05	1.63	67.8	3.10	0.39	1.08
10aG1	B	9.69	8.04	1.60	68.5	3.18	0.40	1.11
	C	9.64	8.76	0.86	67.5	3.00	0.34	0.98
	A	9.07	7.07	1.51	60.5	2.65	0.38	1.05
10aG2	B	9.00	7.99	0.93	60.8	2.87	0.36	1.02
	C	8.92	8.45	0.49	59.7	2.60	0.31	0.89
	A	8.76	8.05	0.43	59.6	2.20	0.27	0.82
10c	B	9.25	8.73	0.42	59.4	2.41	0.28	0.81
	C	8.91	8.19	0.36	59.4	2.38	0.29	0.86
	A	10.73	9.26	1.39	57.3	2.39	0.26	0.80
12c	B	10.64	9.02	1.42	56.9	2.66	0.29	0.88
	C	10.75	9.71	1.31	56.4	2.76	0.28	0.84

these two criteria of TCOD removal rate and methane production rate should be very small. However, it has been estimated that hydrogen methanogenesis can account for as high as 30% of the total COD removal for sewage sludge (McCarty and Smith, 1986). Therefore, when determining COD for samples obtained from the acetogen-active zone (such as the bottom zone of SMAR C), caution should be taken in the interpretation of the COD removal data. This is especially true for heavily loaded systems.

The TCOD removal rate (g/L/d) is a better index than SCOD removal rate in evaluating SMAR performance because the solids retention capability, which is important to SMAR performance, is also considered. Performance evaluation based on effluent TCOD concentration (mg/L) alone is not good because it is the mass TCOD removal rate that needs to be evaluated. It is worth noting that, under steady-state conditions, the difference between the TCOD removal rate and the SCOD removal rate measures the COD synthesis rate into biomass.

In order to evaluate and compare the performance of the three SMARs, TCOD removal rates were plotted against COD loading rates (Figure 31) for all seventeen steady-state runs. It can be seen from the plot that, with the COD loading rate equal to or less than about 4 g/L/d, there was little difference in TCOD removal rate. With the COD loading rate greater than about 4 g/L/d (with or without gassing), SMAR C performed slightly better, except for Run 10c, in which SMAR B performed better. The better performance of SMAR C became greater as the loading rate

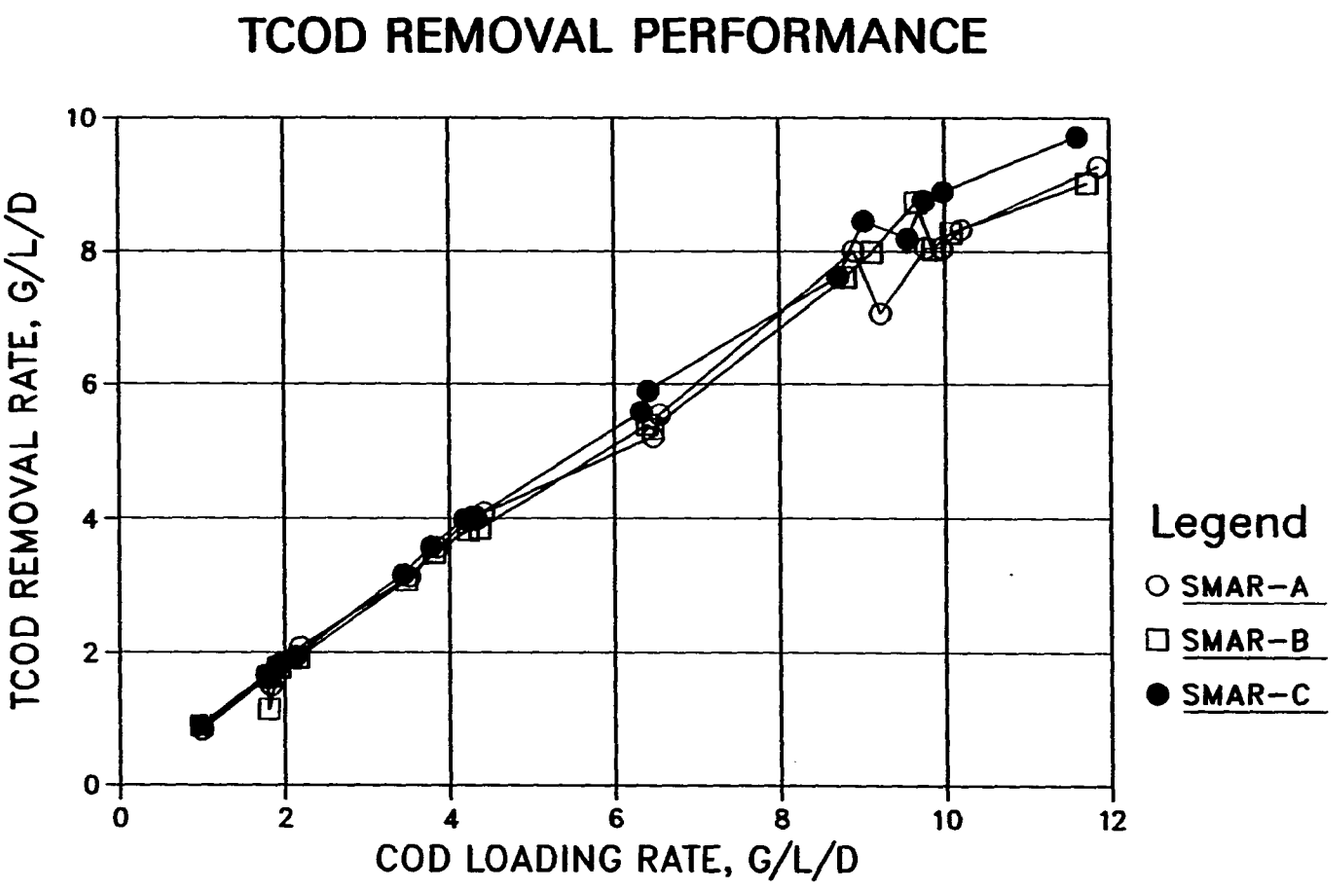

FIGURE 31. Comparison of SMAR steady-state performance in TCOD removal rate

increased in the latter phases of this study. With no gas recycle, SMARs A and B showed little difference in TCOD removal rate for all the loading rates tested. With gas recycle, SMAR B performed better than SMAR A in TCOD removal rate.

SCOD removal rate was also plotted vs. COD loading rate in Figure 32. With no gas recycle, there was little difference among the three SMARs in SCOD removal rate. Comparisons between the plot of TCOD removal rate and the plot of SCOD removal rate reveal that the better performance of SMAR C was likely related to a lower effluent TSS, which results in a lower effluent TCOD. This was especially true for Runs 10c and 12c, in which the TCOD removal rates of SMARs A and B dropped abruptly to about 1 g/L/d less than for SMAR C.

With gas recycle (Runs 10aG1 and 10aG2), SMARs B and C performed better in TCOD removal rate, while SMAR A was likely too short to efficiently retain solids, resulting in a lower TCOD removal rate, even though the SCOD removal rate of SMAR A did improve. The effects of gas recycle will be discussed in more detail later.

Daily average methane production rates (L/L/d) and TSS effluent rates (g/L/d) were also plotted vs. COD loading rate, as shown in Figures 33 and 34, respectively. Both the methane and TSS plots show that SMAR C performed somewhat better in producing more methane and having a lower effluent TSS. This supports the finding, as concluded from TCOD and SCOD plots, that the better performance of SMAR C was related to its better solids retention capability.

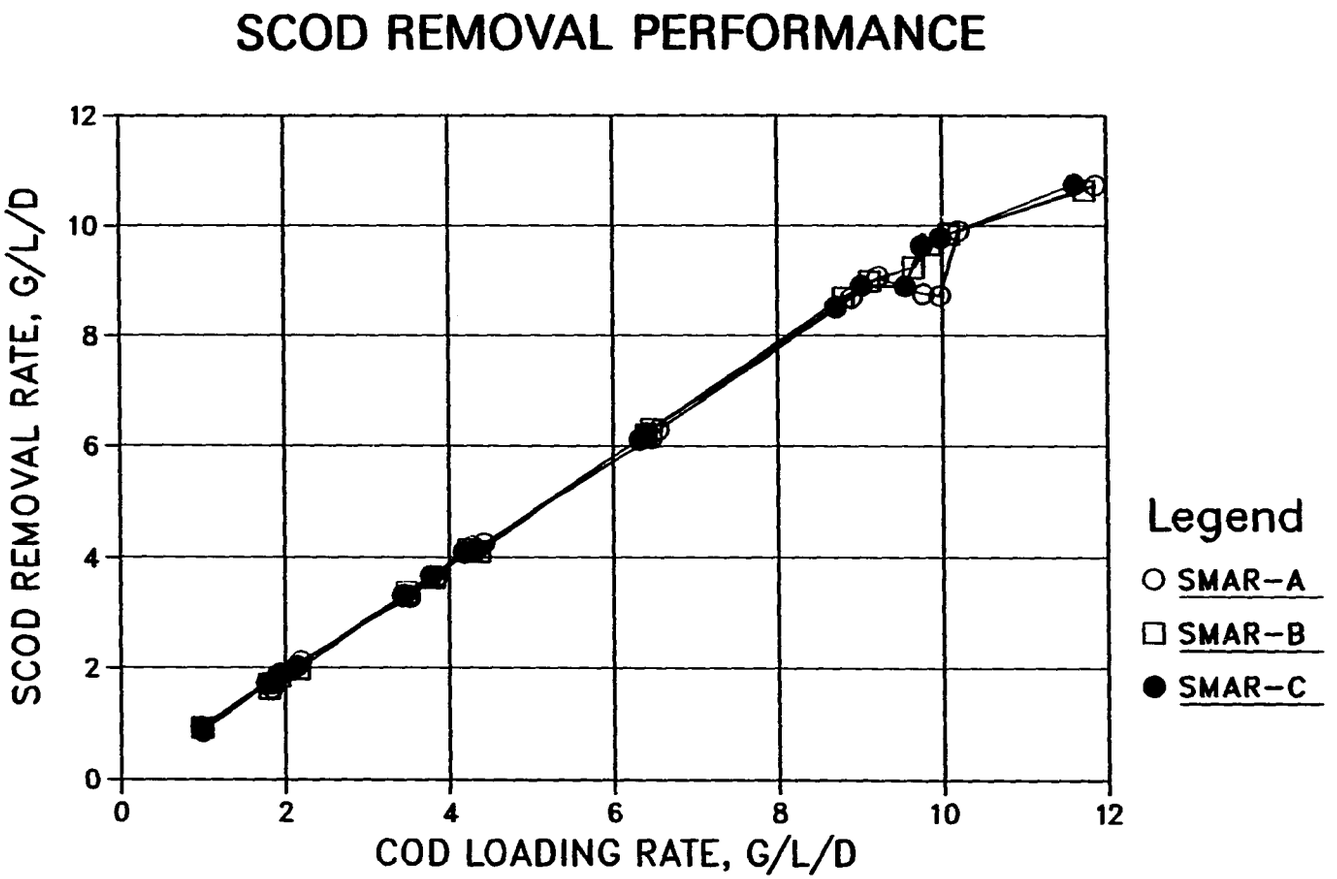

FIGURE 32. Comparison of SMAR steady-state performance in SCOD removal rate

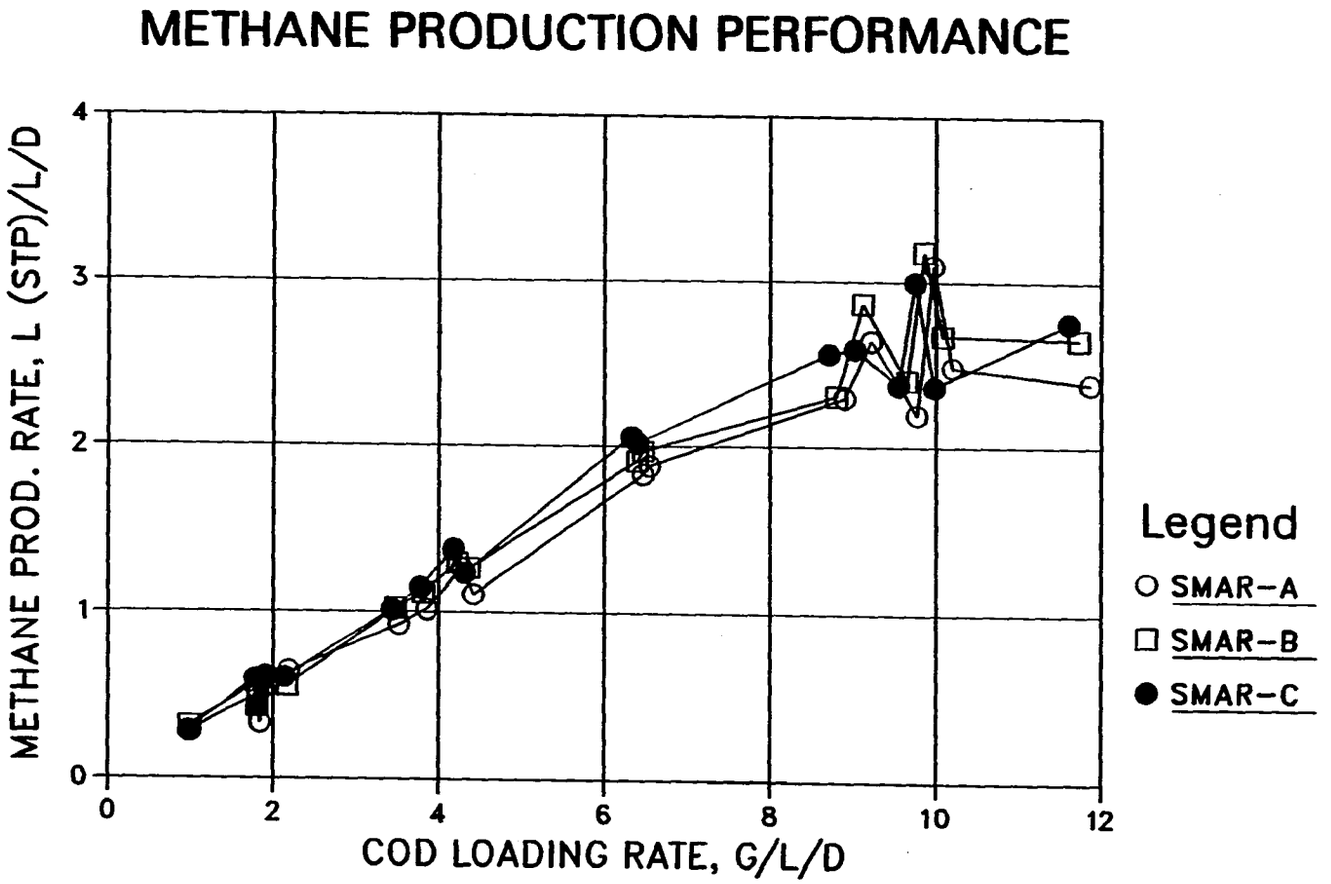

FIGURE 33. Comparison of SMAR steady-state performance in methane production rate

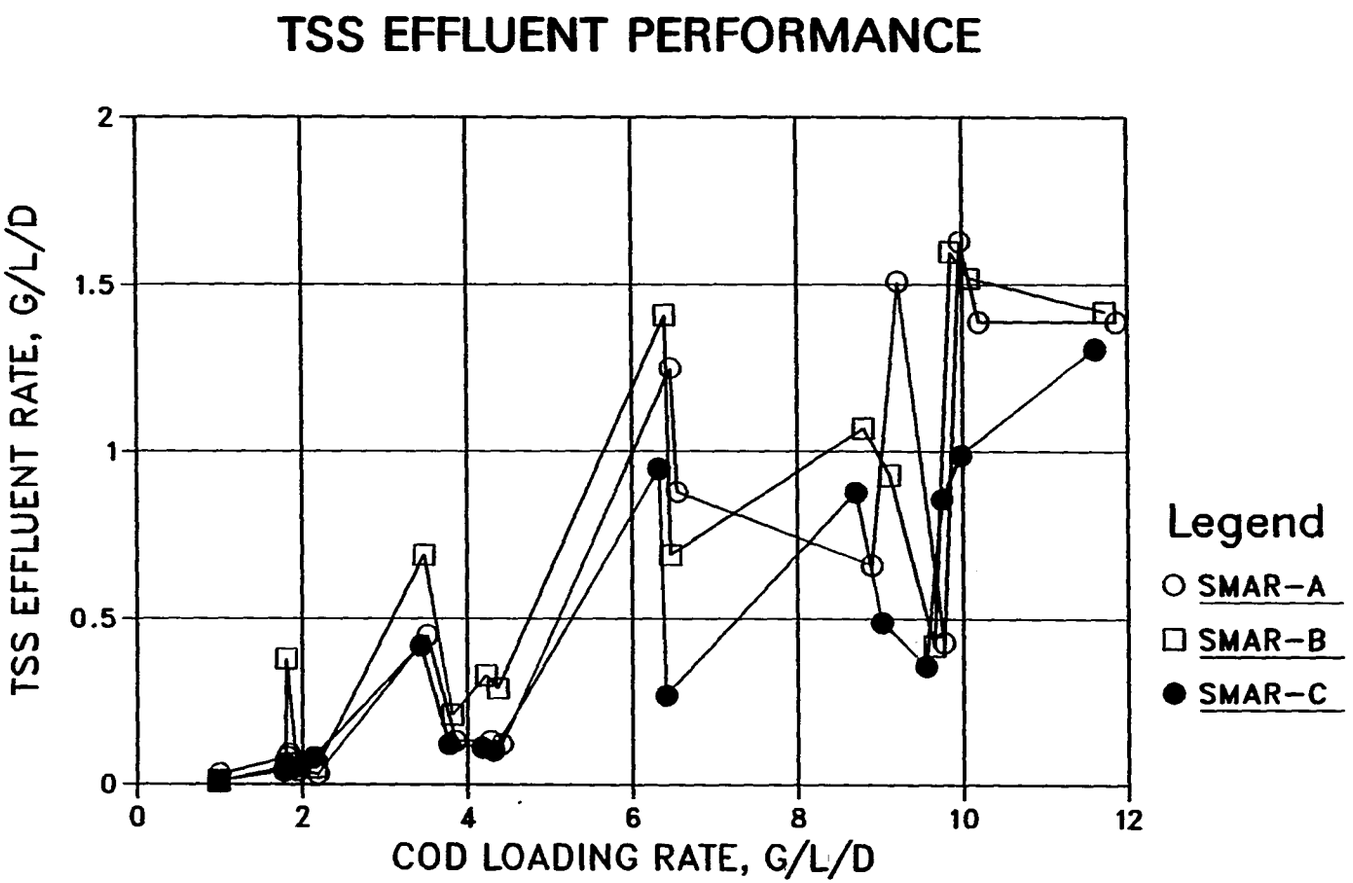

FIGURE 34. Comparison of SMAR steady-state performance in effluent TSS rate

Steady-state treatment performance was also checked for the input-output balance in Table 23. The ratio of methane production rate to TCOD removal rate for each steady-state run was calculated and compared to the theoretical value of 0.35 L CH_4 (STP) produced/g TCOD removed. In general, the calculated ratios were close to the theoretical value, except for those runs with COD loading rates greater than 8 g/L/d with no gas recycle (Runs 10a, 10c, and 12c), as shown in Figure 35. At high loading rates, it was noticed that a large amount of milk aggregates precipitated in the bottom zone of the SMARs. This might be the reason for the poor methane recovery ratios at the high loading rates.

The ratio of [(Methane COD)+ (Effluent TCOD)]/(Influent COD) was also calculated in Table 23. The calculated ratios show the same fact of poor methane recovery at COD loading rates greater than about 8 g/L/d with no gas recycle. These two ratios increased to about their theoretical values with gas recycle (Runs 10aG1 and 10aG2).

Distribution of pH

Appendix E lists data for pH, SCOD, TOA (total organic acids), TSS, and AMA at various sampling heights of the three SMARs for some selected steady-state runs. In general, SMAR A had a fairly uniform pH distribution for all runs studied while SMAR C had the widest variation, especially at high loading rates. This indicates that there was a fundamental difference in the operation of the three SMARs.

In SMAR A, the acid and methane formers were likely mixed together by the mixing effect of the gas produced. This is also evidenced by the distribution in SCOD and TSS, which will be discussed later. However, in SMAR C, as indicated by pH distribution, these two groups of organisms appeared distinctively stratified. For most of runs studied, the distinction occurred at a height of about 1.0-1.5 m of the SMAR C. It is interesting to note that the lowest pH in SMAR C often occurred at port #4 (91.4 cm), where TOA started to drop significantly (such as in Runs 4a, 4b1, 6b1, 6b2, 8a, 10a, and 10c). In SMAR B, the distinction was smaller and often occurred at the lowest port (15.2 cm). However, an increase in flowrate could push the lowest pH to a higher height (such as in Run 4c).

Figure 36 compares pH distribution for different COD loading rates (Run 4a vs. 8a) with the same retention time (about 2 days) and alkalinity addition (alkalinity/COD ratio 1/40). An increase in COD loading from about 4 to 8 g/L/d decreased the entire pH distribution for the three SMARs. The decrease in pH was greater in the lower portions. The pH decrease in the lower portions of SMAR C was the highest among the three SMARs.

pH distribution is also examined for different flowrates (Run 10a vs. 10c) with the same COD loading rate (about 10g/L/d) and alkalinity addition (1/40). As shown in Figure 37, with the same COD loading rate, an increase in flowrate by four times decreases the entire pH distribution for SMARs A and B by almost 0.6 pH unit. This could be

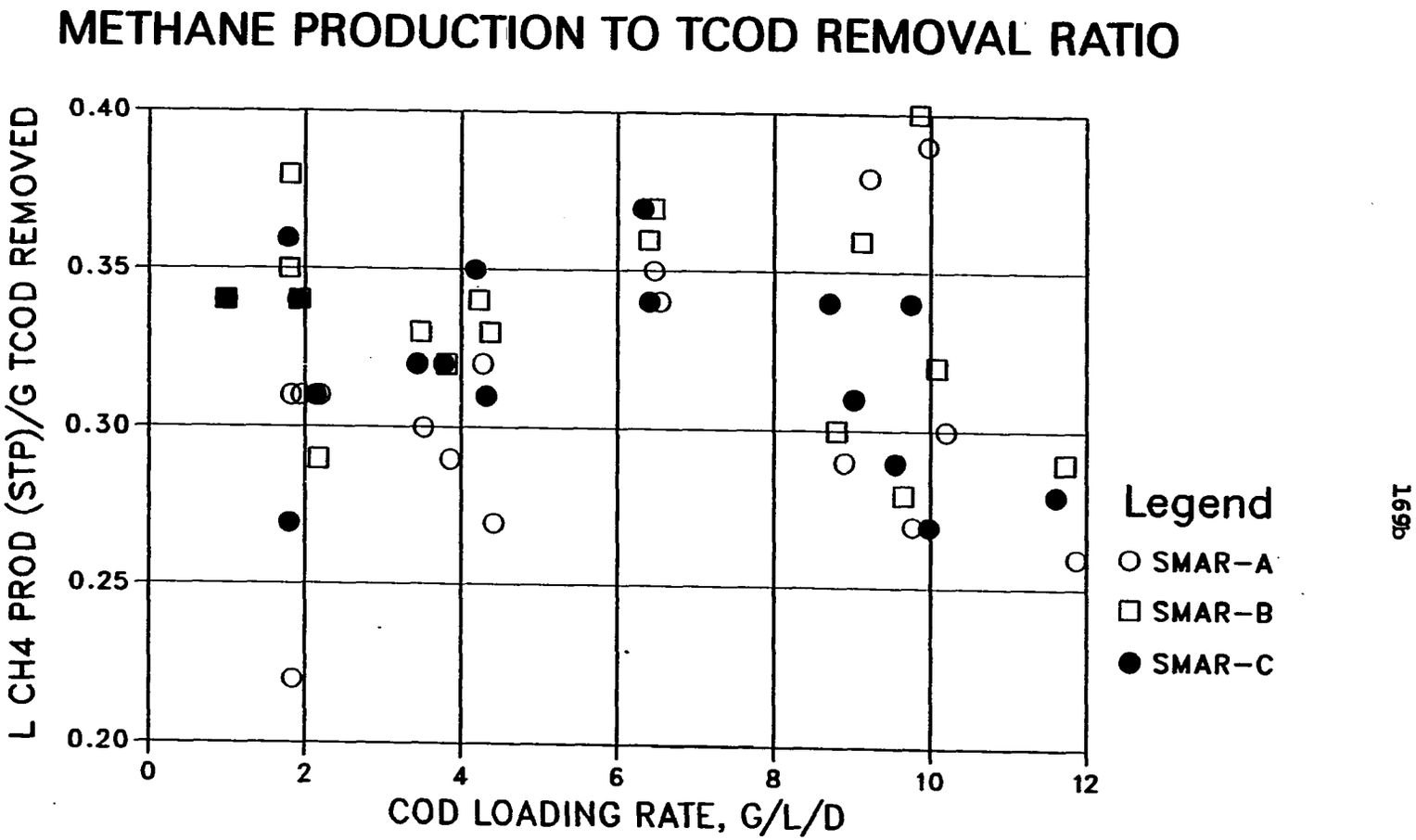

FIGURE 35. Ratios of methane production to COD removal for SMARs at steady-state conditions

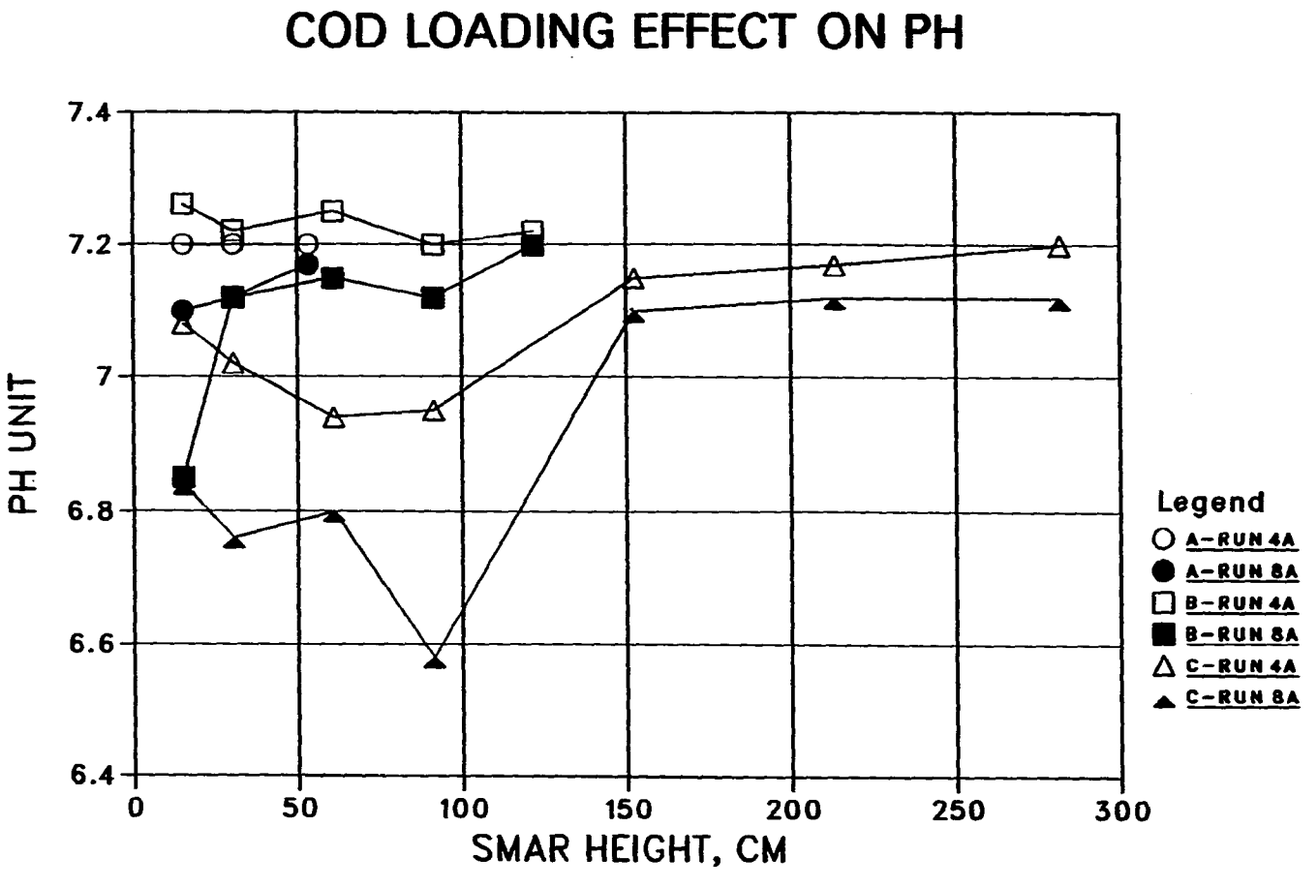

FIGURE 36. Effect of COD loading rate on pH distribution, comparing Run 4a (4 g/L/d) and Run 8a (8 g/L/d), both with retention time of about 1 day

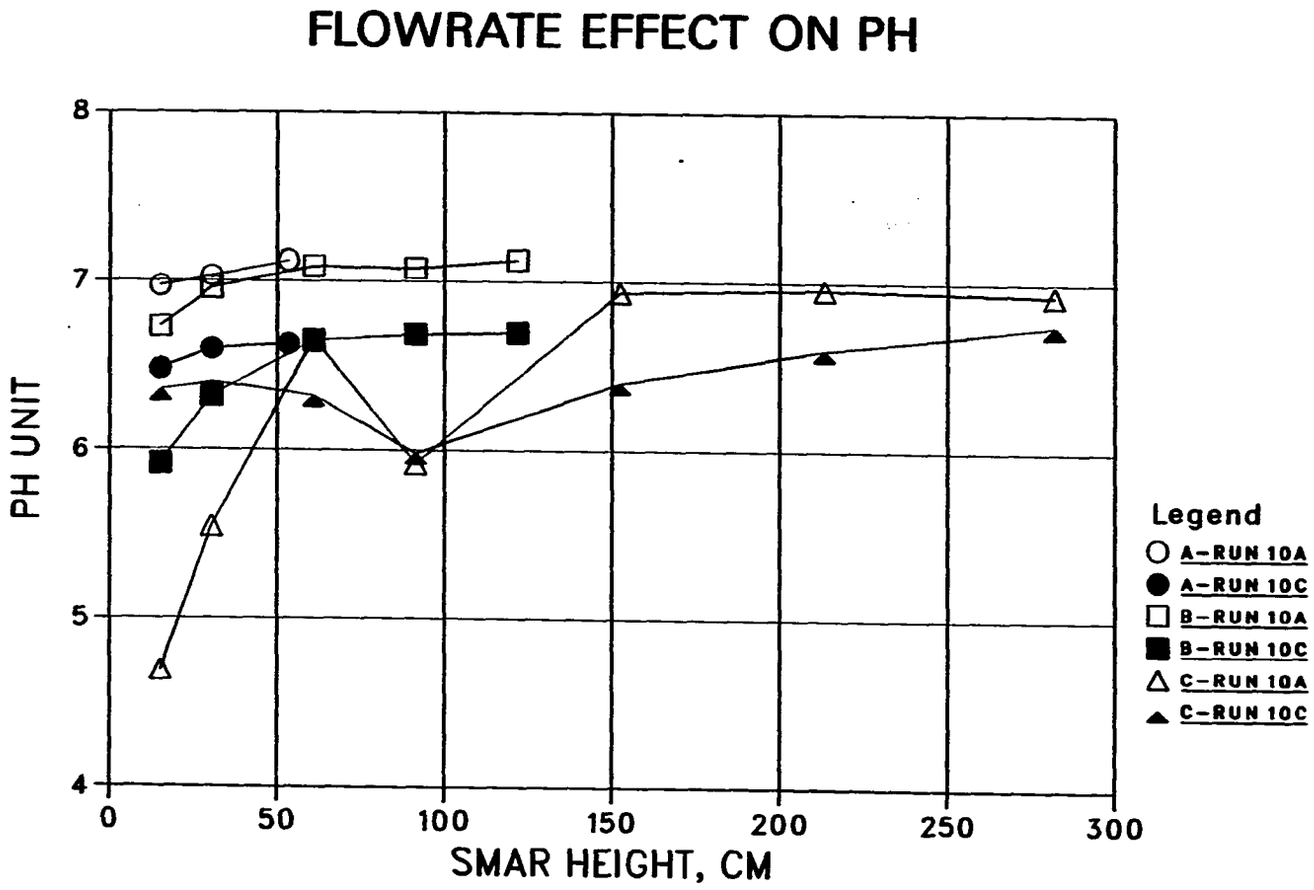

FIGURE 37. Effect of flowrate on pH distribution, comparing Run 10a (retention time of about 2 days) with Run 10c (about 0.5 day), both with a COD loading rate of about 10 g/L/d and a alkalinity/COD ratio of 1/40

explained by a lower existing alkalinity concentration at the higher flowrate, even though the same alkalinity/COD ratio was used. The response of SMAR C to the increased flowrate was quite different and requires a different explanation. At the higher flowrate, the influent COD concentration was lower and consequently resulted in a higher and more uniform pH distribution. However, because of the lower alkalinity concentration, as resulted from a shorter retention time at the higher flowrate, the pH distribution in the upper portions was still lower.

Figure 38 compares Run 6b1 (with alkalinity/COD ratio of 1/4) and Run 6b2 (with 1/40) for the three SMARs. They were operated at a COD loading rate of about 6 g/L/d and a retention time of 1 day. With increased alkalinity addition, pH increased almost in parallel for about 0.2 unit over the entire range in height of SMARs A, B, and in the upper portions of SMAR C. Interestingly, pH distribution in the lower portions of SMAR C decreased. No possible explaination for this could be made.

Distribution of SCOD and Volatile Acids

SCOD distribution in general followed the same pattern as for the total organic acids (TOA) distribution (Appendix E). The TOA is defined as the sum of the C2-C5 volatile acids (Appendix F), expressed as acetic acid. In general, SMAR A was characterized by a more uniform SCOD and TOA distribution, while SMAR C had a high variation, especially at high COD loading rates. The highest variation in SMAR C often occurred at port #3 (61.0 cm) or #4 (91.4 cm), and the greater the COD loading rate

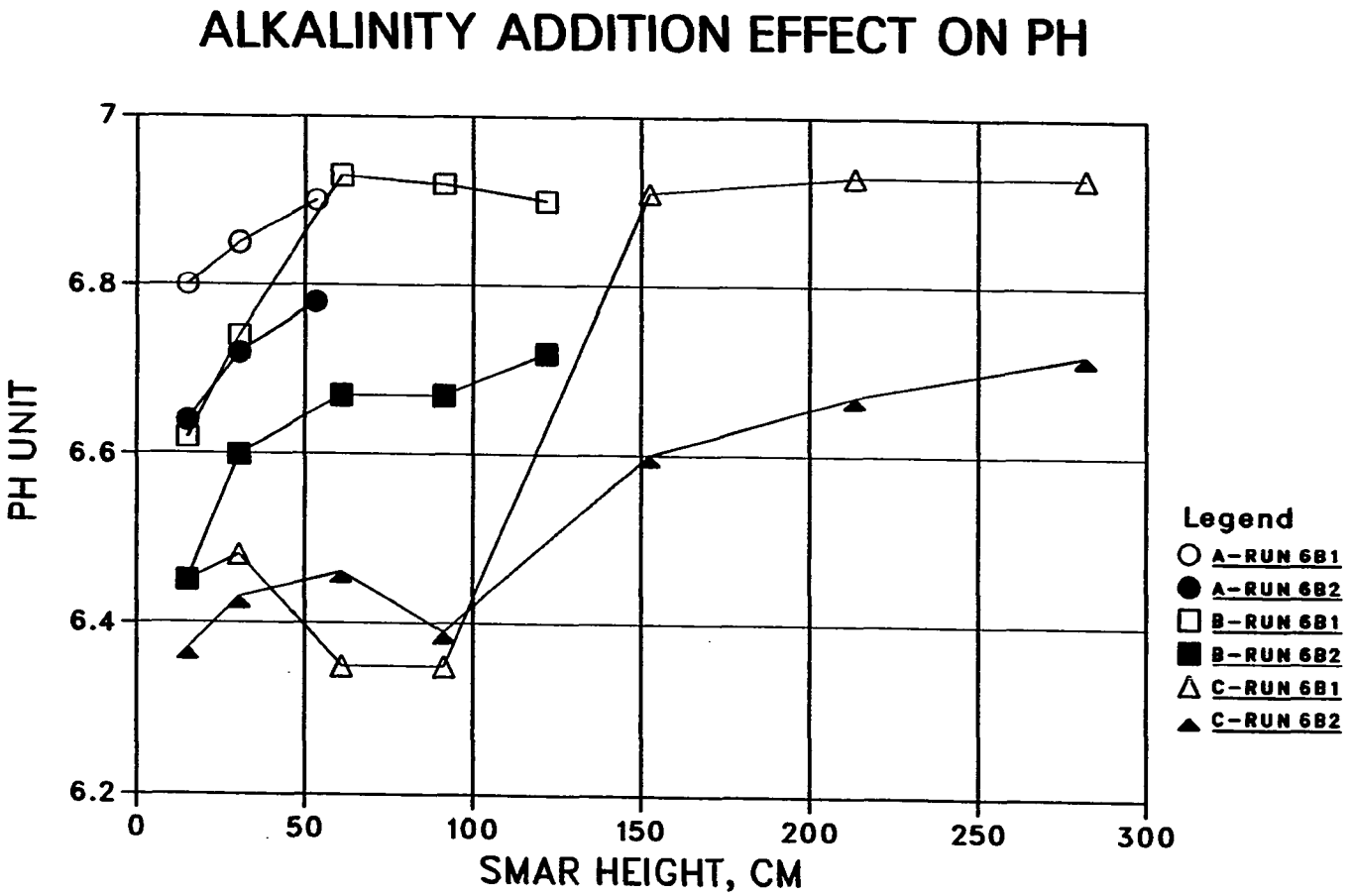

FIGURE 38. Effect of alkalinity addition on pH distribution, comparing Run 6b1 (alkalinity/COD ratio of 1/4) and Run 6b2 (1/40), both with a COD loading rate of about 6 g/L/d and a retention time of about 1 day

the greater the variation. As will be discussed in the following section, the highest variation in TSS distribution in SMAR C also often occurred at the same height. In many runs, SCOD concentration in some lower SMAR heights was lower, especially for the lower portions of SMAR C. This might be due to short circuiting or local deposition of NFDM solution in the SMARs.

Figures 39 through 42 show the effects of loading conditions on SCOD and TOA distribution. As COD loading rate increased from about 4 g/L/d (Run 4c) to about 10 g/L/d (Run 10c) at a retention time of about 0.5 day (Figures 39 and 40), SCOD and TOA distribution of the three SMARs increased almost in parallel. However, at the same COD loading rate of about 10 g/L/d, an increase in influent flowrate decreased the variation in both SCOD and TOA distribution (Run 10a vs. 10c in Figures 41 and 42). This was probably due to the lower influent COD concentration with the higher influent flowrate.

Distribution of Solids and Activity

Appendix E also lists data on total suspended solids (TSS) and some related acetoclastic methanogenic activity (AMA) at various SMAR heights. In general, TSS distribution in SMAR A was rather uniform, indicating a completely mixed hydraulic pattern created by the gas produced. In the runs with COD loading rates of less than about 6 g/L/d, the levels of the TSS distribution in SMAR A were about the same as in the upper zone of SMARs B and C. However, at higher COD loading rates (6 g/L/d or more),

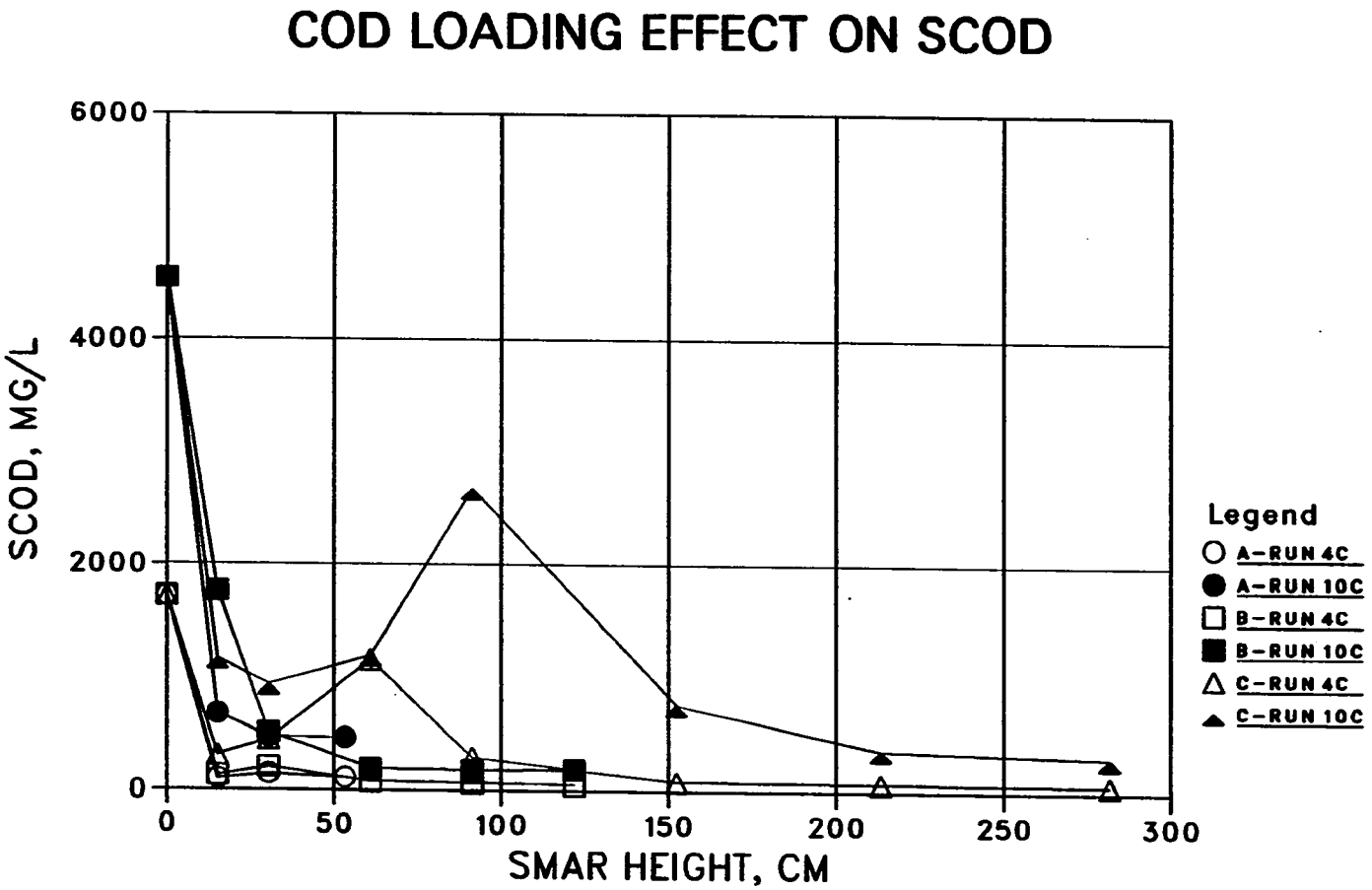

FIGURE 39. Effect of COD loading rate on SCOD distribution, comparing Run 4c (about 4 g/L/d) with Run 10c (about 10 g/L/d), both with a retention time of about 0.5 day

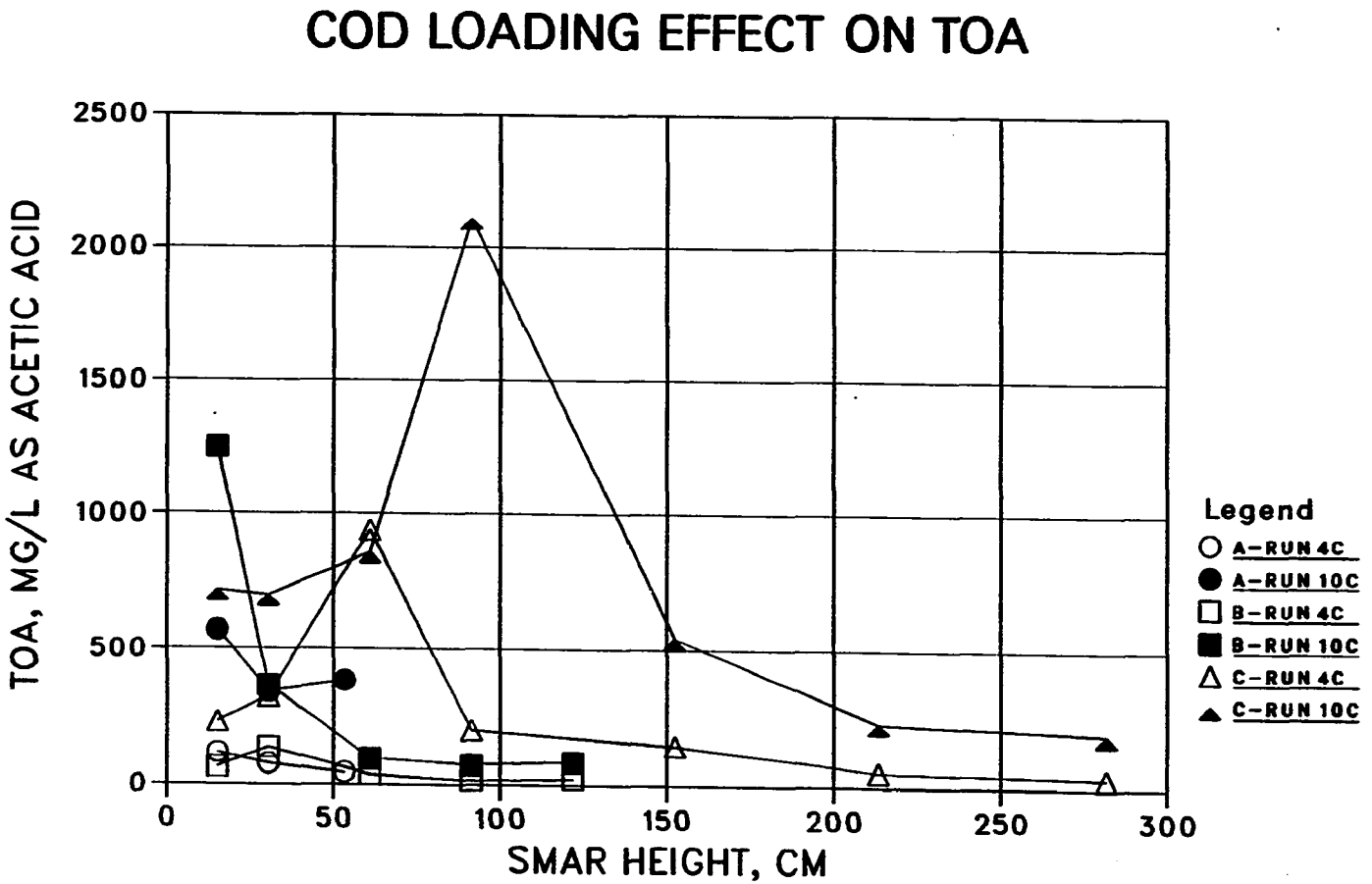

FIGURE 40. Effect of COD loading rate on TOA distribution, comparing Run 4c (about 4 g/L/d) with Run 10c (about 10 g/L/d), both with a retention time of about 0.5 day

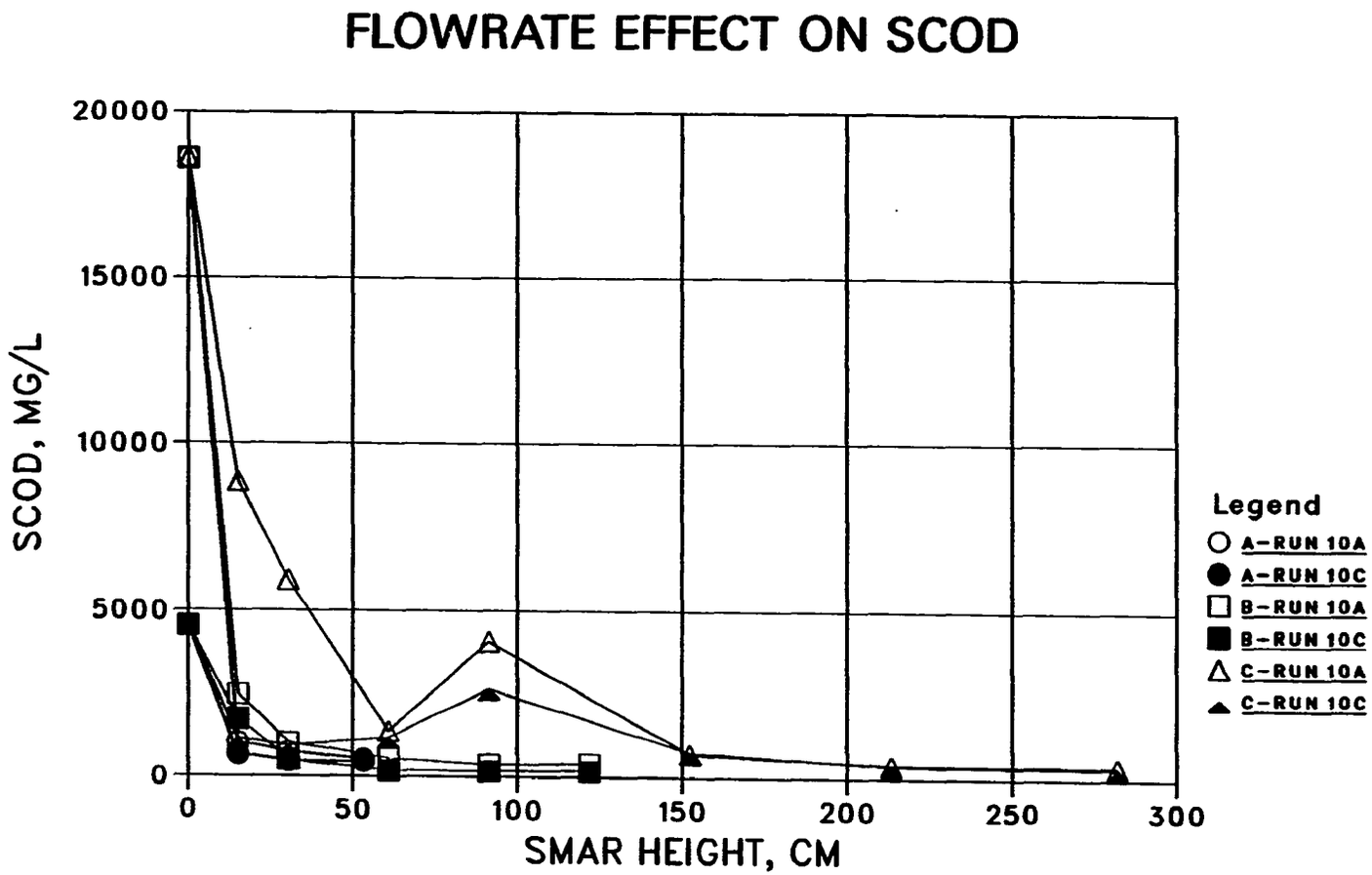

FIGURE 41. Effect of retention time on SCOD distribution comparing Run 10a (about 2 days) with Run 10c (about 0.5 day), both with a COD loading rate of about 10 g/L/d

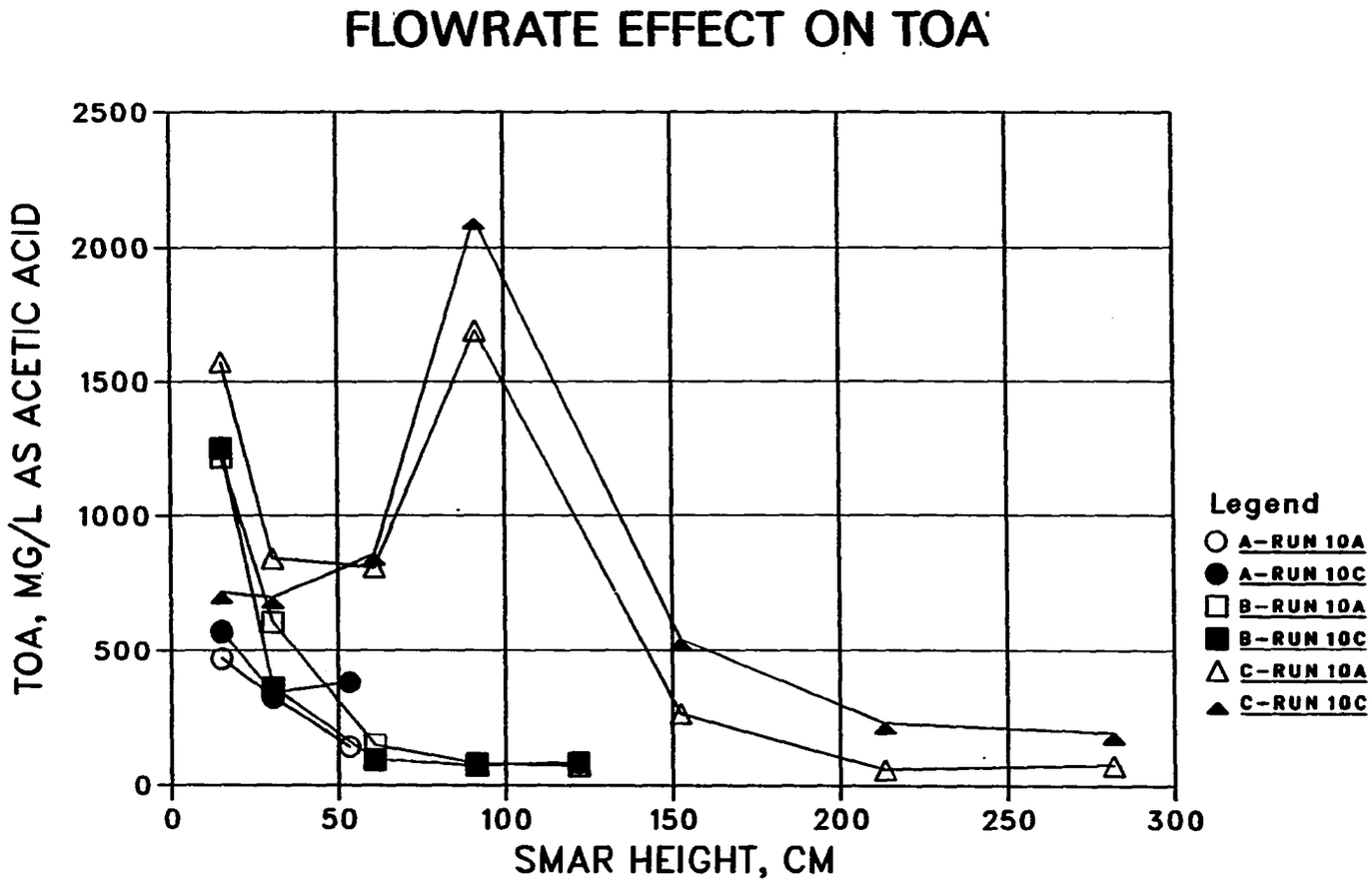

FIGURE 42. Effect of retention time on TOA distribution, comparing Run 10a (about 2 days) with Run 10c (about 0.5 day), both with a COD loading rate of about 10 g/L/d

the levels of TSS distribution in SMAR A became greater than in the upper zones of SMARs B and C. This indicates that SMAR A is too short (53.3 cm to the highest port) to be able to efficiently retain biomass as biomass concentration and biogas mixing intensity increase at the higher loading rates.

TSS distribution in SMAR B was generally uniform at heights between port #3 (61.0 cm) and above. Although SMAR B had a height (121.9 cm to the highest port) of about twice that of SMAR A, TSS data for most runs studied (such as Runs 2a2, 2c, 4a, 4b2, 8a, and 10a) indicate that SMAR B was no better than SMAR A in retaining biomass in the system. Interestingly, most of these runs were operated at the longest retention time tested of about 2 days; therefore the solids uplifting should be due mainly to rising gas. The superficial velocity of the rising gas should be greater in SMAR B than in SMAR A because of the smaller cross-sectional area of SMAR B. With the higher gas superficial velocity, SMAR B might not be better than SMAR A in retaining solids in the system.

As expected, the tallest SMAR (SMAR C) showed the widest variation in TSS distribution. The TSS distribution was generally characterized by two distinct portions separated between port #4 (91.4 cm) and port #5 (152.4 cm). This suggests that the maximum solids expansion height in the SMAR bottom zone was about 1.5 m. The height of the maximum TSS in SMAR C, unlike SMAR B which occurred exclusively at the lowest port (15.2 cm), often occurred at port #2 (30.5 cm) or port #3 (61.0 cm). The maximum TSS concentration was about 1% (10,000 mg/L) for COD loading rates greater than 6 g/L/d studied.

TSS distribution was compared for different COD loading rates with the same influent flowrate in Figure 43 (Run 4a vs. Run 10a) and for different influent flowrates with the same COD loading rates in Figure 44 (Run 10a vs. Run 10c). With the increased COD loading rates at the same influent flowrate, Figure 43 shows that all the TSS distribution increased in parallel, except for the lower parts of SMAR C. It also shows the ability of SMAR C to retain biomass in the bottom 40 cm. However, it is suspected that such a highly concentrated biomass might be resulting from the precipitation of the coagulated milk solution at the higher loading rate. With the increased flowrate at the same COD loading rate, Figure 44 shows that all the TSS distribution decreased in parallel, except for the bottom zone of SMAR C. With the increased flowrate, the wide variation in TSS distribution in the bottom zone of SMAR C decreased. This might be due to the combined effects of more dilute influent COD concentration and higher superficial velocity.

Along with TSS data, Appendix E also lists AMA data for some selected runs. The AMA measures the maximum potential of methane production on acetate in L CH_4 (STP)/g VSS/d. These data show that AMA distribution varies widely with different SMAR heights and loading conditions, especially for SMAR C, with a typical range of 0.10 to 0.70 L/g/d. Assuming a maximum AMA of 1.0 L/g/d, as concluded from pure culture studies (Valcke and Verstraete, 1983), biomass activity could vary from 10% to 70% in their ability to produce methane on acetate. Figure 45 plots AMA vs. VSS for all the runs tested with the three SMARs.

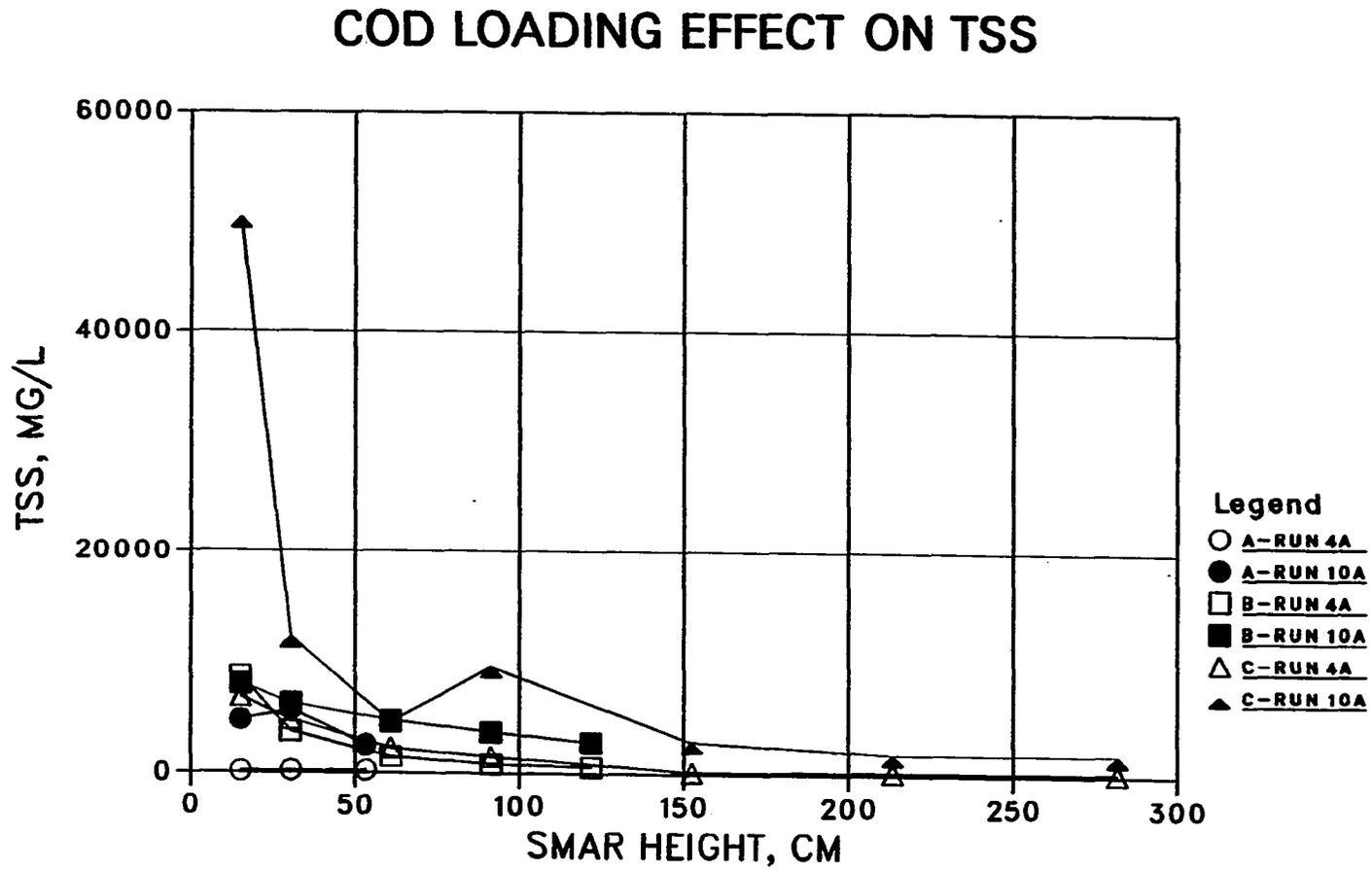

FIGURE 43. Effect of COD loading rates on TSS distribution, comparing Run 4a (about 4 g/L/d) and Run 10a (about 10 g/L/d), both with retention a time of about 2 days

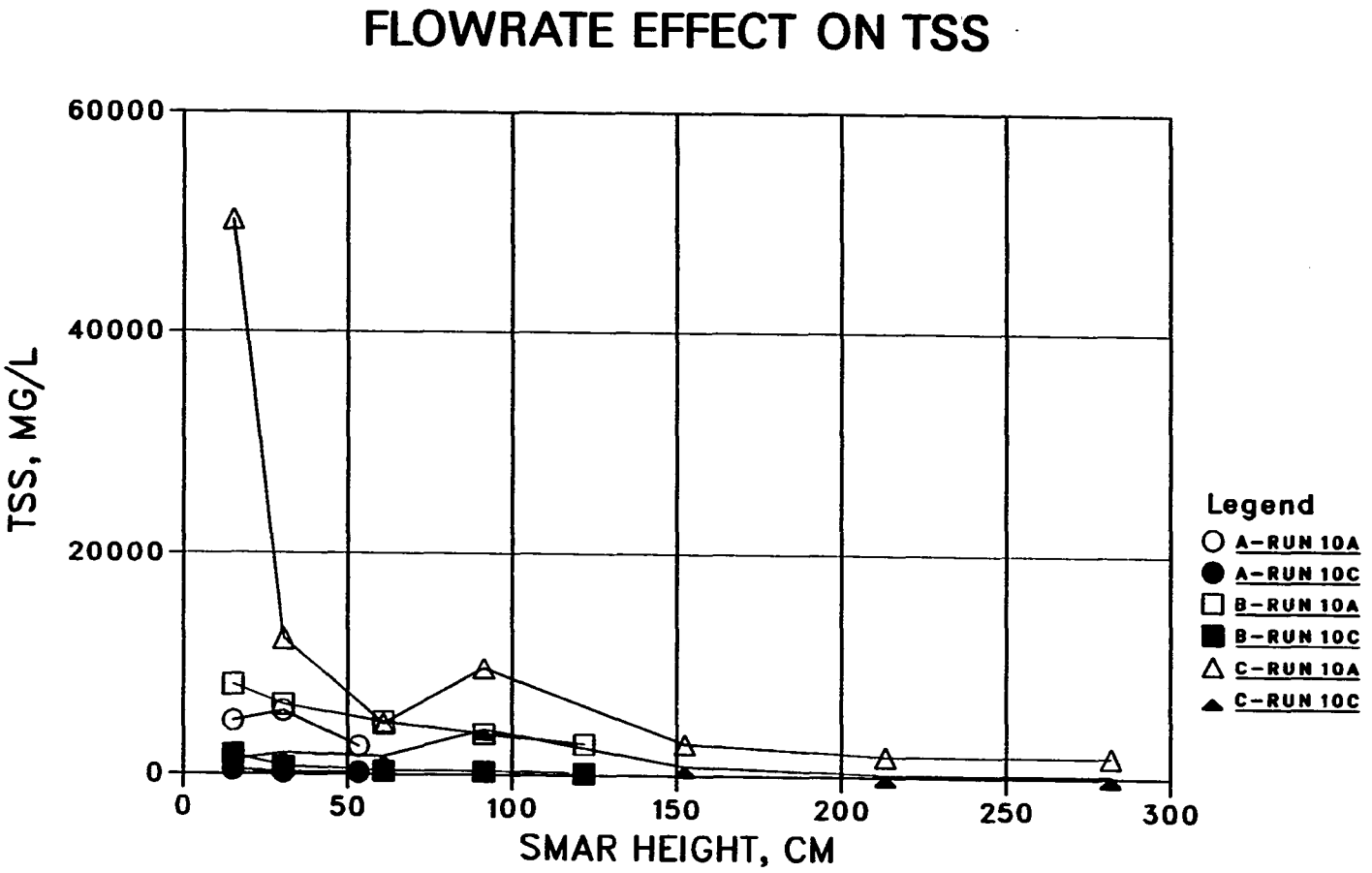

FIGURE 44. Effect of influent flowrate on TSS distribution, comparing Run 10a (about 2 days) and Run 10c (about 0.5 day), both with a COD loading rate of about 10 g/L/d

It can be seen from Figure 45 that, with VSS less than 1 g/L, lower VSS results in higher AMA. However, with VSS greater than 1 g/L, AMA varies within a narrow range of 0.1 to 0.2 L/g/d.

AMA distribution in SMAR A was rather uniform and the distribution level decreased as COD loading rates increased as shown in Figure 46. For example, in Appendix E, AMA in SMAR A was about 0.60 for Run 2a1 (COD loading rate of about 2 g/L/d), about 0.20 for Run 4a (about 4 g/L/d), and about 0.10 for Run 6b1 (about 6 g/L/d). AMA distribution in SMARs B and C was highly varied, especially at SMAR heights between 40 to 60 cm, where TSS varied most. In most runs of SMARs B and C, the lowest AMA often occurred at the lower heights, where higher TSS accumulated. However, in some runs (such as Run 4a, 6b1, 6b2), the lowest AMA occurred in the top portions of SMAR B. This might suggest that inadequate substrate concentration, as occurred in the top portions of the SMARs, could result in lower activity. Operation at a higher flowrate with the same COD loading rate could result in a general increase in AMA distribution (Figure 47).

Effects of Gas Recycle

In the latter phases of this study, as the COD loading rate increased to about 10 g/L/d, it was decided to recycle the gas in the three SMARs. The purpose was to see whether the practice of gas recycle, commonly used in digester operation, could be any benefit to the SMAR systems, especially at high loading rates. This was done by recycling

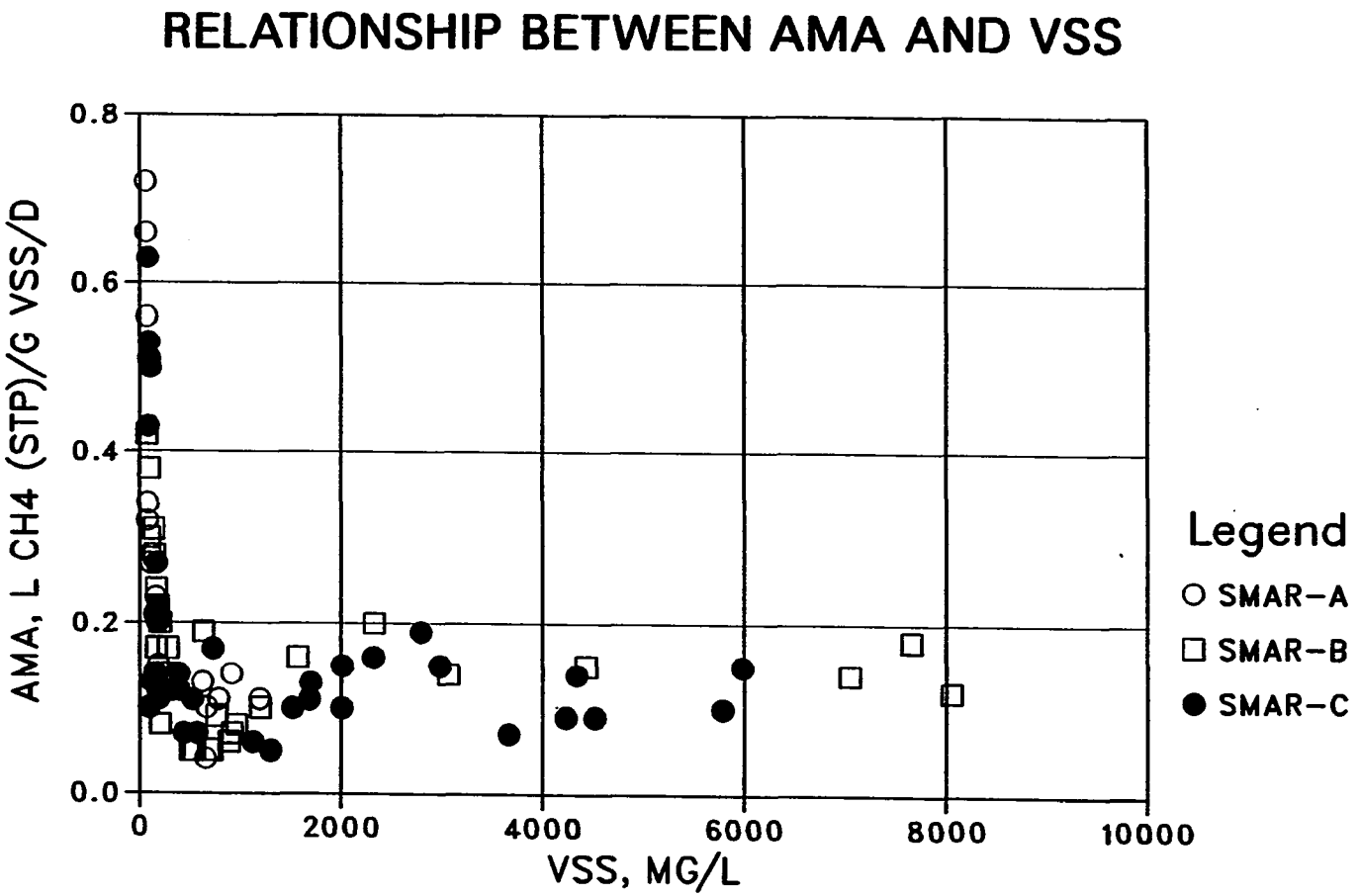

FIGURE 45. Dependence of AMA on VSS, showing with VSS less than 1 g/L, higher VSS results in lower AMA, with VSS greater than 1 g/L, AMA ranges within 0.1-0.2

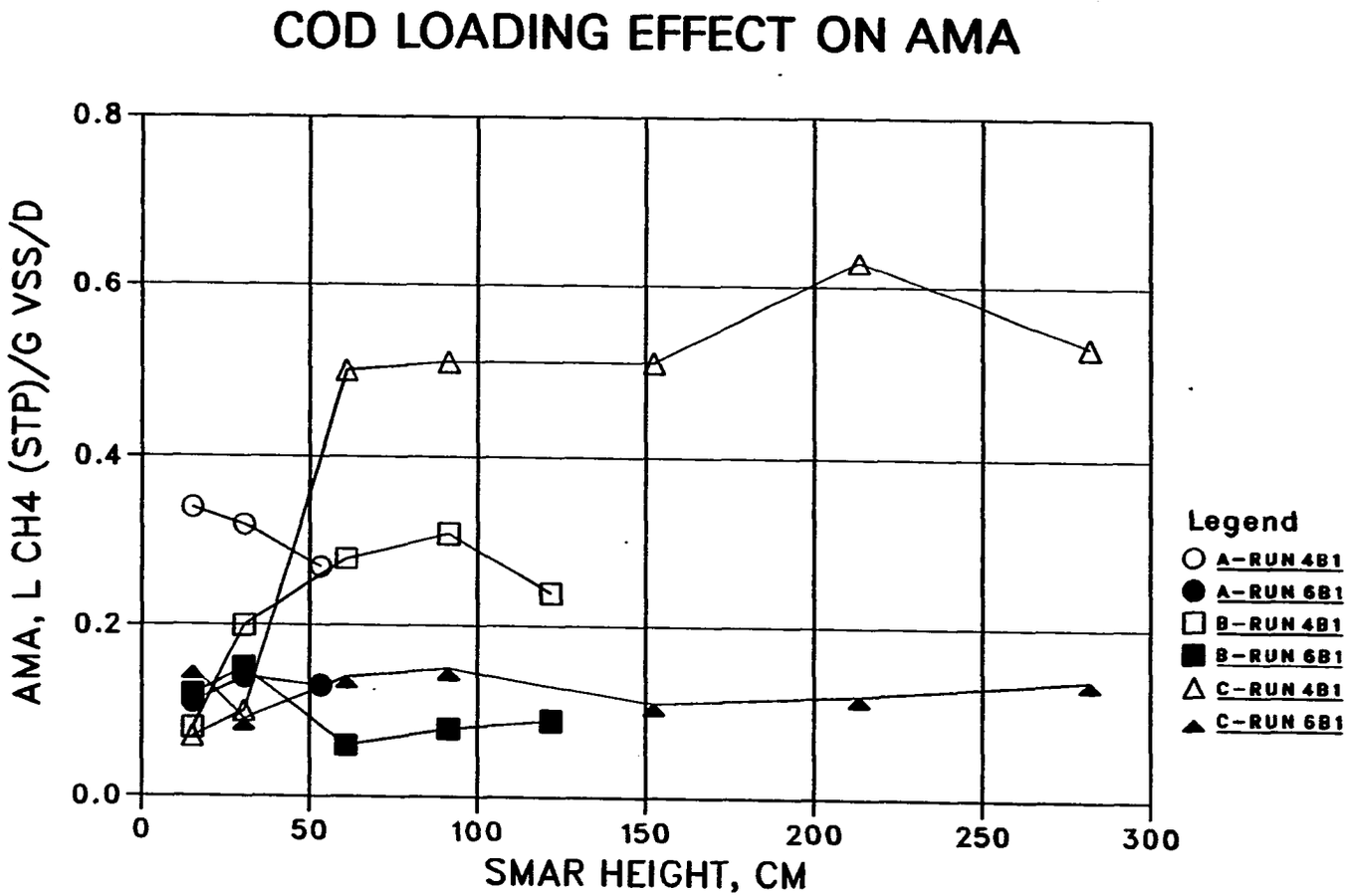

FIGURE 46. Effect of COD loading rates on AMA distribution, comparing Run 4b1 (about 4 g/L/d) and Run 6b1 (about 6 g/L/d), both with retention a time of about 1 day

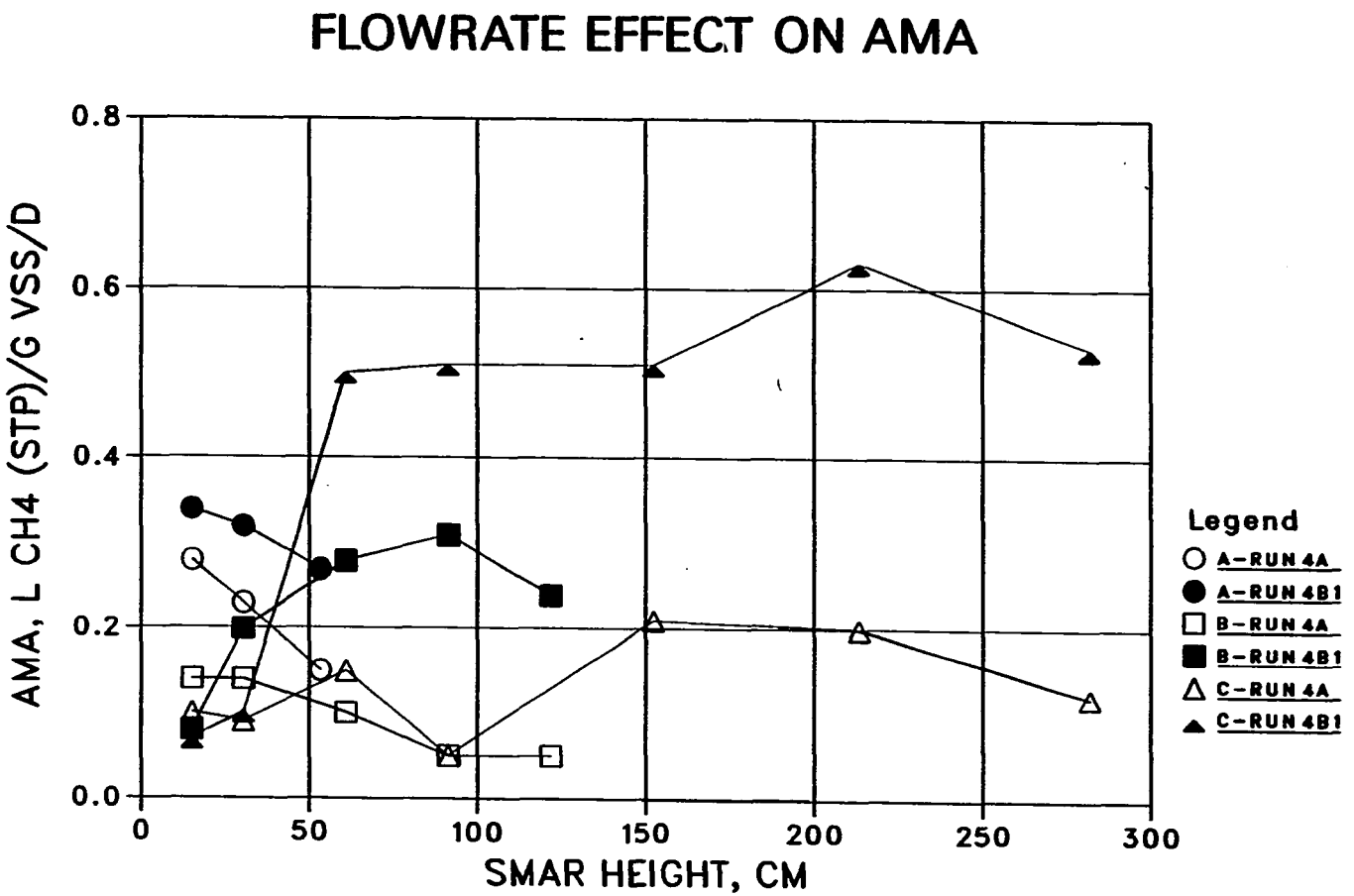

FIGURE 47. Effect of influent flowrate on AMA distribution, comparing Run 4a (about 2 days) and Run 4b1 (about 1 day), both with a COD loading rate of about 4 g/L/d

the exit gas of each SMAR after H_2S scrubbing and directly sparging the gas into each influent line using Masterflex pumps (Figure 13). The gas recycle study was done on two different occasions (Runs 10aG1 and 10aG2) using a recycle rate of about 12 mL/min in Run 10aG1 and 24 mL/min in Run 10aG2. The gas recycle rates account for about 3.5% and 7.0% of the total gas production rate. The COD loading rate was about 10 g/L/d with a retention time of about 2 days for both gas recycle runs. The measured gas recycle pressures at the bottom sparging points were about 3.2, 4.5, and 7.5 psig (or 2.2, 3.2, and 5.3 m of H_2O) for SMARs A, B, and C, respectively. The measured pressures were higher than the calculated water pressures of 0.60, 1.60, and 2.88 m of H_2O for SMARs A, B, and C, respectively.

The effects of gas recycle were remarkable. The methane percentage of the three SMARs increased to about 68% for Run 10aG1 and 60% for Run 10aG2 from about 55% for Run 10a. TCOD removal rates for all the SMARs were correspondingly increased. The increase of methane percentage could be due to two different possible (biological and chemical) mechanisms. First (biological), hydrogen methanogenesis was somehow enhanced with gas recycle, in considering the fact that CO_2 will be reduced with the production of CH_4 in the H_2/CO_2 methanogenesis. Second (chemical), with enhanced hydrogen methanogenesis, the H_2-producing acetogenesis was accordingly enhanced as a result of lower hydrogen partial pressure. This could also enhance acetate methanogenesis. The direct consequence of the enhancements of these reactions was to decrease the total organic

acids and increase the pH. The increase in pH could further result in a higher methane percentage due to a lower CO_2 content in the gas phase.

With gas recycle, CH_4 production rate increased in all three SMARs (Figure 33). There was little difference in the CH_4 production rate among the three SMARs. However, the relative increase of methane production rate in SMAR C was somewhat higher than in SMARs A and B, as a result of gas recycle. This might suggest two possibilities. First, before gas recycle (Run 10a), SMAR C might have been somewhat more inhibited by H_2 gas than SMARs A and B due to the higher hydrostatic pressure in the bottom zone of SMAR C. And second, only the dissolved hydrogen can be utilized by methanogens and the dissolution rate of H_2 gas might be a weak function of pressure with the range tested in this study.

Further examination of the individual volatile acids supports the hypothesis relating to H_2 inhibition. As shown in Appendix F, the concentrations of the H_2-producing volatile acids, especially propionate, n-butyrate, and n-valerate, were all significantly reduced in both gas recycle runs (compared to Run 10a) at most ports of the three SMARs. For example, propionate concentration decreased from 98 mg/L to 14 mg/L at port #1 of SMAR A, from 233 mg/L to 97 mg/L at port #1 of SMAR B, and from 360 mg/L to 202 mg/L at port #4 of SMAR C. However, most of the acids at the bottom two ports of SMAR C (C1 and C2) increased with gas recycle. This might be due to faulty sampling (clogged ports) that leads to the very low acids concentrations for the run without gas recycle.

Acetate concentrations also increased at some ports. An explanation is that, with gas recycle, acetate was produced at a higher rate from acetogenesis of the H_2-producing volatile acids, while, with no gas recycle, acetogenesis was inhibited due to a higher H_2 partial pressure. Figures 48 through 50 compare Run 10a and 10aG2 for the distribution in acetate, propionate, and butyrate, respectively.

With gas recycle, SCOD and TOA distribution decreased at most heights of the three SMARs (Figures 51 and 52), which correspondingly resulted in an increase in pH distribution (Figure 53). Although the gas recycle rates were small (about 3.5% in Run 10G1 and 7.0% in Run 10aG2), TSS distribution (Figure 54) clearly showed that the bottom solids zones in the three SMARs expanded upwards. It appears that SMAR A was too short to retain the expanded solids. In SMARs B and C, solids expansion was limited to the bottom 30 cm.

Gas recycle has been used as a common practice in digester operation to provide mixing for better contact between substrate and organisms. Mixing can also be achieved by using mechanical devices such as low-speed turbines at an equivalent mean velocity gradient (G). In this respect, mixing is simply used for a physical purpose (better contact). However, a recent USEPA report (1987) states that:

> A correlation of equivalent mixing efficiencies with the velocity gradient values for different (mixing) systems has not been demonstrated.

Biogas mixing has been proven to be a more efficient mixing method than mechanical mixing in the operation of many full-scale sludge digesters

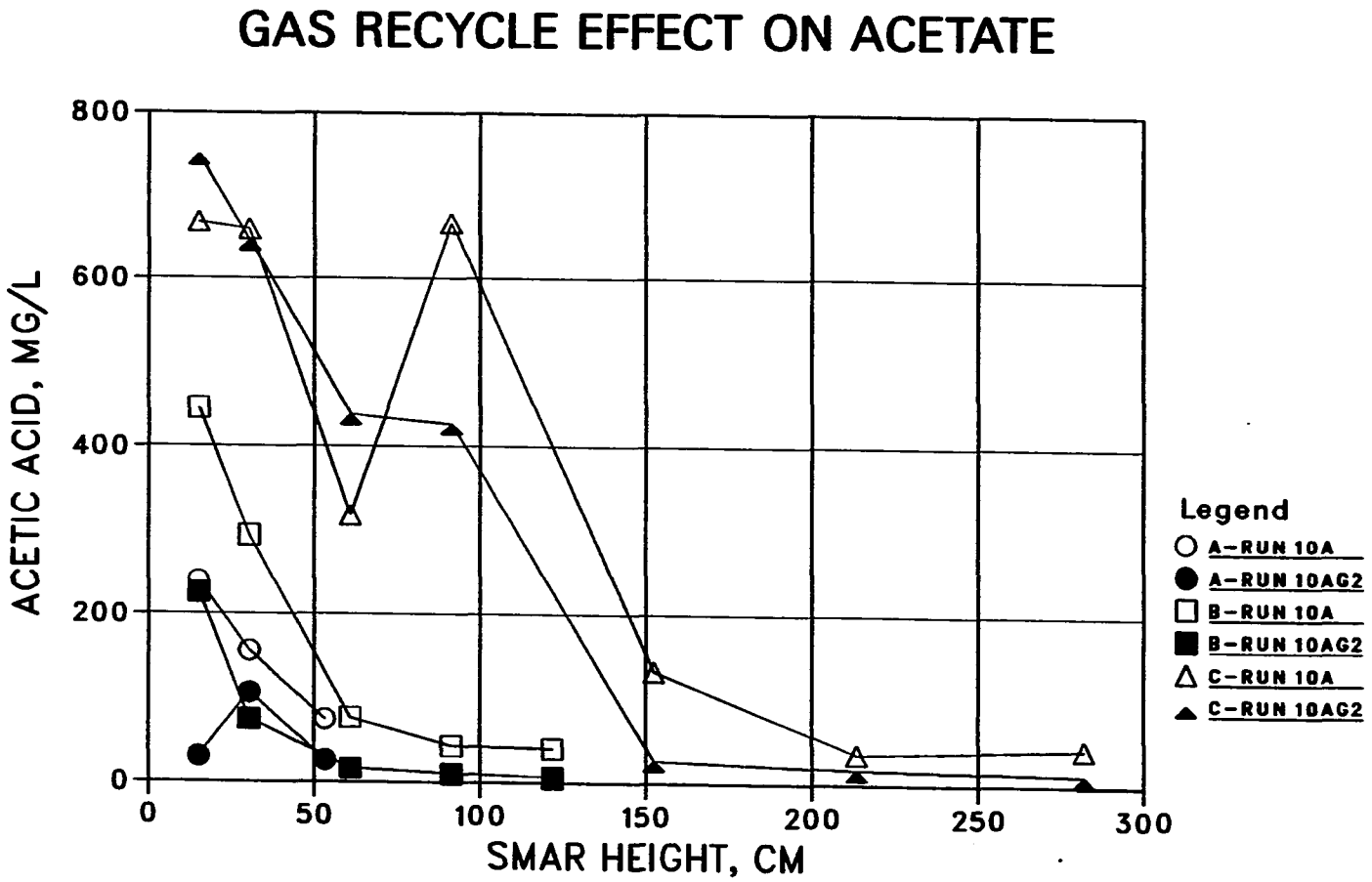

FIGURE 48. Effect of gas recycle on acetate distribution, comparing Run 10a (no recycling) vs. Run 10aG2 (recycling), both with a COD loading rate of about 10 g/L/d and a retention time of about 2 days

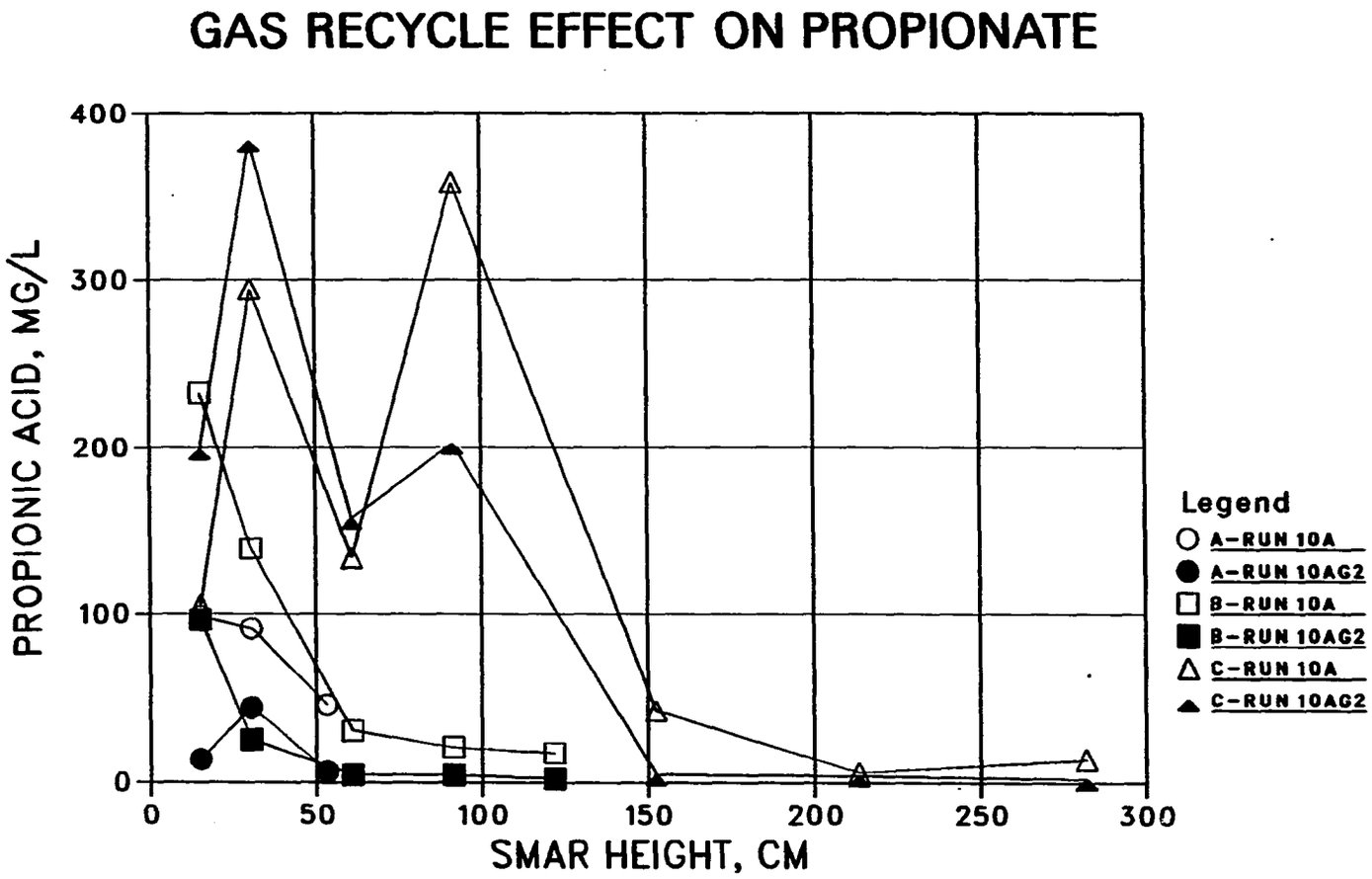

FIGURE 49. Effect of gas recycle on propionate distribution, comparing Run 10a (no recycling) vs. Run 10aG2 (recycling), both with a COD loading rate of about 10 g/L/d and a retention time of about 2 days

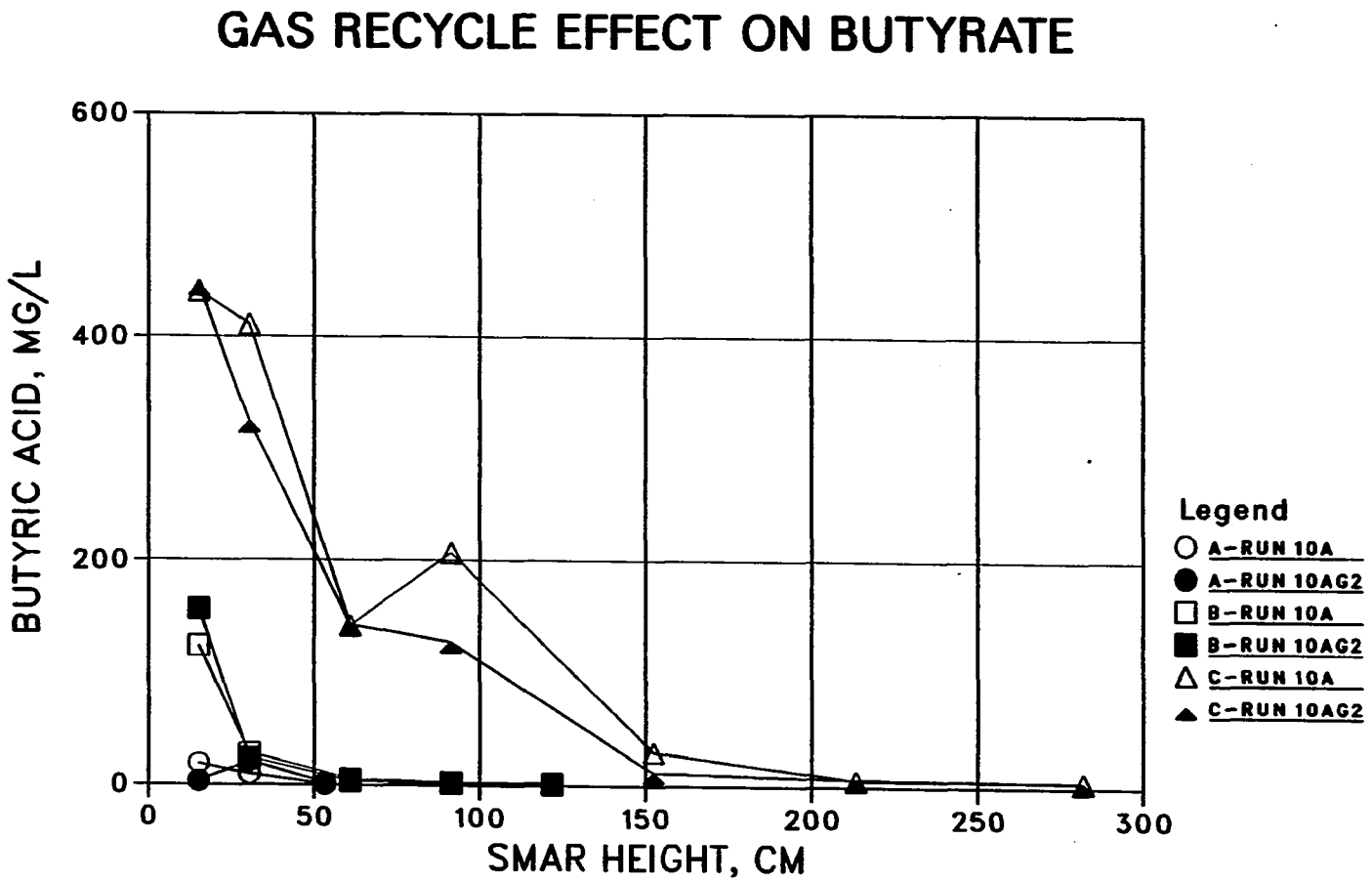

FIGURE 50. Effect of gas recycle on butyrate distribution, comparing Run 10a (no recycling) vs. Run 10aG2 (recycling), both with a COD loading rate of about 10 g/L/d and a retention time of about 2 days

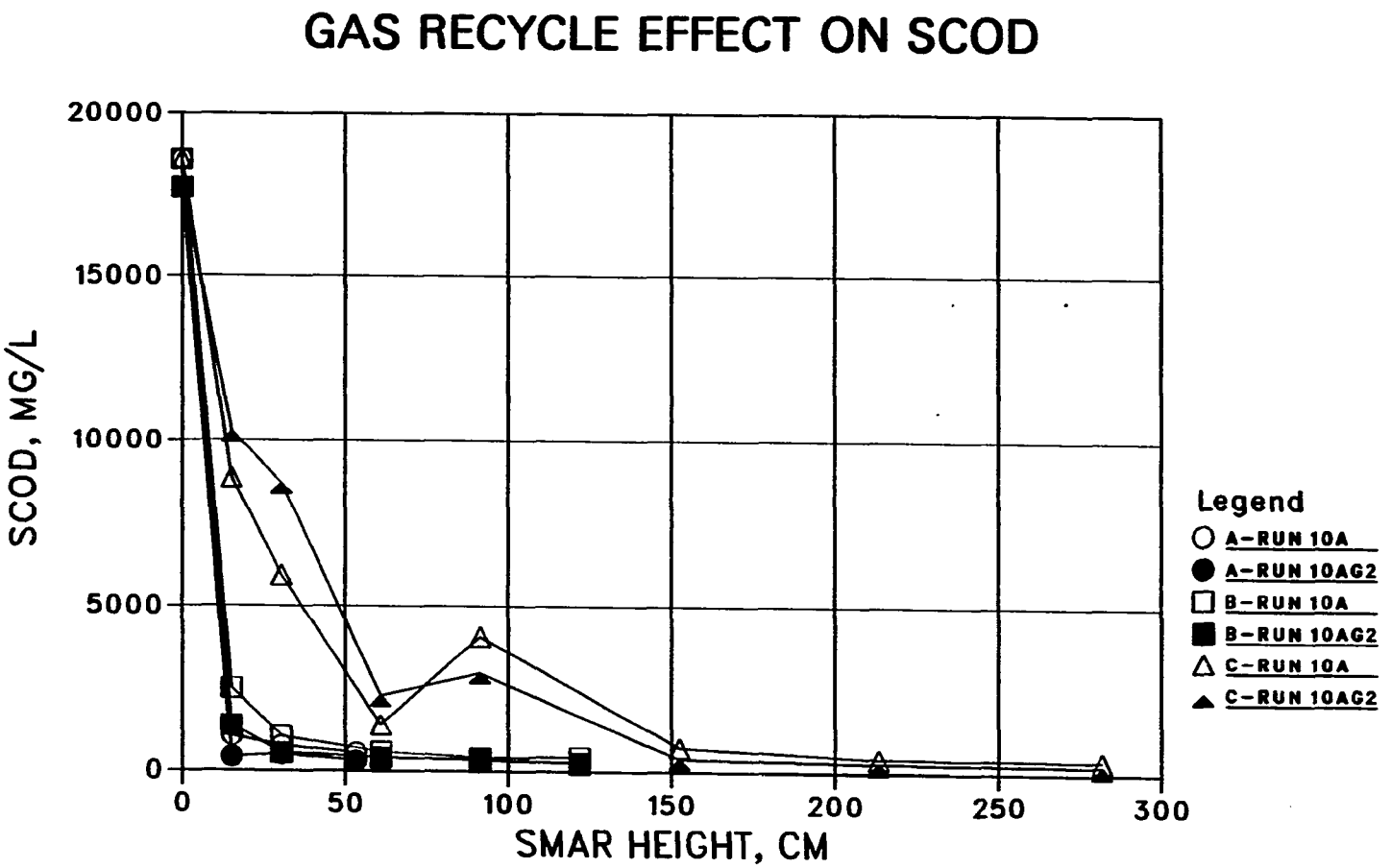

FIGURE 51. Effect of gas recycle on SCOD distribution, comparing Run 10a (no recycling) vs. Run 10aG2 (recycling), both with a COD loading rate of about 10 g/L/d and a retention time of about 2 days

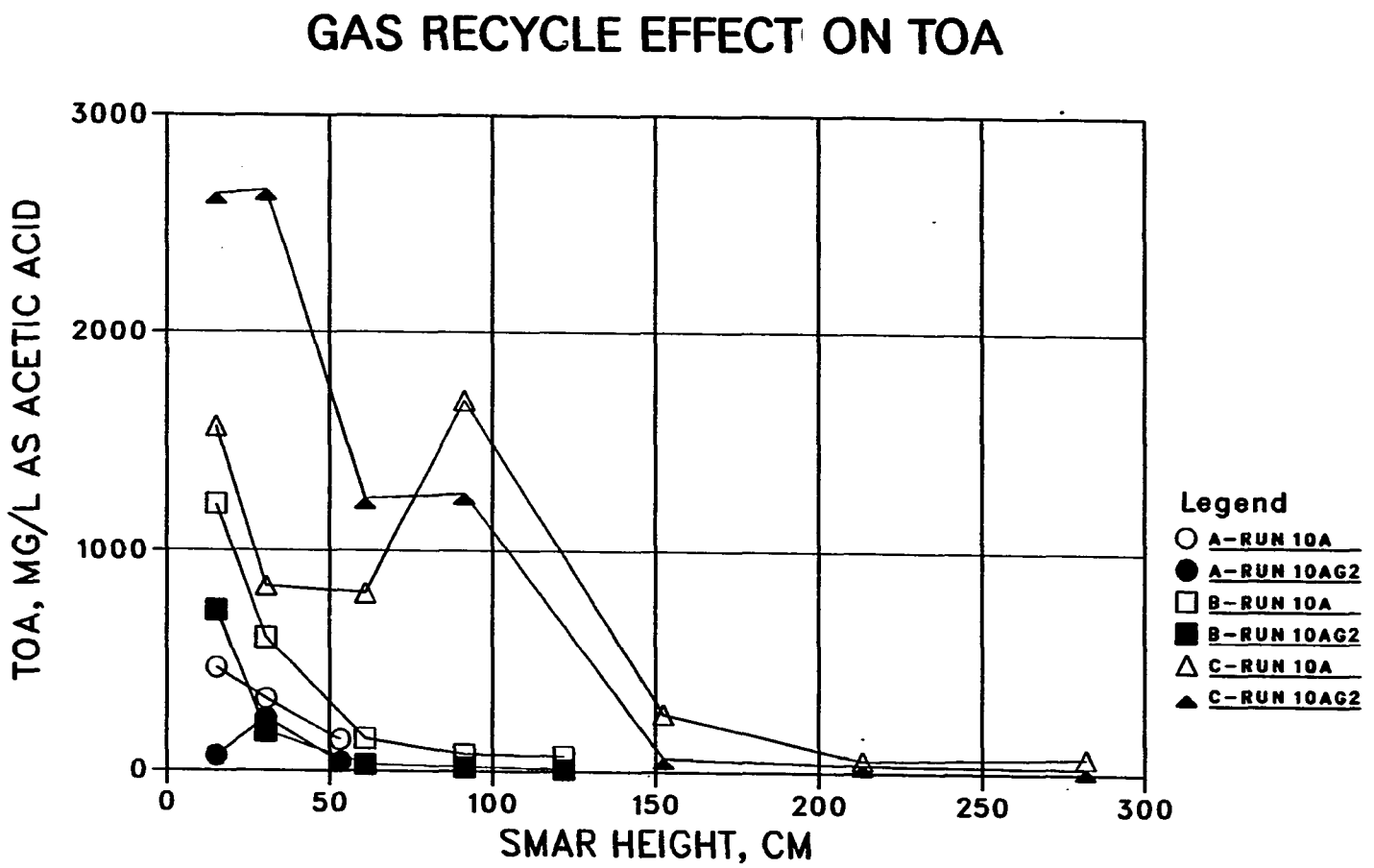

FIGURE 52. Effect of gas recycle on TOA distribution, comparing Run 10a (no recycling) vs. Run 10aG2 (recycling), both with a COD loading rate of about 10 g/L/d and a retention time of about 2 days

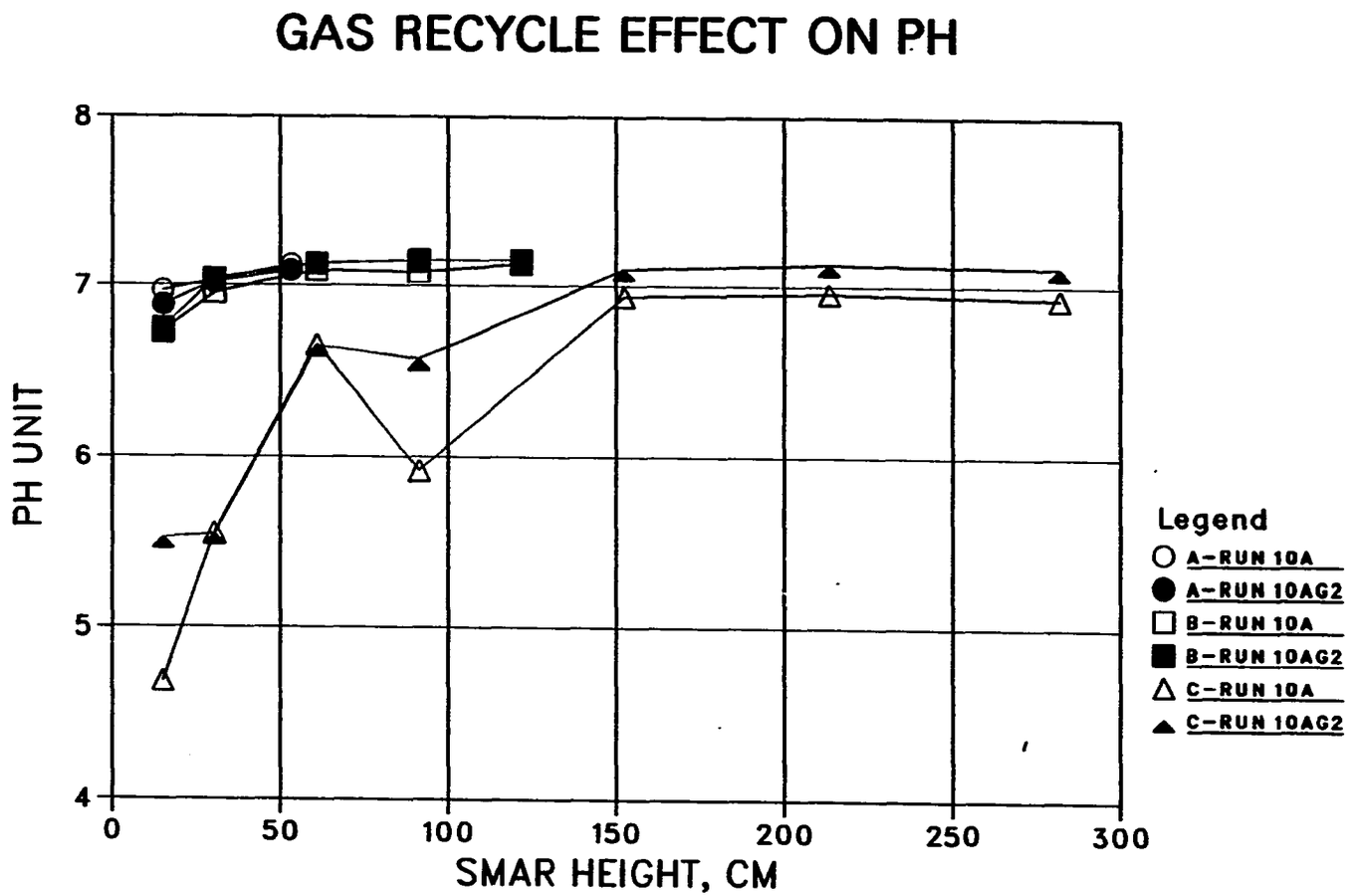

FIGURE 53. Effect of gas recycle on pH distribution, comparing Run 10a (no recycling) vs. Run 10aG2 (recycling), both with a COD loading rate of about 10 g/L/d and a retention time of about 2 days

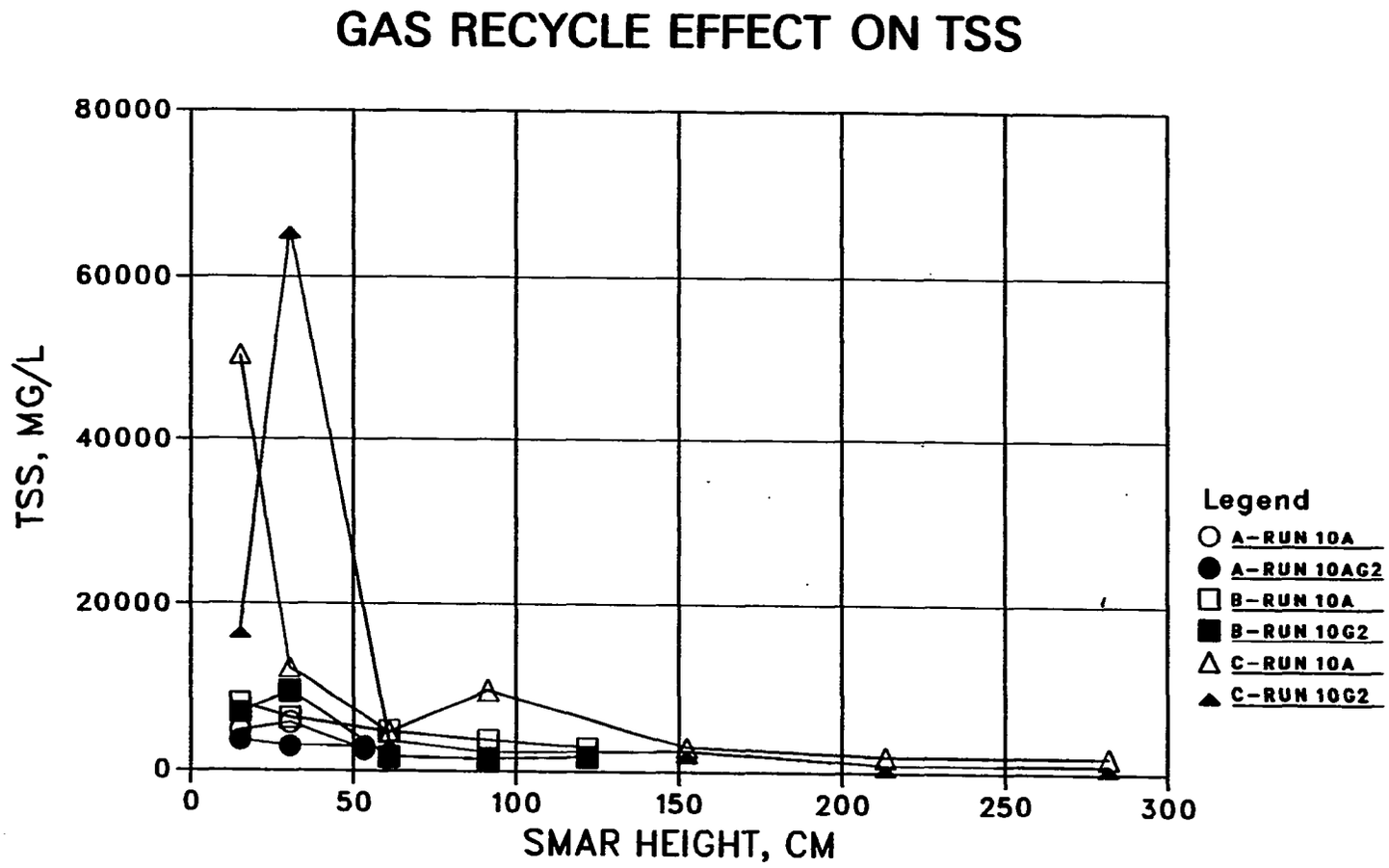

FIGURE 54. Effect of gas recycle on TSS distribution, comparing Run 10a (no recycling) vs. Run 10aG2 (recycling), both with a COD loading rate of about 10 g/L/d and a retention time of about 2 days

(Estruda, 1960). In the onset study of the high-rate sludge digesters, Morgan (1954) observed that the recycle of endproduct biogas can noticeably enhance the sludge digestion rate. He thus termed this as an "autocatalytic reaction". Operations of large-scale pure-culture methanogenic reactors have also shown that methanogenic growth rate on hydrogen (as the sole energy source) can be greatly accelerated (from 0.02 to 0.18 1/hr) when agitation speeds (of six-bladed impeller) increase from 200 rpm to 1000 rpm (Daniels *et al.*, 1984a). All the above information suggests a perception that mixing by gas recycle might have provided a need more than just for a physical reason of a better contact. A biological reason that allows the hydrogen gas in the recycle gas to be more efficiently utilized, consequently enhancing digestion performance, might be a more valid explanation. More studies need to be done to confirm this.

Unsteady-State Response

The general pattern of the unsteady-state responses of the three SMARs to changes in operating conditions is discussed below. Once a steady-state run was completed, loading conditions were changed for the next steady-state study by changing the influent COD concentration and/or flowrate. The general rule was to stepwise increase the volumetric loading rate (g/L/d), but sometimes the loading rate was decreased for a few days and then suddenly increased to observe the response. Appendix D shows the gas production rates for the entire study.

Response to Loading Change

In general, response of gas production to a change in COD loading rate was quick and a steady state was achieved within a few days. For example, on day 75, the loading rate was increased to about 1.0 g/L/d by doubling the influent COD concentration to about 2.0 g/L. The daily gas production rate increased immediately and achieved a steady-state level on day 77. At higher loading rates, such as Run 4b1 on day 273 and Run 8a on day 326, the same quick response was observed.

It seems that operation at higher flowrates resulted in faster responses to change in loading, probably due to the shorter flow-through times required. Response to a sudden large increase in influent flowrates with the same COD loading rates, such as for Run 2c on day 258, was characterized by an initial increase followed by a gradual decrease in gas production. A possible explanation is that, upon the increase of flowrate, the higher influent COD concentration, previously loaded in the SMAR, was quickly displaced upwards and replaced by the lower influent COD concentration. The initial increase and subsequent decrease in gas production was more gradual for SMAR C than for SMARs A and B, probably due to a more plug-flow hydraulic pattern in SMAR C. This might suggest that SMARs that need to treat wastes with a more diurnal or seasonal flowrate change should be designed to enhance plug-flow hydraulics to dampen the changes.

Response to Incidental Air Exposure

On two occasions, air was accidentally pumped into the SMAR system due to clogging in the tap water pressure reducer. The first incident occurred on day 52 (the 2nd day after reseeding) during the re-acclimation period with gas recycle. The system was air-recycled for about 4 hours at a rate of about 250, 120, and 60 mL/min for SMARs A, B, and C, respectively. Gas production decreased by about 20% on the next day, but there was no further decrease thereafter.

The second incident occurred on day 280 right after steady-state Run 4b1. Air was fed through the influent line with no gas recycle for a period of about 1 day. No apparent negative impact was observed. It is explained that, because of the substrate gradient nature of biofloc and biofilm growth in the SMAR system, oxygen which was incidentally fed might not fully reach the growth surface to cause inhibition.

Response to Temperature Change

In a period of day 259-267 (Run 2C), influent temperature fluctuated between 22 and 39° C due to a malfunction in the tap water pressure reducer. Gas production reduced almost by half on day 261 with an influent temperature of 22° C. SMAR C was more stressed than SMARs A and B. An unusual odor was sensed for several days after a constant temperature of 35° C was restored.

Response to Restarting after Long-Term Recession

Response of the three SMARs after a long period of recession was also studied. During the New Years period, COD loading was maintained at a very low rate of about 0.2 g/L/d with a retention time of about 2 days for 22 days. Steady-state gas production was observed in 2 days after the loading was resumed at about 2 g/L/d.

In another incident during the latter phases of this study, the SMAR system was shut off for 12 days (days 368-380) due to a malfunction in the feed pump speed controller. The system was restored at a loading rate of about 8 g/L/d with a retention time of about 0.5 days. Steady-state gas production was achieved in 2 days. SMAR C recovered at a slower rate than SMARs A and B. It is worth noting that, even though the system was operating under acidic conditions (pH 6.0-6.7 along the SMAR height), not considered as an optimum condition in the latter phases of this study, the system was able to recover quickly at such a high loading rate after the long-term recession.

Response to Starving

At the end of the study, influent to the SMAR system was shut off and gas production was monitored for 21 days (day 418 to 438). The purpose of this was to see if there was any difference in decay rate among the three SMARs under starving conditions. The wet test meter for SMAR B was not available at that time, therefore only SMARs A and C were monitored.

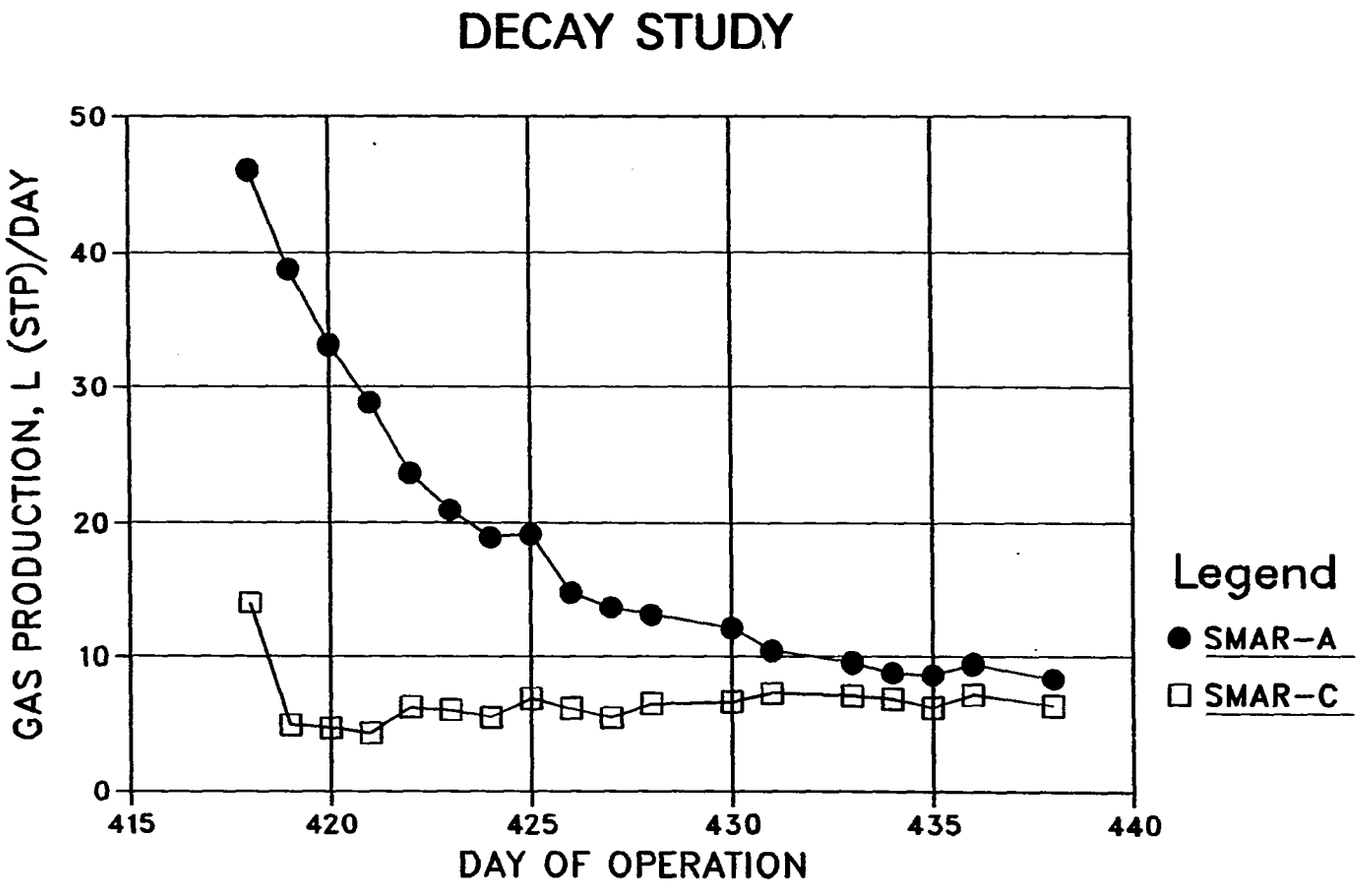

FIGURE 55. Effect of hydrostatic pressure on decay rate

Surprisingly, as shown in Figure 55, SMAR A decayed at a much faster rate than SMAR C. The initial decay rate of SMAR A was about 46 L gas produced/d with a constant rate of change of about 4 L/d/d. The initial decay rate decreased at the constant rate of change for about 10 days and stabilized at a rate of about 9 L/d after. SMAR C, however had a very different response to starving. The gas production rate of SMAR C dropped from about 14 L/d to about 5 L/d on the 2nd day after the start of starving. The gas production then gradually and slightly increased to about 6 L/d at the 5th day and remained at approximately the same rate after that. Gas analysis on day 21 after starving was not successful due to an inadequate gas volume that could be sampled.

The results of the decay study suggest that the decay rate of anaerobic digestion is inversely proportional to the hydrostatic pressure under which the decay occurs. SMARs with higher hydrostatic pressures, as for SMAR C, tend to retain the decaying gas in the systems and retard the decaying process. The same type of retardation (Figure 21) was also observed in most of the AMA tests as pressures built up in the incubation flasks.

SMAR Sizing and Operation

SMAR Sizing Procedures

Based on the results of this study, procedures that could be used for SMAR design are presented below. As shown in Figure 31, TCOD removal rate based on the g/L liquid volume/d appears to be a good design parameter for determining SMAR liquid volume.

SRT is likely to be a better operating index rather than a good parameter for SMAR sizing. This is because the SRT in SMAR systems is usually too long (such as 300-500 days) to be a sensitive design parameter. Also, the concept of SRT fails to differentiate the biomass activity which could vary by a factor of at least ten in a SMAR system (Appendix D). Retention time (T_d) could be used as the design parameter for SMAR sizing with a fairly simple calculation. However, as influent COD concentrations vary, the performance of SMARs is quite different even with the same T_d.

The SMAR sizing procedure presented below is based on three criteria: (1) TCOD removal rate (g/L/d), (2) Theoretical retention time (hour), and (3) Influent substrate flux ($g/cm^2/d$).

(1) Determine the distribution curve of the TCOD removal rates (g/L/d) for a range of COD loading rates and detention times as shown in Figure 31, by pilot-scale tests.

(2) For a design flowrate (Q) and influent COD concentration (S_0), calculate the total daily COD loading rate in g/d (QS_0).

(3) Assume a design SMAR liquid volume (V_l) and calculate the volumetric COD loading rate in g/L/d (QS_0/V_l).

(4) Using the TCOD removal curve established in Step 1, determine the TCOD removal rate (R) at the calculated loading rate determined in step 3.

(5) Decide on a design TCOD removal percentage (p). This could be estimated from the slope of the TCOD removal curve determined in

Step 1. Calculate the total COD required to be treated (pQS_0). It should be noted that a removal percentage beyond the treatment capability determined by the TCOD removal curve in Step 1 should not be used.

(6) Determine the SMAR operating liquid volume (V_2) by pQS_0/R.

(7) If the volume determined in Step 6 is different from the assumed volume in Step 3, repeat Steps 3 through 6 using the volume determined in Step 6 until the volume is the same or within an acceptable range between two consecutive calculating cycles (V_3).

(8) Calculate the theoretical detention time ($T_d = V_3/Q$) to see if it is within the range used in the pilot test for establishing the TCOD removal curve in Step 1. If the T_d is shorter than the shortest value used in the pilot test, a longer T_d should be used to determine the SMAR void volume (V_4).

The SMAR void volume (V_3 or V_4) determined above is based on the actual operating data with the pilot-scale SMARs under actual short-circuiting conditions. Therefore, the short circuiting factor has been considered in the above sizing procedures and needs not be corrected for. However, a scale-up safety factor (f) can be estimated to determine the full-scale SMAR liquid volume ($V_5 = fV_3$ or fV_4). And finally, the SMAR design volume (V) is calculated by dividing V_5 by the packing porosity. It is worth noting that the type of packing that is to be used in full-scale SMARs should be used, in the related pilot-scale studies with the exact same scale, shape, and dimensions (Young, 1985).

To determine SMAR height, the height used in the pilot-scale study could be directly used since this is the height used in establishing the TCOD removal curves in Step 1 above. This also implies that the height of the pilot-scale SMARs should be as close as possible to the height of full-scale SMARs to be designed. This might be somewhat difficult since the height is what needs to be designed. Dague (1982), observing that most removal occurs in the bottom zone, suggests a shallow type of SMAR with a height of about 10 ft (3.3 m). Recently, one full-scale SMAR was designed with a height of 10 ft in the treatment of vegetable processing waste (Roe and Love, 1984). However, the SMAR height should not be scaled up simply using the height/diameter ratio of the pilot-scale SMAR.

Once the volume and height are determined, the cross-sectional area can be calculated. The area (A) should be checked for influent COD flux (QS_0/A). As shown in this study, biomass accumulation in the bottom zone of SMAR C resulted in clogging and serious short-circuiting in the latter phases of this study with a COD loading rate of about 10 g/L/d (Run 10a). With the loading rate, influent COD flux was about 2.8 $g/cm^2/d$ for SMAR C, as compared to about 0.5 for SMAR A and 1.2 for SMAR B. Based on this, a maximum influent COD flux of 2 $g/cm^2/d$ for the NFDM waste is suggested.

Operation with Gas Recycle

Based on the results of the gas recycle studies (Run 10aG1 and 10aG2), the SMAR process should be designed to quickly remove H_2 gas once

it is produced. This is especially true if the SMAR is to be operated at high loading rates, such as above 6 g/L/d. One of the methods, as demonstrated in this study, is to recycle the exit gas. Gas can also be recycled within the bottom active zone, and this is probably a better method to avoid the disturbance in the upper zone, as it would be disturbed with the exit gas recycle.

One of the questions that remains to be answered is what should be the optimal recycling ratio, if there is one. The writer favors a small recycling ratio, such as 5%. It is felt that the key point of gas recycle is to quickly dissolve the insoluble H_2 gas once it is produced. It is also felt that the dissolution rate of H_2 is not a strong function of pressure and mixing intensity, but a strong function of the H_2 bubble size. Therefore a high recycle ratio should not significantly improve the dissolution rate. Also a high ratio might result in the expansion of the bottom solids zone, if gas recycle is not properly designed. If the H_2 dissolution rate is a strong function of H_2 bubble size, fine bubble sparging should be used.

Gas recycle allows H_2 gas in the system to be utilized by the H_2-utilizing methanogens so that the H_2 partial pressure in the system can be reduced. Consequently, methane production and TCOD removal rate can increase and solids become more stabilized. However, if gas recycle is to be used, the height should be carefully reviewed to ensure that effluent solids do not increase.

SUMMARY OF RESULTS AND CONCLUSIONS

Tracer studies:

(1) Tracer studies were done on both clean and dirty-bed SMARs, using lithium chloride with a slug input. This appears to be appropriate with a fair lithium recovery of 80-100 percent. Inadequate recovery due to absorption and/or adsorption by biomass in this study was not as great as in a previous study by Mueller and Mancini (1976), using a dye tracer.

(2) The clean-bed tests were done with and without air gassing at a theoretical hydraulic retention time of about 0.5 day. With no gassing, the three SMARs had about the same degree of dispersion with a dispersion number (N_d) of 0.10-0.12. Based on the ratio of actual retention time to theoretical retention time (T/T_d), SMARs A and B had very little short-circuiting, while SMAR C (the tallest column) had slight short-circuiting (0.92), probably due to a higher superficial velocity.

(3) Bottom single-point air gassing was used for the clean-bed tracer test at a mean velocity gradient of about 40 1/sec. Under this gassing condition, SMARs A and B had a very large dispersion (N_d = 0.8-0.9) and SMAR C had a large dispersion (0.3). The shortest column (SMAR A) had the most short-circuiting (0.78) and the tallest column (SMAR C) had the least (0.95). This suggests that gassing has a significant effect on SMAR hydraulics, and, by increasing the SMAR height, short circuiting can be reduced.

(4) Two dirty-bed tests were conducted at COD loading rates of about 4 g/L/d and 8 g/L/d and a hydraulic retention time of about 0.5 days. Compared to the clean bed with gassing, the dirty beds displayed more short-circuiting (0.6-0.8), even at lower mean velocity gradients (10-40 1/s). At the COD loading rate of 4 g/L/d, the tallest column (SMAR C) had the least short-circuiting (0.83) and dispersion (0.17). However, at the COD loading rate of 8 g/L/d, SMARs A and C were more short-circuiting (0.60) than SMAR B (0.71). SMAR A was probably too short to retain its contents under the effect of biogas mixing. For SMAR C, the higher short-circuiting probably resulted from the accumulation of highly concentrated biomass in the bottom. This suggests that, under normal operating conditions, biogas mixing and accumulation of biomass has a significant effect on SMAR hydraulics to cause short-circuiting, and it appears that there is an optimal height/diameter ratio (such as for SMAR B) in reducing the short-circuiting.

(5) Clean-bed tracer tests cannot be used to estimate SMAR hydraulics under normal operating conditions. The actual SMAR hydraulics under normal operating conditions is a plug flow with a strong dispersion with the dispersion number (N_d) ranging from 0.2 to 1.0 and a dispersion coefficient (D_d) ranging from 1 to 90 cm^2/min.

(6) The dispersion numbers obtained in this study cannot be correlated with the mean velocity gradient induced by biogas mixing. The SMAR configuration must be considered.

Activity test:

(1) The test criteria listed in Table 13 and the procedure shown in Appendix C for the acetoclastic methanogenic activity (AMA) test developed in this study appears to be appropriate, as evidenced by a strong linear specific gas production rate (L/g VSS/hour) and a fair success rate.

(2) In general, the anaerobic procedures of N_2 gas purging and sulfide addition are adequate to provide the anaerobic requirement. Stabilization for one hour after seeding is adequate for the depletion of air exposed in sample transfer. Gentle hand mixing appears to be appropriate for data reproducibility.

(3) The manometer calibration procedure by incrementally withdrawing gas from incubation flasks appears to be appropriate, as evidenced by the almost perfect least squares linear correlation of the calibration curves.

(4) A reproducibility study with four repetitions gives the activity test a variation coefficient of 6.5% at a mean AMA of 0.39 L CH_4 (STP)/gm VSS/d.

SMAR performance:

Three different shapes of cylindrical SMARs with the same packing volume of about 85 liters were operated at 35 ^{o}C for 415 days with a COD loading rate ranging from 1 to 12 g/L/d at three hydraulic retention times of about 0.5, 1, and 2 days. The feed substrate was made of low-heat non-fat dry milk with mineral supplement. The effect of biogas

mixing was also evaluated by recycling exit gas after the H_2S scrubbers and directly injecting the gas into the bottom feed lines.

Throughout the entire study, pseudo steady-state performance of the three SMARs was evaluated in seventeen runs, as shown in Figure 22. Analyses on samples from various heights and effluent included total and soluble chemical oxygen demand (TCOD and SCOD), pH, alkalinity, total volatile acids (TVA), individual organic acids (C2-C5), and the activity test (AMA). Daily gas production and the methane content of the exit gas were also determined. The following observations can be made:

(1) TCOD removal rate, instead of SCOD removal rate, should be used in the treatment performance evaluation of the SMAR process so that its solids retention capability can be also considered.

(2) Based on TCOD removal rates (Figure 31), the tallest column (SMAR C) performed slightly better with COD loading rate above 4 g/L/d (with and without gas recycle). With COD loading rate equal to or below 4 g/L/d, there was little difference in TCOD removal rate among these three SMARs. With no gas recycle, SMARs A (the shortest column) and B showed little difference in TCOD removal rate. With gas recycle, SMAR B performed better than SMAR A in TCOD removal rate.

(3) With no gas recycle, there was little difference in SCOD removal rate among the three SMARs (Figure 32). Comparisons between TCOD removal rate and SCOD removal rate suggests that the better performance of SMAR C was related to its better solids retention capability, resulting in less effluent solids. Evaluation based on

daily average methane production rate (Figure 33) and TSS effluent rate (Figure 34) agrees with the findings based on TCOD and SCOD removal rates.

(4) In general, SMAR A had a fairly uniform distribution in pH, SCOD, TOA, TSS, and AMA with height (Appendix E), while SMAR C had the widest variation. This suggests that there was a fundamental difference in the operation of the three SMARs. In SMAR A, the acid and methane formers were more uniformly mixed together by the self-induced biogas. In SMAR C, these two groups appear distinctively stratified, especially at high loading rates.

(5) Acetoclastic methanogenic activity (AMA) ranged from 0.05 to 0.72 L CH_4 (STP)/gm VSS/d in this study. For VSS less than 1 g/L, a higher AMA is associated with lower VSS concentrations (Figure 45). For VSS greater than 1 g/L, AMA varies within a narrow range of 0.1 to 0.2 L CH_4 (STP)/gm VSS/d.

(6) Unsteady-state operating data indicate that, the SMAR system is capable of a quick response to organic shock loadings and hydraulic shock loadings. The system can tolerate a certain degree of air exposure and low temperature. The system can also recover from a long-term recession at a full loading rate within 2 to 3 days.

Effects of gas recycle:

(1) Gas recycle studies were done on two occasions with recycle ratios of about 3.5% and 7.0% and a COD loading rate of about 10 g/L/d at a hydraulic retention time of about 2 days. Compared to the run with

the similar operating conditions without gas recycle, gas recycle result in a 5-13% increase in CH_4 content. Comparisons in distributions of SCOD, individual volatile acids (C2-C5), and pH show interrelated effects of the improved performance with gas recycle. However, there is little difference in the improved performance among these three SMARs with gas recycle.

(2) With gas recycle, data in TSS distribution show that the bottom solids zones in the three SMARs expanded upwards. It appears that SMAR A is too short to retain the expanded solids. In SMARs B and C, solids expansion was limited in the bottom 30 cm.

SMAR design procedure:

(1) Based on the results of this study, a rational SMAR design procedure is proposed. The procedure is based on three criteria: TCOD removal rate (g/L/d), theoretical detention time (hours), and influent substrate flux ($g/cm^2/d$). The last criterion is set to prevent systems from the bottom accumulation of highly concentrated solids that could result in serious short-circuiting and clogging problems.

(2) When conducting SMAR pilot studies, the height of the pilot-scale SMARs should be as close as possible to the height of the full-scale SMARs to be designed. Considering that most removal occurs in the bottom zone, a shallow type of SMAR, say about 10 ft (3.3 m) can be used, as opposed to a 20-30 ft SMAR height used by Taylor (1972) and Witt *et al.* (1979).

(3) Based on the results of the gas recycle studies, the SMAR process can be designed for gas recycle to improve performance, especially at high loading rates. It is suggested that the key point of gas recycle is to quickly dissolve the insoluble H_2 gas once it is produced. It is also suggested that a small recycle ratio, such as 5%, be used to minimize bottom solids expansion. If the H_2 dissolution rate is a strong function of H_2 bubble size, fine bubble sparging should be used. If gas recycle is used, the height should be carefully reviewed to ensure that effluent solids do not increase.

RECOMMENDATIONS FOR FURTHER RESEARCH

Hydrostatic Pressure:

A type of retardation in gas production was observed in two separate tests during this study. The first was in conducting the AMA tests for samples obtained from various heights of the SMARs. In most runs, retardation was observed when the pressure built up after 5-6 hours of incubation. The retardation could not be due to substrate limitation, since an adequate F/M ratio was insured throughout the entire period of incubation. The incubation under high pressures could not be further studied because of the use of the manometer, which could only hold a maximum pressure of about 20-25 cm acetylene tetrabromide ($C_2H_2Br_4$, s.g. 2.96 g/cm^3).

The second test was in conducting the SMAR decay test under starving conditions at the end of this study. SMAR C, which has a higher hydrostatic pressure, decayed at a much slower initial rate than did SMAR A (Figure 45). It is suggested that the type of retardation under high pressure be further studied during acclimation and normal operating conditions. The importance of the study can be related to the scale-up problem. Many full-scale anaerobic reactors are operated at a much higher hydrostatic pressure (20-30 ft H_2O) than the pilot-scale reactors (0.5-5 ft H_2O) used to establish design loadings.

The retardation test can be done by using a pressure transducer with a signal readout device in the AMA test. Another method is to operate CSTRs with a pressurized water lock. The first method is easier while

the second method can provide information with continuous feeding under acclimation or normal operating conditions.

Fine bubble sparging:

The results of the gas recycle study suggest a hypothesis that, at high loading rates, anaerobic digestion can be rate-limited by the dissolution rate of hydrogen gas produced in the system. Indeed, hydrogen gas is very insoluble in water (about 1.6 g/L at 25° C). When hydrogen is produced by hydrogen-producing acetogens, it is in the dissolved form. The dissolved hydrogen that is not utilized in time tends to volatilize into the gas phase. The hydrogen gas, which cannot be utilized by methanogens (or even sulfate-reducers), builds up and eventually reaches a level that inhibits the hydrogen-producing acetogenesis, especially of low-carbon volatile acids, such as propionate and butyrate.

One can also speculate that the dissolution rate of hydrogen gas is a strong function of hydrogen bubble size. It is suggested that further studies be done to verify this hypothesis. This can be done by operating several CSTRs with hydrogen gas sparging through diffusers with different pore sizes. This would allow for establishing the relationship between hydrogen utilization rate and hydrogen dissolution rate with different bubble sizes. Also, biofilm or biofloc reactors such as anaerobic filters can be operated at high loading rates using complex wastes and sparged with recycled gas using fine-bubble diffusers. This would allow

for study of the optimal gas recycling rate (if there is one) and demonstrate a practical use of the hypothesis.

BIBLIOGRAPHY

Andrews, J. F. and Pearson, E. A. "Kinetics and characteristics of volatile acid production in anaerobic fermentation processes." International Journal of Air and Water Pollution, 9, 439-461 (1965).

Argonne National Laboratory. Anaerobic Filters: An Energy Plus for Wastewater Treatment. Proceedings of the Seminar/Workshop, Howey-In-The-Hill, Florida, ANL/CNSV-TM-50 (1980).

Arora, H. C. and Chattopadhya, S. N. "Anaerobic contact filter process: a suitable method for the treatment of vegetable tanning effluents." Water Pollution Control, 79, 501-506 (1980).

Bache, R. and Pfennig, N. "Selective isolation of *Acetobacterium woodi* on methoxylated aromatic acids and determination of growth yields." Archives of Microbiology, 130, 255-261 (1981).

Backman, R. C., Blanc, F. C., and O'Shaughnessy, J. C. "The treatment of dairy wastewater by the anaerobic up-flow packed bed reactor." Proceedings of the 40th Industrial Waste Conference, Purdue University, West Lafayette, Indiana (1986).

Balch, W. E., Fox, G. E., Magrum, L. J., Woese, C. R., and Wolfe, R. S. "Methanogens: reevaluation of a unique biological group." Microbiology Review, 43, 260-296 (June, 1979).

Baresi, L., Mah, R. A., Ward, D. M., and Kaplan, I. R. "Methanogenesis from acetate: enrichment studies." Applied and Environmental Microbiology, 36, 1, 186-197 (July, 1978).

Barker, H. A. "Studies on methane producing bacteria." Archives of Microbiology, 7, 420-436 (1936).

Barker, H. A. Bacterial Fermentations. John Wiley & Sons Inc., New York (1956).

Barker, H. A. "Fermentation of nitrogenous organic compounds." The Bacteria--Metabolism. Volume II. I. C. Gunsalus and R. Y. Stainer (Eds.). Academic Press, New York (1961).

Barnes, D., Bliss, P. J., Grauer, B., Kuo, E. M., Robins, K, and Maclean, G. "Influence of organic shock loads on the performance of anaerobic fluidized bed system." Proceedings of the 38th Industrial Waste Conference, Purdue University, West Lafayette, Indiana (1983).

Belay, N., Sparling, R., and Daniels, L. "The assimilatory reduction of N_2 and NO_3^- by *Methanococcus thermolithotrophicus*." Proceedings of Biotechnology Advanced Processing Municipal Wastes, Fuels, and Chemicals. A. A. Antonopoulos (Ed.). Argonne National Laboratory, ANL/CNSV-TM-167 (1985).

Belyaev, S. S., Wolkin, R., Kenealy, N. J., DeNiro, S. E., and Zeikus, J. G. "Methanogenic bacteria from the Bondyuzhskoe oil field: general characterization and analysis of stable-carbon isotopic fractionation." Applied and Environmental Microbiology, 45, 626-632 (1983).

Bergey's Manual of Determinative Bacteriology. 8th Edition. R. E. Buchanan and N. E. Gibbons (Eds.). Williams and Wilkins Co., Baltimore (1974).

Blum, D. J. W., Hergenroeder, R., Parkin, G. F., and Speece, R. E. "Anaerobic treatment of coal conversion wastewater constituents: biodegradability and toxicity." Journal of Water Pollution Control Federation, 58, 2, 122-131 (February, 1986).

Boone, D. R. and Bryant, M. P. "Propionate-degrading bacterium *Syntrophobacter wolinii*, sp. nov. gen. nov. from methanogenic ecosystems." Applied and Environmental Microbiology, 40, 3, 626-632 (September, 1980).

Brand, J. M. and Markovetz, A. J. "Some thermodynamic considerations for establishing coculture conditions for H_2-producing bacteria with H_2-utilizing bacteria." Department of Biochemistry, University of Fort Hare, Alice 5700, South Africa (1984).

Bryant, M. P. "Microbial methane production--theoretical aspects." Journal of Animal Science, 48, 1, 193-201 (1979).

Bull, M. A., Sterritt, R. M., and Lester, J. N. "The distribution of bacterial activity in an anaerobic fluidized bed reactor." Water Research, 18, 8, 1017-1024 (August, 1984).

Chian, E. S. K. and DeWalle, F. B. "Removal of heavy metals from a fatty acid wastewater with a completely mixed anaerobic filter." Proceedings of the 31st Industrial Waste Conference, Purdue University, West Lafayette, Indiana (1977).

Chiang, C. F. Development of a Design Model for the Static-Bed Submerged Media Anaerobic Reactors. M.S. thesis, University of Iowa, Iowa City, Iowa (July, 1983).

Chiang, C. F. "Nutrition and taxonomy of methanogens." Individual Study, Course No. 061:161. University of Iowa, Iowa City, Iowa (June, 1985).

Chiang, C. F. and Seagren, E. "A new approach to chemical oxygen demand analysis: micro closed-reflux titration-calibration curve method." Presented at the 10th Midwest Water Chemistry Workshop, University of Iowa, Iowa City, Iowa (October, 1987).

Chynoweth, D. P. and Mah, R. A. "Volatile acid formation in sludge digestion." Anaerobic Biological Treatment Processes. R. F. Gould (Ed.). Advances in Chemistry Series 105. American Chemical Society, Washington, D. C. (1971).

Clark, R. H. and Speece, R. E. "The pH tolerance of anaerobic digestion." Advances in Water Pollution Research, Volume II. S. H. Jenkins (Ed.). University of Texas, Austin, Texas (1970).

Contois, D. E. "Kinetics of bacterial growth: relationship between population density and specific growth rate of continuous cultures". Journal of General Microbiology, 21, 40-50 (August, 1959).

Corder, R. E., Hook, C. A., Larkin, J. M., and Frea, J. I. "Isolation and characterization of two new methane-producing cocci: *Methanogenium olentangyi* sp. nov. and *Methanococcus deltae* sp. nov." Archives of Microbiology, 134, 28-32 (1983).

Cornish-Bowden, A. and Eisenthal, R. "Statistical considerations in the estimation of enzyme kinetic parameters by the direct linear plot and other methods." Biochemical Journal, 139, 721-730 (1974).

Crawford, G. V., Alkema, T., Yue, M., and Thorne, M. "Treatment of high strength liquors from sludge thermal conditioning systems using anaerobic packed bed reactors." Presented at the 53rd Annual Conference of the Water Pollution Control Federation, Las Vegas, Nevada (September, 1980).

Dague, R. R. "Principles of anaerobic filter design." Presented at the 26th Annual Great Plains Wastewater Design Conference, Omaha, Nebraska (March, 1982).

Dague, R. R. and Chiang, C. F. "A two-culture model for the submerged media anaerobic reactor." Presented at the 57th Annual Conference of the Water Pollution Control Federation, New Orleans, Louisiana (1984).

Dague, R. R. and Porter, J. R., Jr. "High pH and free ammonia in anaerobic filter inhibition." Abstract Submitted to the 55th Annual Conference of Water Pollution Control Federation, St. Louis, Missouri (1982).

Dague, R. R., McKinney, R. E., and Pfeffer, J. T. "Anaerobic activated sludge." Journal of Water Pollution Control Federation, 38, 2, 220-226 (February, 1966).

Dague, R. R., McKinney, R. E., and Pfeffer, J. T. "Solids retention in anaerobic waste treatment systems." Journal of Water Pollution Control Federation, 42, 2, Part 2, R29-R46 (February, 1970).

Dague, R. R., Brindley, D. R., and Liang, P. S. "Anaerobic filter treatment of recycle from thermal sludge conditioning and dewatering." Presented at the 53rd Annual Conference of the Water Pollution Control Federation, Las Vegas, Nevada (September, 1980).

Daniels, L. "Biological methanogenesis: physiological and practical aspects." Trends in Biotechnology, 2,4, 91-98 (1984).

Daniels, L., Belay, N, and Mukhopadahyay, B. "Considerations for the use and large-scale growth of methanogenic bacteria." Biotechnology and Bioengineering Symposium, 14, 199-213 (1984a).

Daniels, L., Sparling, R., and Sprott, G. D. "The bioenergetics of methanogenesis." Biochimica et Biophysica Acta, 768, 113-163 (1984b).

Daniels, L., Belay, N, and Rajagopal, B. S. "Assimilatory reduction of sulfate, sulfite, and thiosulfate by methanogenic bacteria." Applied and Environmental Microbiology, 51, 4, 703-709 (April, 1986).

Daniels, L., Fuchs, G., Thauer, R. K., and Zeikus, J. G. "Carbon monoxide oxidation by methanogenic bacteria." Journal of Bacteriology, 132, 118-126 (1977).

DeWalle, F. B. and Chian, E. S. K. "Kinetics of substrate removal in a completely mixed anaerobic filter." Biotechnology and Bioengineering, 18, 1275-1295 (1976).

DiLallo, R. and Albertson, O. E. "Volatile acids by direct titration." Journal of Water Pollution Control Federation, 33, 4, 356-365 (April, 1961).

Estruda, A. A. "Design and cost considerations in high rate sludge digestion." Journal of the Sanitary Engineering Division, Proceedings of the American Society of Civil Engineers, 86, SA3, 111-127 (May, 1960).

Finney, C. D. and Evans, R. S., II "Anaerobic digestion: the rate-limiting process and the nature of inhibition." Science, 190, 1088-1089 (December, 1975).

Fox, G. E., Magrum, L. J., Balch, W. E., Wolfe, R. S., and Woese, C. R. "Classification of methanogenic bacteria by 16S ribosomal RNA characterization." Proceedings of National Academy of Science, USA (1977).

Frostell, B. "Anaerobic treatment in a sludge bed system compared with filter system." Journal of Water Pollution Control Federation, 53, 2, 216-222 (February, 1981).

Grady, C. P., Jr. and Lim, H. C. Biological Wastewater Treatment: Theory and Applications. Marcel Dekker, Inc., New York (1980).

Gulevich, W., Renn, C. E., and Liebman, J. C. "Role of diffusion in biological waste treatment." Environmental Science and Technology, 2, 2, 113-119 (February, 1968).

Guyot, J. P., Traore, I., and Garcia, J. L. "Methane production from propionate by methanogenic mixed culture." Federation of European Microbiological Societies (FEMS) Microbiology Letters, 26, 329-332 (1985).

Hansson, G. and Molin, N. "End product inhibition in methane fermentations: effects of carbon dioxide on fermentative and acetogenic bacteria." European Journal of Applied Microbiology and Biotechnology, 13, 242-247 (1981).

Harper, S. R. and Pohland, F. G. "Enhancement of anaerobic treatment efficiency through process modification." Journal of Water Pollution Control Federation, 59, 3, 152-161 (March, 1987).

Harris, J. E., Pinn, P. A., and Davis, R. P. "Isolation and characterization of a novel thermophilic, freshwater methanogen." Applied and Environmental Microbiology, 48, 6, 1123-1128 (1984).

Harvey, M., Forsberg, C. W., Beveridge, T. J., Pos, J., and Ogilvie, J. R. "Methanogenic activity and structural characteristics of the microbial biofilm on a needle-punched polyester support." Applied and Environmental Microbiology, 48, 3, 633-638 (September, 1984).

Haug, R. J., Raksit, S. K., and Wong, G. G. "Anaerobic filter treats waste activated sludge." Water and Sewage Works, 124, 40-43 (February, 1977).

Heyes, R. H. and Hall, R. J. "Kinetics of two subgroups of propionate-using organisms in anaerobic digestion." Applied and Environmental Microbiology, 46, 3, 710-715 (September, 1983).

Hoover, S. R. and Porges, N. "Assimilation of dairy wastes by activated sludge II: the equation of synthesis and rate of oxygen utilization." Sewage and Industrial Waters, 24, 3, 306-312 (March, 1952).

Huber, H., Thomm, M., Konig, H., Thies, G., and Stetter, K. O. "*Methanococcus thermolithotrophicus*, a novel thermophilic lithotrophic methanogen." Archives of Microbiology, 132, 47-50 (1982).

Hungate, R. E., Smith, W., Bauchop, T., Yu, I, and Rabinowitz, J. C. "Formate as an intermediate in the bovine rumen fermentation." Journal of Bacteriology, 102, 389-397 (1970).

Huser, B. A., Wuhrmann, K., and Zehnder, A. J. B. " *Methanothrix soehgenii* gen. nov. sp. nov., a new acetotrophic non-hydrogen-oxidizing methane bacteria." Archives of Microbiology, 132, 1-9 (1982).

Hydroscience, Inc. Pilot-Scale Anaerobic Filter Treatment of Heat Treatment Liquid. EPA-600/2-81-114. Hydroscience, Inc., Westwood, New Jersey (July, 1981).

Jenkins, S. R., Morgan, J. M., and Sawyer, C. L. "Measuring anaerobic sludge digestion and growth by a simple alkalimetric titration." Journal of Water Pollution Control Federation, 55, 5, 448-453 (May, 1983).

Jennett, J. C. and Dennis, N. D., Jr. "Anaerobic filter treatment of pharmaceutical waste." Journal of Water Pollution Control Federation, 47, 1, 104-121 (January, 1975).

Johnson, L. D. and Young, J. C. "Inhibition of anaerobic digestion by organic priority pollutants." Journal of Water Pollution Control Federation, 55, 12, 1441-1449 (December, 1983).

Jones, W. J., Paynter, M. J. B., and Gupta, R. "Characterization of *Methanococcus maripaludis* sp. nov., a new methanogen isolated from saltmarsh sediment." Archives of Microbiology, 135, 91-97 (1983a).

Jones, W. J., Leigh, J. A., Mayer, F., Woese, C. R., and Wolfe, R. S. "*Methanococcus jannaschii* sp. nov., an extremely thermophilic methanogen from a submarine hydrothermal vent." Archives of Microbiology, 136, 254-261 (1983b).

Kaspar, H. F. and Wuhrmann, K. "Kinetic parameters and relative turnovers of some important catabolic reactions in digesting sludge." Applied and Environmental Microbiology, 36, 1, 1-7 (1978).

Kelly, C. R. and Switzenbaum, M. S. "Anaerobic treatment: temperature and nutrient effects." Agricultural Wastes, 10, 135-154 (1984).

Kerby, R., Niemczura, W., and Zeikus, J. G. "Single-carbon catabolism in acetogens: analysis of carbon flow in *Acetobacterium woodii* and *Butyribacterium methylotrophicum* by fermentation and ^{13}C nuclear magnetic resonance measurement." Journal of Bacteriology, 155, 1208-1218 (September, 1983).

Konig, H. and Stetter, K. O. "Isolation and characterization of *Methanolobus tindarius* sp. nov., a coccoid methanogen growing only on methanol and methylamines." Zentralblatt fuer Bakteriologie Mikrobiologie und Hygiene, I, Abstract, Origin, c3, 478-490 (1982).

Kouadio, S. K. Evaluation of the Methods of Linear Least Squares Based on Linearized Models of the Completely Mixed Flow Activated Sludge Process for Estimating the Monod Kinetic Parameters and Alternative Methods for Estimating the Monod Kinetic Parameters. M.S. Thesis. University of Iowa, Iowa City, Iowa (August, 1984).

Lau, A. O., Strom, P. F., and Jenkins, D. "The competitive growth of floc-forming and filamentous bacteria: a model for activated sludge bulking." Journal of Water Pollution Control Federation, 56, 1, 52-61 (January, 1984).

Lawler, D. F., Chung, Y. J., Hwang, S. J., and Hull, B. A. "Anaerobic digestion: effects on particle size and dewaterability." Journal of Water Pollution Control Federation, 58, 12, 1107-1123 (December, 1986).

Lawrence, A. W. and McCarty, P. L. "Kinetics of methane fermentation in anaerobic treatment." Journal of Water Pollution Control Federation, 41, 2, part 2, R1-R17 (February, 1969).

Lee, K. M. and Stensel, H. D. "Aeration and substrate utilization in a sparged packed-bed biofilm reactor." Journal of Water Pollution Control Federation, 58, 11, 1066-1072 (November, 1986).

Lettinga, G., Van Velsen, A. F. M., Hobma, S. W., De Zeeuw, W., and Klapwijk, A. "Use of the upflow sludge blanket (USB) reactor concept for biological wastewater treatment, especially for anaerobic treatment." Biotechnology and Bioengineering, 22, 699-734 (1980).

Levenspiel, O. and Smith, W. K. "Notes on the diffusion-type model for the longitudinal mixing of fluids in flow." Chemical Engineering Science, 6, 227-233 (1957).

Levine, A. D., Tchobanoglous, G., and Asano, T. "Characterization of the size distribution of contaminants in wastewater: treatment and reuse implications." Journal of Water Pollution Control Federation, 57, 7, 805-816 (July, 1985).

Mah, R. A. "Isolation and characterization of *Methanococcus mazei*." Current Microbiology, 3, 321-326 (1980).

Mah, R. A. and Kuhn, D. A. "Transfer of the type species of the genus *Methanococcus* to the genus *Methanosarcina*, naming it *Methanosarcina mazi* (Barker 1936) comb. nov. et. emend. and conservation of the genus *Methanococcus* (approved lists 1980) with *Methanococcus vannielii* (approved lists 1980) as the type species." International Journal of Systematic Bacteriology, 34, 1174-1184 (1984).

Mahoney, E. M., Varangu, L. K., Cairns, W. L., and Kosaric, N. "Cell surface and aggregation studies of microbes from anaerobic systems." Presented at the 57th Annual Conference of the Water Pollution Control Federation, New Orleans, Louisiana (1984).

McCarty, P. L. "Anaerobic waste treatment fundamentals: part one--chemistry and microbiology." Public Works, 95, 107-112 (September, 1964a).

McCarty, P. L. "Anaerobic waste treatment fundamentals: part two--environmental requirements and control." Public Works, 95, 123-126 (October, 1964b).

McCarty, P. L. "Anaerobic treatment of soluble wastes." Advances in Water Quality Improvement. Volume I. E. F. Gloyna and W. W. Eckenfelder, Jr. (Eds.). University of Texas, Austin, Texas (1966).

McCarty, P. L. "Energetics and bacterial growth." Presented at the 5th Rundolf Research Conference, Rutgers-the State University, New Brunswick, New Jersey (1969).

McCarty, P. L. "Historical trends in the anaerobic treatment of dilute wastewaters." Anaerobic Treatment of Sewage. M. S. Swizenbaum (Ed.). University of Massachusetts, Amherst, Massachusetts (June, 1985).

McCarty, P. L. and Smith, D. P. "Anaerobic wastewater treatment." Environmental Science and Technology, 20, 1200-1206 (November, 1986).

McInerney, M. J. and Bryant, M. P. "Anaerobic degradation of lactate by syntrophic associations of *Methanosarcina barkeri* and *Desulfovibrio* species and effect of H_2 on acetate degradation." Applied and Environmental Microbiology, 41, 2, 346-354 (1981).

McInerney, M. J., Bryant, M. P., and Pfennig, N. "Anaerobic bacterium that degrades fatty acids in syntrophic association with methanogens." Archives of Microbiology, 122, 129-131 (1979).

McInerney, M. J., Bryant, M. P., Hespell, R. B., and Costerton, J. W. "*Syntrophomonas wolfei* gen. nov. sp. nov., an anaerobic syntrophic, fatty acid-oxidizing bacterium." Applied and Environmental Microbiology, 41, 4, 1029-1039 (April, 1981).

Metcalf and Eddy, Inc. Wastewater Engineering: Treatment, Disposal, Reuse. 2nd Edition. McGraw-Hill, New York (1972).

Meunier, A. D. and Williamson, K. J. "Packed bed biofilm reactors: simplified model." Journal of the Environmental Engineering Division, Proceedings of the American Society of Civil Engineering, 107, EE2, 307-317 (April, 1981).

Miller, T. L. and Wolin, M. J. "Oxidation of hydrogen and reduction of methanol to methane is the sole energy source for a methanogen isolated from human feces." Journal of Bacteriology, 153, 1051-1055 (1983a).

Miller, T. L. and Wolin, M. J. "Stability of *Methanobrevibacter smithii* populations in the microbial flora excreted from the human large bowel." Applied and Environmental Microbiology, 45, 317-318 (1983b).

Monod, J. "The growth of bacterial cultures." Annual Review of Microbiology, 3, 371-394 (1949).

Morgan, P. F. "Studies of accelerated digestion of sewage sludge." Sewage and Industrial Wastes, 26, 4, 462-478 (April, 1954).

Mosey, F. E. "Anaerobic filtration: a biological treatment process for warm industrial effluents." Water Pollution Control, 77, 370-378 (1978).

Mueller, J. A. and Mancini, J. L. "Anaerobic filter--kinetics and application." Proceedings of the 30th Industrial Waste Conference, Purdue University, West Lafayette, Indiana (1976).

Novak, J. T. and Carlson, D. A. "The kinetics of anaerobic long chain fatty acid degradation." Journal of Water Pollution Control Federation, 42, 11, 1932-1943 (November, 1970).

Oleszkiewicz, J. A. and Koziarski, S. "Low temperature anaerobic biofiltration in upflow reactors." Journal of Water Pollution Control Federation, 54, 11, 1465-1471 (November, 1982).

O'Rourke, J. T. Kinetics of Anaerobic Waste Treatment at Reduced Temperatures. Ph.D. Dissertation. Stanford University (March, 1968).

Parkin, G. F., Speece, R. E., Yang, C. H. J., and Kocher, W. M. "Response of methane fermentation systems to industrial toxicants." Journal of Water Pollution Control Federation, 55, 1, 44-53 (January, 1983).

Pfeffer, J. T. and Liebman "Energy from refuse by bioconversion, fermentation, and residual disposal processes." Resource Recovery Conversion, 1, 295-313 (1976).

Plummer, A. H., Jr., Malina, J. F., Jr., and Eckenfelder, W. W., Jr. "Stabilization of a low solids carbohydrate waste by an anaerobic submerged filter." Proceedings of the 23rd Industrial Waste Conference, Purdue University, West Lafayette, Indiana (1969).

Podolak, P. L., Friedman, A. A., and LaGrega, M. D. "Effect of reduced partial pressure on anaerobic rotating biological contactor." Proceedings of the 2nd International Conference on Fixed Film Biological Processes, University of Pittsburgh, Pittsburgh, Pennsylvania (July, 1984).

Polprasert, C. and Hoang L. H. "Kinetics of bacteria and bacteriophages in anaerobic filters." Journal of Water Pollution Control Federation, 55, 4, 385-391 (April, 1983).

Powell, G. E., Hilton, M. G., Archer, D. B., and Kirsop, B. H. "Kinetics of the methanogenic fermentation of acetate." Journal of Chemical Technology and Biotechnology, 33B, 209-215 (1983).

Ripley, L. E., Boyle, W. C., and Converse, J. C. "Improved Alkalimetric monitoring for anaerobic digestion of high-strength wastes." Journal of Water Pollution Control Federation, 58, 5, 406-411 (May, 1986).

Rittmann, B. E. "The effect of shear stress on biofilm loss rate." Biotechnology and Bioengineering, 24, 501-506 (1982).

Rittmann, B. E., Strubler, C. E., and Ruzicka, T. "Anaerobic-filter pretreatment kinetics." Journal of the Environmental Division, Proceedings of the American Society of Civil Engineers, 108, EE5, 900-912 (October, 1982).

Rivard, C. J. and Smith P. H. "Isolation and characterization of a thermophilic marine methanogenic bacterium, *Methanogenium thermophilicum* sp. nov." International Journal of Systematic Bacteriology, 32, 430-436 (1982).

Rivard, C. J., Henson, J. M., Thomas, M. V., and Smith, P. H. "Isolation and characterization of *Methanomicrobium paynteri* sp. nov., a mesophilic methanogen isolated from marine sediments." Applied and Environmental Microbiology, 46, 484-490 (1983).

Robinson, R. W., Akin, D. E., Nordstedt, R. A., Thomas, M. V., and Aldrich, H. L. "Light and electron microscopic examination of methane-producing biofilms from anaerobic fixed-bed reactors." Applied and Environmental Microbiology, 48, 1, 127-136 (July, 1984).

Roe, S. F., Jr. and Love, L. S. "Anaerobic digestion of vegetable processing waste." Presented at the 2nd International Conference on Fixed Film Biological Processes, Arlington, Virginia (May, 1984).

Sachs, E. F., Jennett, J. C., and Rand, M. C. "Pharmaceutical waste treatment by anaerobic filter." Journal of the Environmental Engineering Division, Proceedings of the American Society of Civil Engineers, 108, EE2, 297-314 (1982).

Sahm, H. Anaerobic Wastewater Treatment--Advances in Biological Engineering/Biotechnology. Springer-Verlag, Inc., New York, (1984).

Scheifinger, C. C. and Wolin, M. J. "Propionate formation from cellulose and soluble sugars by combined cultures of *Bacteroides succinogenes* and *Selenomonas ruminatium*." Applied Microbiology, 26, 5, 789-795 (1973).

Schink, B. and Pfenning, N. "*Propionigenium modestum*, gen. nov. sp., a new strictly anaerobic, nonsporing bacterium growing on succinate." Archives of Microbiology, 133, 209-216 (1982).

Shames, I. H. Mechanics of Fluids. 2nd Edition. McGraw-Hill Book Company, New York (1982).

Shea, T. G., Pretorius, W. A., Cole, R. D., and Pearson, E. A. "Kinetics of hydrogen assimilation in the methane fermentation." Water Research, 2, 833-848 (1968).

Sohngen, N. L. Waterstof En Metan. Ph.D. Dissertation. University of Technology, Delft, The Netherlands (1906).

Song, K.-H. and Young, J. C. "Media design factors for fixed-bed filters." Journal of Water Pollution Control Federation, 58, 2, 115-121 (February, 1986).

Sorensen, J., Christensen, D., and Jorgenesn, B. B. "Volatile fatty acids and hydrogen as substrates for sulfate-reducing bacteria in anaerobic marine sediment." Applied and Environmental Microbiology, 42, 1, 5-11 (July, 1981).

Sowers, K. R. and Ferry, J. G. "Isolation and characterization of a methylotrophic marine methanogen, *Methanococcoides methylutens* gen. nov., sp. nov." Applied and Environmental Microbiology, 45, 684-690 (1983).

Sowers, K. R., Baron, S. F., and Ferry, J. G. " *Methanosarcina acetivorans* sp. nov., an acetotrophic methane-producing bacterium isolated from marine sediments." Applied and Environmental Microbiology, 47, 971-978 (1984).

Speece, R. E. "Anaerobic biotechnology for industrial wastewater treatment." Environmental Science and Technology, 17, 9, 416A-427A (1983).

Speece, R. E. and McCarty, P. L. "Nutrient requirements and biological solids accumulation in anaerobic digestion." Advances in Water Pollution Research. Volume 2. W. W. Eckenfelder (Ed.). University of Texas, Austin, Texas (September, 1962).

Standard Methods for the Examination of Water and Wastewater. 16th Edition. American Public Health Association, Washington, D. C. (1985).

Stetter, K. O. and Gagg, G. "Reduction of molecular sulphur by methanogenic bacteria." Nature, 305, 309-311 (1983).

Stetter, K. O., Thomm, M., Winter, J., Wildgruber, G., Huber, H., Zillig, W., Janecovic, D., Konig, H., Palm, P., and Wunderl, S. "*Methanothermus fervidus*, sp. nov., a novel extremely thermophilic methanogen isolated from an Icelandic hot spring." Zentralblatt fuer Bakteriologie Mikrobiologie und Hygiene, I, Abstract, Origin c2, 166-178 (1981).

Suidan, M. T. "Performance of deep biofilm reactors." Journal of the Environmental Engineering Division, 112, 1, 78-93 (February, 1986).

Taylor, D. W. "Full-scale anaerobic trickling filter evaluation." Proceedings of National Symposium on the 3rd Food Processing Wastes, New Orleans, Louisiana. EPA-R2-72-018 (November, 1972).

Thauer, K. R., Jungermann, K. and Decker, K. "Energy conservation in chemotrophic anaerobic bacteria." Bacteriological Reviews, 41, 1, 100-180 (March, 1977).

Torpey, W. N. "Loading to failure of a pilot high-rate digester." Sewage Works, 27, 2, 121-148 (February, 1955).

Trulear, M. G. and Characklis, W. G. "Dynamics of biofilm processes." Journal of Water Pollution Control Federation, 54, 9, 1288-1300 (September, 1982).

U. S. Environmental Protection Agency. Operations Manual Anaerobic Sludge Digestion. EPA-430/9-76-001 (February, 1976).

U. S. Environmental Protection Agency. Methods of Chemical Analysis of Water and Wastes. EPA-625/6-74-003a (1978).

U. S. Environmental Protection Agency. Handbook for analytical quality control in water and wastewater laboratories. EPA-600/4-79-019 (March, 1979).

U. S. Environmental Protection Agency. Process Design Manual for Sludge Treatment and Disposal. EPA-625/1-79-011 (September, 1979).

U. S. Environmental Protection Agency. "Design information report--Anaerobic digester mixing systems." Journal of Water Pollution Control Federation, 59, 3, 162-170 (March, 1987).

Van Den Berg, L. and Lentz, C. P. "Comparison between up- and down-flow anaerobic fixed film reactors of varying surface-to-volume ratios for the treatment of bean blanching waste." Proceedings of the 34th Industrial Waste Conference, Purdue University, West Lafayette, Indiana (1979).

Van Der Meer, R. R. and De Vletter, R. "Anaerobic treatment of wastewater: the gas-liquid-sludge separator." Journal of Water Pollution Control Federation, 54,11, 1482-1492 (November, 1982).

Valcke, D. and Verstraete, W. "A Practical Method to Estimate the Acetoclastic Methanogenesis Biomass in Anaerobic Sludges." Journal of Water Pollution Control Federation, 55, 9, 1191-1196 (September, 1983).

Wang, Y.-T., Suidan, M. T., and Rittman, B. E. "Kinetics of methanogens in an expanded-bed reactor." Journal of Environmental Engineering, 112, 1, 155-171 (February, 1986).

Weber, W. J., Jr. Physicochemical Processes for Water Quality Control. John Wiley & Sons, New York (1972).

Weimer, P. J. and Zeikus, J. G. "Fermentation of cellulose and cellobiose by *Clostridium thermocellum* in the absence and presence of *Methanobacterium thermoautotrophicum*." Applied and Environmental Microbiology, 33, 289-297 (1977).

Wildgruber, G., Thomm, M., Konig, H., Ober, K., Ricchiuto, T., and Stetter, K. O. "*Methanoplanus limicola*, a plate-shaped methanogen, representing a novel family, the *Methanoplanaceae*." Archives of Microbiology, 132, 31-36 (1982).

Williamson, K. and McCarty, P. L. "A model of substrate utilization by bacterial films." Journal of Water Pollution Control Federation, 48, 1, 9-24 (January, 1976a).

Williamson, K. and McCarty, P. L. "Verification studies of the biofilm model for bacterial substrate utilization." Journal of Water Pollution Control Federation, 48, 2, 281-296 (February, 1976b).

Winter, J., Lerp, C., Zabel, H. P., Wildenauer, F. X., Konig, H., and Schindler, F. *Methanobacterium wolfei*, sp. nov., a new tungsten-requiring, thermophilic, autotrophic methanogen." Systematic Applied Microbiology, 5, 457-466 (1984).

Witt, E. R., Humphrey, W. J., and Roberts, T. E. "Full-scale anaerobic filter treats high strength wastes." Proceedings of the 34th Industrial Waste Conference, Purdue University, West Lafayette, Indiana (1979).

Wood, W. A. "Fermentation of carbohydrates and related compounds." The Bacteria--Metabolism. Volume II. I. C. Gunsalus and R. Y. Stainer (Eds.). Academic Press, New York (1961).

Young, J. C. The Anaerobic Filter for Waste Treatment. Ph.D. Dissertation. Stanford University, Stanford, California (1968).

Young, J. C. "Anaerobic filters for pretreatment of industrial wastes." Presented at the 7th International Symposium on Alternative Energy Sources, Miami Beach, Florida (December, 1985).

Young, J. C. and Dahab, M. F. "Effect of media design on the performance of fixed-bed anaerobic filters." Presented at the International Association of Water Pollution Research Seminar on Anaerobic Treatment of Wastewater in Fixed-Film Reactors, Technical University of Denmark, Copenhagen, Denmark (June, 1982).

Young, J. C. and McCarty, P. L. "The anaerobic filter for waste treatment." Journal of Water Pollution Control Federation, 41, 5, part 2, R160-R173 (May, 1969).

Zeikus, J. G. "Microbial population in digesters." Presented at the 4rd International Symposium on Anaerobic Digestion, Kwangchow, Kwangtung, China (1985).

Zeikus, J. G., Lynd, L. H., Thompson, T. E., Krzycki, J. A., Weimer, D. J., and Hegge, P. W. "Isolation and characterization of a new, methylotrophic, acidogenic anaerobe, the Marburg strain." Current Microbiology, 3, 381-386 (1980).

Zhilina, T. N. "A new obligate halophilic methane-producing bacterium." Mikrobiologiia, 52, 3, 375-382 (1983).

Zimpro, Inc. Determination of Chemical Oxygen Demand. ZP-166, Zimpro, Inc., Rothschild, Wisconsin (1980).

Zinder, S. H. and Mah, R. A. "Isolation and characterization of a thermophilic strain of *Methanosarcina* unable to use H_2-CO_2 for methanogenesis." Applied and Environmental Microbiology, 38, 996-1008 (1979).

ACKNOWLEDGEMENTS

The sincerest appreciation is extended to the author's major professor, Dr. Richard R. Dague, for his continued guidance, encouragement, and patience, throughout the author's graduate work. The financial support from the Iowa State Engineering Research Institute is gratified.

The author's graduate committee, Dr. E. Robert Baumann, Dr. John L. Cleasby, Dr. Peter J. Reilly, Dr. Lacy Daniels, and Dr. Gene Parkin, who provide many invaluable helps and comments to this study, are appreciated.

Appreciation is also extended to many of the author's colleagues and friends for their companionship and assistance: Eric Seagren, Ann Spiesman, Johannes Haarhoff, Suingill Choi, David You, James Lin, Ravindra Srivastava, Peter Gunther, Adrian Hanson, David Sabatini, Delvin DeBoer, and Charles Lee.

APPENDIX A. TAXONOMY OF METHANOGENS BASED ON BALCH'S SCHEME (1979)

RECENT ISOLATES ARE LISTED WITH APPROPRIATE REFERENCES

No.	Organism	Strain	History	Energy Source	G+C (%)	μ_m (1/d)	pH	Temp (°C)	NaCl (%)	Reference
Order I. Methanobacteriales										
Family I-I. Methanobacteriacea										
Genus I-I-I. Methanobacterium										
1.	*Mb. formicicum*	MF	M.P. Bryant, digester	H2,f	40.7					
2.	*Mb. bryantii*	M.o.H.	Former *Mb.* sp. isolated from *M. omelianskii* (Barker, 1963)	H2	32.7					
2a.	*Mb. bryantii*	M.o.H.G.	former *Mb.* sp.	H2	33.2					
3.	*Mb. thermo-autotrophicum*	ΔH	Sewage sludge digester	H2	49.7		8.0	65.0		

H2 = hydrogen f = formate m = methanol a = acetate ma = methylamides

No.	Organism	Strain	History	Energy Source	G&C (%)	μ_m (1/d)	pH	Temp (°C)	NaCl (%)	Reference
3a.	*Mb. thermo-autotrophicum*	JW510		H2						
3b.	*Mb. thermo-autotrophicum*	Marburg		H2		10.4				
3c.	*Mb. thermo-autotrophicum*	W	from ΔH	H2	46.0					
3d.	*Mb. Thermo-autototrophium*	S		H2	46.0					
3e.	*Mb. Thermo-autotrophicum*	GC1		H2						
4.	*Mb. wolfei*	W	Mixture of sewage sludge and river sed.	H2	61.0	4.8	7.2	60.0	1.0	Winter *et al.* (1984)
	Mb. sp.	Kuznetsov	Ground water	H2,f	48.8	1.0	7.2	37.0	14.0	Belyaev *et al.* (1983)
	Mb. sp.	Omeliansky	Oil field	H2	37.3	0.9	6.9	45.0	14.0	Belyaev *et al.* (1983)
	Mb. sp.	Ivanov	Oil field USSR	H2	36.6	1.0	7.2	45.0	No	Belyaev *et al.* (1983)

No.	Organism	Strain	History	Energy Source	G&C (%)	μ_m (1/d)	pH	Temp (°C)	NaCl (%)	Reference
	Genus I-I-II. Methanobrevibactor									
5.	*Mbr. ruminantium*	M1	bovine rumen Former *Mb.* sp. of Smith & Hungate (1958)	H2,f	30.6					
6.	*Mbr. arbophilius*	DH1	Wet wood Former *Mb.* sp. of Zeikus & Hennig (1975)	H2	27.5					
6a.	*Mbr. arbophilius*	DC	Former *Mb.* sp. Former *Mb.* sp. of Castignetti & Klain (1977)	H2	27.7					
6b.	*Mbr. arbophilius*	AZ	Sewage sludge digester Former *Mb.* sp. of Zehender & Wuhrmann (1977)	H2	31.6					
7.	*Mbr. smithii*	P5	Sewage sludge digester Former *Mb.* sp. of Smith (1961)	H2,f	31.0					
	Family I-II. Methanothermaceae (Stetter et al., 1981)									
	Genus I-II-I. Methanothermus (Stetter et al., 1981)									
8.	*Mt. fervidus*	V24S	Volcano spring sed.	H2	33.0	5.9	6.5	83.0		Stetter *et al.* (1981)

No.	Organism	Strain	History	Energy Source	G&C (%)	μ_m (1/d)	pH	Temp (°C)	NaCl (%)	Reference
Order II. Methanococcales										
Family II-1. Methanococcaceae										
Genus II-I-I. Methanococcus										
9.	*Mc. vannielii*	SB	San Fransisco Bay sed.	H2,f	31.1	2.1	8.0	40.0	2.4	
10.	*Mc. voltae*	PS	Estuary sed. Former *Mc.* sp. of Word (1970)	H2,f	30.7	5.5	7.0	38.0	4.0	
11.	*Mc. thermo-lithotrophicus*	SN1	Volcano	H2,f	31.3	18.5	7.0	65.0	4.0	Huber *et al.* (1982)
12.	*Mc. delta*	RC	Missi. river	H2,f	40.5	8.3		37.0	4.0	Corder *et al.* (1983)
13.	*Mc. maripaludis*	JJ	Salt marsh sed.	H2,f	33.0	8.3	7.0	38.0	0.6	Jones *et al.* (1983b)
14.	*Mc. jannaschii*	JAL-1	East Pacific ocean hydro-thermal vent	H2	31.0	41.6	6.0	85.0	2.9	Jones *et al.* (1983a)
15.	*Mc. halophilus*									Zhilina (1983)
	Mc. species		Human feces	H2/m						Miller & Wolin (1983b)

No.	Organism	Strain	History	Energy Source	G&C (%)	μ_m (1/d)	pH	Temp (°C)	NaCl (%)	Reference
Order III. Methanomicrobiales										
Family III-I. Methanomicrobiacea										
Genus III-I-I. Methanomicrobium										
16.	*Mm. mobilis*	BP	Bovine rumen	H2,f	48.8					
17.	*Mm. paynteri*	G2000	Marine sed.	H2	44.9	3.5	7.0	40.0	0.9	Rivard *et al.* (1983)
Genus III-I-II. Methanogenium										
18.	*Mg. cariaci*	JR11	Cariaco Trench sed.	H2,f	51.6		7.0	25.0	2.9	
19.	*Mg. marisnigri*	JR1m	Black Sea	H2,f	61.2		6.4	25.0	1.2	
20.	*Mg. tatii*									
21.	*Mg. thermophilicum*		Marine sed.	H2,f				55.0		Rivard & Smith (1982)
22.	*Mg. olentangyi*	RC/ER	Fresh water river sed.	H2	54.4	1.5		37.0	1.0	Corder *et al.* (1983)
23.	*Mg. Frittony*	FR4	Fresh water lake sed.	H2,f	49.2	13.9	7.3	57.0	1.0	Harris *et al.* (1984)

No.	Organism	Strain	History	Energy Source	G&C (%)	μ_m (1/d)	pH	Temp (°C)	NaCl (%)	Reference
	Genus III-I-III. Methanospirillum									
24.	*Msp. hungateii*	JF1	Sewage sludge digester	H2,f	45.0			40.0		
24a.	*Msp. hungateii*	GP1	Pear waste digester	H2,f	46.5		7.0	35.0		
	Genus III-I-IV. Methanococcodies (Sowers & Ferry, 1983)									
25.	*Mcc. methylutens*	TMA10	19.8 m deep digester	m,ma	42.0	3.2	7.3	35.0	2.6	Sowers & Ferry, (1983)
	Family III-II. Methanoplanaceae (Wildgruber et al., 1982)									
	Genus III-II-I. Methanoplanus (Wildgruber et al., 1982)									
26.	*Mpl. limicola*	M3	Steam *drilling*	H2,f	47.5	2.4	7.0	40.0	1.0	Wildgruber *et al.* (1982)

No.	Organism	Strain	History	Energy Source	G&C (%)	μ_m (1/d)	pH	Temp (°C)	NaCl (%)	Reference
Family III-III. Methanosarcina				**Genus III-III-I. Methanosarcina**						
27.	*Ms. barkeri*	MS	Sewage sludge digester	H2,m ma,a	38.8					
27a.	*Ms. barkeri*		Sewage sludge digester	H2,m ma,a	38.8	0.28				
27b.	*Ms. barkeri*	W		H2,m ma,a	40.5					
27c.	*Ms. barkeri*	UBS		H2,m ma,a	43.5					
27d.	*Ms. barkeri*	Z		H2,m ma,a	51.0					
27e.	*Ms. barkeri*	R1M3		H2,m ma,a						
28. (1984)	*Ms. mazei*	S6	Lab digester digester	H2,m ma,a	42.0	1.0	7.0	35.0	7.0	Mah & Kuhn Mah (1980)
29.	*Ms. acetivorans*	C2A	Marine sed.	m,ma a	42.0	3.2	6.7	40.0	1.2	Sowers *et al.* (1984)
	Ms. species	TM1	Lab digester digester	m,ma	42.0	3.3	6.0	50.0		Zinder & Mah (1979)
Genus III-III-II. Methanothrix (Huster, 1982)										
30.	*Mtx. soehngenii*	Opfikon	Sewage sludge digester	a	51.9	0.2	7.6	37.0		Huser *et al.* (1982)
Genus III-III-III. Methanolobus (Konig & Stetter, 1982)										
31.	*Ml. tindarius*	Tindari3	Marsh pond sed.	m,ma	40.0			25.0		Konig & Stetter (1982)

APPENDIX B. GROWTH YIELD AND KINETIC DATA OF SOME SELECTED FERMENTATIVE AND METHANOGENIC BACTERIA FOR BOTH PURE AND MIXED CULTURES

Reactions	Temp (°C)	Y_m[a] (g/e)	μ_m[b] (1/d)	k_d[c] (1/d)	K_s[d] (me/L)	$Y_m/\Delta G^o$ (g/kal)	μ_m/Y_m (e/g/d)	Reference
Group IIIa (Homoacetogenesis)								
Methanol → Acetate (ΔG^o = -2.36 kcal/e)								
A. woodii	28.0	0.88	-			0.37	-	Bache & Pfennig (1981)
B. methylotrophicum (w/HCOOH)	37.0	-	3.30			-	-	Kerby *et al.* (1983)
(w/CO)	37.0	-	1.51					
Group IIIb (Homopropionogenesis)								
Succinate → propionate (ΔG^o = -0.27 kcal/e)								
P. modestum	33.0	0.17	3.70			0.63	21.8	Schink & Pfennig (1982)
P. modestum (w/yeast)	33.0	-	6.65			-	-	
Group IIIc (Homobutyrogenesis)								
Methanol → butyrate (ΔG^o = -1.07 kcal/e)								
B. methylotrophicum (w/acetate)			37.0	-	0.83	-	-	Zeikus *et al.* (1980)

[a]True yield coefficient in g VSS or VS/elec. equiv. used.

[b]Maximum specific growth rate in 1/d = 0.693/doubling time.

[c]Decay rate constant in 1/d.

[d]Half-saturation constant in m elec. equiv./L.

Reactions	Temp (°C)	Y_m[a] (g/e)	μ_m[b] (1/d)	k_d[c] (1/d)	K_s[d] (me/L)	$Y_m/\Delta G^o$ (g/kal)	μ_m/Y_m (e/g/d)	Reference
Group IV (Methanogenesis)								
Formate → Methane (ΔG^o = -5.72 kcal/e)								
Mb. formicicum	-	0.73	-			0.13		Daniels *et al.* (1984b)
Mb. formicicum (org. sup.)	-	0.60	-			0.11		
CO → Methane (ΔG^o = -5.54 kcal/e)								
H_2/CO_2 → Methane (ΔG^o = -3.91 kcal/e)								
Ms. barkeri	-	0.80	-			0.21		Daniels *et al.* (1984b)
Mb. formicicum (org. sup.)	-	0.44	-			0.11		
Mb. bryantii	-	0.30	-			0.08		
Mb. thermoautotrophicum	-	0.20	-			0.05		
Mixed cultures	37.0	0.34	1.05	0.009	0.75	0.09	3.09	Shea *et al.* (1968)
Mathematical model	-	0.25	0.50			0.06	2.00	McCarty (1969)
Mixed cultures	33.0	-	-		0.11			Kaspar and Wuhrmann (1978)
Methanol → Methane (ΔG^o = -3.20 kcal/e)								
Ms. barkeri	-	0.75	-			0.23		Daniels *et al.* (1984b)
Ml. tindarius	-	0.51	-			0.16		

Reactions	Temp (°C)	Y_m[a] (g/e)	μ_m[b] (1/d)	k_d[c] (1/d)	K_s[d] (me/L)	$Y_m/\Delta G^o$ (g/kal)	μ_m/Y_m (e/g/d)	Reference
Acetate → Methane (ΔG^o = -0.85 kcal/e)								
Ms. barkeri (org. sup.)	-	0.37				0.44		Daniels *et al.* (1984b)
Ms. barkeri	-	0.28				0.33		
Mtx. soehngenii	-	0.16				0.19		
Mathematical model	-	0.14	0.27			0.17	2.00	McCarty (1969)
Mixed cultures	35.0	0.32	0.34	0.02	20.6	0.38	1.08	Lawrence & McCarty (1969)
	30.0	0.43	0.27	0.04	44.5	0.51	0.64	
	25.0	0.40	0.24	0.01	116.2	0.47	0.62	
Mixed cultures (13.2% atm)	35.0	0.35	2.62	0.44	33.4	0.41	7.49	Finney & Evans II (1975)
Mixed cultures	33.0	-	-		2.67			Kaspar and Wuhrmann (1978)
Mixed cultures	37.0	-		0.69	19.3			Powell *et al.* (1983)
Fluidized bed modeling	35.0	-	-		1.15		0.55	Wang *et al.* (1985)
Propionate → Methane (ΔG^o = -0.905 kcal/e)								
S. wolinii/Msp. hungateii	35.0		0.10					Boone & Bryant (1980)
S. wolinii/Desulfovibrio	35.0		0.19					
Mixed cultures	35.0	0.34	0.44	0.01	4.38	0.38	1.28	Lawrence & McCarty (1969)
	25.0	0.41	0.54	0.04	82.0	0.45	1.31	
Mixed cultures	33.0				22.0			Kaspar and Wuhrmann (1978)
Mixed cultures								
t_d=14.5 d, w/ glucose	35.0		0.13		2.18			Heyes & Hall (1983)
t_d= 8.2 d, w/ glucose	35.0		0.96		77.5			
t_d= 8.2 d, w/o glucose	35.0		1.20		62.4			
Mixed cultures	35.0		1.16					Guyot *et al.* (1985)

Reactions	Temp (°C)	Y_m[a] (g/e)	μ_m[b] (1/d)	k_d[c] (1/d)	K_s[d] (me/L)	$Y_m/\Delta G^o$ (g/kal)	μ_m/Y_m (e/g/d)	Reference
Butyrate → Methane (ΔG^o = -2.04 kcal/e)								
S. wolfei/Msp. hungatei	35.0	-	0.18			-	-	McInerney *et al.* (1981)
S. wolfei/Desulfovibrio	35.0	-	0.31					
Mixed cultures	35.0	0.38	0.79	0.027	0.67	0.19	2.09	Lawrence & McCarty (1969)
Valerate → Methane								
S. wolfei/Msp. hungatei	-	0.92	-			-	-	McInerney *et al.* (1981)
S. wolfei/Desulfovibrio	-	0.18	-					
Amino & fatty acids → Methane								
Mixed cultures	35.0	0.43	-	0.038		-	-	Speece & McCarty (1962)
Glucose & starch → Methane								
Mixed cultures	35.0	3.68	-	0.088		-	-	Speece & McCarty (1962)
Nutrient broth → Methane								
Mixed cultures	35.0	0.61	-	0.014			-	Speece & McCarty (1962)

Reactions	Temp (°C)	Y_m[a] (g/e)	μ_m[b] (1/d)	k_d[c] (1/d)	K_s[d] (me/L)	$Y_m/\Delta G^o$ (g/kal)	μ_m/Y_m (e/g/d)	Reference
Dextrose → Methane								
Mixed culture	35.0	1.12	0.92		0.020		0.82	Andrews & Pearson (1965)
Lipids → Methane								
Mixed cultures	35.0	-			250.0		0.83	O'Rourke (1968)
	25.0	-			465.0		0.58	
	20.0	-			577.5		0.48	
Saturated acids → Methane								
Mixed cultures								
Stearic (18-C)	37.0	-			52.1		0.01	Novak & Carlson (1970)
Palmitic(16-C)	37.0	-			17.9		0.13	
Myristic(14-C)	37.0	-			13.1		0.12	
Unsaturated acids → Methane								
Mixed culture								
Oleric (18-C)	37.0	-			397.5		0.50	Novak & Carlson (1970)
Linoleic(18-C)	37.0	-			227.0		0.63	

APPENDIX C. OUTLINE OF ACETOCLASTIC METHANOGENIC ACTIVITY (AMA) TEST PROCEDURES

Phase I. Preparation of Experimental Apparatus and Buffer Solution

A. Preparation of manometer

(1) Fill the manometer half-way with a suitable density of liquid. Avoid air trap in the liquid.

B. Preparation of incubation flask and connection

(1) Prepare 500-mL wide-mouth Erlenmeyer flasks.

(2) Install a #10 butyl rubber stopper with 2 septa.

(3) Prepare a suitable length of low permeability tubing. Install one end of the tubing with a hypodermic needle and connect the other end to the manometer.

C. Leak check

(1) Fill the incubation flask with 450 mL water and cap it with the 2-septum rubber stopper.

(2) Shake the flask rigorously for a few minutes and stand by in the 35° C room for at least 1 hour before use.

(3) Adapt the flask with central septum to the manometer.

(4) Pressurize the flask to 30 cm of manometer liquid and stand by for at least 1 hour for leak check.

D. Preparation of buffer solution

(1) Prepare a suitable amount of buffer solution of 0.27 gm KH_2PO_4/L, 0.35 gm K_2HPO_4/L, and 1.2 gm $NaHCO_3$/L, if sample dilution is required or attached growth is to be tested.

(2) Measure a suitable amount of buffer solution into incubation flasks so that the final incubation volume is to be 450 mL.

(3) Purge the buffer solution in the flask with nitrogen gas at a gasing rate of 0.5 L/min for 1 min to remove DO. Cap the flask right after the purging.

(4) Add 1 mL of reducing agent Na_2S through septum using a syringe to make 1mM of sulfide.

(5) Partially release the nitrogen pressure in the flask using a syringe and place the solution in the constant temperature room. Allow for at least 1 hour before use.

Phase II. Sample Collection and Seeding

E. Sample collection and seeding

(1) Purge the sampling bottles with nitrogen gas right before sampling at a gasing rate of 0.5 mL/min for 1 min.

(2) Secure a suitable a amount of biomass from reactors.

(3) Carefully open the flask and inoculate a suitable amount of biomass so that the total amount of biomass is not more than 0.5 gm VSS and the final volume is 450 mL.

(4) Be sure to include a reagent blank (without seeding) for comparison.

Phase III. Culturing and Monitoring

F. Sample stabilization

(1) Cap the flask right after the seeding and inject another 1 mL Na_2S to the flask to make the solution 1 mM of sulfide.

(2) Standby the flask in the constant temperature room for at least 1 hour to allow for recovery from oxygen exposure.

G. Adding substrate and starting monitoring

(1) Inject 5 mL of NaAc to make the solution of 1.67 gm HAc.

(2) Gently shake the flask. Adapt the flask to the manometer and zero the manometer to start monitoring.

(3) Read the manometer every 0.5 hour for at least 6 hours of incubation.

(4) Gently shake the flask by hand for 30 sec every 30 min after each reading.

(5) Record the local barometric pressure and operating temperature several times throughout the incubation period.

Phase IV. Calibration of Manometer

H. Calibration of manometer

(1) Read the manometer after incubation.

(2) Withdraw gas from flasks with an increment of 2000 μL gas using a microsyringe through the side septum and record the corresponding manometer readings (h).

(3) Convert the amount of each accumulated gas withdrawn at the operating barometric pressure and temperature (v_p) to conditions of 0° and 1 atm (v_s).

(4) Plot v_s against h and calculate the slope and linearity, using the least square linear regression method.

Phase V. Methane/VSS Analysis and Data Handling

I. Methane and VSS analysis

(1) At the end of the incubation, withdraw a suitable amount of biogas from the flask in the incubation room, using a microsyringe.

(2) Inject the withdrawn biogas into a gas chromatograph to determine the methane content using at least 3 replicates.

(3) Harvest the biomass after the GC analysis to determine the VSS at 550° C according to the Standard Method.

J. Data handling

(1) Calculate the methane production rate.

(2) Calculate the AMA (L CH_4 produced at STP/gm VSS/day).

(3) Report the AMA values with the incubation temperature if other than 35° C is used.

APPENDIX D. SMAR AVERAGE DAILY GAS PRODUCTION

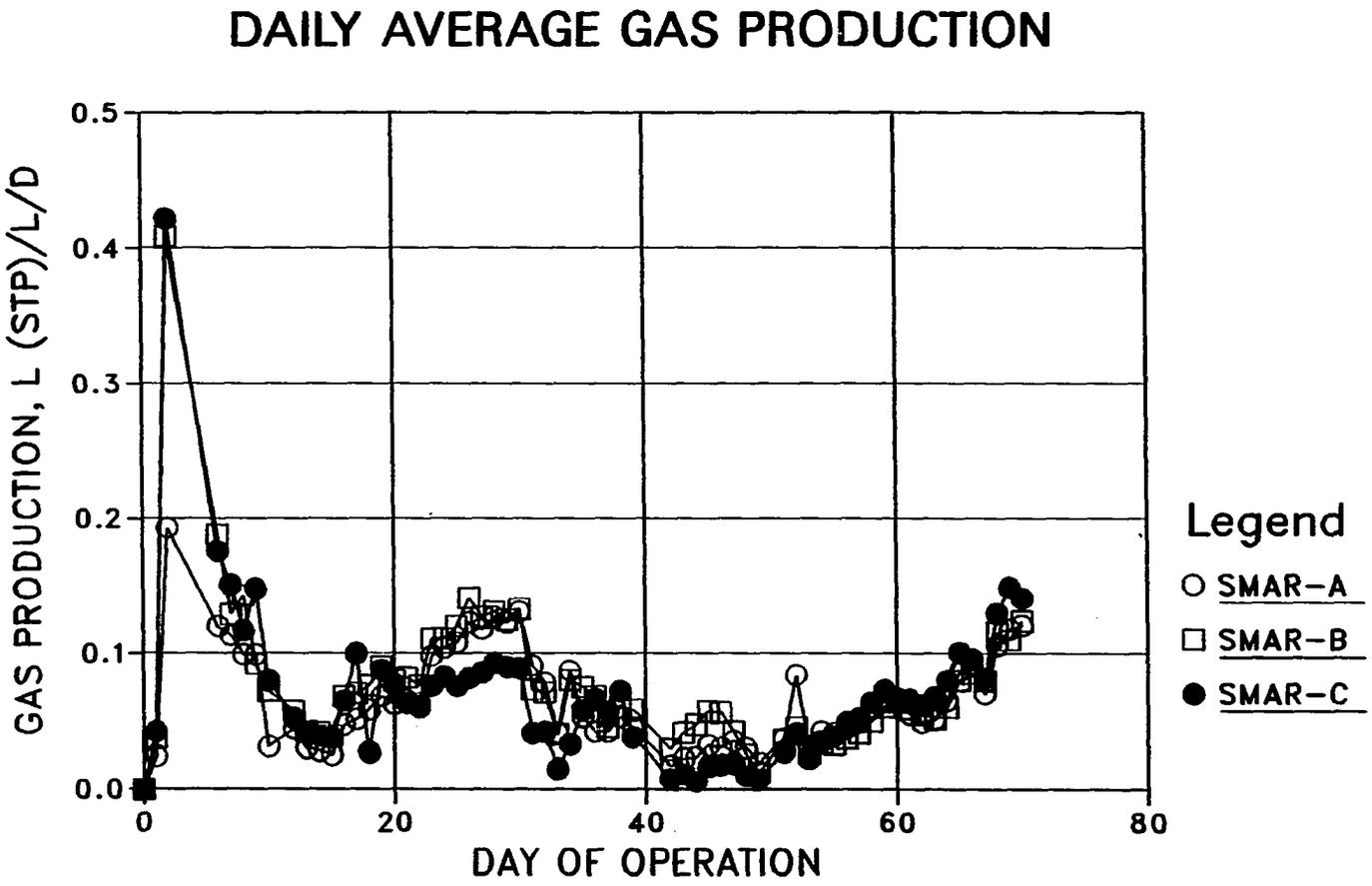

FIGURE 56. SMAR average daily gas production (day 0 to 70)

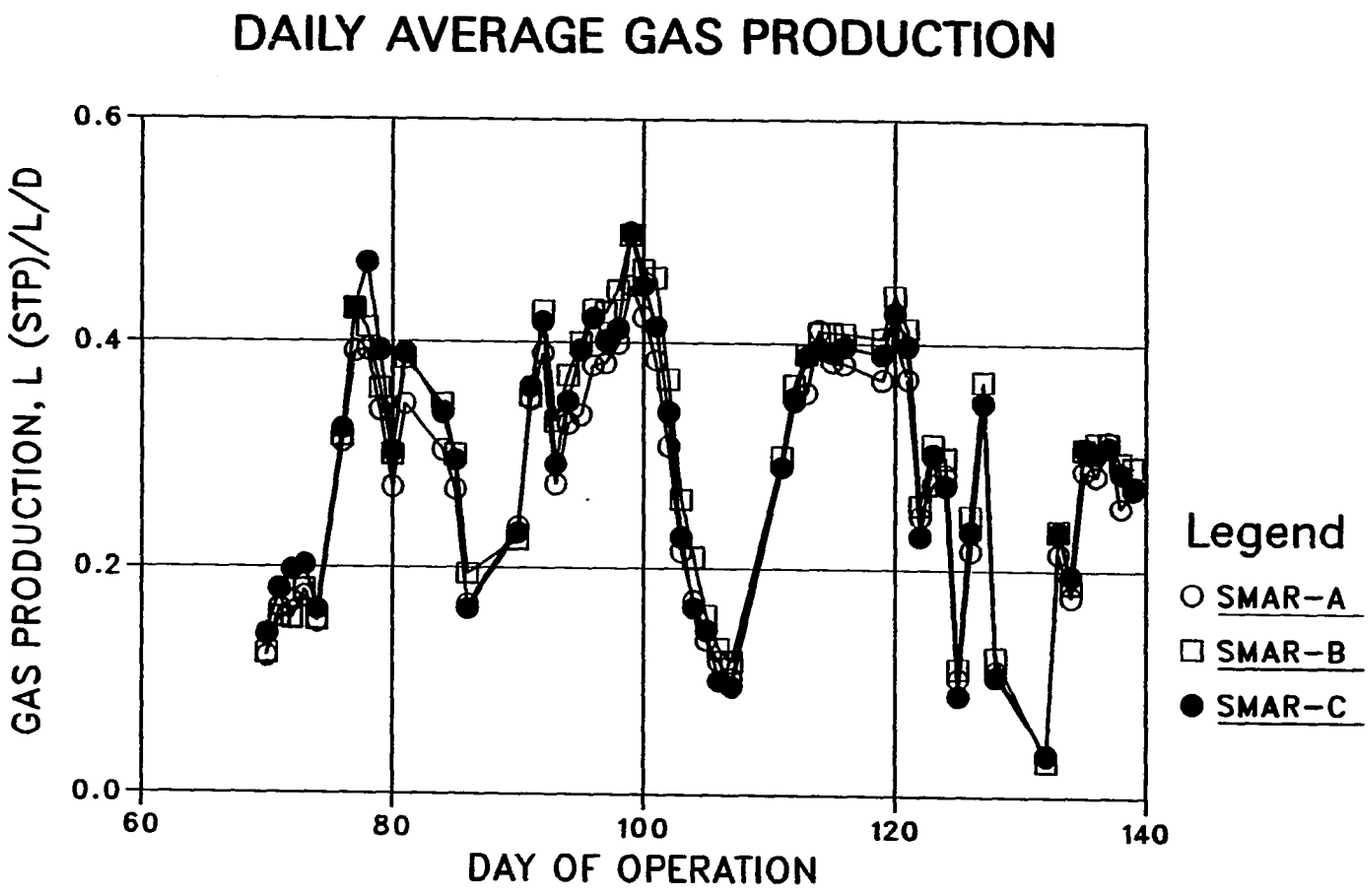

FIGURE 57. SMAR average daily gas production (day 70 to 140)

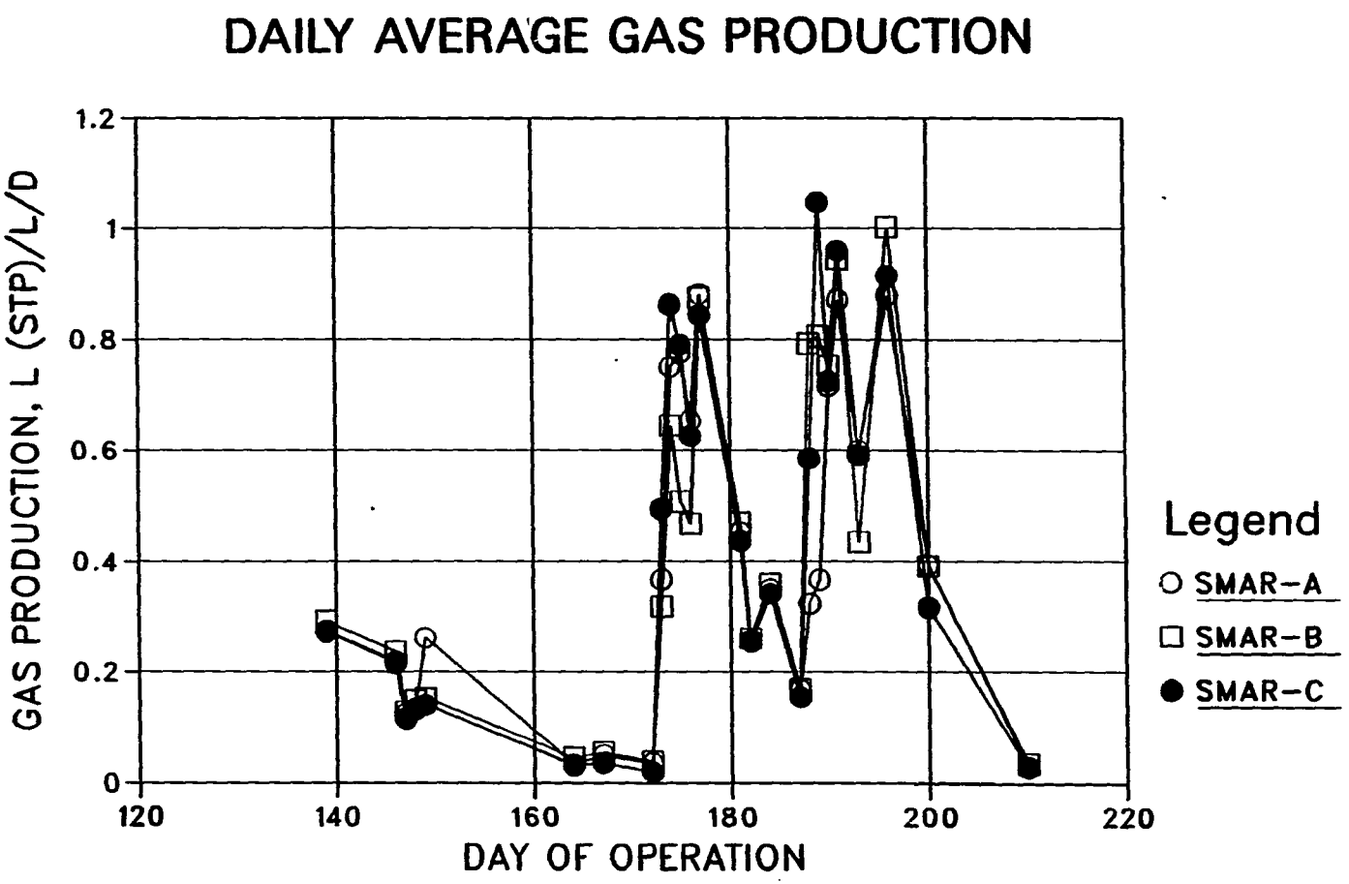

FIGURE 58. SMAR average daily gas production (day 140 to 210)

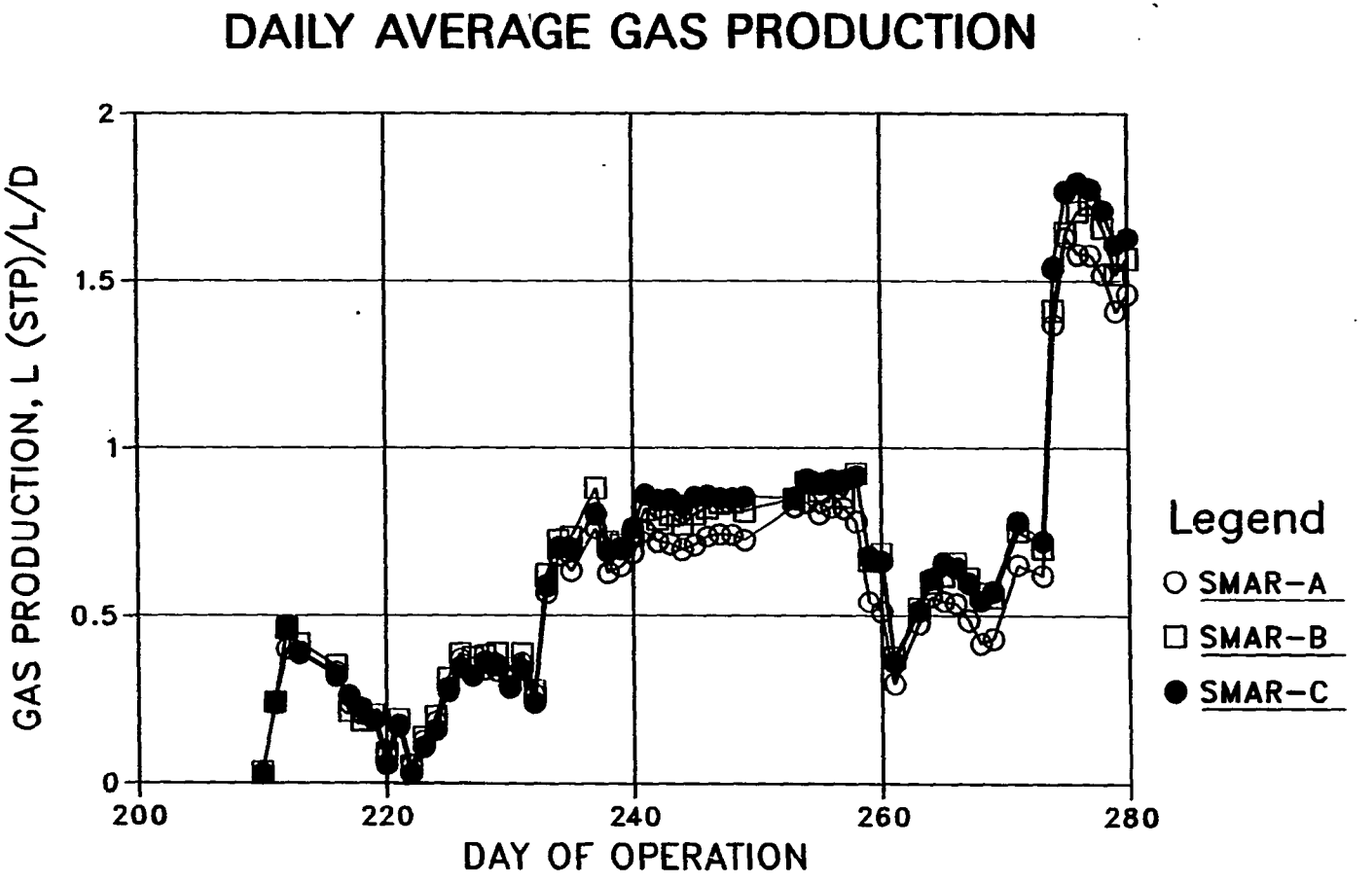

FIGURE 59. SMAR average daily gas production (day 210 to 280)

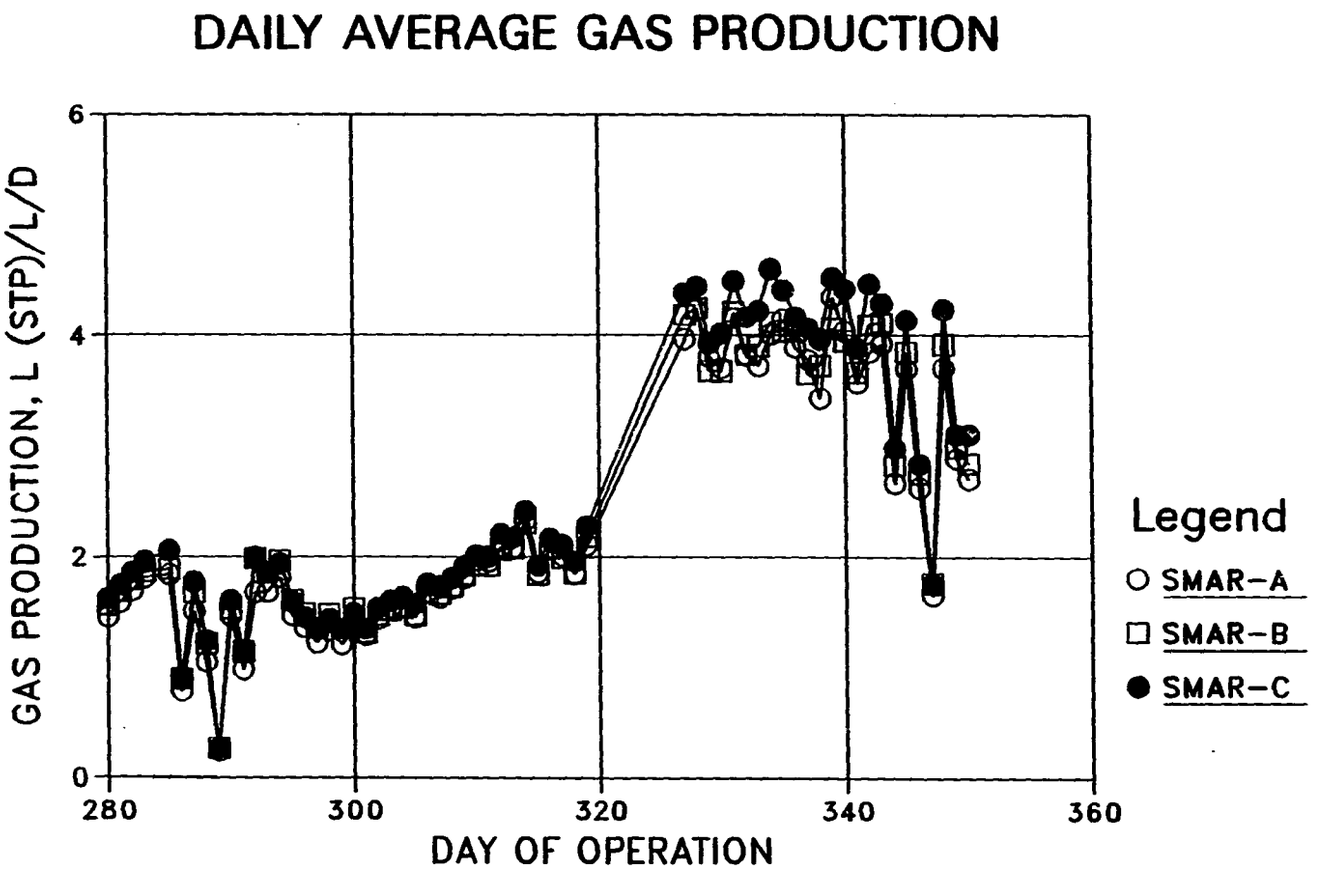

FIGURE 60. SMAR average daily gas production (day 280 to 350)

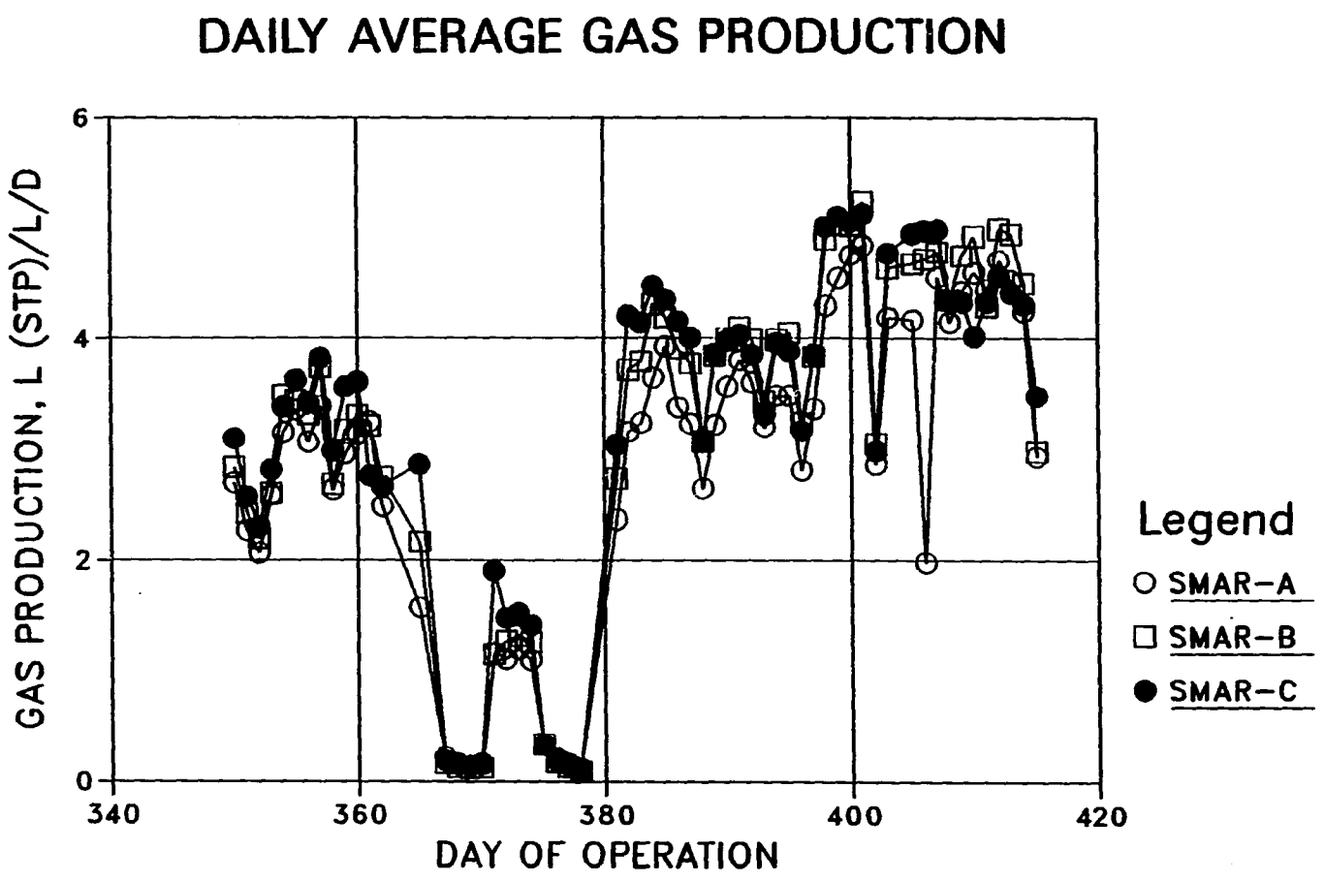

FIGURE 61. SMAR average daily gas production (day 350 to 415)

APPENDIX E. SMAR STEADY-STATE PROFILE DATA

Run 1a

SMAR Port	Height (cm)	SCOD (mg/L)	TOA (mg/L)	TSS (mg/L)	VSS (%)	AMA (L/g/d)	pH
(Inf)	0.0	1910					
A-1	15.2	125	NA	60	82	NA	NA
A-2	30.5	206		60	85		
A-3	53.3	250		60	87		
	0	1910					
B-1	15.2	104		ERR	ERR		
B-2	30.5	112		90	72		
B-3	61.0	151		40	80		
B-4	91.4	171		30	81		
B-5	121.9	130		20	82		
	0	1910					
C-1	15.2	137		ERR	ERR		
C-2	30.5	96		ERR	ERR		
C-3	61.0	96		80	79		
C-4	91.4	91		50	87		
C-5	152.4	95		30	81		
C-6	213.4	82		20	82		
C-7	281.8	90		20	75		

Run 2a1

SMAR Port	Height (cm)	SCOD (mg/L)	TOA (mg/L)	TSS (mg/L)	VSS (%)	AMA (L/g/d)	pH
(Inf)	0.0	4130					
A-1	15.2	172		80	93	0.56	NA
A-2	30.5	138		60	100	0.66	
A-3	53.3	143		60	93	0.72	
	0	4130					
B-1	15.2	124		180	67	ERR	
B-2	30.5	257		260	71	0.22	
B-3	61.0	328		130	76	0.30	
B-4	91.4	370		130	74	0.38	
B-5	121.9	355		90	81	0.42	
	0	4130					
C-1	15.2	1146		390	72	ERR	
C-2	30.5	210		160	73	ERR	
C-3	61.0	219		250	75	0.22	
C-4	91.4	205		220	75	0.27	
C-5	152.4	192		200	74	0.21	
C-6	213.4	189		120	71	0.43	
C-7	281.8	208		160	74	0.13	

Run 2a2

SMAR Port	Height (cm)	SCOD (mg/L)	TOA (mg/L)	TSS (mg/L)	VSS (%)	AMA (L/g/d)	pH
(Inf)	0.0	3760					
A-1	15.2	80	NA	80	80	NA	NA
A-2	30.5	79		80	83		
A-3	53.3	101		70	96		
	0	3760					
B-1	15.2	77		1060	78		
B-2	30.5	77		290	78		
B-3	61.0	98		70	91		
B-4	91.4	111		110	85		
B-5	121.9	181		110	86		
	0	3760					
C-1	15.2	625		10460	83		
C-2	30.5	364		2710	83		
C-3	61.0	137		160	85		
C-4	91.4	89		120	85		
C-5	152.4	96		90	80		
C-6	213.4	73		90	80		
C-7	281.8	70		90	85		

Run 2b

SMAR Port	Height (cm)	SCOD (mg/L)	TOA (mg/L)	TSS (mg/L)	VSS (%)	AMA (L/g/d)	pH
(Inf)	0	1760					
A-1	15.2	41	30	37	79	NA	NA
A-2	30.5	46	7	33	78		
A-3	53.3	78	23	80	89		
	0	1760					
B-1	15.2	85	37	580	72		
B-2	30.5	65	20	53	74		
B-3	61.0	42	5	40	75		
B-4	91.4	42	4	44	78		
B-5	121.9	85	39	48	74		
	0	1760					
C-1	15.2	909	486	2560	86		
C-2	30.5	119	119	470	80		
C-3	61.0	68	22	54	78		
C-4	91.4	59	15	49	81		
C-5	152.4	59	4	51	84		
C-6	213.4	48	12	49	74		
C-7	281.8	55		36	80		

Run 2c

SMAR Port	Height (cm)	SCOD (mg/L)	TOA (mg/L)	TSS (mg/L)	VSS (%)	AMA (L/g/d)	pH
(Inf)	0	870					
A-1	15.2	182	83	50	96	NA	NA
A-2	30.5	124	46	50	87		
A-3	53.3	104	37	40	81		
	0	870					
B-1	15.2	172	76	1560	80		
B-2	30.5	170	80	550	80		
B-3	61.0	47	11	60	88		
B-4	91.4	59	17	120	79		
B-5	121.9	100	44	180	87		
	0	870					
C-1	15.2	325	152	520	89		
C-2	30.5	378	167	500	82		
C-3	61.0	189	57	360	88		
C-4	91.4	84	22	50	92		
C-5	152.4	46	8	40	83		
C-6	213.4	40	1	20	82		
C-7	281.8	41	2	20	75		

Run 4a

SMAR Port	Height (cm)	SCOD (mg/L)	TOA (mg/L)	TSS (mg/L)	VSS (%)	AMA (L/g/d)	pH
(Inf)	0	7790					
A-1	15.2	151	30	150	75	0.28	7.20
A-2	30.5	153	52	200	80	0.23	7.20
A-3	53.3	148	65	240	79	0.15	7.20
	0	7790					
B-1	15.2	128	91	8700	81	0.14	7.26
B-2	30.5	332	235	3740	82	0.14	7.22
B-3	61.0	201	86	1480	81	0.10	7.25
B-4	91.4	165	43	830	83	0.05	7.20
B-5	121.9	153	27	610	83	0.05	7.22
	0	7790					
C-1	15.2	532	276	6890	84	0.10	7.08
C-2	30.5	690	339	4810	88	0.09	7.02
C-3	61.0	866	560	2290	88	0.15	6.94
C-4	91.4	787	580	1480	88	0.05	6.95
C-5	152.4	184	80	180	83	0.21	7.15
C-6	213.4	152	35	220	82	0.20	7.17
C-7	281.8	152	29	210	85	0.12	7.20

Run 4b1

SMAR Port	Height (cm)	SCOD (mg/L)	TOA (mg/L)	TSS (mg/L)	VSS (%)	AMA (L/g/d)	pH
(Inf)	0	3820					
A-1	15.2	85	31	110	75	0.34	7.20
A-2	30.5	82	18	100	76	0.32	7.30
A-3	53.3	191	70	130	78	0.27	7.28
	0	3820					
B-1	15.2	171	41	260	79	0.08	7.15
B-2	30.5	144	42	270	77	0.20	7.40
B-3	61.0	132	13	190	77	0.28	7.40
B-4	91.4	122	19	190	73	0.31	7.25
B-5	121.9	177	46	210	79	0.24	7.32
	0	3820					
C-1	15.2	563	337	670	85	0.07	6.88
C-2	30.5	806	620	120	78	0.10	6.86
C-3	61.0	221	120	130	80	0.50	7.25
C-4	91.4	137	37	130	77	0.51	7.22
C-5	152.4	98	26	110	81	0.51	7.20
C-6	213.4	99	14	100	80	0.63	7.28
C-7	281.8	112	16	120	76	0.53	7.35

Run 4c

SMAR Port	Height (cm)	SCOD (mg/L)	TOA (mg/L)	TSS (mg/L)	VSS (%)	AMA (L/g/d)	pH
(Inf)	0	1720					
A-1	15.2	99	116	250	81	ERR	6.68
A-2	30.5	144	77	280	88		6.52
A-3	53.3	109	44	220	80		6.52
	0	1720					
B-1	15.2	128	64	3620	73		6.62
B-2	30.5	205	136	2180	83		6.48
B-3	61.0	79	37	600	75		6.52
B-4	91.4	67	16	330	77		6.56
B-5	121.9	53	23	340	79		6.46
	0	1720					
C-1	15.2	309	231	3760	76		6.52
C-2	30.5	449	325	2310	88		6.52
C-3	61.0	1163	940	1650	85		6.11
C-4	91.4	292	201	350	70		6.38
C-5	152.4	82	146	210	70		6.49
C-6	213.4	70	52	250	66		6.54
C-7	281.8	62	34	210	57		6.54

Run 6b1

SMAR Port	Height (cm)	SCOD (mg/L)	TOA (mg/L)	TSS (mg/L)	VSS (%)	AMA (L/g/d)	pH
(Inf)	0	6310					
A-1	15.2	618	504	2020	59	0.11	6.80
A-2	30.5	431	330	1600	57	0.14	6.85
A-3	53.3	311	230	1220	51	0.13	6.90
	0	6310					
B-1	15.2	753	499	11190	72	0.12	6.62
B-2	30.5	346	187	6160	72	0.15	6.74
B-3	61.0	135	65	1620	55	0.06	6.93
B-4	91.4	143	71	1690	57	0.08	6.92
B-5	121.9	180	100	1390	55	0.09	6.90
	0	6310					
C-1	15.2	780	400	4590	65	0.15	6.45
C-2	30.5	2460	1967	6850	66	0.09	6.48
C-3	61.0	4673	2972	6290	69	0.14	6.35
C-4	91.4	ERR	3898	9350	64	0.15	6.35
C-5	152.4	256	221	1090	48	0.11	6.91
C-6	213.4	207	107	960	41	0.12	6.93
C-7	281.8	203	96	950	41	0.14	6.93

Run 6b2

SMAR Port	Height (cm)	SCOD (mg/L)	TOA (mg/L)	TSS (mg/L)	VSS (%)	AMA (L/g/d)	pH
(Inf)	0	6220					
A-1	15.2	514	324	990	79	0.11	6.64
A-2	30.5	394	240	840	79	0.10	6.72
A-3	53.3	247	111	840	78	0.04	6.78
	0	6220					
B-1	15.2	1182	649	9230	83	0.18	6.45
B-2	30.5	417	252	2810	83	0.20	6.60
B-3	61.0	146	82	1120	82	0.07	6.67
B-4	91.4	137	58	860	83	0.05	6.67
B-5	121.9	156	52	660	82	0.05	6.72
	0	6220					
C-1	15.2	1432	973	2070	82	0.13	6.37
C-2	30.5	759	515	2480	81	0.10	6.43
C-3	61.0	670	411	2870	81	0.16	6.46
C-4	91.4	875	556	3370	83	0.19	6.39
C-5	152.4	258	181	390	78	0.12	6.60
C-6	213.4	173	65	500	88	0.07	6.67
C-7	281.8	169	78	260	72	0.11	6.72

Run 8a

SMAR Port	Height (cm)	SCOD (mg/L)	TOA (mg/L)	TSS (mg/L)	VSS (%)	AMA (L/g/d)	pH
(Inf)	0	17070					
A-1	15.2	556	388	1430	86	NA	7.10
A-2	30.5	539	297	1560	89		7.12
A-3	53.3	408	222	1260	88		7.17
	0	17070					
B-1	15.2	535	320	12950	84		6.85
B-2	30.5	278	163	5170	86		7.12
B-3	61.0	148	43	2460	83		7.15
B-4	91.4	146	24	2370	86		7.12
B-5	121.9	182	44	2070	87		7.20
	0	17070					
C-1	15.2	1884	1315	5450	87		6.84
C-2	30.5	ERR	1833	8890	89		6.76
C-3	61.0	2019	1368	8050	90		6.80
C-4	91.4	5226	2253	7610	87		6.58
C-5	152.4	917	392	2330	88		7.10
C-6	213.4	376	33	1940	90		7.12
C-7	281.8	338	131	1720	90		7.12

Run 10a

SMAR Port	Height (cm)	SCOD (mg/L)	TOA (mg/L)	TSS (mg/L)	VSS (%)	AMA (L/g/d)	pH
(Inf)	0	18600					
A-1	15.2	1050	470	4820		NA	6.97
A-2	30.5	758	328	5740			7.03
A-3	53.3	536	143	2540			7.12
B-1	15.2	2506	1215	8080			6.73
B-2	30.5	1036	606	6300			6.96
B-3	61.0	565	151	4760			7.09
B-4	91.4	387	81	3720			7.08
B-5	121.9	414	73	2820			7.13
C-1	15.2	8857	1573	50330			4.69
C-2	30.5	5921	842	12250			5.55
C-3	61.0	1392	811	4620			6.66
C-4	91.4	4096	1691	9600			5.92
C-5	152.4	718	266	2880			6.94
C-6	213.4	392	58	1860			6.96
C-7	281.8	354	74	1860			6.93

Run 10aG2

SMAR Port	Height (cm)	SCOD (mg/L)	TOA (mg/L)	TSS (mg/L)	VSS (%)	AMA (L/g/d)	pH
(Inf)	0	17740					
A-1	15.2	412	70	3640		NA	6.89
A-2	30.5	503	241	2920			7.02
A-3	53.3	298	43	2910			7.09
		17740					
B-1	15.2	1376	732	6980			6.75
B-2	30.5	538	182	9500			7.04
B-3	61.0	385	32	1600			7.13
B-4	91.4	331	21	1440			7.15
B-5	121.9	234	12	1860			7.15
		17740					
C-1	15.2	10269	2636	17000			5.52
C-2	30.5	8691	2654	65900			5.54
C-3	61.0	2273	1243	3560			6.65
C-4	91.4	2988	1264	2180			6.57
C-5	152.4	371	64	2360			7.10
C-6	213.4	265	37	920			7.13
C-7	281.8	209	26	960			7.11

Run 10c

SMAR Port	Height (cm)	SCOD (mg/L)	TOA (mg/L)	TSS (mg/L)	VSS (%)	AMA (L/g/d)	pH
(Inf)	0	4550					
A-1	15.2	684	571	400	83	0.12	6.48
A-2	30.5	476	342	180	87	0.14	6.60
A-3	53.3	469	384	200	84	0.14	6.63
	0	4550					
B-1	15.2	1767	1251	1810	87	0.16	5.92
B-2	30.5	517	366	740	86	0.19	6.32
B-3	61.0	193	96	330	86	0.17	6.65
B-4	91.4	184	74	340	84	0.14	6.69
B-5	121.9	190	85	200	84	0.17	6.70
	0	4550					
C-1	15.2	1169	716	1280	88	0.06	6.35
C-2	30.5	942	697	1960	86	0.11	6.40
C-3	61.0	1196	857	1670	91	0.10	6.32
C-4	91.4	2665	2106	4120	89	0.07	5.98
C-5	152.4	770	543	850	86	0.17	6.40
C-6	213.4	367	231	190	87	0.13	6.60
C-7	281.8	306	194	170	84	0.14	6.75

APPENDIX F. SMAR STEADY-STATE C2-C5 VOLATILE ACIDS

Total organic acids (TOA) is defined as the sum of the acetic acid (HAc), propionic acid (HPr), iso-butyric acid (I-But), n-butyric acid (n-But), 2-methyl butyric acid (2-m But), iso-valeric acid (I-Val), and n-valeric acid (n-Val), in the expression of acetic acid. Each individual acid is expressed as its acid, in mg/L.

Sample ID	HAc (mg/L)	HPr (mg/L)	I-But (mg/L)	n-But (mg/L)	2-m But (mg/L)	I-Val (mg/L)	n-Val (mg/L)	TOA (mg/L)
Run 2b								
A1	13.2	1.6	0.7	3.1	0.0	2.5	3.1	30.3
A2	4.9	0.4	0.0	1.0	0.0	0.0	0.0	6.8
A3	12.0	0.0	1.0	4.0	1.1	1.2	0.0	23.2
B1	17.4	4.2	0.9	5.6	1.4	1.4	0.5	37.3
B2	9.5	1.9	0.6	2.9	0.7	0.8	0.5	20.4
B3	1.2	0.1	0.9	0.9	0.2	0.3	0.0	4.8
B4	1.4	0.5	0.2	1.4	0.0	0.0	0.0	4.4
B5	17.4	5.5	2.0	3.3	1.8	1.6	1.1	39.4
C1	170.4	93.8	17.5	64.2	16.0	18.7	12.5	486.1
C2	55.9	15.1	2.5	19.1	2.9	3.6	1.0	119.0
C3	11.4	0.1	0.8	3.2	1.0	1.5	0.0	21.6
C4	7.9	1.1	0.5	2.3	0.3	0.3	0.0	14.5
C5	9.0	0.9	0.4	1.4	0.6	0.6	0.0	14.7
C6	2.6	0.0	0.0	0.6	0.3	0.2	0.0	4.2
C7	9.3	0.5	0.4	0.7	0.2	0.2	0.0	12.1
Run 2c								
A1	38.9	11.0	6.2	7.5	1.1	3.4	1.8	83.2
A2	28.6	5.1	2.0	4.0	0.0	0.8	0.4	45.7
A3	18.1	6.6	2.7	1.6	1.2	1.5	0.1	37.4
B1	38.0	8.9	2.8	10.9	1.6	2.0	0.6	76.2
B2	41.6	9.4	1.6	12.2	1.2	1.7	0.9	79.8
B3	5.7	2.2	0.7	1.0	0.0	0.0	0.0	11.0
B4	7.9	2.0	2.1	2.5	0.0	0.0	0.0	17.1
B5	18.8	4.7	4.9	4.5	1.4	1.6	0.3	44.1
C1	74.8	20.6	5.0	20.5	2.7	3.9	1.9	151.7
C2	84.2	20.2	4.5	26.1	2.6	3.4	1.8	167.1
C3	31.3	7.7	1.7	6.7	0.9	1.4	0.0	57.1
C4	11.2	2.0	3.9	1.1	0.2	0.4	0.0	21.9
C5	2.6	0.4	0.0	3.6	0.0	0.0	0.0	8.3
C6	0.9	0.0	0.0	0.1	0.0	0.0	0.0	1.1
C7	1.0	0.0	0.0	0.6	0.0	0.0	0.0	1.8

SMAR Steady-State C2-C5 volatile acids

Sample ID	HAc (mg/L)	HPr (mg/L)	I-But (mg/L)	n-But (mg/L)	2-m But (mg/L)	I-Val (mg/L)	n-Val (mg/L)	TOA (mg/L)
Run 4a								
A1	14.5	7.8	0.8	0.6	0.0	0.5	1.7	30.0
A2	28.3	12.7	1.5	0.8	0.3	1.5	0.8	51.8
A3	34.7	18.1	1.7	0.6	0.8	2.1	0.0	65.4
B1	35.4	24.2	3.9	3.7	0.0	3.7	4.8	90.7
B2	100.3	57.6	10.7	10.8	6.1	7.1	5.6	234.9
B3	44.8	24.4	1.4	1.1	1.4	1.9	1.2	86.1
B4	26.9	8.9	0.6	0.5	0.6	0.8	0.5	42.5
B5	17.5	5.9	0.4	0.2	0.2	0.5	0.3	27.2
C1	111.7	81.3	9.3	8.5	7.3	9.5	5.3	275.6
C2	136.5	96.3	10.3	11.1	8.8	11.5	10.3	338.6
C3	197.5	157.6	19.4	22.8	16.6	22.9	22.7	559.6
C4	225.0	157.4	18.8	22.2	16.2	23.1	19.8	579.7
C5	46.1	18.3	1.8	0.9	1.5	1.5	1.6	80.3
C6	21.0	6.9	0.7	0.4	0.5	0.4	1.3	34.8
C7	19.1	5.4	0.7	0.2	0.5	0.6	0.4	29.5
Run 4b1								
A1	12.8	4.2	1.9	2.3	0.0	2.1	2.2	31.4
A2	7.9	2.5	0.7	1.3	0.2	1.3	0.6	17.6
A3	30.4	15.1	2.9	4.6	1.8	3.1	1.0	70.1
B1	19.0	6.9	1.8	2.6	1.7	1.3	0.9	40.5
B2	17.3	7.3	3.2	3.0	0.9	2.1	0.7	41.7
B3	8.5	1.7	0.4	0.5	0.2	0.5	0.0	13.1
B4	11.4	3.3	0.6	0.8	0.4	0.5	0.0	19.2
B5	22.5	9.4	1.5	2.0	1.5	1.5	0.9	46.0
C1	129.2	80.9	14.6	19.0	11.9	13.7	8.9	336.9
C2	229.9	136.0	20.1	65.9	18.0	22.5	16.3	620.4
C3	42.2	35.1	4.3	8.4	3.2	4.1	1.9	119.7
C4	14.6	4.8	1.0	5.3	1.5	1.9	0.7	36.7
C5	13.7	4.8	1.0	1.4	0.7	1.3	0.0	26.4
C6	8.7	2.3	0.4	0.5	0.3	0.3	0.0	13.9
C7	8.8	1.9	0.5	0.6	0.9	0.8	0.0	15.6

SMAR Steady-State C2-C5 volatile acids

Sample ID	HAc (mg/L)	HPr (mg/L)	I-But (mg/L)	n-But (mg/L)	2-m But (mg/L)	I-Val (mg/L)	n-Val (mg/L)	TOA (mg/L)
Run 4c								
A1	51.9	28.4	3.8	5.0	0.9	3.6	5.1	116.1
A2	32.8	19.8	2.4	4.0	1.4	2.8	1.7	76.8
A3	19.5	11.0	1.6	1.5	0.8	2.0	0.6	43.5
B1	26.1	16.5	2.2	2.7	1.5	2.5	1.9	63.7
B2	54.7	35.7	4.8	6.6	3.8	4.8	3.8	136.3
B3	17.0	9.9	1.1	0.8	0.9	1.3	0.8	36.9
B4	5.9	5.6	0.4	0.2	0.1	0.3	0.9	15.8
B5	5.3	12.3	0.3	0.2	0.0	0.3	0.6	22.7
C1	94.8	62.7	7.5	9.5	6.1	8.0	6.2	231.4
C2	99.8	110.6	12.1	10.7	9.3	14.3	8.7	324.6
C3	304.7	249.3	28.0	96.2	22.6	34.9	28.2	940.1
C4	83.7	48.5	3.9	23.0	3.3	4.7	2.6	201.2
C5	78.7	28.4	6.1	4.2	0.0	4.0	6.0	145.8
C6	21.7	14.1	2.4	3.0	0.0	2.8	0.0	51.8
C7	13.6	15.3	1.3	0.0	0.0	0.0	0.0	34.4
Run 6b1								
A1	224.0	101.0	19.3	30.8	12.0	17.0	19.3	504.0
A2	149.6	76.1	11.8	16.1	7.8	9.5	9.5	329.8
A3	108.5	60.1	7.2	6.3	5.3	5.6	5.3	229.9
B1	135.7	157.8	27.9	5.6	30.8	24.8	14.7	499.1
B2	66.4	56.2	8.1	4.5	7.3	6.0	6.0	187.0
B3	34.4	17.3	1.4	0.7	1.1	1.4	1.2	64.9
B4	38.3	20.0	1.3	0.8	0.9	0.7	1.5	71.3
B5	53.0	27.8	1.9	1.4	1.4	2.3	1.1	100.3
C1	148.2	155.0	11.1	4.6	11.7	6.5	4.1	400.2
C2	488.9	488.3	98.5	144.3	78.2	119.9	107.9	1967.3
C3	602.8	707.0	146.4	214.0	130.5	206.0	233.1	2971.9
C4	647.3	784.5	216.4	360.2	169.6	281.3	394.8	3898.2
C5	98.1	51.4	6.7	8.3	4.8	8.0	9.0	220.6
C6	57.0	23.3	2.9	2.2	3.0	2.7	2.4	107.1
C7	55.4	21.4	2.6	1.2	1.7	2.3	1.2	96.3

SMAR Steady-State C2-C5 volatile acids

Sample ID	HAc (mg/L)	HPr (mg/L)	I-But (mg/L)	n-But (mg/L)	2-m But (mg/L)	I-Val (mg/L)	n-Val (mg/L)	TOA (mg/L)
Run 6b2								
A1	137.8	63.0	10.7	23.3	9.5	8.3	16.6	324.0
A2	113.3	51.9	8.3	10.8	6.4	6.1	7.9	240.0
A3	54.7	23.8	3.5	3.6	2.8	2.2	4.9	111.5
B1	164.1	156.8	41.9	29.6	33.9	35.8	40.2	649.0
B2	110.7	50.1	11.2	16.7	7.8	7.5	7.3	251.6
B3	41.1	17.3	2.1	1.4	2.8	2.8	3.1	82.2
B4	33.2	18.8	1.2	0.0	0.0	0.0	0.0	58.1
B5	29.4	16.1	1.7	0.0	0.0	0.0	0.0	51.8
C1	284.0	188.4	40.3	100.1	37.9	51.1	58.3	972.8
C2	193.8	100.4	19.6	49.0	14.1	17.9	25.1	515.3
C3	177.6	82.0	13.2	36.5	10.5	10.3	14.2	411.1
C4	220.5	108.9	20.5	56.1	14.6	15.3	22.2	555.6
C5	80.9	39.1	5.3	11.5	1.4	6.0	8.9	181.4
C6	39.5	17.1	1.7	1.7	0.0	0.0	0.0	65.5
C7	37.3	18.4	1.5	2.2	3.0	2.7	1.9	78.3
Run 8a								
A1	216.2	72.7	12.5	15.2	8.5	9.7	6.0	387.6
A2	167.8	62.0	8.8	8.3	5.1	6.5	4.8	297.4
A3	136.9	50.0	7.1	3.0	2.5	2.3	0.0	221.6
B1	126.0	82.2	15.8	5.5	11.7	11.6	12.9	320.3
B2	74.3	31.9	5.5	2.8	7.0	7.4	7.4	163.0
B3	30.7	9.0	1.1	0.0	0.0	0.0	0.0	43.4
B4	9.6	7.3	1.4	2.2	0.0	0.0	0.0	23.9
B5	31.9	8.6	0.7	0.5	0.0	0.0	0.0	44.3
C1	503.6	291.0	55.3	76.0	41.1	58.7	53.1	1314.9
C2	562.4	440.3	86.7	125.9	59.7	92.5	92.5	1833.5
C3	505.5	324.3	58.7	72.2	43.1	60.7	55.2	1367.7
C4	624.4	531.0	96.7	234.8	72.5	97.7	116.4	2252.5
C5	194.3	87.0	11.1	10.9	11.8	13.8	8.5	391.8
C6	17.6	8.9	1.3	1.4	0.0	0.0	0.0	32.5
C7	74.5	28.5	2.0	1.7	4.0	5.1	0.0	130.7

SMAR Steady-State C2-C5 volatile acids

Sample ID	HAc (mg/L)	HPr (mg/L)	I-But (mg/L)	n-But (mg/L)	2-m But (mg/L)	I-Val (mg/L)	n-Val (mg/L)	TOA (mg/L)
Run 10a								
A1	238.7	98.6	14.3	19.0	9.6	9.3	16.9	469.7
A2	156.5	91.5	8.2	9.3	5.9	4.5	8.8	327.7
A3	75.1	46.1	1.9	0.6	1.3	1.2	1.8	143.0
B1	446.1	233.0	45.7	124.3	34.4	37.7	64.6	1215.2
B2	293.0	138.9	18.7	28.2	14.5	11.9	16.3	605.8
B3	77.3	30.7	5.6	5.2	0.9	5.2	5.6	151.0
B4	43.5	20.9	1.8	2.5	0.5	1.8	1.0	81.1
B5	40.8	17.5	3.1	2.0	0.4	1.0	0.4	73.0
C1	667.7	105.2	10.8	440.3	8.6	9.4	49.0	1572.9
C2	656.9	294.8	26.9	410.6	26.7	17.7	61.2	1841.6
C3	317.5	133.4	21.6	142.5	12.5	10.8	28.7	811.3
C4	666.7	358.6	47.5	206.9	34.5	21.3	67.3	1691.5
C5	134.2	43.0	6.6	30.6	5.2	2.1	6.8	265.7
C6	36.0	5.7	0.9	5.7	1.7	0.0	1.5	58.1
C7	43.0	13.8	1.0	5.2	0.4	0.5	2.0	74.1
Run 10aG1								
A3	27.6	11.5	1.5	4.4	1.4	1.3	1.4	57.3
B5	13.2	5.4	0.5	2.4	0.4	0.5	0.6	26.5
C7	7.7	5.5	0.2	3.5	0.4	0.2	0.9	22.4
Run 10aG2								
A1	30.5	13.9	3.4	3.5	0.3	3.3	3.9	70.4
A2	107.4	44.7	9.0	21.2	5.2	7.4	7.6	241.3
A3	26.2	6.5	1.2	1.8	0.7	1.1	0.7	42.8
B1	226.1	96.6	30.3	157.2	18.2	18.5	29.0	731.6
B2	75.3	25.7	9.4	24.1	5.0	4.1	6.5	182.4
B3	16.4	4.5	1.1	3.6	0.5	0.8	0.7	31.8
B4	10.3	4.5	0.6	1.8	0.5	0.3	0.3	21.3
B5	6.4	2.2	0.3	1.0	0.1	0.0	0.6	12.3
C1	749.0	198.9	167.9	445.5	146.6	231.1	59.0	2636.2
C2	645.1	383.2	132.4	323.4	129.0	177.8	203.7	2654.0
C3	438.9	156.5	51.3	143.4	34.5	93.0	63.9	1242.7
C4	427.7	202.4	56.5	127.8	37.2	58.2	90.8	1264.2
C5	26.9	4.7	2.2	11.6	1.0	1.5	4.1	64.3
C6	16.8	3.9	0.8	6.8	0.7	1.2	0.7	37.2
C7	11.7	2.2	0.6	4.7	0.5	1.0	1.1	26.5

SMAR Steady-State C2-C5 volatile acids

Sample ID	HAc (mg/L)	HPr (mg/L)	I-But (mg/L)	n-But (mg/L)	2-m But (mg/L)	I-Val (mg/L)	n-Val (mg/L)	TOA (mg/L)
Run 10c								
A1	203.1	102.0	19.5	73.9	13.3	21.8	26.9	571.3
A2	111.6	76.0	12.7	35.5	9.1	13.4	16.4	341.9
A3	142.1	101.1	13.0	21.8	10.8	14.5	13.6	383.8
B1	352.8	244.2	55.3	153.9	43.3	49.8	77.4	1250.7
B2	129.6	74.7	12.9	34.7	14.5	14.0	15.3	365.9
B3	39.2	30.1	2.2	4.2	1.6	2.0	2.5	96.3
B4	30.1	24.8	1.4	1.7	1.3	1.5	2.0	74.4
B5	26.7	31.7	1.3	0.6	1.8	3.9	4.2	85.3
C1	245.8	143.3	25.5	67.2	21.0	31.6	40.0	715.7
C2	270.4	143.4	26.2	55.1	18.5	26.6	31.9	697.4
C3	279.7	183.3	33.2	68.2	27.5	42.2	49.5	857.2
C4	526.4	441.6	84.5	228.1	71.4	114.8	152.8	2105.5
C5	208.5	112.8	14.6	51.2	13.7	20.4	24.0	542.8
C6	91.5	63.7	5.6	13.4	5.3	7.4	6.7	231.0
C7	82.5	51.9	6.2	6.2	6.3	7.4	3.5	194.0